PROTOCOLO CINVA- MNT-243

"EVALUACIÓN DE PÉPTICOS IN VITRO E IN VIVO RADIOMARCADOS PARA EL DIAGNÓTICO ESPECÍFICO DE LESIONES TUMORALES POR IMÁGENES GAMMAGRAFICAS EN MEDICINA NUCLEAR".

INVESTIGADOR: DRA.MARTA PEDRAZA LÓPEZ

DEPARTAMENTO: MEDICINA NUCLEAR

INSTITUTO NACIONAL DE
CIENCIAS MÉDICAS
Y NUTRICIÓN
SALVADOR ZUBIRÁN

24 de abril de 2017

Dra. Norma Bobadilla Sandoval
Coordinadora de la Comisión en Animales
PRESENTE

Distinguida Dra. Norma Bobadilla

En respuesta al oficio CINVA 006-17, anexo la información solicitada referente al protocolo **EVALUACIÓN *IN VITRO* E *IN VIVO* DE PÉPTIDOS RADIOMARCADOS PARA EL DIAGNÓSTICO ESPECÍFICO DE LESIONES TUMORALES POR IMÁGENES GAMMAGRÁFICAS EN MEDICINA NUCLEAR" CINVA 243**.

El protocolo se registró en julio 2007 y finalizó en julio 2008, se adjunta forma única.
Se solicitó una prórroga para continuar con el protocolo hasta diciembre 2015.
Finalmente se solicitó el cierre del protocolo el 11 de febrero de 2016.
Se adjuntan copias de los oficios.

De este proyecto se derivaron 8 publicaciones:

1. P.P. Surujpaul, C. Gutierrez Wing, B Ocampo-García, F. de M Ramírez, C. Artega de Murphy, M. Pedraza-López and G. Ferro-Flores.Gold Nanoparticles Conjugated to [Tyr^3] Octreotide Peptide. **Biophysical Chemistry 2008; 138: 83-90.**

2. F. A. López-Durán, M. Pedraza-López, C. Arteaga de Murphy, E. Hernández-Hernández, R. García-Becerra, D. Ordaz-Rosado. Pharmacokinetics and uptake of ^{99m}Tc-HYNIC-cRGD in $\alpha_v\beta_3$ for imaging angiogenesis in induced malignant tumors. ***Bioquimia* (2009) 34:61-68.**

3. C.L. Santos-Cuevas, G. Ferro-Flores, C. Arteaga de Murphy, F. de M. Ramírez, M.A. Luna-Gutiérrez, M. Pedraza-López, R. García-Becerra, D. Ordaz-Rosado. Design, preparation, *in vitro* and *in vivo* evaluation of 99mTc-N2S2-TAT(49-57)-bombesin: a target-specific hybrid radiopharmaceutical. **Int. J. Pharmaceutics (2009) 375:75-83**

4. Avila-Rodriguez, M.A. Ferro-Flores, G., Pedraza-Lopez, M., Arteaga de Murphy, C. **Preparation and evaluation of ^{68}Ga-DOTA-Glu-[cyclo(Arg-Gly-Asp-D-Phe-Lys)]2 labeled with cyclotron produced gallium-68.** 19th International Symposium on Radiopharmaceutical Science, Amsterdarm, ***J. Labelled Cpd.Radiopharm. 2011; 54: S1-P264; S353.***

5. Nallely Jiménez-Mancilla, Guillermina Ferro-Flores, Blanca Ocampo-García, Myrna Luna-Gutiérrez, Flor De María Ramírez, Martha Pedraza-López, Eugenio Torres-García. Multifunctional Targeted Radiotherapy System for Induced Tumours Expressing Gastrin-releasing Peptide Receptors. ***Current Nanoscience (2012)*** 8: 193-201.

Avenida Vasco de Quiroga No. 15
Colonia Belisario
Dominguez Seccion XVI
Delegacion Tlalpan
Codigo Postal 14080
Mexico, Distrito Federal
Tel: 55 2598 3900
www.incmnsz.mx

INSTITUTO NACIONAL DE CIENCIAS MÉDICAS Y NUTRICIÓN SALVADOR ZUBIRÁN

6. V. López-Rodríguez, R.E. Gaspar-Carcamo, V.M. Lara-Camacho, M. Avila-Garcia, G. Ferro-Flores, M. Pedraza-López, C. Arteaga de Murphy, M.A. Ávila-Rodríguez, 66Ga labeled DOTA-E-(c(RGDfK))2 and NODAGA-E-(c(RGDfK))2 to target tumors over-expressing αvβ3 integrin receptors, ***J Label Compd Radiopharm 56, S356 (2013).***

7. A. Vilchis-Juárez, G. Ferro-Flores, C. Santos-Cuevas, Enrique Morales-Avila, Blanca Ocampo-García, Lorenza Díaz-Nieto, M. Luna-Gutiérrez, N. Jiménez-Mancilla, M. Pedraza-López, L. Gómez-Oliván. Molecular Targeting Radiotherapy with cyclo-RGDfK(C) Peptides Conjugated to ^{177}Lu-Labeled Gold Nanoparticles in Tumor-Bearing Mice. ***J. Biomed. Nanotechnol 10(3) 393-404 (2014)***

8. V. Lopez-Rodriguez, R.E. Gaspar-Carcamo, M. Pedraza-Lopez, C. Arteaga de Murphy, G. Ferro-Flores, M.A. Avila-Rodriguez. Preparation and preclinical evaluation of 66Ga-DOTA-E(c(RGDfK))2 as a Potential theranostic radiopharmaceutical . **Nucl. Med. Biol. 42(2): 109-114 (2015)**

Sin otro particular por el momento, reciba un cordial saludo.

Atentamente,

Dra. Martha Pedraza López
Investigador en Ciencias Médicas "C"
Departamento de Medicina Nuclear.

c.c.p. Dr. Gerardo Gamba Ayala, Director de Investigación
M.V.Z. Mariela Contreras Escamilla, Jefa del DIEB

Avenida Vasco de Quiroga No. 15
Colonia Belisario Domínguez Sección XVI
Delegación Tlalpan
Código Postal 14080
México, Distrito Federal
Tel: 10 84 00 30
www.incmnsz.mx

Bioquímia

Artículo original
Farmacología

Radiopharmacokinetics and uptake of ^{99m}Tc-cRGD in $\alpha_v\beta_3$ integrins for imaging angiogenesis in induced malignant tumors in athymic mice

Fred A. López-Durán,* Martha Pedraza-López,** Consuelo Arteaga de Murphy,** Edith Hernández-Hernández,*** Rocío García-Becerra,**** David Ordaz-Rosado****

ABSTRACT

The multistep process of angiogenesis offers several targets for therapeutic interventions. One molecular target structure is the alfa five beta three ($\alpha_v\beta_3$) integrin which is expressed on vascular endothelial cells and over-expressed in cancer tumor angiogenesis. To image neoangiogenesis in athymic mice with induced pancreatic, breast and prostate malignant tumors a new radiopharmaceutical was developed. The ^{99m}Tc-EDDA/HYNIC-cyclic-Arg-Gly-Asp-D-Phe-Lys (^{99m}Tc-cRGD) targets integrin receptors $\alpha_v\beta_3$ and was prepared with an average radiochemical purity > 95 %. ^{99m}Tc-cRGD shows high in vivo *stability, fast blood clearance and rapid renal excretion in mice. There are statistical differences between tumor/muscle ratios for the 3 tumors studied. The highest tumor/non-target ratio was found in breast cancer (7.2 after 24 h) and a representative dorsal SPECT image was obtained where the tumor showed up very clearly over the background tissue. The high resolution of the image implies that ^{99m}Tc-cRGD will be of great value in nuclear medicine as a potential radiopharmaceutical for $\alpha_v\beta_3$ integrins receptor uptake and for imaging neoangiogenesis in neoplastic tissue and to follow up cancer tumor progression.*

Key words: *Radiolabelled RGD-peptide, integrin $\alpha_v\beta_3$, molecular imaging, angiogenesis.*

RESUMEN

Los receptores de integrinas $\alpha_v\beta_3$ se encuentran en la pared endotelial de los vasos sanguíneos y están sobreexpresados, sobre todo en los nuevos vasos de los tumores malignos. Para visualizar la neoangiogénesis en tumores inducidos con células cancerosas de páncreas, mama y próstata en ratones atímicos se desarrolló un nuevo radiofármaco de tecnecio-99m (^{99m}Tc). El péptido cíclico con los aminoácidos: -Arg-Gly-Asp-D-Phe-Lys- se marcó con ^{99m}Tc por medio del ligante bifuncional ácido hidracinonicotínico (HYNIC) y del coligante etilendiaminodiacético (EDDA). El ^{99m}Tc-EDDA/HYNIC-cyclic-Arg-Gly-Asp-D-Phe-Lys (^{99m}Tc-cRGD) con pureza radioquímica > 95%, se une *in vivo* a los receptores de integrinas $\alpha_v\beta_3$ con alta especificidad. En los ratones atímicos con cáncer inducido presenta rápida depuración sanguínea y eliminación renal y hay diferencias estadísticamente significativas entre la captación del tumor comparada contra la captación en músculo, en los tres tipos de neoplasias. La relación más alta tumor/músculo fue de 7.2 a las 24 h para el cáncer de mama y se visualizó la neoangiogénesis en este tumor. La alta resolución de la imagen demuestra que en la medicina nuclear el ^{99m}Tc-cRGD será de gran valor como un radiofármaco que se une específicamente a receptores de integrinas $\alpha_v\beta_3$ y por consiguiente permite obtener imágenes moleculares de tumores malignos con alta resolución.

Palabras clave: Péptido -RGD-^{99m}Tc, integrina $\alpha_v\beta_3$, imagen molecular, angiogénesis.

* Faculty of Medicine, Universidad Autónoma del Estado de México. Toluca, México.
** Nuclear Medicine Department, Instituto Nacional de Ciencias Médicas y Nutrición Salvador Zubirán, México.
*** Department of Radioactive Materials, Instituto Nacional de Investigaciones Nucleares, México.
**** Department of Reproductive Biology, Instituto Nacional de Ciencias Médicas y Nutrición Salvador Zubirán, México.

Correspondencia:
Martha Pedraza López, Ph.D.
Departamento de Medicina Nuclear. Instituto Nacional de Ciencias Médicas y Nutrición Salvador Zubirán. Vasco de Quiroga Núm. 15. Delegación Tlalpan. 14000. México, D.F. México.
Fax +52(55) 5655 1076, E-mail: mpedraza_lopez@yahoo.com.mx

Recibido: 29-07-2009
Aceptado: 20-05-2009

INTRODUCTION

Angiogenesis is a complex natural physiologic process that results in the formation of new vessels in a tissue and during angiogenesis a group of cell membrane receptors (transmembrane heterodimeric glucoproteins), called integrins modulate cell migration, cell-cell interactions and cell binding to the extracellular matrix.[1-3]

Angiogenesis is increased in several pathologic entities including cancer. The integrins enhance vascular and lymphatic permeability and are directly involved in cancer tumor-induced angiogenesis.[2,4] Several studies have shown that there is a correlation between $\alpha_v\beta_3$ receptor expression, angiogenesis and the metastatic potential of the corresponding cancer tumor.[5]

The multistep process of angiogenesis offers several targets for therapeutic interventions. One target structure is the $\alpha_v\beta_3$ integrin, which is overexpressed in vascular endothelial cells, and recognizes certain specific amino acid sequences.[4,6] It is of interest to study the development of targeting radiopharmaceuticals for $\alpha_v\beta_3$ integrin receptors that could serve as antiangiogenic therapeutics.[7] Radiolabeled peptides containing the specific amino acid sequence —arginine-glycine-aspartic acid— (RGD) have been used for targeting $\alpha_v\beta_3$ integrin receptors and thus imaging angiogenesis.

RGD peptides have been labeled with ^{99m}Tc, ^{111}In, ^{90}Y, ^{123}I, ^{64}Cu, ^{68}Ga. and ^{18}F.[8-12] There is especial interest in positron emitters for PET (positron emission tomography) integrin $\alpha_v\beta_3$ expression imaging in cancer tumors. It was shown that constraining the mobility of the linear RDG, by forming a cyclic peptide, increased their integrin receptor affinity *in vitro*.[13] Tetramer and octamer RDG peptides have been labeled with copper-64 for PET imaging of induced glioblastomas in a mice model.[14] Gallium-68 was conjugated to cyclic RGDs through a macrocyclic chelator.[11,12] For ^{18}F labeling chemistry many linkers and conjugated molecules in cyclic, monomeric and polymeric structures have been used for PET. Some radiopharmaceuticals are: ^{18}F-galacto-RGD, the dimeric cyclic ^{18}F-E[c(RGDyK)]2 and the ^{18}F-bombesin heterodimer. The tetrameric fluorinated aldehydes that were conjugated to an amino-oxy-bearing RGD peptide and linked to a polyethyleneglycol prosthetic group gave the best biodistribution in mice.[15-19] Nevertheless ^{99m}Tc labeling is still the best option for *in situ* radiopharmaceutical preparations useful for the hybrid SPECT/CT (single-photon emission computed tomography/computed tomography).[20]

A considerable number of synthetic peptides modified from the five amino acid parent or lead structure arginine-glycine-aspartic acid-phenilalanine-valine amino acids (RGDfV) have been assayed. Kok et al. reported that substituting the valine of the parental cRGDfV peptide for a lysine amino acid shows high affinity for $\alpha_v\beta_3$ integrins.[7] The cyclized-Arg-Gly-Asp-D-Phe-Lys (cRGDfK), as a monomer or dimer, can be technetium-99m labeled for targeting $\alpha_v\beta_3$ receptors. The lysine side chain provides primary amine functionality for coupling bifunctional chelating agents such as hydrazinonicotinic acid (HYNIC).[3,21-23]

Decristoforo et al. described the radiolabeling of a HYNIC-derivatized cyclic monomeric RGD peptide containing tyrosine and lysine amino acids [c(RGDyK (HYNIC)] using tricine and ethylendiaminodiacetic acid (EDDA) as coligands.[24]

The aim of this research was to easily prepare a ^{99m}Tc-EDDA/HYNIC-cyclic-Arg-Gly-Asp-D-Phe-Lys (^{99m}Tc-cRGD) radiopharmaceutical, to determine its biopharmacokinetics, estimate $\alpha_v\beta_3$ integrin receptor uptake and to image angiogenesis in athymic mice with induced malignant pancreatic, breast and prostate tumors.

METHODS

Preparation of ^{99m}Tc-EDDA/HYNIC-cyclic-Arg-Gly-Asp-D-Phe-Lys (^{99m}Tc-cRGD)

The cyclic-Arg-Gly-Asp-D-Phe-Lys pentapeptide (cRGD) (Bachem, USA) was conjugated to hydrazinonicotinic acid (HYNIC) via *o*-(7-azabenzotriazolyl)-1,1,3,3-tetramethyluronium hexafluorophosphate (HATU). The HYNIC-cRGD conjugate was > 98%, chemically pure as analyzed by reversed phase high-performance liquid chromatography (HPLC, Waters instrument running Millenium software with both radioactivity and UV photodiode array in-line detectors).

The lyophilized kit was prepared with the HYNIC-cRGD conjugate plus ethylendiaminodiacetic acid (EDDA) and tricine as coligands and $SnCl_2$ as a reducing agent.

The radiopharmaceutical ^{99m}Tc-EDDA/HYNIC-cyclic-Arg-Gly-Asp-D-Phe-Lys (^{99m}Tc-cRGD) was prepared by adding ^{99m}Tc-pertechnetate obtained from a GETEC ^{99}Mo/^{99m}Tc generator (ININ-Mexico) to the lyophilized sterile kit and incubated for 15 min in boiling water.[25]

Evaluation of radiochemical purity

Radiochemical purity analyses were performed by solid phase extraction (Sep-Pak C-18 cartridges), reverse phase high-performance liquid chromatography (HPLC) and by instant thin-layer chromatography on silica gel (ITLC-SG, Gelman Sciences) with three different mobile phases: 2-butanone to determine the amount of free $^{99m}TcO_4^-$ (Rf = 1); 0.1 M sodium citrate pH 5 to determine ^{99m}Tc-EDDA coligand and $^{99m}TcO_4^-$ (Rf = 1) and, methanol: 1 M ammonium acetate (1:1 v/v) for ^{99m}Tc-colloid (Rf = 0).[25]

Cancer cell lines

Three cancer producing cell lines were used:

a) The AR42J murine pancreatic cancer cell line (ATTC, Rockville, MD, USA) over-expresses somatostatin receptors (SS). The cells were routinely cultivated at 37 °C in 5% CO_2 and 85% air humidified atmosphere in Dulbecco's minimum essential culture medium (DMEM) (Life Technologies, Inc, Gaithersburg, MD) which was supplemented with 5% fetal-bovine-serum and 100 U/mL of penicillin and 100 μg/mL streptomycin.
b) The MCF-7 cell line is derived from human breast cancer and overexpresses cholecystokinin receptors (CCK). The cells were cultivated in DMEM and 10 nM estradiol and incubated in 5% CO_2 at 37 °C, 85% atmosphere and humidity.
c) The PC-3 human prostate cancer cell line PC-3 was originally obtained from ATCC (USA) and overexpresses gastrin releasing peptide receptors (GRP). PC-3 cells were routinely grown in "RPMI" culture medium supplemented with 10% newborn calf serum and streptomycin (100 μg/mL) at 37 °C, with 5% CO_2 atmosphere and 85% humidity.[26]

Induced cancer tumors in athymic mice

Animal experiments were carried out in compliance with the Official Mexican Norm (NOM 062-Zoo-1999): rules and regulations for safe and adequate laboratory animal handling.

Athymic adult male mice (20-22 g) were kept in sterile cages with beds of sterile wood shavings, constant temperature, humidity, noise and 12:12 light periods. Water and feed (standard PMI 5001 feed) were given *ad libitum*. The cancer cells (1 x 10^6 in 0.1 mL) were implanted in 36 athymic mice by subcutaneous injection into the animal's back (12 mice injected with the AR42J cells, 12 mice injected with the MCF-7 cells and 12 mice injected with the PC-3 cells). Tumor growth was monitored frequently and the length and width were measured in cm^2 with calipers. The final volume (cm^3), after sacrifice, was expressed in grams.

In vivo biokinetics and cancer tumor uptake

When the tumors became visible (< 1 cm^2) a mean of 18.5 MBq of the radiopeptide, was injected in a tail vein (n = 3) for each time interval. After 0.5, 1, 3 and 24 h the mice were sacrificed in a CO_2 chamber. The tumor and the organs or tissues (blood, heart, lung, liver, spleen, pancreas, kidneys, thigh muscle and femur) were excised, blotted dry and put into plastic test tubes, previously weighed. The weight of the organ and the anatomic characteristics of the tumors were recorded. Activity of the tumor and organs was measured in a crystal scintillation [NaI (Tl)] well-type detector. The mean of 3 diluted aliquots of the injected activity (I.A.) were considered as the 100% uptake. Percentage uptake or activity A (number of disintegrations per unit time) of each organ or tissue was calculated and the results were expressed as the percentage of injected activity per gram of tissue (%IA/g). Tumor/blood and tumor/muscle ratios were calculated. Each value represents the mean and SD of three animals.

To evaluate the kinetics of the system a compartmental model was developed using the OLINDA/EXM code. The program allows the user to enter kinetic data and fit it to one or more exponential terms. The total number of disintegrations (N), in source regions, was calculated, integrated over time and expressed per unit of initial activity in the source region: MBq-h/MBq (previously considered as residence time in the MIRD code) equation 1.[27]

$$N_{SOURCE} = \int_{t=0}^{t=\infty} A_{SOURCE}\,dt \qquad (1)$$

Image acquisition

Imaging of mice injected with ^{99m}Tc-cRGD was performed with a Siemens E-cam SPECT single head gamma camera with a pinhole collimator.

Statistical strategy

The mean % uptake for each lot of 3 mice per time interval was calculated. The statistical method em-

ployed was the t-Student's test for the activity of the tumor *vs.* muscle for each time interval after administration. The significance level was $p = 0.05$.

RESULTS

The average radiochemical purity of ^{99m}Tc-cRGD was > 95% in all cases. Free $^{99m}TcO_4$ was < 2 %; 2-3% of ^{99m}Tc-EDDA and < 1.0% of ^{99m}Tc-colloid.

The biodistribution of ^{99m}Tc-cRGD in the three models of induced cancer tumors are summarized in *table I*. The radiopeptide shows favorable pharmacokinetic properties such as rapid blood clearance and renal elimination. Activity was accumulated mainly in the liver, spleen and kidneys.

There was a high *in vivo* stability in the induced tumors (pancreas, breast and prostate). Low muscle uptake (background activity) was observed in all the mice. Twenty four hours after radiopharmaceutical administration the mean percentage of the injected activity per gram of tissue (%IA/g) found in the murine pancreatic cancer tumor was 0.73 ± 0.36% (AR42J cells); 1.31 ± 0.24% in breast cancer (MCF-7 cells) and 0.67 ± 0.02% in the prostatic cancer (PC-3 cells), *(Table I)*. The anatomical characteristics for the xenograft pancreatic tumor were of a large, friable hemorrhagic mass; the breast tumor was white, compact and hard; the prostatic tumor was white with a discreet beige coloring, compact and hard to the touch. The tumor/blood ratios of % IA/g tissue in 24 h after administration were 14.6 for the AR42J cell line; 10.9 for the MCF-7 cell line; 9.5 for the PC-3 cell line. The tumor to muscle ratio after 24 h in the pancreatic tumor induced with the AR42J cell line was 4.0; in the hard, compact breast cancer (MCF-7 cell line) was 7.2 and for the PC-3 cell line (prostate) the ratio was 3.5 *(Table II)*. The reason for these differences might be that in the hemorrhagic pancreatic tumor the activity leaks out, in the compact dense breast tumor it remains inside the tumor and in the poorly vascular prostatic tumor the activity is minor.

Table I. Biodistribution data for ^{99m}Tc-cRGD in an athymic mice model bearing induced tumors expressed as % injected activity / gram of tissue (%IA/ g tissue), at different time intervals (0.5 to 24 h).

		% IA /g tissue		
Organ	Time p.i. (h)	AR42J (Pancreas)	MCF-7 (Breast)	PC-3 (Prostate)
Blood	0.5	3.15 ± 0.48	1.66 ± 0.21	0.88 ± 0.52
	1	2.86 ± 0.38	0.68 ± 0.10	0.70 ± 0.10
	3	0.31 ± 0.05	0.31 ± 0.02	0.34 ± 0.07
	24	0.05 ± 0.03	0.12 ± 0.04	0.07 ± 0.01
Liver	0.5	2.14 ± 0.57	2.15 ± 0.24	2.14 ± 0.04
	1	2.79 ± 0.47	1.60 ± 0.18	2.45 ± 0.43
	3	2.31 ± 0.60	1.51 ± 0.13	1.57 ± 0.40
	24	0.83 ± 0.31	0.91 ± 0.15	1.16 ± 0.47
Spleen	0.5	2.53 ± 0.03	1.72 ± 0.19	2.02 ± 0.37
	1	1.09 ± 0.07	1.56 ± 0.65	2.11 ± 0.20
	3	1.11 ± 0.19	1.42 ± 0.40	1.48 ± 0.28
	24	0.53 ± 0.18	1.16 ± 0.21	1.89 ± 0.57
Kidneys	0.5	3.75 ± 0.74	4.04 ± 0.12	6.62 ± 0.79
	1	9.75 ± 1.84	3.07 ± 0.01	3.02 ± 0.14
	3	2.65 ± 0.41	3.02 ± 0.30	2.28 ± 0.36
	24	1.37 ± 0.44	1.95 ± 0.04	1.53 ± 0.33
Muscle	0.5	0.90 ± 0.06	0.73 ± 0.14	0.65 ± 0.04
	1	1.09 ± 0.14	0.46 ± 0.09	0.58 ± 0.06
	3	0.33 ± 0.05	0.32 ± 0.02	0.34 ± 0.06
	24	0.18 ± 0.03	0.18 ± 0.03	0.19 ± 0.05
Tumor	0.5	2.26 ± 0.24	2.00 ± 0.60	1.59 ± 0.27
	1	2.84 ± 0.14	1.71 ± 0.52	1.48 ± 0.19
	3	2.15 ± 0.15	1.61 ± 0.37	1.23 ± 0.29
	24	0.73 ± 0.36	1.31 ± 0.24	0.67 ± 0.02

There is a statistical difference ($p < 0.05$) in % IA/g tumor *vs* muscle for the 3 tumors and for each mean time interval *(Table III)*.

Figure 1 shows 0.5-24 h uptake tumor data for each cell line inductor. The optimal time for activity concentration was observed between 1 h to 3 h for the three cell lines. The total number of disintegrations N in the source organs is shown in *Table IV*.

The back bearing induced human breast cancer tumor showed the highest uptake (6.15%). A dorsal SPECT image of one representative athymic mouse 3 h after injection is shown in *figure 2*.

DISCUSSION

For their growth cancer tumors require new blood vessel formation via angiogenic factors and one of these factors is the $\alpha_v \beta_3$ integrin. Besides alfa5 beta3 receptors the 3 tumors studied overexpress specific receptors: somatostatin in pancreatic cancer, cholecystokinin (CCK) in breast cancer and gastrin releasing peptide (GRP) in prostate cancer and the 3 tumors showed different degrees of radiopharmaceutical uptake which might be due to the differences in vasculature and to the amount of integrins present in the blood vessels regardless of other specific receptors.

As mentioned above, angiogenesis is a complex natural physiologic process that refers to the remodeling of the vascular tissue and it is characterized by the branching out of new blood vessels from preexisting vessels. Pathologic angiogenesis is found in cancer tumors and in several other pathologic entities. Angiogenesis can be imaged because of integrin targeting and uptake of radiopharmaceuticals. Early attempts using direct ^{99m}Tc labeling approaches were reported without showing specific *in vivo* uptake.[28,29] Other groups of researchers have reported indirect ^{99m}Tc labeling using HYNIC conjugated to peptide analogues.

Janssen et al. have compared the tumor targeting characteristics of a monomeric radiolabelled RGD-peptide with those of a dimeric analogue.[3] Both peptides were radiolabelled with ^{99m}Tc via HYNIC to form ^{99m}Tc-HYNIC-c(RGDfK) and ^{99m}Tc-HYNIC-E[c(RGDfK)]2. *In vitro*, the IC_{50} showed a 10-fold higher affinity of the dimer as compared to the monomer (0.1 *vs.* 1.0 nM). In athymic female BALB/c mice with subcutaneously growing OVCAR-3 ovarian car-

Table II. Tumor-to-organ ratios in an athymic mice model bearing induced tumors at different time intervals (0.5 to 24 h).

	Time p.i. (h)	AR42J (Pancreas)	MCF-7 (Breast)	PC-3 (Prostate)
Tumor/blood	0.5	0.71	1.20	1.80
	1	0.99	2.51	2.11
	3	6.93	5.19	3.61
	24	14.6	10.91	9.57
Tumor /muscle	0.5	2.51	2.73	2.44
	1	2.60	3.71	2.55
	3	6.51	5.03	3.61
	24	4.05	7.27	3.52

Table III. Statistical analysis of the tumor activity *vs* muscle activity for each induced tumor per time intervals (t-Student's test) n = 3 for each time.

AR42J	%IA/g tissue							
	0.5 h		1 h		3h		24 h	
	Muscle	Tumor	Muscle	Tumor	Muscle	Tumor	Muscle	Tumor
Mean	0.93	2.43	1.08	2.84	0.32	2.15	0.17	0.73
Variance	0.003	0.092	0.045	0.039	0.006	0.045	0.001	0.171
	t = 8.40		t = 8.58		t = 11.42		t = 2.66	
	p = 0.001		p = 0.013		p = 0.008		p = 0.037	
MCF7								
Mean	0.73	2.00	0.46	1.71	0.32	1.61	0.18	1.31
Variance	0.031	0.543	0.011	0.400	6.11E-4	0.201	4.0E-4	0.090
	t = 2.90		t = 3.36		t = 4.97		t = 6.47	
	p = 0.044		p = 0.028		p = 0.007		p = 0.003	
PC3								
Mean	0.65	1.59	0.58	1.48	0.34	1.23	0.19	0.67
Variance	0.002	0.151	0.006	0.054	0.005	0.127	0.004	0.001
	t = 4.57		t = 6.32		t = 4.25		t = 9.83	
	p = 0.019		p = 0.003		p = 0.013		p = 0.002	

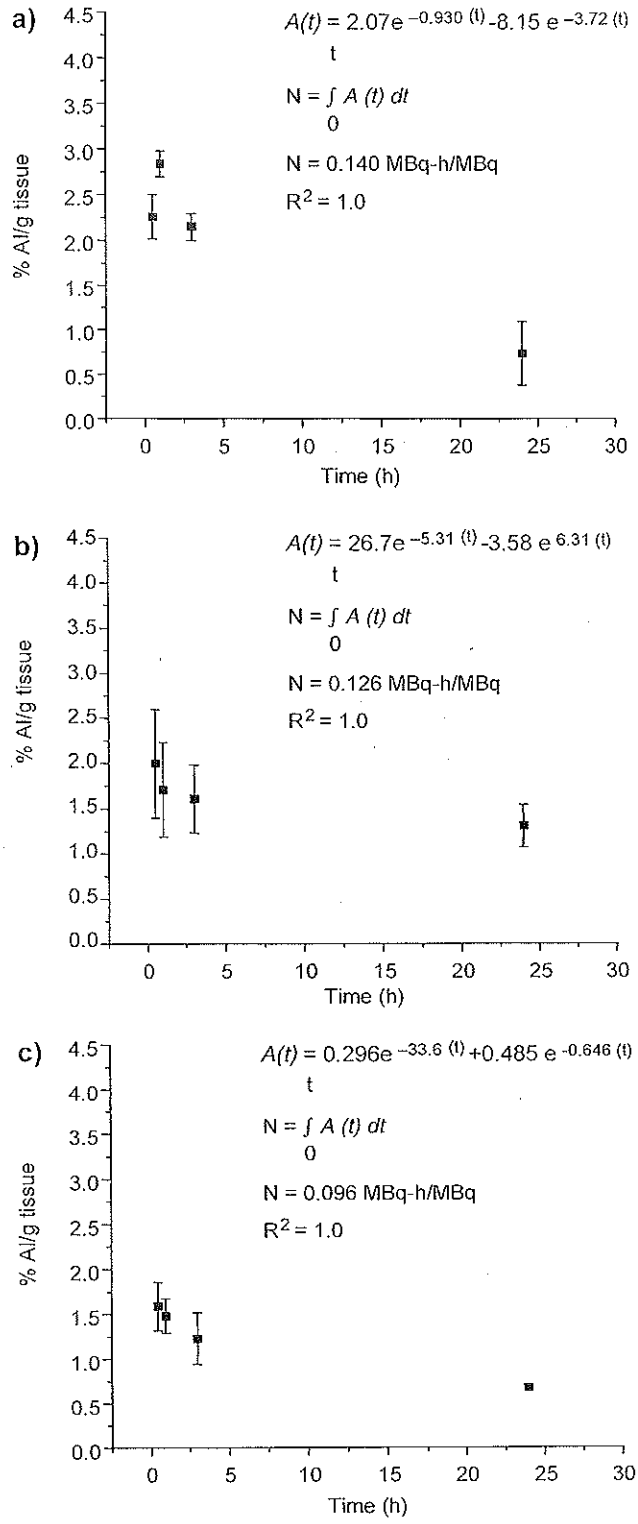

Figure 1. Biokinetics of ^{99m}Tc-cRGD in cancer tumors induced with cell lines a) AR42J (murine pancreas cancer); b) MCF-7 (human breast cancer) and c) PC-3 (human prostate) in 0.5 to 24 h.

Table IV. Total number of disintegrations (N) in the source organs of athymic mice with induced cancer tumors expressed per unit activity administered, (OLINDA/EXM).

	Total number of disintegrations (N) MBq-h/MBq Induced cancer tumor		
Organ	Pancreas	Breast	Prostate
Blood	0.061	0.040	0.030
Heart	0.030	0.037	0.031
Lung	0.074	0.061	0.057
Liver	0.181	0.193	0.015
Spleen	0.143	0.154	0.154
Pancreas	0.038	0.043	0.030
Kidneys	0.279	0.342	0.251
Intestine	0.211	0.255	0.244
Muscle	0.024	0.029	0.027
Bone	0.016	0.058	0.034
Tumor	0.140	0.126	0.096

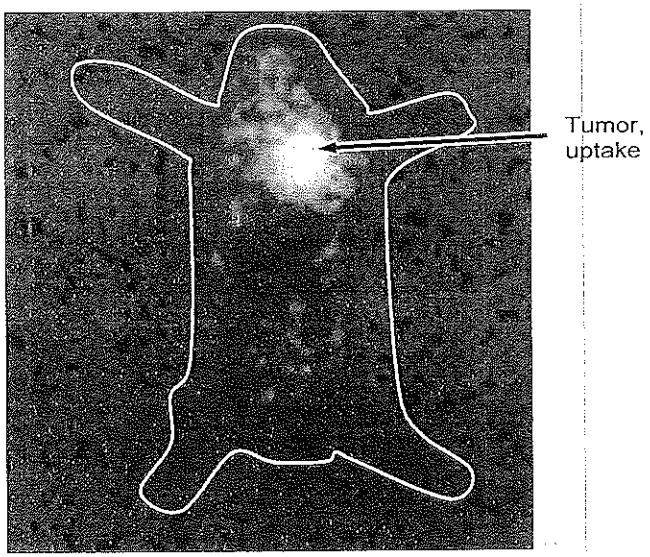

Figure 2. A selected image of an athymic mouse with induced tumor of human breast cancer 3 h after injection of ^{99m}Tc-cRGD was taken after dissection of internal viscera to highlight the tumor uptake (tumor/muscle ratio 6.15).

cinoma xenografts, the dimeric RGD peptide showed better retention in the tumor than the monomeric analogue, most likely due to the bivalent interaction with the target cell.

The cyclic HYNIC-derivatized monomeric RGD peptide [c(RGDyK(HYNIC)] was successfully ^{99m}Tc labeled using EDDA and tricine as coligands.[24]

Evaluation of radiolabeling of linear and cyclic RGD peptides was determined using a carbonil precursor $[^{99m}Tc(H_2O)_3(CO)_3]^+$ and the uptake of the

cRGDfK-His was higher than that with the linear peptide.[30]

^{99m}Tc-RGD has been used in many studies as a dimer or as a trimeric, tetrameric, octameric and multimeric molecules for imaging of tumor integrin $\alpha_v\beta_3$ expression, with good tumor uptake and favorable pharmacokinetics However all these peptides need to be synthetized.[3,11,14,31]

We used the commercial cyclic pentapeptide containing a phenylalanine amino acid (cyclic-Arg-Gly-Asp-D-Phe-Lys) which was conjugated with HYNIC and EDDA and tricine as coligands to form ^{99m}Tc-EDDA/HYNIC-cyclic-Arg-Gly-Asp-D-Phe-Lys (^{99m}Tc-cRGD).

Our research has led us to conclude that a highly stable, radiochemically pure, freeze dried kit can be ^{99m}Tc radio labeled in any hospital radiopharmacy. The ^{99m}Tc-cRGD targets $\alpha_v\beta_3$ integrin receptors in cancer tumor angiogenesis and allows noninvasive imaging of malignant tumors in a murine model. This could be a promising radiopharmaceutical for imaging cancer tumor angiogenesis in human beings.

The advantage of this lyophilized formulation of the cRGD peptide conjugated to HYNIC and with the added coligands EDDA and tricine over other reported formulations is that cRGD kit is easily labeled in one step with technetium-99m in any hospital radiopharmacy. The radiopharmaceutical ^{99m}Tc-cRGD targeted $\alpha_v\beta_3$ integrin receptors in athymic mice with 3 xenografted pancreas, breast and prostate cancer tumors and the tumor to muscle ratio are high allowing a better resolution of the tumor uptake over the muscle background in the SPECT image.

This non invasive nuclear medicine procedure demonstrated that ^{99m}Tc-cRGD will be of great value as a radiopharmaceutical for $\alpha_v\beta_3$ integrin receptor uptake and for imaging angiogenesis in neoplastic tissue.

ACKNOWLEDGMENTS

This study was supported by the CONACyT-Mexico 52633-M project.

Our gratitude to Jesús Sepúlveda-Méndez MD; Ma. Minerva Méndez-Fernández NMT; Ma. Guadalupe Soto-Gutiérrez NMT; Manuel Maury-Ruiz NMT; Armando Jiménez-Yedra NMT for obtaing the mice images.

REFERENCES

1. Carmeliet P, Jain RK. Angiogenesis in cancer and other diseases. *Nature*. 2000; 407: 249-57.
2. Haubner R. $\alpha_v\beta_3$-integrin imaging: a new approach to characterize angiogenesis? *Eur J Nucl Med Mol Imaging*. 2006; 33: 54-63.
3. Janssen M, Oyen WJ, Massuger LF, Frielink C, Dijkgraaf I, Edwards DS, et al. Comparison of a monomeric and dimeric radiolabeled RGD-peptide for tumor targeting. *Cancer Biother Radiopharm*. 2002; 17: 641-6.
4. Line BR, Mitra A, Nan A, Ghandehari H. Targeting tumor angiogenesis: Comparison of peptide and polymer-peptide conjugates. *J Nucl Med*. 2005; 40: 1552-60.
5. Felding-Habermann B, Mueller BM, Romerdahl CA, Cheresh DA. Involvement of integrin alphaV gene expression in human melanoma tumourigenicity. *J Clin Invest*. 1992; 89: 2018-22.
6. D'Andrea LD, Del Gatto A, Pedone C, Benedetti E. Peptide-based molecules in angiogenesis. *Chem Biol Drug Des*. 2006; 67: 115-26.
7. Kok RJ, Schraa AJ, Bos EJ, Moorlag HE, Asgeirsdóttir SA, Everts M, et al. Preparation and functional evaluation of RGD-modified proteins as alpha(v)beta(3) integrin directed therapeutics. *Bioconjug Chem*. 2002; 13: 128-35.
8. Haubner R, Wester HJ, Reuning U, Senekowitsch-Schmidtke R, Diefenbach B, Kessler H, et al. Radiolabeled alpha(v)beta$_3$ integrin antagonists: A new class of tracers for tumor targeting. *J Nucl Med*. 1999; 40: 1061-71.
9. Haubner R, Wester HJ. Radiolabed tracers for imaging of tumour angiogenesis and evaluation of anti-angiogenic therapies. *Curr Pharm Des*. 2004; 10: 1439-55.
10. Yoshimoto M, Ogawa K, Washiyama K, Shikano N, Mori H, Amano R, et al. Alpha(v)beta(3) Integrin-targeting radionuclide therapy and imaging with monomeric RGD peptide. *Int J Cancer*. 2008; 123: 709-15.
11. Li ZB, Chen K, Chen X. (68)Ga-labeled multimeric RGD peptides for microPET imaging of integrin alpha(v)beta (3) expression. *Eur J Nucl Med Mol Imaging*. 2008; 35: 1100-8.
12. Jeong JM, Hong MK, Chang YS, Lee YS, Kim YJ, Cheon GJ, et al. Preparation of a promising angiogenesis PET imaging agent: 68Ga-labeled c(RGDyK)-isothiocyanatobenzyl-1,4,7-triazacyclononane-1,4,7-triacetic acid and feasibility studies in mice. *J Nucl Med*. 2008; 49: 830-6.
13. Knight LC. *In handbook of radiopharmaceuticals*; Welch MJ, and Redvanly CS, eds. England: John Wiley & Sons; 2003. p. 643-84.
14. Li ZB, Cai W, Cao Q, Chen K, Wu Z, He L, et al. 64Cu-Labeled tetrameric and octameric RGD peptides for small-animal PET of tumor $\alpha_v\beta_3$ integrin expression. *J Nucl Med*. 2007; 48: 1162-71
15. Haubner R, Weber WA, Beer AJ, Vabuliene E, Reim D, Sarbia M, et al. Noninvasive visualization of the activated $\alpha_v\beta_3$ integrin in cancer patients by positron emission tomography and [18F]galacto-RGD. *PLoS Med*. 2005; 2: 29.
16. Zhang X, Xiong Z, Wu Y, Cai W, Tseng JR, Gambhir SS, et al. Quantitative PET imaging of tumor integrin $\alpha_v\beta_3$ expression with ^{18}F-FRGD2. *J Nucl Med*. 2006; 47: 113-21.
17. Li ZB, Wu Z, Chen K, Ryu EK, Chen X. 18F-labeled BBN-RGD heterodimer for prostate cancer imaging. *J Nucl Med*. 2008; 49: 453-61.
18. Glaser M, Morrison M, Solbakken M, Arukwe J, Karlsen H, Wiggen U, et al. Radiosynthesis and biodistribution of cyclic RGD peptides conjugated with novel [18F]fluorinated aldehyde-containing prosthetic groups. *Bioconjug Chem*. 2008; 19: 951-7.
19. Wu Z, Li ZB, Chen K, Cai W, He L, Chin FT, et al. Micro-PET of tumor integrin alpha-beta3 expression using 18F-

labeled PEGylated tetrameric RGD peptide (18F-FPRGD4). *J Nucl Med.* 2007; 48: 1536-44.
20. Liu S, Edwards DS. 99mTc-Labeled small peptides as diagnostic radiopharmaceuticals. *Chem Rev.* 1999; 99: 2235-68.
21. Bock M, Bruchertseifer F, Haubner R, Senekowitsch-Schmidtke R, Kessler H, Schwaiger M, et al. Tc-99m-, Re-188- and Y-90-labeled $\alpha_v \beta_3$ antagonists: promising tracer for tumor-induced angiogenesis. *J Nucl Med.* 2000; 41: 41P.
22. Su ZF, Liu G, Gupta S, Zhu Z, Rusckowski M, Hnatowich DJ. *In vitro* and *in vivo* evaluation of a technetium-99m-Labeled cyclic RGD peptide as a specific marker of $\alpha_v \beta_3$ integrin for tumor imaging. *Bioconjugate Chem.* 2002; 13: 561-70.
23. Liu S, Hsieh WY, Kim YS, Mohammed SI. Effect of coligands on biodistribution characteristics of ternary ligand 99mTc complexes of a HYNIC-conjugated cyclic RGDfK dimer. *Bioconjugate Chem.* 2005; 16: 1580-8.
24. Decristoforo C, Faintuch-Linkowski B, Rey A, von Guggenberg E, Rupprich M, Hernandez-Gonzales I, et al. [99mTc]HYNIC-RGD for imagin integrin $\alpha_v \beta_3$ expression. *Nucl Med Biol.* 2006; 33: 945-52.
25. Ferro-Flores G, Arteaga de Murphy C, Rodríguez-Cortés J, Pedraza-López M, Ramírez-Iglesias T. Preparation and evaluation of 99mTc-EDDA/HYNIC-[Lys^3]-Bombesin for imaging of gastrin-releasing peptide receptor-positive tumours. *Nucl Med Commun.* 2006; 27: 371-6.
26. Larrea F, García-Becerra R, Lemus AE, García GA, Pérez-Palacios G, Jackson KJ, et al. A-ring reduced metabolites of 19-nor synthetic progestins as subtype selective agonists for ERa. *Endocrinology.* 2001; 142: 3791-9.
27. Stabin MG, Sparks RB, Crowe E. OLINDA/EXM: The second-generation personal computer software for internal dose assessment in nuclear medicine. *J Nucl Med.* 2005; 46: 1023-7.
28. Sivolapenko GB, Skarlos D, Pectasides D, Stathopoulou E, Milonakis A, Sirmalis G, et al. Related imaging of metastatic melanoma utilizing a technetium-99m labelled RGD-containing synthetic pepetide. *Eur J Nucl Med.* 1998; 25: 1383-9.
29. Noiri E, Goligorsky MS, Wang GJ, Wang J, Cabahug CJ, Sharma S, et al. Biodistribution and clearance of 99mTc-labeled Arg-Gly-Asp(RGD) peptide in rats with ischemic acute renal failure. *J Am Soc Nephrol.* 1996; 7: 2682-8.
30. Fani M, Psimadas D, Zikos C, Xanthopoulos S, Loudos GK, Bouziotis P, et al. Comparative evaluation of linear and cyclic 99mTc-RGD peptides for targeting of integrins in tumor angiogenesis. *Anticancer Res.* 2006; 26: 431-4.
31. Chen X, Sievers E, Hou Y, Park R, Tohme M, Bart R, et al. Integrin $\alpha_v \beta_3$-Targeted Imaging of Lung Cancer. *Neoplasia.* 2005; 7: 271-9.

UNIVERSIDAD AUTONOMA DEL ESTADO DE MEXICO

INSTITUTO NACIONAL DE INVESTIGACIONES NUCLEARES

ININ

FACULTAD DE MEDICINA

ESTUDIO BIOCINETICO DEL $|^{99m}Tc|$-Lys-D-PHE-RGD en un Modelo Murino: Comparación con el $|^{99m}Tc|$-HYNIC-TOC y $|^{99m}Tc|$-HYNIC-BN

T E S I S

QUE PARA OBTENER EL GRADO DE

MAESTRO EN CIENCIAS CON ESPECIALIDAD EN FÍSICA MÉDICA

P R E S E N T A

FRED ALONSO LÓPEZ DURÁN

Director de Tesis: **Dra. Martha Pedraza López**

Revisores:

TOLUCA, MÉXICO AGOSTO 2009

Nuclear Medicine and Biology 42 (2015) 109–114

Contents lists available at ScienceDirect

Nuclear Medicine and Biology

journal homepage: www.elsevier.com/locate/nucmedbio

Preparation and preclinical evaluation of ^{66}Ga-DOTA-E(c(RGDfK))$_2$ as a potential theranostic radiopharmaceutical

V. Lopez-Rodriguez [a], R.E. Gaspar-Carcamo [a], M. Pedraza-Lopez [b], E.L. Rojas-Calderon [c], C. Arteaga de Murphy [b], G. Ferro-Flores [c], M.A. Avila-Rodriguez [a,*]

[a] Unidad PET, Facultad de Medicina, Universidad Nacional Autónoma de México, México, D.F., Mexico
[b] Instituto Nacional de Ciencias Médicas y Nutrición Salvador Zubirán, México, D.F., Mexico
[c] Instituto Nacional de Investigaciones Nucleares, Estado de México, Mexico

ARTICLE INFO

Article history:
Received 28 August 2014
Received in revised form 26 September 2014
Accepted 30 September 2014

Keywords:
Gallium-66
RGD peptides
Integrin $\alpha_v\beta_3$
Angiogenesis
Theranostics
PET imaging

ABSTRACT

Introduction: Integrin $\alpha_v\beta_3$ plays an important role in angiogenesis and is over-expressed in tumoral endothelial cells and some other tumor cells. RGD (Arg-Gly-Asn) peptides labeled with ^{68}Ga ($t_{1/2}$ = 68 min) have showed good characteristics for imaging of $\alpha_v\beta_3$ expression using positron emission tomography (PET). Gallium-66 has been proposed as a PET imaging alternative to ^{68}Ga and given the unique high energy of its emitted positrons (E_{max} 4.15 MeV) it may also be useful for therapy. The aim of this research is to prepare [^{66}Ga]DOTA-E-[c(RGDfK)]$_2$ and evaluate in mice its potential as a new theranostic radiopharmaceutical.

Methods: High specific activity ^{66}Ga was produced via the ^{66}Zn(p,n) reaction, and the labelling method of DOTA-E-[c(RGDfK)]$_2$ with ^{66}Ga was optimized. Radiochemical purity was determined by TLC, and *in vitro* stability and protein binding were determined. Serial microPET imaging and biodistribution studies were carried out in nude mice bearing C6 xenografts. Radiation absorbed dose estimates were based on the biodistribution studies, where tumor and organs of interest were collected at 0.5, 1, 3, 5 and 24 h post-injection of [^{66}Ga]DOTA-E-[c(RGDfK)]$_2$.

Results: Our results have shown that [^{66}Ga]DOTA-E-[c(RGDfK)]$_2$ can be prepared with high radiochemical purity (>97%), specific activity (36–67 GBq/μmol), *in vitro* stability, and moderate protein binding. MicroPET imaging up to 24 post-injection showed contrasting tumors reflecting $\alpha_v\beta_3$-targeted tracer accumulation. Biodistribution studies and dosimetry estimations showed a stable tumor uptake, rapid blood clearance, and favorable tumor-to-tissue ratios.

Conclusions: The peptide conjugated DOTA-E-[c(RGDfK)]$_2$ labeled with ^{66}Ga may be attractive as a theranostic agent for tumors over-expressing $\alpha_v\beta_3$ integrins.

1. Introduction

During the past three decades, several radiopharmaceuticals have been developed for the early diagnosis of cancer through the use of novel molecular targets and predictive biomarkers, especially those aberrantly overexpressed in biological malignancy, invasiveness, metastasis and apoptosis [1–5].

It has been shown that peptides based on the Arg-Gly-Asp (RGD) amino acid sequence have a high affinity and selectivity for $\alpha_v\beta_3$ integrin receptors; specifically, it was found that cyclic analogues of RGD containing 5 amino acids (RGD sequence + a hydrophobic amino acid in position 4 + an additional amino acid in position 5) have the highest $\alpha_v\beta_3$ binding affinities [6,7]. Alpha(V)beta(3) integrin receptors are over expressed on endothelial cells during blood vessel formation affecting tumor growth, invasiveness and metastatic potential, and are therefore potential targets for receptor-mediated tumor imaging and therapy.

New approaches have been addressed in order to improve, with various ligands, the affinity of RGD. Due to the natural mode of interaction between $\alpha_v\beta_3$ and peptides containing the amino acid sequence RDG that may involve multivalent binding sites, the use of multivalent cyclic RGD peptides could improve the binding affinity and tumor uptake. Several research groups have compared the cyclic RGDfK monomer, dimer (E-[c(RGDfK)]$_2$) and tetramer (E-[c(RGDfK)]$_4$) as targeting biomolecule for diagnostic and therapeutic applications [8–11]. The short distances between the cyclic RGD peptides in dimmers (~20 bond distance), make it unlikely simultaneous binding to the adjacent $\alpha_v\beta_3$ receptors. It has been proposed that the binding of one RGD motif to the integrin $\alpha_v\beta_3$ will significantly increase "local concentration" of the multivalent RGD motif in the vicinity of the receptor-binding site leading to an enhanced integrin $\alpha_v\beta_3$ binding rate or the reduced dissociation rate of the cyclic RDG peptide from the integrin $\alpha_v\beta_3$ [12]. This may explain the higher tumor uptake and longer tumor retention times of radiolabelled cyclic RGD tetramer and dimmer as compared

* Corresponding author at: Unidad PET, Facultad de Medicina, UNAM, Ciudad Universitaria, Delegación Coyoacán, México, D.F., C.P. 04510, Mexico. Tel.: +52 55 56232288; fax: +52 55 56232115.
E-mail address: avilarod@uwalumni.com (M.A. Avila-Rodriguez).

http://dx.doi.org/10.1016/j.nucmedbio.2014.09.010
0969-8051/

to their monomeric analogues [11–13]. The tetrameric RGD peptide labeled with ^{64}Cu ([^{64}Cu]DOTA-E{E-[c(RGDfK)]$_2$}$_2$), showed significantly higher receptor binding affinity than monomeric and dimeric RGD analogues, but demonstrated lower kidney clearance which may be related to the positively charge differences [14].

The positron emitting radionuclide ^{66}Ga ($t_{½}$ = 9.49 h, 56.5% β^+, 43.5% EC) has been proposed as a PET imaging alternative to ^{68}Ga. ^{66}Ga is of special interest because of its relative long half-life which makes it a suitable tracer for the study of long-term physiological processes and labeling of macromolecules with slow pharmacokinetics [15–17]. In addition, the most abundant positrons emitted by ^{66}Ga have a unique high energy (E_{max} 4.15 MeV, mean range 7.6 mm in tissue), which may also be useful for therapy [17].

At the intersection between treatment and diagnosis, interest has grown in combining both paradigms into clinically effective pharmaceuticals. This concept, recently named as theranostics, is highly relevant to agents that target molecular biomarkers of disease and is expected to contribute to personalized medicine [18].

The aim of this research was to prepare, characterize and perform the preclinical evaluation and dosimetry of [^{66}Ga]DOTA-Glu-[cyclo(Arg-Gly-Asp-D-Phe-Lys)]$_2$ ([^{66}Ga]DOTA-E-[c(RGDfK)]$_2$) in order to evaluate its potential as a theranostic radiopharmaceutical for molecular imaging diagnosis and targeted radiotherapy of $\alpha_v\beta_3$ over-expressing tumors.

2. Materials and methods

2.1. Reagents

All reagents used were TraceSelect grade, and water employed to prepare solutions was of Milli-Q grade (18 MΩ-cm) to ensure heavy metal-free aqueous solutions. Ultrapure HCl, HEPES and NH_4OAc (>99.999%) were purchased from Sigma-Aldrich (St. Louis, MO, USA). Cation exchange resin (AG50W-X4, 100–200 mesh) was purchased from BioRad (Hercules, CA, USA). Isotopically enriched ^{66}Zn (98.72 %) was obtained from Isoflex (San Francisco, CA, USA). DOTA-E-[c(RGDfK)]$_2$ was purchased from ABX advanced biomedical compounds GmbH (Radeberg, Germany), and centrifugal filters (cellulose, 30,000 MW cut off) and Millex-GV syringe filters (0.22 μm, PVDF, 33 mm) were obtained from Millipore (Bedford, MA, USA).

2.2. Cell lines and animal model

C6 rat glioma cell line was purchased from the American Type Culture Collection (ATCCW CCL-107, Rockville, USA). The cells were grown in RPMI 1640 medium (Invitrogen, USA) supplemented with 10% fetal bovine serum and antibiotics (100 mg/ml streptomycin) and incubated at 37 °C in an atmosphere with 5% CO_2.

Experimental animals were handled observing the technical specifications for the production, care and use of laboratory animals stated in the Official Mexican Norm NOM 0062-ZOO-1999. Studies with mice in this specific work were performed according to protocols approved by the Research and Ethics Committee of the Faculty of Medicine, at the National Autonomous University of Mexico (UNAM).

Female athymic Balb-C nu/nu mice (20–25 g) were supplied by the National Institute of Medical Sciences and Nutrition Salvador Zubiran (INCMNSZ), Mexico City, Mexico. All animals were kept in a pathogen free environment and fed *ad lib.*

C6 xenografts were induced by subcutaneous injection of 1×10^6 cells resuspended in 0.1 ml of phosphate buffered saline, in the dorsal surface of the scapula. The sites of injection were observed at regular intervals for the appearance of tumor formation and progression, and mice were used for *in vivo* experiments when the diameter of tumor reached about 0.5 cm.

2.3. Gallium-66 production

Gallium-66 was produced in a Siemens Eclipse HP cyclotron via the ^{66}Zn (p,n) ^{66}Ga reaction with 11 MeV protons as previously described by Engle et al. [19]. Briefly, ^{66}Zn was electrodeposited on Au backing and then irradiated for 10 to 20 min at a beam current of 10 to 20 μA. Radiochemical separation was performed by ion exchange chromatography using AG 50 W X-4 resin. The reactivity or effective specific activity of ^{66}Ga was determined by titration of [^{66}Ga]$GaCl_3$ with DOTA (1,4,7,10-Tetraazacyclododecane-1,4,7,10-tetraaceic acid).

2.4. Preparation of [^{66}Ga]DOTA-E-[c(RGDfK)]$_2$

For radiolabelling of DOTA-E-[c(RGDfK)]$_2$, 25 μl of the conjugated peptide solution (400 μg/ml, 1% EtOH), 25 μl 1.0 M HEPES (pH 7.0), and 25 μl 0.25 M NH_4OAc (pH 5.5), were mixed with 200–370 MBq of ^{66}Ga stock solution (50 μl 0.1 M HCl) and incubated for 20 min at 95 °C in a compact thermomixer (Eppendorf, USA) at 300 rpm [12]. When needed, purification of the final product was performed by SPE using Sep-Pak C18 Light cartridges. The final product was sterilized by passing through a 0.22 μm syringe filter (Millex-GV). The structural formula of [^{66}Ga]DOTA-E-[c(RGDfK)]$_2$ is shown in Fig. 1 [20].

2.5. Radiochemical purity

The radiochemical purity (RCP) was determined by thin layer chromatography (TLC) using silica gel (SG) strips as stationary phase and 1:1 MeOH:10% NH_4OAc (w/v) as mobile phase [21]. Evaluation of the TLC plates was performed by autoradiography in a Cyclone Plus Storage Phosphor System (Perkin Elmer).

2.6. In vitro stability

To determine the *in vitro* stability of [^{66}Ga]DOTA-E-[c(RGDfK)]$_2$ in physiological saline and serum, an aliquot (50 μl) of the labelled compound solution was incubated at 37 °C with 1 ml of 0.9% NaCl and fresh human serum. Radiochemical purity stability was evaluated up to 24 h by TLC-SG as described above.

2.7. Protein binding

To determine serum protein binding of [^{66}Ga]DOTA-E-[c(RGDfK)]$_2$, and aliquot of the labeled compound (100 μl) was incubated at 37 °C with 1 ml of fresh human serum up to 4 hours. After incubation the solution was analyzed by ultrafiltration (30,000 MW). Protein binding was determined by measuring the activity remaining in the filter, while the unbound [^{66}Ga]DOTA-E-[c(RGDfK)]$_2$ passed through the filter.

2.8. MicroPET imaging

Mice bearing glioma C6 tumors were scanned after a tail vein injection of 20 ± 0.5 MBq of [^{66}Ga]DOTA-E[c(RGDfK)]$_2$ under isoflourane anesthesia (1–3%). PET images were acquired in a MicroPET Focus 120 (Concorde Microsystems, Knoxville, TN, USA) at different post injection (p.i.) times (0.5, 1, 3, 5 and 24 h). Scan time was 20 min for images acquired at 0.5, 1, and 3 h p.i., 30 min for images acquired 5 h p.i., and 60 min for images acquired at 24 h. After PET acquisitions animals were sacrificed to perform the biodistribution studies. MicroPET images were reconstructed using a 3-D ordered subset expectation maximization (OSEM 3D) algorithm.

2.9. Biodistribution studies

After PET imaging acquisitions, animals were sacrificed by cervical dislocation at 0.5, 1, 3, 5, and 24 h p.i. (n = 3 per time point), and tissues

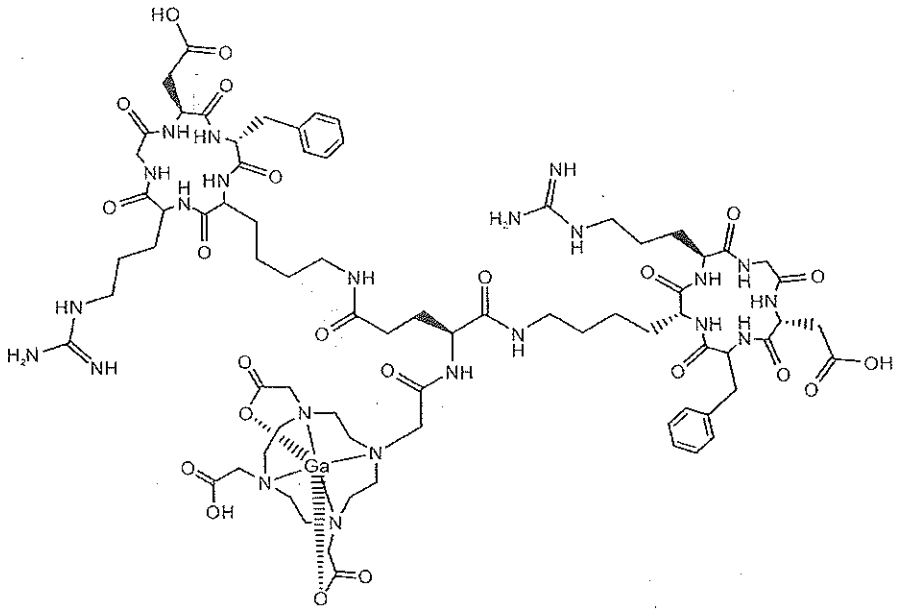

Fig. 1. Structural formula of the DOTA conjugated dimeric-RGD peptide labeled with Ga isotope [20].

of interest (blood, brain, heart, lungs, liver, spleen, blander, kidneys, bowel, muscle, femur and tumor) were removed immediately and

The labeling yield of [^{66}Ga]DOTA-E-[c(RGDfK)]$_2$ was almost quantitative using 5.5 nmol of the conjugated peptide. It was observed that a

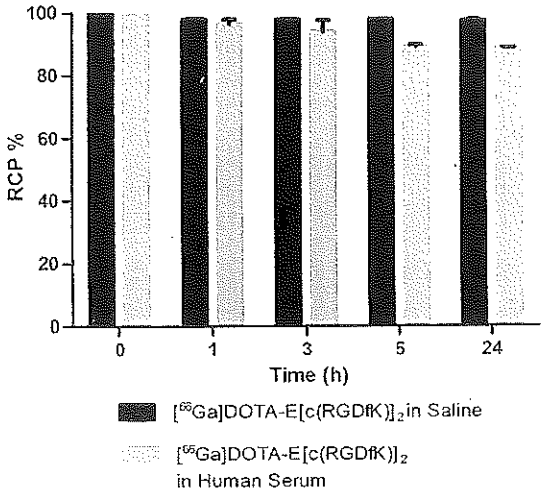

Fig. 3. Stability studies showed high stability of $[^{66}Ga]$DOTA-E-$[c(RGDfK)]_2$ up to 24 h in human serum and phisiological saline.

clearance from blood and kidneys and high uptake in the liver and spleen, which was consistent with biodistribution data.

Biodistribution data (%ID/g and %ID/organ) of $[^{66}Ga]$DOTA-E-$[c(RGDfK)]_2$ are shown in Fig. 5. High uptake was observed in organs such as liver, kidneys, lung, spleen, heart, bladder, and muscle at early times, but significantly decreased at 5 h p.i. Rapid blood clearance was also observed, reaching a blood uptake of only 2.81 ± 0.32 %ID/g at 1 h p.i. Uptake of $[^{66}Ga]$DOTA-E-$[c(RGDfK)]_2$ by the C6 tumor xenograft indicated stable retention of the tracer with minimal wash-out up to 24 h. Tumor-to-muscle ratios (% ID/g) were 1.40 ± 0.97 and 1.78 ± 0.57 at 0.5 h and 24 h p.i., respectively, while tumor-to-blood ratio was 0.20 ± 0.09 at 0.5 h, increasing to 1.97 ± 0.37 at 24 h p.i.

Fig. 6 shows the radiation absorbed doses normalized to unit injected activity (mGy/MBq) and the tumor-to-tissue absorbed dose ratios. As expected, the highest radiation absorbed dose was deposited in the tumor (65.53 ± 8.39 mGy/MBq), followed by the liver (48.06 ± 17.01), kidneys (32.72 ± 4.42), and spleen (27.2 ± 7.29). The biological residence time for the C6 glioma tumors was 5.57 h.

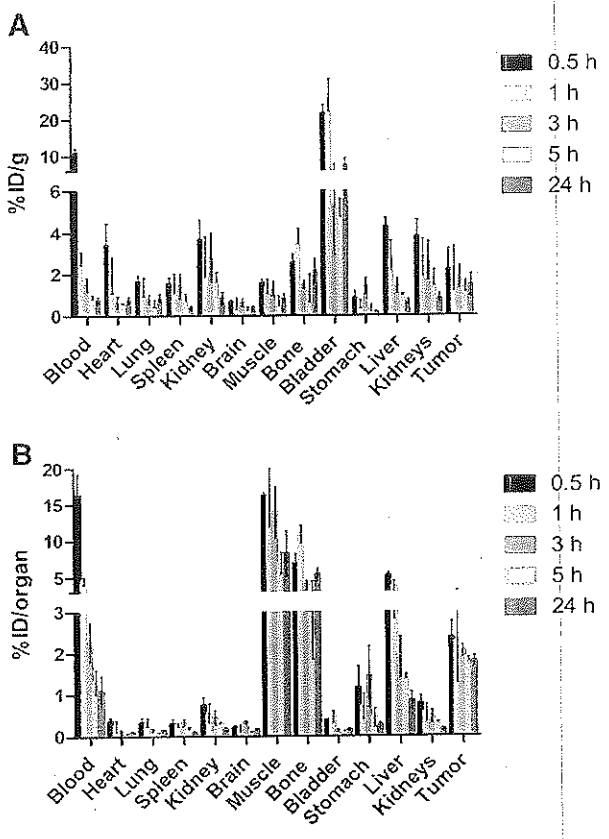

Fig. 5. Biodistribution data for $[^{66}Ga]$DOTA-E-$[c(RGDfK)]_2$ in mice 0.5, 1, 3, 5 and 24 h p.i. Results are shown as A) %ID/g (mean ± SD) and B) %ID/organ (mean ± SD).

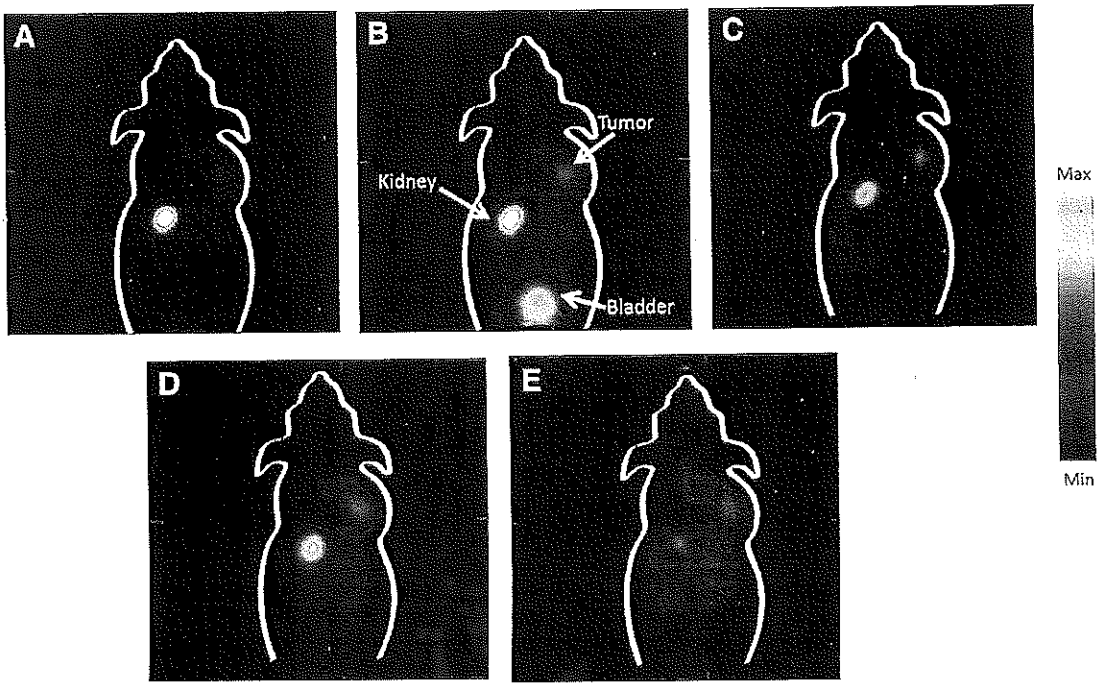

Fig. 4. Coronal microPET images of $[^{66}Ga]$DOTA-E-$[c(RGDfK)]_2$ in nude mice bearing C6 tumor xenograft at 0.5 h (A), 1 h (B), 3 h (C), 5 h (D) and 24 h (C) after injection of 20 ± 0.5 MBq of tracer under isoflourane anesthesia. Acquisition time was 20 min for A,B, and C); 30 min for D, and 60 min for E.

A

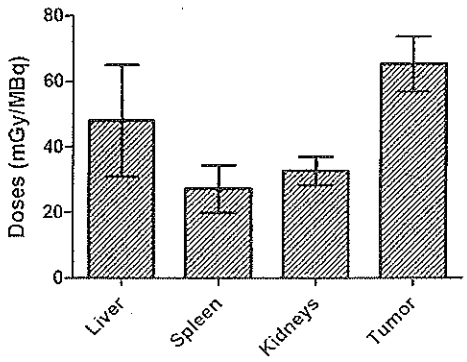

B

Tissue	Tumor to tissue absorbed dose ratio
Liver	1.36
Spleen	2.41
Kidneys	2.01
Tumor	1

Fig. 6. A)Estimated radiation absorbed doses normalized to unit injected activity and B) tumor-to-tissue absorbed dose ratios of [^{66}Ga]DOTA-E-[c(RGDfK)]$_2$ in nude mice bearing C6 tumor xenograft.

4. Discussion

During the past few years different multivalent cyclic RGD peptide conjugates have been used to target tumors over-expressing $\alpha_v\beta_3$ integrin receptors [25–39]; however, it has been demonstrated that the dimeric conjugate is more suitable for both, imaging and therapeutic applications. Li et al. [34] showed that despite the fact that the tetrameric peptide conjugate labeled with ^{68}Ga had the highest tumor uptake, its poor tumor-to-kidney ratio makes this compound less useful than the dimeric and monomeric counterparts. It was also found that the dimeric and monomeric peptide had similar tumor-to-kidney ratios but the dimer had higher tumor uptake and a prolonged retention time, making it more suitable than the monomer. On the other hand, Luna-Gutierrez et al. [25] investigated the potential of ^{177}Lu-labeled monomeric and dimeric cyclic RGD peptides ([c(RGDfK)]$_n$) for the treatment of tumors over-expressing $\alpha_v\beta_3$ integrins. *In vivo* evaluation in a mouse U87MG xenograft model showed that [^{177}Lu]DOTA-E-[c(RGDfK)]$_2$ had a higher uptake in tumor and a higher tumor-to-kidney ratio than [^{177}Lu]DOTA-E-c(RGDfK), making the dimer more suitable than the monomer for therapeutic applications.

In this light we evaluated the dimeric conjugated DOTA-E-[c(RGDfK)]$_2$ labeled with ^{66}Ga to target tumors over expressing $\alpha_v\beta_3$ integrin receptors. The glioma cell line used in this research was the C6 which is known to have a high tumor density of integrin $\alpha_v\beta_3$ receptors on the surface (1.51×10^{11} number of receptors/mg protein) [28], making this cell line a good candidate to evaluate theranostic applications with peptides containing the amino acid sequence RDG, labeled with the appropriate radionuclide. For imaging purposes, ^{68}Ga had shown to be a suitable radionuclide as it can be easily obtained from a ^{68}Ge/^{68}Ga generator [29–32], while for therapeutic applications the beta emitter ^{177}Lu is promising [34–37]. However, due to its decay scheme and the unique high energy of emitted positrons, ^{66}Ga has the potential to serve a dual role in the development of agents for PET-molecular imaging and radioimmunotherapy drugs for oncology. Additionally, high specific activity ^{66}Ga, in enough quantity and quality for clinical applications, can be efficiently produced in compact biomedical cyclotrons using enriched target material, which is relatively inexpensive (~2–3 USA dll/mg, ^{66}Zn > 99%) [19].

The most important feature of targeted radionuclide therapy is to deliver a tumoricidal dose for tumor ablation, without compromising other vital organs [38]. The [^{66}Ga]DOTA-E-[c(RGDfK)]$_2$ evaluated in this research showed good pharmacokinetic characteristics with a relatively stable tumor uptake and a rapid blood clearance. Dosimetry estimations from our biodistribution data showed that critical organs such as liver, kidneys, and spleen can receive a considerable radiation dose per unit injected activity, but in all cases the dose was lower than the one received by the tumor. Of particular interest in this research was to determine the tumor-to-tissue ratios that better define tumor targeting properties.

The 65 mGy/MBq radiation absorbed dose normalized to unit injected activity determined in this research for [^{66}Ga]DOTA-E-[c(RGDfK)]$_2$ in C6 tumors was significantly lower than the 230 mGy/MBq reported by Luna-Gutierrez et al. [25] for [^{177}Lu]DOTA-E-[c(RGDfK)]$_2$ in U87MG tumors; however, the tumor-to-tissue ratios reported in both cases are very similar. Note that for comparison purposes the higher density of integrin $\alpha_v\beta_3$ receptors on the surface of U87MG *vs.* C6 cells [28] is compensated in some way by the higher specific activity of ^{177}Lu *vs.* ^{66}Ga [25]. These results suggest that [^{66}Ga]DOTA-E-[c(RGDfK)]$_2$ possesses potential for targeted radionuclide therapy of tumors over expressing integrin $\alpha_v\beta_3$ receptors. Additionally, we had shown that, despite the high energy positrons emitted by ^{66}Ga, it is possible to get good quality microPET-images.

Since [^{66}Ga]DOTA-E-[c(RGDfK)]$_2$ combines imaging and radiotherapy in one preparation, it could be useful as a theranostic radiopharmaceutical for tumors over-expressing $\alpha_v\beta_3$ integrins. To plan a diagnosis/treatment scheme for an individual patient, the diagnosis and prospective radiation absorbed dose estimates could be made by administering a tracer activity of the radiopharmaceutical and subsequently the larger therapeutic activity. The quantitative patient-specific dosimetry work-up using a diagnostic dose before the therapeutic dose would be useful to identify cancer patients for whom the treatment is most likely to be effective, eliminating those patients for whom it would be unsuccessful ("personalized medicine"). In agreement with other radionuclide therapy protocols, positively charged amino acids could be coinfused to reduce the radiopeptide kidney retention considering that the maximum tolerated dose (MTD) for kidney is 25 Gy, while for spleen and liver the MTD value is almost twice [39].

5. Conclusions

To summarize, ^{66}Ga labeled DOTA-E-[c(RGDfK)]$_2$ was prepared with high yield, specific activity and radiochemical purity. The microPET imaging and biodistribution studies showed high affinity for the $\alpha_v\beta_3$ integrin receptors, with rapid blood clearance; and the radiation absorbed dose estimation suggested sub-toxic doses to critical organs. These results support the idea that [^{66}Ga]DOTA-E-[c(RGDfK)]$_2$ may be attractive as a theranostic agent for tumors over-expressing $\alpha_v\beta_3$ integrins.

Acknowledgements

We are grateful to A. Zarate-Morales and A. Flores-Moreno for cyclotron irradiations and to V.M. Lara-Camacho and M. Avila-Garcia for microPET imaging. This research was supported by CONACYT Grant

179218, UNAM-DGAPA-PAPIIT TA200512 and the International Atomic Energy Agency RC16467.

References

[1] Kai C, Conti PS. Target-specific delivery of peptide-based probes for PET imaging. Adv Drug Deliv Rev 2010;62:1005–22.

[2] Tolmachev V, Stone-Elander S. Radiolabelled proteins for positron emission tomography: pros and cons of labelling methods. Biochim Biophys Acta 1800;2010: 487–510.

[3] Lee S, Xie J, Chen X. Peptides and peptide hormones for molecular imaging and disease diagnosis. Chem Rev 2010;110:3087–111.

[4] Schottelius M, Wester HJ. Molecular imaging targeting peptide receptors. Methods 2009;48:161–77.

[5] Kaur S, Venktaraman G, Jain M, Senapati S, Garg PK, Batra SK. Recent trends in antibody-based oncologic imaging. Cancer Lett 2012;315:97–111.

[6] Plow EF, Haas TA, Zhang L, Loftusi J, Smith JW. Ligand binding to integrins. J Biol Chem 2000;275:21785–8.

[7] Gurrath M, Muller G, Kessler H, Aumailley M, Timpl R. Conformation/activity studies of rationally designed potent anti-adhesive RGD peptides. Eur J Biochem 1992;210: 911–21.

[8] Barrett JA, Croker AC, Onthank DC, Heminway S, Rajopadhye M, Liu S, et al. RP593 a ^{99m}Tc-labeled $\alpha_v\beta_3/\alpha_v\beta_5$ antagonist, rapidly detects spontaneous tumors in mice and dogs. Nucl Med Commun 2000;21:564.

[9] Janssen ML, Oyen WJ, Dijkgraaf I, Massuger LF, Frielink C, Edwards DS, et al. Tumor targeting with radiolabeled alpha(v)beta(3) integrin binding peptides in a nude mouse model. Cancer Res 2002;62:6146–51.

[10] Janssen ML, Oyen WJ, Massuger LF, Frielink C, Dijkgraaf I, Edwards DS, et al. Comparison of a monomeric and dimeric radiolabeled RGD-peptide for tumor targeting. Cancer Biother Radiopharm 2002;17:641–6.

[11] Janssen ML, Frielink C, Dijkgraaf I, Oyen WJ, Edwards DS, Liu S, et al. Improved tumor targeting of radiolabeled RGD peptides using rapid dose fractionation. Cancer Biother Radiopharm 2004;19:399–404.

[12] Dijkgraaf I, Yim C-B, Franssen MG, Schuit CR, Luurtsema G, et al. PET imaging of αvβ3 integrin expression in tumours with ^{68}Ga-labelled mono-, di- and tetrameric RGD peptides. Eur J Nucl Med Mol Imaging 2011;38:128–37.

[13] Chen X, Liu S, Hou Y, Tohme M, Park R, Bading JR, et al. MicroPET imaging of breast cancer alphav-integrin expression with ^{64}Cu-labeled dimeric RGD péptidos. Mol Imaging Biol 2004;6:350–9.

[14] Wu Y, Zhang X, Xiong Z, Cheng Z, Fisher DR, Liu S, et al. microPET imaging of glioma integrin αvβ3 expression using ^{64}Cu-labeled tetrameric RGD peptide. J Nucl Med 2005;46:1707–18.

[15] Lewis MR, Reichert DE, Laforest R, Margenau WH, Shefer RE, Klinkowstein RE, et al. Production and purification of gallium-66 for preparation of tumor-targeting radiopharmaceuticals. Nucl Med Biol 2002;29:701–6.

[16] Graham MC, Pentlow KS, Mawlawi O, Finn RD, Daghighian F, Larson SM. An investigation of the physical characteristics of ^{66}Ga as an isotope for PET imaging and quantification. Med Phys 1997;24:317–26.

[17] Ugur Ömer, Kothari Paresh J, Finn Ronald D, Zanzonico Pat, Ruan Shutian, Guenther Ilonka, et al. Ga-66 labeled somatostatin analogue DOTA-DPhe^1-Tyr^3-octreotide as a potential agent for positron emission tomography imaging and receptor mediated internal radiotherapy of somatostatin receptor positive tumors. Nucl Med Biol 2002;29:147–57.

[18] Janib SM, Moses AS, MacKay JA. Imaging and drug delivery using theranostic nanoparticles. Adv Drug Deliv Rev 2010;62:1052–63.

[19] Engle JW, Lopez Rodriguez V, Gaspar Carcamo RE, Valdovinos HF, Valle Gonzalez M, Trejo Ballado F, et al. Very high specific activity $^{66/68}$Ga from zinc targets for PET. Appl Radiat Isot 2012;70:1792–6.

[20] Kubíček Vojtěch, Havlíčkova Jana, Kotek Jan, Tircsó Gyula, Hermann Pert, Tóth Éva, et al. Gallium(III) complexes of DOTA and DOTA-monoamide: kinetic and thermodynamic studies. Inorg Chem 2010;49:10960–9.

[21] Karolin Pohle, Johannes Notni, Johanna Bussemer, Horst Kessler, Markus Schwaiger, Beer Ambros J. ^{68}Ga-NODAGA-RGD is a suitable substitute for ^{18} F-Galacto-RGD and can be produced with high specific activity in a cGMP/GRP compliant automated process. Nucl Med Biol 2012;39:777–84.

[22] Petty C. Research Techniques in the Rats. Springfield, IL: Charles C. Thomas; 1982.

[23] Frank DW. Physiological data of laboratory animals. Boca Raton, FL: CRC Press; 1976.

[24] Jimenez-Mancilla NP, Ferro-Flores G, Ocampo-García B, Luna-Gutiérrez M, Pedraza-Lopez M, Torres-Garcia E. Multifunctional targeted radiotherapy system for induced tumours expressing gastrin-releasing peptide receptor. Curr Nanosci 2012;8: 193–201.

[25] Luna-Gutiérrez M, Ferro-Flores G, Ocampo-García B, Jiménez-Mancilla NP, Morales-Avila E, De León Rodríguez LM, et al. ^{177}Lu-labeled monomeric, dimeric and multimeric RGD peptides for the therapy of tumors expressing α(v)β(3) integrins. J Labelled Comp Radiopharm 2012;50:140–8.

[26] Miller WH, Hartmann-Siantar C, Fisher D, Descalle MA, Daly T, Lehmann J, et al. Evaluation of beta-absorbed fraction in a mouse model for ^{90}Y, ^{188}Re, ^{166}Ho, ^{149}Pm, ^{64}Cu and ^{177}Lu radionuclides. Cancer Biother Radiopharm 2005;20:436–49.

[27] Stabin MG, Sparks RB, Crowe E. OLINDA/EXM: The second-generation personal computer software for internal dose assessment in nuclear medicine. J Nucl Med 2005: 46:1023–7.

[28] Zhang X, Xiong Z, Wu Y, Cai W, Tseng JR, Gambhir SS, et al. Quantitative PET imaging of tumor integrin αvβ3 expression with ^{18} F-FRGD$_2$. J Nucl Med 2006;47:113–21.

[29] Knetsch PA, Petrik M, Griessinger CM, Rangger C, Fani M, Kesenheimer C, et al. [^{68}Ga] NODAGA-RGD for imaging αvβ3 integrin expression. Eur J Nucl Med Mol Imaging 2011;38:1303–12.

[30] Knetsch PA, Petrik M, Rangger C, Seidel G, Pietzsch HJ, Virgolini I, et al. [68Ga]NS3-RGD and [68Ga] Oxo-DO3A-RGD for imaging $\alpha_v\beta_3$ integrin expression: synthesis, evaluation, and comparison. Nucl Med Biol 2013;40:65–72.

[31] Decristoforo C, Gonzalez Hernandez I, Carlsen J, Rupprich M, Huisman M, Virgolini I, et al. ^{68}Ga- and ^{111}In-labelled DOTA RGD peptides for imaging of $\alpha_v\beta_3$ integrin expression. Eur J Nucl Med Mol Imaging 2008;35:1507–15.

[32] Smith Daniel L, Breeman Wouter AP, Sims-Mourtada Jennifer. The untapped potential of Gallium68-PET:The next wave of ^{68}Ga-agents. Appl Radiat Isot 2013;76: 14–23.

[33] Oxboel Jytte, Brandt-Larsen Malene, Schjoeth-Eskesen Christina, Myschetzky Rebecca, El-Ali Henrik H, Madsen Jacob, et al. Comparison of two new angiogenesis PET tracers ^{68}Ga-NODAGA-E[c(RGDyK)]$_2$ and ^{64}Cu-NODAGA-E[c(RGDyK)]$_2$: in vivo imaging studies in human xenograft tumors. Nucl Med Biol 2014;41:259–67.

[34] Li ZB, Chen K, Chen X. ^{68}Ga-labeled multimeric RGD peptides for microPET imaging of integrin $\alpha_v\beta_3$ expression. Eur J Nucl Med Mol Imaging 2008;35:1100–8.

[35] Chakraborty S, Sarma HD, Vimalnath KV, Pillai MR. Tracer level radiochemistry to clinical dose preparation of ^{177}Lu-labeled cyclic RGD peptide dimer. Nucl Med Biol 2013;40:946–54.

[36] Jin-Hwan Kim, Jae-Cheong Lim, Ki-Cheol Yun, Sun-Ju Choi, Young-Don Hong. Preparation and preliminary biological evaluation of ^{177}Lu-labeled GluDTPA-cyclo (RGDfK) for integrin $\alpha_v\beta_3$ receptor-positive tumor targeting. J Labelled Comp Radiopharm 2012;55:10–7.

[37] Ju Chang Hwan, Jeong Jae Min, Lee Yun-Sang, Kim Young Joo, Lee Byung Chul, Lee Dong Soo, et al. Development of a ^{177}Lu-Labeled RGD derivative for targeting angiogenesis. Cancer Biother Radiopharm 2010;25:687–91.

[38] Fawwaz RA, Wang TS, Srivastava SC, Hardy MA. The use of radionuclides for tumor therapy. Int J Rad Appl Instrum B 1986;13:429–36.

[39] Zaknun J, Bodei L, Mueller-Brand J, Pavel ME, Baum RP, Hörsch D, et al. The joint IAEA, EANM, and SNMMI practical guidance on peptide receptor radionuclide therapy (PRRNT) in neuroendocrine tumours. Eur J Nucl Med Mol Imaging 2013;40: 800–16.

International Journal of Pharmaceutics 375 (2009) 75–83

Contents lists available at ScienceDirect

International Journal of Pharmaceutics

journal homepage: www.elsevier.com/locate/ijpharm

Design, preparation, *in vitro* and *in vivo* evaluation of ^{99m}Tc-N_2S_2-Tat(49–57)-bombesin: A target-specific hybrid radiopharmaceutical

Clara L. Santos-Cuevas[a,b], Guillermina Ferro-Flores[a,*], Consuelo Arteaga de Murphy[c], Flor de M. Ramírez[a], Myrna A. Luna-Gutiérrez[a,b], Martha Pedraza-López[c], Rocío García-Becerra[c], David Ordaz-Rosado[c]

[a] *Instituto Nacional de Investigaciones Nucleares, Mexico*
[b] *Universidad Autónoma del Estado de México, Mexico*
[c] *Instituto Nacional de Ciencias Médicas y Nutrición Salvador Zubirán, Mexico*

ARTICLE INFO

Article history:
Received 24 December 2008
Received in revised form 11 April 2009
Accepted 14 April 2009
Available online 22 April 2009

Keywords:
Radiolabeled bombesin
Hybrid radiopharmaceutical
Peptide-receptor imaging
Tat-bombesin

ABSTRACT

The gastrin-releasing peptide receptor (GRP-r) is over-expressed in various human tumors. Recently, ^{99m}Tc-EDDA/HYNIC-Lys^3-bombesin (^{99m}Tc-BN) was reported as a radiopharmaceutical with specific cell GRP-r binding and images in breast cancer patients demonstrated distinct radioactivity accumulation in malignant tissue. The HIV Tat-derived peptide has been used to deliver a large variety of cargoes into cells. Therefore, a new hybrid radiopharmaceutical of type ^{99m}Tc-N_2S_2-Tat(49–57)-Lys^3-bombesin (^{99m}Tc-Tat-BN) would increase cell uptake. The aim of this research was to prepare and assess *in vitro* and *in vivo* uptake kinetics in cancer cells of ^{99m}Tc-Tat-BN and to compare its cellular internalization with that of ^{99m}Tc-BN. Structures of N_2S_2-Tat-BN and Tc(O)N_2S_2-Tat-BN were calculated by an MM procedure. ^{99m}Tc-Tat-BN was synthesized and stability studies carried out by HPLC and ITLC-SG analyses in serum and cysteine solutions. *In vitro* internalization was tested using human prostate cancer PC-3 cells and breast carcinoma cell lines MDA-MB231 and MCF7. Biodistribution was determined in PC-3 tumor-bearing nude mice. Results showed a minimum energy of 271 kcal/mol for N_2S_2-Tat-BN and 300 kcal/mol for Tc(O)N_2S_2-Tat-BN. ^{99m}Tc-Tat-BN radiochemical purity was >90%. *In vitro* studies demonstrated stability in serum and cysteine solutions, specific cell receptor binding and internalization in three cell lines was significantly higher than that of ^{99m}Tc-BN ($p < 0.05$). The tumor-to-muscle radioactivity ratio was 8.5 for ^{99m}Tc-Tat-BN and 7 for ^{99m}Tc-BN. Therefore, this hybrid is potentially useful in breast and prostate cancer imaging.

1. Introduction

Molecular imaging is defined as the visualization, characterization and measurement of biological processes at the molecular and cellular levels in humans and other living systems (Thakur and Lentle, 2005). Cancer imaging techniques using radiotracers targeted to specific receptors have yielded successful results demonstrating the utility of such approaches for developing specific radiopharmaceuticals.

Regulatory peptide receptors are over-expressed in numerous human cancer cells. These receptors have been used as molecular targets for radiolabeled peptides to localize cancer tumors. The useful clinical results achieved during the last decade with somatostatin receptor-expressing neuroendocrine tumor imaging, have been extended to the study of other radiopeptides to target alternative cancer-associated peptide receptors such as gastrin-releasing peptide, cholecystokinin, peptide ligands for integrin receptors or neurotensin. The improvement of radiopeptide analogues allows specific clinical imaging of different tumor types, including breast, prostate, intestine, pancreas and brain tumors (Ferro-Flores et al., 2006a; de Visser and Verwijnen, 2008).

The bombesin (BN) peptide was isolated from frog skin and belongs to a large group of neuropeptides with many biological functions. The human equivalent is the gastrin-releasing peptide (GRP, 27 amino acids) and its receptors (GRP-r) are over-expressed in the tumor cell membrane in an early stage of carcinogenesis (Lui et al., 2003). GRP and BN differ by only 1 of 10 carboxy-terminal residues and this explains the similar biological activity of the two peptides (Reubi, 2003). The strong-specific BN–GRP-r binding is the basis for labeling BN with radionuclides (Baidoo et al., 1998; La Bella et al., 2002; Varvarigou et al., 2002; Smith et al., 2003; Faintuch et al., 2005; Nock et al., 2005; Lin et al., 2005; Alves et al., 2006; Zhang et al., 2006a; Garcia-Garayoa et al., 2007; Kunstler et al., 2007).

^{99m}Tc-EDDA/HYNIC-Lys^3-BN (^{99m}Tc-BN) obtained from lyophilized kit formulations has been reported as a radiopharma-

* Corresponding author at: Departamento de Materiales Radiactivos, Instituto Nacional de Investigaciones Nucleares, Carretera México-Toluca S/N, La Marquesa, Ocoyoacac, Estado de México, C.P. 52750, Mexico. Tel.: +52 55 53297200x3863; fax: +52 55 53297306.
E-mail addresses: ferro_flores@yahoo.com.mx, guillermina.ferro@inin.gob.mx (G. Ferro-Flores).

0378-5173/$ – see front matter © 2009 Elsevier B.V. All rights reserved.
doi:10.1016/j.ijpharm.2009.04.018

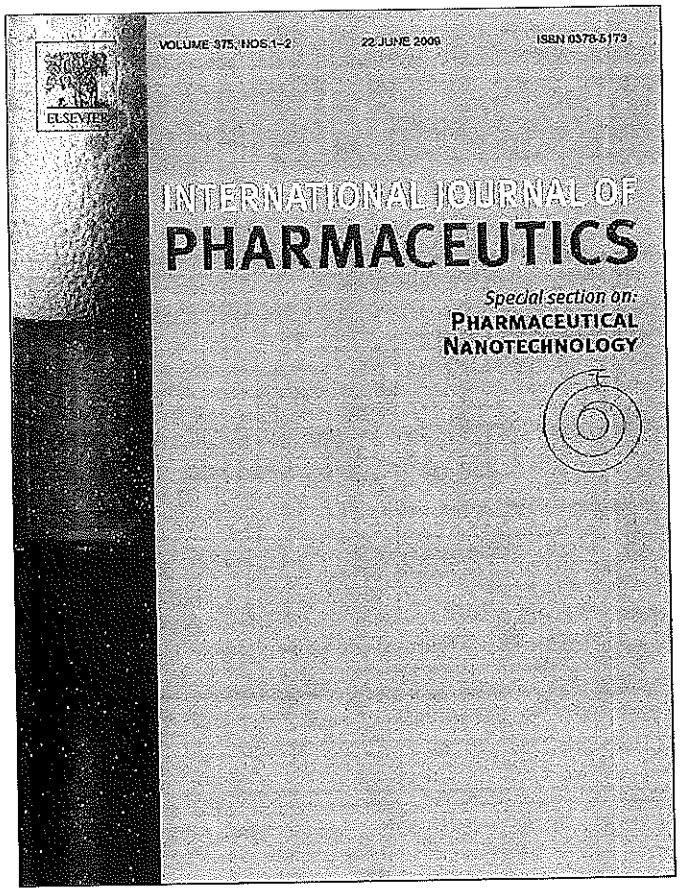

ceutical with high stability in human serum, specific cell receptor binding and rapid internalization. Biodistribution data in mice showed rapid blood clearance, with predominant renal excretion and specific binding towards GRP receptor-positive tissues such as pancreas and PC-3 tumors (Ferro-Flores et al., 2006b). Images of GRP-r expression in breast cancer patients demonstrated distinct radioactivity accumulation in malignant tissue (Santos-Cuevas et al., 2008).

Targeted entry into cells is an increasingly important research area. Disease diagnoses and treatment by novel methods would be greatly enhanced by efficiently transporting materials to living cell nuclei. Penetrating peptides are emerging as attractive drug delivery tools. The HIV Tat-derived peptide is a small basic peptide called "trojan horse" for successfully delivering a large variety of cargoes into cells such as nanoparticles, proteins, peptides and nucleic acids. The "transduction domain" or region conveying cell penetrating properties appears to be confined to a small stretch of basic amino acids with the sequence RKKRRQRRR and known as Tat(49–57) (Koch et al., 2003; Dietz and Bähr, 2004; Deshayes et al., 2005; Zhang et al., 2006b; Hu et al., 2007; Jain et al., 2007; Youngblood et al., 2007; Chen and Harrison, 2007; Cornelissen et al., 2008).

Therefore, a new hybrid radiopharmaceutical of type ^{99m}Tc-N_2S_2-Tat(49–57)-Lys^3-bombesin (^{99m}Tc-Tat-BN) would significantly increase cancer cell uptake and consequently image contrast of cancer tumors and their metastases, improving sensitivity and specificity of diagnostic studies in breast cancer.

The aim of this research was to prepare and assess *in vitro* and *in vivo* uptake kinetics in GRP receptor-positive cancer cells of ^{99m}Tc-Tat-BN and to compare its cellular internalization with that of ^{99m}Tc-BN.

2. Experimental

2.1. Design and preparation of hybrid N_2S_2-Tat(49–57)-Lys^3-BN peptide

Tat(49–57) peptide (H-Arg-Lys-Lys-Arg-Arg-Gln-Arg-Arg-Arg-NH_2) was conjugated to Gly-Gly-Cys-Gly-Cys(Acm)-Gly-Cys(Acm)-NH_2 to produce the Tat(49–57)-spacer-N_2S_2 peptide (H-Arg^1-Lys^2-Lys^3-Arg^4-Arg^5-Gln^6-Arg^7-Arg^8-Arg^9-Gly^{10}-Gly^{11}-Cys^{12}-Gly^{13}-Cys^{14}(Acm)-Gly^{15}-Cys^{16}(Acm)-NH_2). The sequence Gly^{13}-Cys^{14}(Acm)-Gly^{15}-Cys^{16}(Acm)-NH_2 was added for use as the specific N_2S_2 chelating site for ^{99m}Tc (Fig. 1).

Lys^3-bombesin (Pyr-Gln-Lys-Leu-Gly-Asn-Gln-Trp-Ala-Vla-Gly-His-Leu-Met-NH_2) was conjugated to maleimidopropyl (MPA) through Lys^3 and the MPA group used as the branch position forming a thioether with the Cys^{12} side chain of Tat(49–57)-spacer-N_2S_2 peptide (Fig. 1). Synthesis, HPLC analysis, Mass Spectral Analysis (MALDI), Amino Acid Analysis (AAA) and peptide content determination were carried out in the Bachem Laboratories obtaining a certified white powder product with chemical purity >90% and molecular weight of 3779.5 g/mol (Bachem, CA, USA).

2.2. Molecular modeling

The N_2S_2-Tat(49–57)-Lys^3-BN peptide molecule was built taking into account valence, bond type, charge and hybridization. The minimum energies (Molecular Mechanics calculations by Augmented MM3 procedure) and the lowest energy conformer (CONFLEX procedure) associated to the optimized geometry of its structure were calculated using the CAChe Pro 5.02 and/or 5.04 program package for windows® (Fujitsu Ltd., 2000–2001). Sequential application of Augmented MM3/CONFLEX procedures yielded the most stable conformers for the N_2S_2-Tat(49–57)-Lys^3-BN and for Tc(O)N_2S_2-Tat(49–57)-Lys^3-BN structures.

2.3. Technetium-99 labeling of N_2S_2-Tat(49–57)-Lys^3-BN

^{99m}Tc-pertechnetate was obtained from a GETEC ^{99}Mo/^{99m}Tc generator (ININ-Mexico). All the other reagents were purchased from Sigma–Aldrich Chemical Co., and used as received.

Acetamidomethyl (Acm) groups deprotection and N_2S_2-Tat(49–57)-Lys^3-bombesin labeling were accomplished in one step by pertechnetate reduction with stannous chloride in ammonium acetate and sodium tartrate presence at room temperature. Alkalinity (pH 9.5) was necessary to de-acetylate Cys^{14}(Acm) and Cys^{16}(Acm) side chains of TAT(49–57)-spacer-N_2S_2 peptide that are essential for oxotechnetate binding (Bogdanov et al., 2001; Zhang et al., 2006a,b).

One milligram of N_2S_2-Tat(49–57)-Lys^3-BN was dissolved in 200 μL of injectable water (Pisa®, Mexico). Ten microliters of this solution were added to 25 μL of sodium ^{99m}Tc-pertechnetate (185 MBq) followed by 7 μL of deprotection mixture (50 mg/mL sodium tartrate in 0.1 M NH_4OH/NH_4CH_3COOH, pH 9.5) and 3 μL of reducing solution (0.5 mg $SnCl_2$/mL in 0.05 M HCl). The final mixture was incubated for 20 min at room temperature.

2.4. Evaluation of ^{99m}Tc-N_2S_2-Tat(49–57)-Lys^3-BN (^{99m}Tc-Tat-BN) radiochemical purity

Radiochemical purity analyses were performed by instant thin-layer chromatography on silica gel (ITLC-SG, Gelman Sciences), solid phase extraction (Sep-Pak C-18 cartridges) and reverse phase high-performance liquid chromatography (HPLC).

ITLC-SG analysis was accomplished using 2 different mobile phases: 2-butanone to determine the amount of free $^{99m}TcO_4^-$ (Rf = 1) and 0.1 M sodium citrate pH 5 to determine ^{99m}Tc-tartrate and $^{99m}TcO_4^-$ (Rf = 1). Rf value of the radiolabeled peptide in each system was 0.0.

The Sep-Pak cartridges were preconditioned with 5 mL of ethanol followed by 5 mL of 1 mM HCl and 5 mL of air. An aliquot of 0.1 mL of the labeled peptide was loaded on the preconditioned Sep-Pak cartridge followed by 5 mL of 1 mM HCl to elute free $^{99m}TcO_4^-$ and ^{99m}Tc-tartrate. The radiolabeled peptide was eluted with 3 mL of ethanol:saline (1:1) mixture and the hydrolyzed-reduced ^{99m}Tc or ^{99m}Tc-colloid remained in the cartridge.

HPLC analyses were carried out with a Waters instrument running Millennium software with both radioactivity and UV-photodiode array in-line detectors and YMC ODS-AQ S5 column (5 μm, 4.6 mm × 250 mm). The gradient was run at a flow rate of 1 mL/min with the following conditions: 0.1% trifluoroacetic acid (TFA)/water (solvent A) and 0.1% TFA/acetonitrile (solvent B). The gradient started with 100% solvent A for 3 min, changed to 50% solvent A over 10 min, was maintained for 10 min, changed to 30% solvent A over 3 min and finally returned to 100% solvent A over 4 min. In this system retention times for free $^{99m}TcO_4^-$, and ^{99m}Tc-Tat-BN were 3–4 min and 10–10.5 min, respectively.

2.5. Serum stability

Size exclusion HPLC analysis and a ITLC-SG were used to estimate serum stability of ^{99m}Tc-Tat-BN. A 50 μL volume of labeled peptide solution (0.5 μg/50 μL) was incubated at 37 °C with 1 mL of fresh human serum. Radiochemical stability was determined from samples of 10 μl taken at different times from 20 min to 24 h for analysis. A shift of the HPLC radioactivity profile to higher molecular weight indicates protein binding, while lower-molecular weight peaks indicate labeled catabolites or serum cysteine binding.

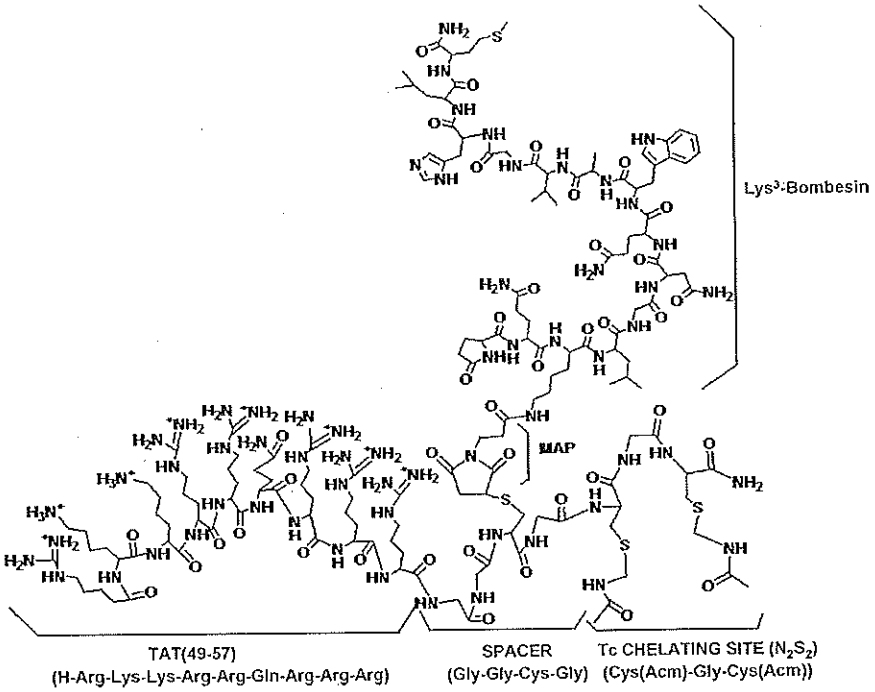

Fig. 1. General scheme of the N_2S_2-Tat(49–57)-Lys³-BN hybrid peptide.

2.6. Cysteine challenge

^{99m}Tc-Tat-BN was tested for instability towards cysteine. A fresh cysteine solution was prepared (10 mg/mL in 0.1 M PBS, pH 7.0) and diluted to different concentrations. Then 10 μL of each cysteine solution was mixed with 90 μL of 20 μM of the labeled peptide solutions. The molar ratios of cysteine to peptide were 5:1, 50:1 and 500:1. Each test tube was incubated at 37 °C and radiochemical purity analyzed 1 h later by ITLC.

2.7. Preparation of ^{99m}Tc-EDDA/HYNIC-Lys³-BN (^{99m}Tc-BN)

As previously reported, a lyophilized formulation containing HYNIC-Lys³-BN, EDDA, tricine, and stannous chloride was prepared (Ferro-Flores et al., 2006b). The radiolabeling procedure was carried out by adding 1 mL of 0.2 M phosphate buffer pH 7.0 to the freeze-dried kit formulation and immediately 740–1110 MBq (1 mL) of ^{99m}Tc-pertechnetate followed by incubation in boiling water for 15 min. Radiochemical purity was also evaluated by reverse phase HPLC and ITLC.

2.8. In vitro kinetic studies

2.8.1. Cell lines

Human prostate cancer cell PC-3 line and human breast carcinoma cell lines MDA-MB231 and MCF7 were originally obtained from ATCC (USA). The cells were routinely grown at 37 °C, with 5% CO_2 atmosphere and 100% humidity in RPMI medium supplemented with 10% newborn calf serum and antibiotics (100 μg/mL streptomycin).

2.8.2. Internalization assay and non-specific binding

PC-3 or MDA-MB231 or MCF7 cells supplied in fresh medium were diluted to 1×10^6 cells/tube and incubated with about 200,000 cpm of ^{99m}Tc-BN (0.3 nmol total peptide) or ^{99m}Tc-Tat-BN (0.3 nmol total bombesin) in triplicate at 37 °C for 0.083, 2, 4, 6 and 24 h. The test tubes were centrifuged (3 min, 500 g), washed twice with phosphate buffer saline (PBS), and the activity of the cell pellet determined in a crystal scintillation well type detector. Radioactivity in the cell pellet represents both externalized peptide (surface bound) and internalized peptide. An aliquot with the initial activity was taken to represent 100%, and the cell uptake activity was then calculated.

The externalized peptide activity was removed with 1 mL of 0.2 M acetic acid/0.5 M NaCl solution added to the resuspended cell pellet. The test tubes were centrifuged, washed with PBS, re-centrifuged, and pellet activity was considered as internalization. The cell pellet was re-suspended with 1 M NaOH to break up the membranes, centrifuged and washed with PBS. The supernatant activity represents cytoplasm uptake. Non-specific binding was determined in parallel but in presence of 10 μM Lys³-BN (Bachem-USA) (blocked receptor cells).

2.8.3. Statistical analysis

Differences between the *in vitro* cell data for BN-radiopharmaceuticals were evaluated with the Student *t*-test.

2.9. Biodistribution studies

Biodistribution and tumor uptake studies in mice were carried out according to the rules and regulations of the Official Mexican Norm 062-ZOO-1999.

Healthy 6-week-old Balb-C mice were used for biodistribution studies. ^{99m}Tc-Tat-BN, 1.11 MBq (30 μCi) in 0.04 mL was injected in a tail vein. The mice ($n=3$) were sacrificed at 0.25, 05, 2, 4 and 24 h post-injection. Whole heart, lung, liver, spleen, pancreas, kidneys, intestines, muscle, bone and blood samples were saline rinsed, paper blotted and placed into pre-weighed plastic test tubes. The activity was determined in a well-type scintillation detector (*Canberra*) along with six 0.5 mL aliquots of the diluted standard representing 100% of the injected activity. Mean activities were used to

obtain the percentage of injected activity per gram of tissue % IA/g.

2.9.1. Tumor induction in athymic mice

Athymic male mice (20–22 g) were kept in sterile cages with sterile wood-shavings bed, constant temperature, humidity, noise and 12:12 light periods. Water and feed (standard PMI 5001 feed) were given *ad libitum*.

Prostate tumors were induced by subcutaneous injection of PC-3 cells (1×10^6) resuspended in 0.2 mL of phosphate-buffered saline, into the upper back of four 6–7-week-old nude mice. Injection sites were observed at regular intervals for tumor formation and progression.

2.9.2. Imaging

The nude mice with the implanted tumors were sacrificed and scanned with a gamma camera with a pinhole collimator 2 h after ^{99m}Tc-Tat-BN or ^{99m}Tc-BN administration in the tail vein (3 MBq in 0.04 mL). Finally, complete dissection was carried out to determine percentage of injected activity per gram of tissue % IA/g as described above.

3. Results

3.1. Design of $(Acm)_2S_2N_2$-Tat-Lys^3-bombesin and $Tc(O)S_2N_2$-Tat-Lys^3-bombesin by semiempirical calculations

A good molecular modeling yields structures which are similar to those obtained experimentally. However, this similarity could be affected by the size, charge and mobility of the molecule, e.g. in the case of big and charged peptides. Without forgetting this fact, the hybrid N_2S_2-Tat(49–57)-Lys^3-BN peptide (Fig. 2A) was designed using semiempirical calculations to investigate the feasibility of its formation. The minimum energies of its most stable structure and conformer were 271 and 233 kcal/mol, respectively.

The technetium-oxo complex formed with this hybrid peptide was also modeled considering two well-known facts of this type of chelating site: (1) the two terminal thiols $S_2(Acm)_2$ are able to be ionized by removing the acetamidomethyl protecting groups (Canney et al., 1993; Bandoli et al., 2001), (2) the amide groups easily undergo deprotonation (Bandoli et al., 2001). Then it is expected that the chelating site yields a $[N_2S_2]^{4-}$ coordination around the $[Tc(O)]^{3+}$ core forming this way a negative charged five-coordinate complex. Based on the latter, the molecule of the $[TcO(N_2S_2)]^{-1}$-

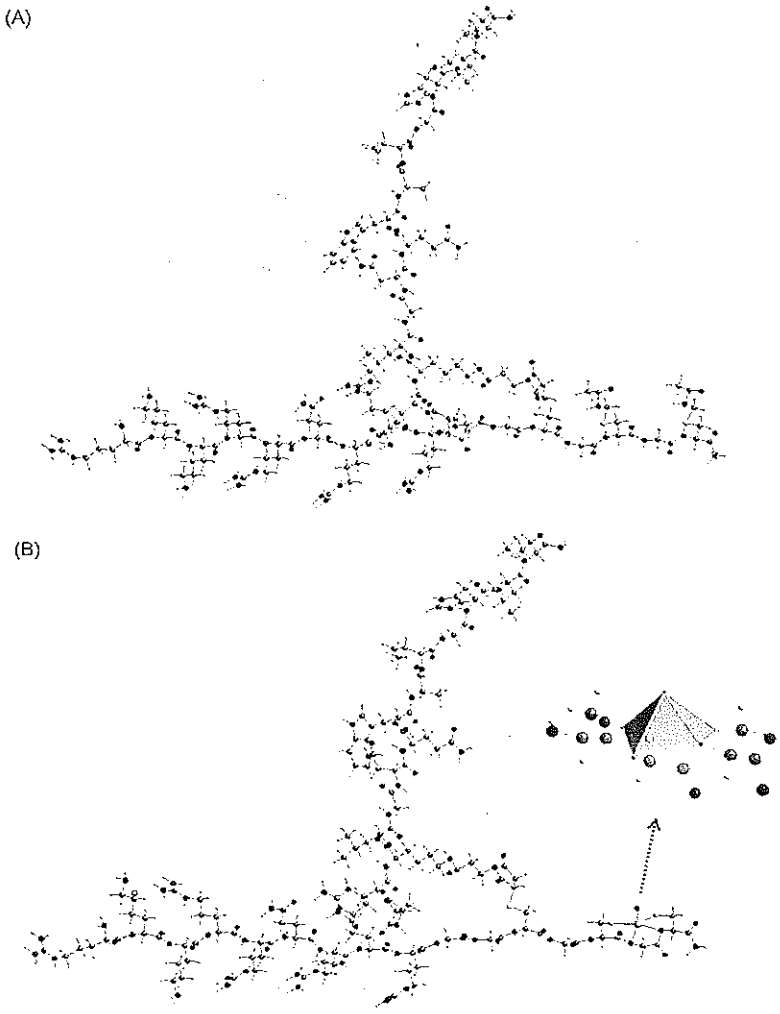

Fig. 2. (A) The most stable conformer of the modeled N_2S_2-Tat(49–57)-Lys^3-BN hybrid peptide molecule using CONFLEX. (B) The most stable conformer of the modeled $Tc(O)N_2S_2$-Tat(49–57)-Lys^3-BN hybrid peptide molecule using CONFLEX. The expanded geometry of the Tc(O) chelate: $[Tc(O)N_2S_2]^{-1}$ is given for clarity.

Table 1
Bond distances of the calculated Tc(O)-N_2S_2-Tat-Lys^3-BN complex using Augmented MM3 and CONFLEX semiempirical procedures.

Compound	Geometry	Bond distances (Å)	Bond distance ratio
$[^{99m}Tc$-$(N_2S_2DADS)]^{-1}$	Square pyramid[a]	Tc-N1: 2.002 Tc-N2: 1.984 Tc-S1: 2.300 Tc-S2: 2.286 Tc=O: 1.667	R_N = 1.009 R_S = 1.006 TcN2/TcO = 1.190 TcS1/TcO = 1.38
$[(^{99m}Tc(O)$-$(N_2S_2))^{-1}$-Tat-Lys^3-BN	Distorted square pyramid	Tc-N1: 2.314 Tc-N2: 2.308 Tc-S1: 2.618 Tc-S2: 2.611 Tc=O: 2.210	R_N = 1.003 R_S = 1.003 TcN2/TcO = 1.04 TcS1/TcO = 1.19

[a] By X-ray diffraction (Canney et al., 1993).

TAT(49–57)-Lys^3-BN peptide complex was calculated (Fig. 2B) using the most stable conformer of the hybrid peptide molecule. The minimum energy of the optimized structure was 300 kcal/mol and that of the most stable conformer equal to 262 kcal/mol. In Table 1 are given some geometrical parameters of this complex.

3.2. Evaluation of ^{99m}Tc-Tat-BN radiochemical purity and stability

The results obtained by ITLC, Sep-Pak and HPLC analyses showed a mean radiochemical purity for ^{99m}Tc-Tat-BN of 92 ± 2% (n > 30) and remains stable after 24 h without post-labeling purification (Fig. 3). The average specific activity was 14 MBq/nmol. After 1 h in human serum the radiochemical purity remained >90% and decreased to 82% and 65% after 3 and 24 h, respectively. Protein binding was 36.4 ± 2.7 at 2 h without ^{99m}Tc transchelation to cysteine (Fig. 4). After incubation with 5:1, 50:1 and 500:1 molar ratios of cysteine to peptide, ITLC analysis revealed that the radioactivity dissociated from ^{99m}Tc-Tat-BN was 7%, 16% and 41%, respectively, indicating adequate radiopharmaceutical stability towards cysteine present in blood.

3.3. In vitro uptake

The *in vitro* results showed an important uptake in the three cancer cell lines PC3, MCF7 and MDA-MB231 which is inhibited significantly by pre-incubation with cold bombesin (Table 2). In general cell binding in blocked cells was less than 3% of total activity for ^{99m}Tc-BN and less than 9% for ^{99m}Tc-Tat-BN in all cell lines and during all times. This confirmed *in vitro* specificity of both radiopharmaceuticals for GRP receptors found in cell membranes of the three cell lines due to the fact that both compounds contain BN. However, the hybrid ^{99m}Tc-Tat-BN shows a higher uptake (p < 0.05) due to Tat's capacity to internalize the molecule into the cytoplasm and even into the nucleus (Costantini et al., 2008).

Internalization increase of ^{99m}Tc-Tat-BN compared with that of ^{99m}Tc-BN in the cell lines is shown in Fig. 5, demonstrating that the hybrid peptide has the ability to penetrate the cell membrane. Maximum internalization is reached in PC3 and MCF7 cells between 2 and 4 h after incubation. However MDA-MB231 cells showed a distinct pattern where cellular internalization reaches a maximum during the first few minutes decreasing with time.

The percentage activity in cytoplasm of the total internal activity (Fig. 6) shows a great difference between both radiopharmaceuticals. Most of ^{99m}Tc-BN remains in the cell membrane while ^{99m}Tc-Tat-BN is released in the cytoplasm, where it can be internalized into the nucleus because of its amino acid nuclear localization sequence (NLS) (Costantini et al., 2008).

3.4. Biodistribution and imaging

^{99m}Tc-Tat-BN biodistribution is shown in Table 3. Renal excretion is predominantly observed but hepatobiliary clearance is also present. GRP-r receptors are naturally expressed in lungs showing radiopharmaceutical uptake (Shriver et al., 2000). However, pancreas shows higher uptake than non-excretory organs such as spleen, muscle and even lungs because of its GRP-r expression, indicating that BN acts as the targeting vector.

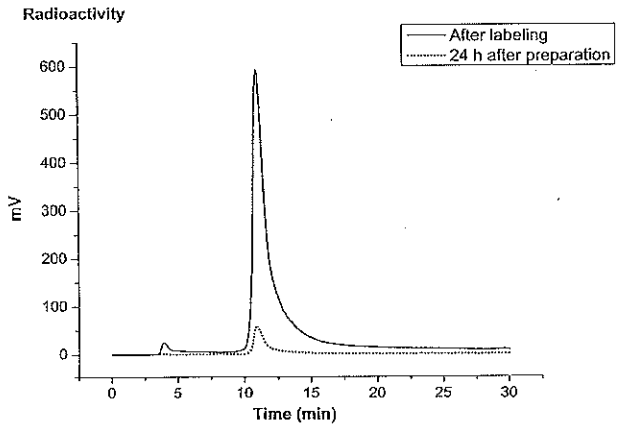

Fig. 3. Reverse phase HPLC radiochromatograms of ^{99m}Tc-N_2S_2-Tat(49–57)-Lys^3-BN after labeling, and 24 h after preparation (kept at room temperature).

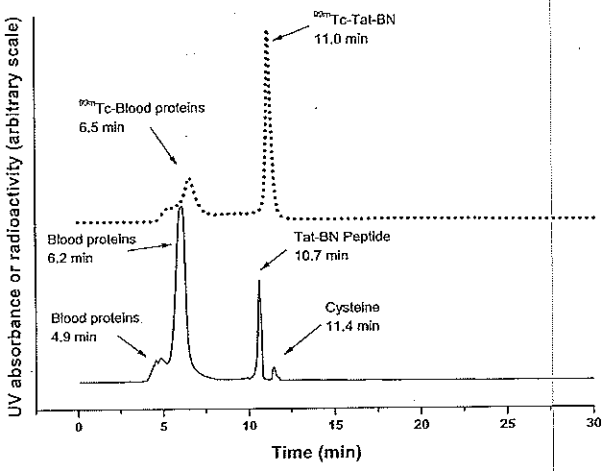

Fig. 4. Size-exclusion HPLC. Solid line represents the UV-chromatogram (280 nm) of human serum proteins and dotted line the radiochromatogram of ^{99m}Tc-N_2S_2-Tat(49–57)-Lys^3-BN 2 h after incubation in human serum at 37 °C.

Table 2
^{99m}Tc-N_2S_2-Tat(49–57)-Lys^3-BN (^{99m}Tc-Tat-BN) and ^{99m}Tc-EDDA/HYNIC-Lys^3-BN (^{99m}Tc-BN) cell uptake in different cancer cell lines (% of total activity ± SD).

Time (h)	PC3		MCF7		MDA-MB231	
	^{99m}Tc-Tat-BN	^{99m}Tc-BN	^{99m}Tc-Tat-BN	^{99m}Tc-BN	^{99m}Tc-Tat-BN	^{99m}Tc-BN
0.083	22.01 ± 2.08	10.29 ± 1.47	19.27 ± 3.55	7.83 ± 0.71	24.33 ± 2.82	5.91 ± 0.26
1	21.43 ± 2.91	8.59 ± 0.59	17.43 ± 1.13	6.79 ± 0.45	19.43 ± 1.30	5.48 ± 0.21
2	24.88 ± 2.12	12.85 ± 0.90	18.27 ± 2.14	8.97 ± 0.92	15.98 ± 1.07	5.06 ± 0.57
4	28.10 ± 3.86	17.62 ± 1.86	13.15 ± 1.27	7.48 ± 0.30	14.40 ± 1.79	4.16 ± 0.39
6	25.43 + 1.79	9.63 + 0.47	12.65 + 0.94	7.98 + 0.22	13.60 + 0.96	4.19 + 0.52
24	23.91 ± 1.53	8.21 ± 0.64	12.30 ± 1.16	2.32 ± 0.49	14.24 ± 0.34	3.43 ± 0.27

Table 3
Biodistribution of ^{99m}Tc-N_2S_2-Tat(49–57)-Lys^3-BN in healthy Balb-C mice at different times after radiopharmaceutical administration ($n = 3$ in each time).

Tissue	% IA/g (mean + SD)				
	0.25 h	0.5 h	2 h	4 h	24 h
Blood	7.81 ± 2.62	6.02 ± 2.59	1.12 ± 0.17	1.00 ± 0.03	0.07 ± 0.02
Heart	2.43 ± 0.78	1.62 ± 0.63	0.33 ± 0.07	0.32 ± 0.03	0.09 ± 0.10
Lungs	2.68 ± 0.94	2.26 ± 0.44	0.60 ± 0.08	0.56 ± 0.04	0.09 ± 0.03
Liver	4.91 ± 1.57	3.97 ± 1.70	2.03 ± 0.04	2.11 ± 0.32	0.52 ± 0.17
Spleen	1.28 ± 0.40	0.80 ± 0.30	0.35 ± 0.05	0.55 ± 0.17	0.23 ± 0.07
Pancreas	2.89 ± 1.01	2.65 ± 0.77	1.87 ± 0.11	1.43 ± 0.24	0.21 ± 0.04
Kidneys	16.87 ± 4.85	22.99 ± 8.57	29.02 ± 2.78	27.72 ± 2.18	8.45 ± 0.81
Intestine	3.70 ± 1.49	11.30 ± 7.71	2.06 ± 0.33	2.05 ± 0.98	0.17 ± 0.08
Muscle	1.47 ± 0.26	1.28 ± 0.70	0.58 ± 0.23	0.43 ± 0.14	0.03 ± 0.02
Bone	2.44 ± 0.79	1.74 ± 0.60	0.42 ± 0.05	0.78 ± 0.26	0.19 ± 0.17

Table 4 shows biodistribution in mice with induced PC-3 tumors. Tumor-to-blood, tumor-to-muscle and pancreas-to-blood ratios for ^{99m}Tc-BN were 4.4, 7 and 8.2, respectively, and 3.2, 8 and 1.4 for ^{99m}Tc-Tat-BN correspondingly. *In vivo* images showed a clear tumor uptake and a dissection process to eliminate internal viscera, highlighted the ^{99m}Tc-BN and ^{99m}Tc-Tat-BN uptake in tumor PC-3 cells (Fig. 7). The tumor/muscle ratio obtained from image counts per pixel corresponding to ^{99m}Tc-BN was 7 and for ^{99m}Tc-Tat-BN was 8.5, demonstrating a minimal difference between the two.

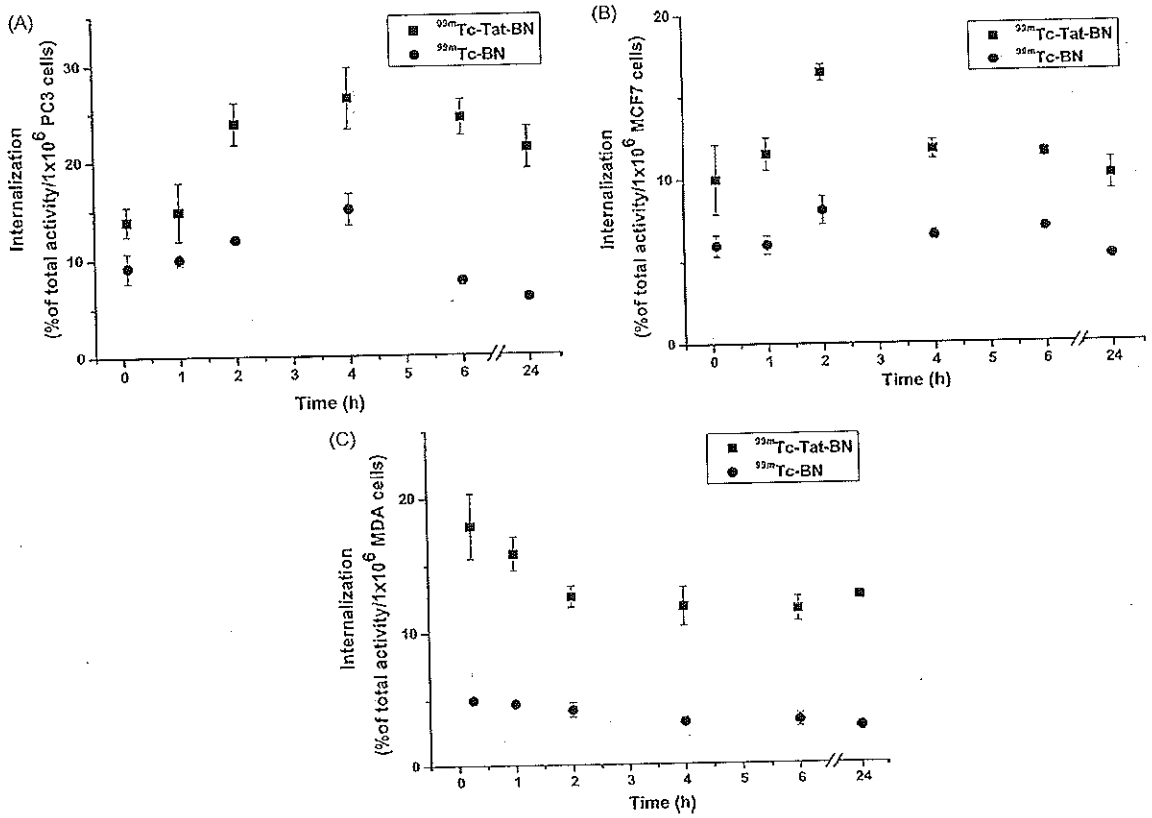

Fig. 5. Time dependent internalization of ^{99m}Tc-N_2S_2-Tat(49–57)-Lys^3-BN (^{99m}Tc-Tat-BN) and ^{99m}Tc-EDDA/HYNIC-Lys^3-BN (^{99m}Tc-BN) in (A) PC3, (B) MCF7 and (C) MDA-MB231 cancer cell lines.

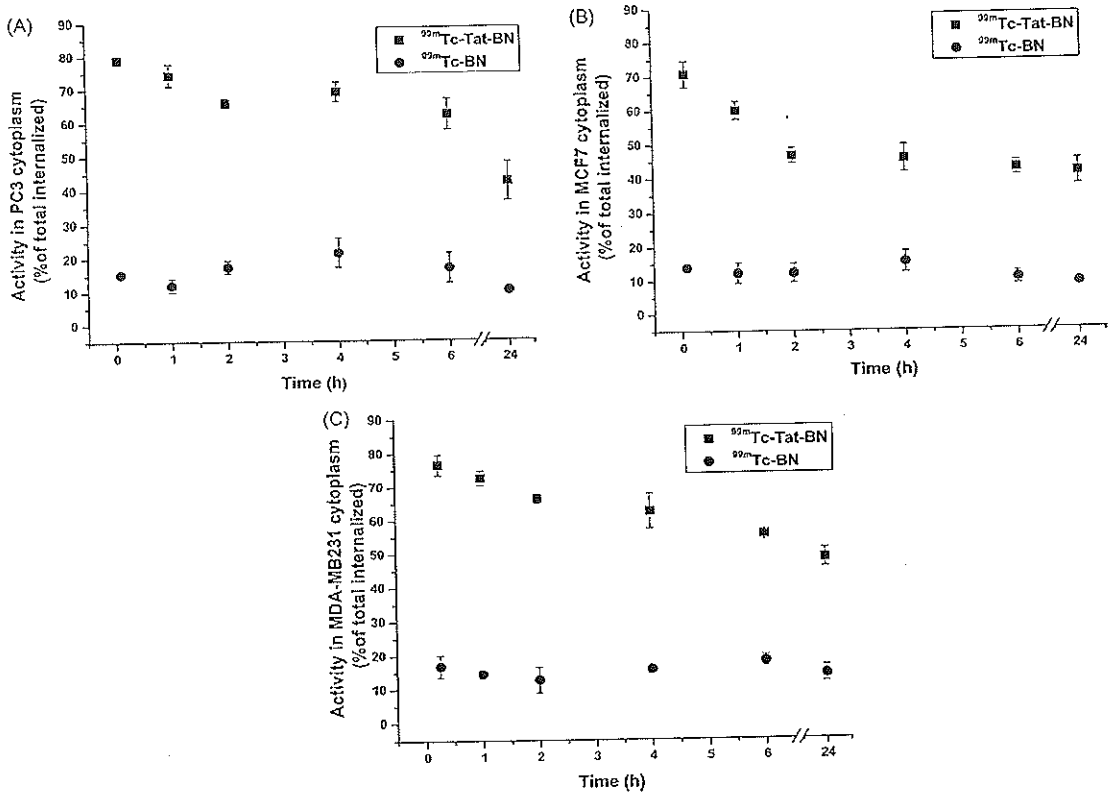

Fig. 6. Uptake of ^{99m}Tc-N_2S_2-Tat(49–57)-Lys^3-BN (^{99m}Tc-Tat-BN) and ^{99m}Tc-EDDA/HYNIC-Lys^3-BN (^{99m}Tc-BN) in the cytoplasm of (A) PC3, (B) MCF7 and (C) MDA-MB231 cancer cell lines.

Table 4
Biodistribution in nude mice with induced PC-3 tumors 2 h after administration of ^{99m}Tc-N_2S_2-Tat(49–57)-Lys^3-BN (^{99m}Tc-Tat-BN) ($n=3$) or ^{99m}Tc-EDDA/HYNIC-Lys^3-BN (^{99m}Tc-BN) ($n=3$).

Tissue	%IA/g (mean ± SD)	
	^{99m}Tc-BN	^{99m}Tc-Tat-BN
Blood	0.40 ± 0.03	1.22 ± 0.16
Heart	0.25 ± 0.02	0.43 ± 0.08
Lung	0.50 ± 0.04	0.54 ± 0.07
Liver	0.85 ± 0.04	2.14 ± 0.05
Spleen	0.40 ± 0.05	0.42 ± 0.04
Pancreas	3.29 ± 0.21	1.69 ± 0.12
Kidney	23.5 ± 1.21	28.12 ± 2.18
Intestine	0.85 ± 0.13	1.96 ± 0.23
Muscle	0.25 ± 0.03	0.48 ± 0.05
Tumor	1.75 ± 0.11	3.84 ± 0.25

4. Discussion

The minimum energies of the calculated hybrid peptide are adequate for its molecular structure since the large size, complexity and high charge of this peptide impose steric and electrostatic repulsions against its stabilization at lower minimum energies. However, the comparison of its minimum energy (271 kcal/mol) to those reported for other calculated structures of smaller charged peptides like UBI(29–41) (Melendez-Alafort et al., 2003), Tat-Scr (Ferro-Flores et al., 2004), 90 and 72–90 kcal/mol, respectively, suggested that the hybrid peptide has to be stable. In addition, the conformation acquired by the peptide molecule does not interfere with the recognition capability of BN. These facts supported the proposal that the preparation of the hybrid peptide has to be viable and the specificity maintained.

$[TcO(N_2S_2)]^{-1}$-Tat(49–57)-Lys^3-BN peptide structure acquired in the chelating site a distorted square pyramidal geometry with the oxo group at the apical position of the pyramid and Tc about the center of the plane formed by the N_2S_2 donors (see expanded segment of the molecule, Fig. 2B). This geometry has been found by X-ray diffraction for other five-coordinate Tc(O) complexes neutral or charged compounds like negatively charged five coordinate $Tc(O)N_2S_2$ complexes (Bandoli et al., 2001; Canney et al., 1993). The minimum energy of this complex does not differ significantly from that of the hybrid peptide before coordination to $[Tc(O)]^{3+}$. This evidence together the geometrical arrangement acquired by the complexed hybrid peptide (Fig. 2B) demonstrate that the recognition capability of the peptide is little affected by the formation of the $Tc(O)N_2S_2$ complex. However, the stability of the $[Tc(O)(N_2S_2)]^{-1}$ chelate itself could be affected.

In general ^{99m}Tc-Tat-BN did not show the excellent radiochemical characteristics as that previously reported for ^{99m}Tc-BN (Ferro-Flores et al., 2006b), since the first one showed slightly lower radiochemical purity (>95% for ^{99m}Tc-BN) and lower stability in cysteine and human serum. These results were expected since HYNIC core with additional co-ligands has demonstrated to be highly stable for labeling peptides (Liu and Edwards, 1999; Decristoforo et al., 2000). Nevertheless, the technetium-binding region consisting of Gly-Gly-Cys-NH_2 or Cys-Gly-Cys-NH_2 peptide (to form a $-N_2S_2-$ or $-N_3S-$ ligand) has been successfully used to prepare stable complexes with the $Tc{=}O^{3+}$ core producing minimum alteration of the molecule bioactivity in agreement with results obtained in this research (Bogdanov et al., 2001; Francesconi et al., 2004; Zhang et al., 2006b).

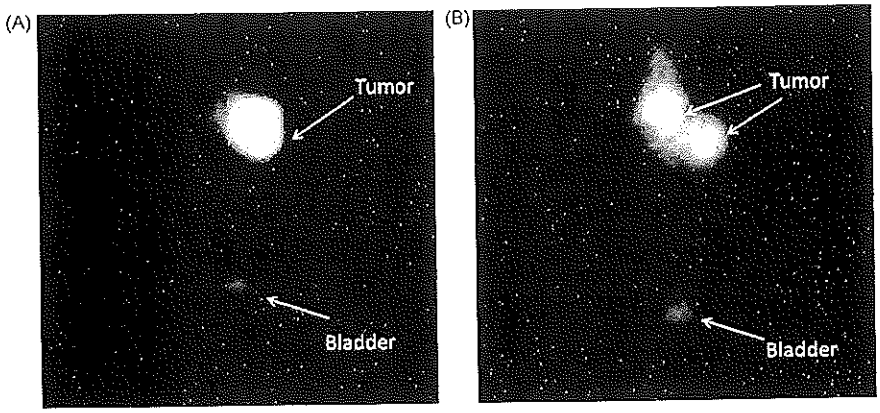

Fig. 7. Uptake of (A) ^{99m}Tc-N_2S_2-Tat(49–57)-Lys^3-BN (^{99m}Tc-Tat-BN) and (B) ^{99m}Tc-EDDA/HYNIC-Lys^3-BN (^{99m}Tc-BN) in tumor PC3 cells in athymic mouse 2 h after radiopharmaceutical administration (mice with dissection of internal viscera to highlight tumor uptake).

^{99m}Tc-Tat-BN binds to plasmatic proteins approximately 20% more than ^{99m}Tc-BN. These data indicate that in spite of the fact that both radiopharmaceuticals contain BN and are labeled with ^{99m}Tc, the positive charges of Tat due to arginines and lysines contained in its amino acid sequence, tend to interact faster and in a strong way with proteins, besides that it is not targeted to a specific receptor (Costantini et al., 2008; Cornelissen et al., 2008). This cationic property is necessary to penetrate the cell membrane and localize the nucleus (Drin et al., 2003), but these characteristics can have an effect in blood elimination rate by binding to plasmatic proteins as well as increasing interaction and internalization in cells and healthy tissue (e.g. plasmatic cells, spleen and liver). Although cancer cell uptake was significantly higher for ^{99m}Tc-Tat-BN with respect to ^{99m}Tc-BN, the higher activity in blood for the first one did not produce a very high increase in the contrast of tumor image in mice (Fig. 7).

The maximum uptake of both radiopharmaceuticals was presented at the same times in all cancer cells, in PC3 at 4 h (^{99m}Tc-BN, 17.62 ± 1.86%; ^{99m}Tc-Tat-BN, 28.1 ± 2.86%), in MCF7 at 2 h (^{99m}Tc-BN, 8.97 ± 0.92%; ^{99m}Tc-Tat-BN, 18.27 ± 2.14%) and in MDA-MB231 at 5 min (^{99m}Tc-BN, 5.91 ± 0.26%; ^{99m}Tc-Tat-BN, 24.33 ± 2.82%) with differences only attributed to GRP-r cell expression. In this point it is important to mention that although MCF7 and MDA-MB231 are both breast cancer cell lines, the first one is estrogen-dependent and the latter is estrogen-independent, and it has been suggested that the GRP-r expression is estrogen-dependent in the early stages of breast carcinoma (Halmos et al., 1995). The elimination of the radiopharmaceuticals in the following times is due to the fact that the internalization process of the ligand/GRP-r complex involves lysosomes final trapping upon binding, where, in the case of the peptides, are quickly degraded. Due to this immediate lysosome degradation, no radioactivity accumulation in cells was expected (La Bella et al., 2002).

Receptor proteins in cells are considered targets in molecular nuclear medicine. In general cell internalization was receptor specific with ^{99m}Tc-BN and in the ^{99m}Tc-Tat-BN case 9% of total activity was non-specific as demonstrated uptake results in GRP-r blocked cell experiments because of Tat nuclear localizing sequence (NLS) (Costantini et al., 2008).

In this work the nucleus of the cytoplasm was not separated to quantify nuclear internalization. Nevertheless it was considered necessary to carry out this test with the purpose of estimating cellular dosimetry because of ^{99m}Tc-auger electron emission.

Biodistribution studies showed a slow blood clearance for ^{99m}Tc-Tat-BN, the contrary was observed in non-target organs, however, maximum uptake was observed in kidneys indicating principal renal excretion. These results coincide with ^{99m}Tc-BN biodistribution studies where excretion is mainly renal and uptake in non-target organs was lower with faster blood clearance. Nevertheless both radiopharmaceuticals showed good tumor localization for PC3 cells in athymic mice. However ^{99m}Tc-Tat-BN showed a slightly better tumor/muscle ratio of 8.5 compared to 7 for ^{99m}Tc-BN.

High ^{99m}Tc-Tat-BN uptake in kidneys and in non-target organs shows the need for an improved method for reducing radioactivity background which could be done by the co-administration of a cold lysine–arginine infusion as previously reported for other peptide-radiopharmaceuticals (Bodei et al., 2003).

5. Conclusions

^{99m}Tc-N_2S_2-Tat(49–57)-Lys^3-BN has been developed as a hybrid radiopharmaceutical composed of a penetrating peptide with specific targeting moiety (Tat conjugated to BN) producing a stable labeled molecule able to overcome the lypophilic cell membrane barrier with higher internalization in GRP-receptor positive cancer cells with respect to ^{99m}Tc-EDDA/HYNIC-Lys^3-BN. Therefore, this hybrid is potentially useful in breast and prostate cancer imaging.

Acknowledgements

This study was supported by the CONACyT-SALUD-69051-Mexico and the International Atomic Energy Agency (Contract No. 14539/RO).

References

Alves, S., Correia, J.D., Santos, I., Veerendra, B., Sieckman, G.L., Hoffman, T.J., Rold, T.L., Figueroa, S.D., Retzloff, L., McCrate, J., Prasanphanich, A., Smith, C.J., 2006. Pyrazolyl conjugates of bombesin: a new tridentate ligand framework for the stabilization of fac-{M(CO)$_3$}^{1} moiety. Nucl. Med. Biol. 33, 625–634.

Baidoo, K.E., Lin, K.S., Zhan, Y., Finley, P., Scheffel, U., Wagner, H.N., 1998. Design, synthesis, and initial evaluation of high-affinity technetium bombesin analogues. Bioconjugate Chem. 9, 218–225.

Bandoli, G., Dolmella, A., Porchia, M., Refosco, F., Tisato, F., 2001. Structural overview of technetium compounds (1993–1999). Coord. Chem. Rev. 214, 43–90.

Bodei, L., Cremonesi, M., Zoboli, S., Grana, C., Bartolomei, M., Rocca, P., Caracciolo, M., Macke, H.R., Chinol, M., Paganelli, G., 2003. Receptor-mediated radionuclide therapy with ^{90}Y-DOTATOC in association with amino acid infusion: a phase 1 study. Eur. J. Nucl. Med. 30, 207–216.

Bogdanov, A., Tung, C.-H., Bredow, S., Weissleder, R., 2001. DNA binding chelates for nonviral gene delivery imaging. Gene Ther. 8, 515–522.

Canney, D.J., Billings, J., Francesconi, L.C., Guo, Y.-Z., Haggerty, B.S., Rheingold, A.L., Kung, H.F., 1993. Dicarboxylate diamide dimercaptide (N_2S_2) technetium-99m complexes: synthesis and biological evaluation as potential renal radiopharmaceuticals. J. Med. Chem. 36, 1032–1040.

Chen, L., Harrison, S.D., 2007. Cell-penetrating peptides in drug development: enabling intracellular targets. Biochem. Soc. Trans. 35, 821–825.
Cornelissen, B., McLarty, K., Kersemans, V., Scollard, D., Reilly, R., 2008. Properties of [^{111}In]-labeled HIV-1 tat peptide radioimmunoconjugates in tumor-bearing mice following intravenous or intratumoral injection. Nucl. Med. Biol. 35, 101–110.
Costantini, D.L., Hu, M., Reilly, R., 2008. Peptide motifs for insertion of radiolabeled biomolecules into cells and routing to the nucleus for cancer imaging or radiotherapeutic applications. Cancer Biother. Radiopharm. 23, 3–23.
Decristoforo, C., Melendez-Alafort, L., Sosabowski, J.K., Mather, S.J., 2000. ^{99m}Tc-HYNIC-[Tyr^3]-octreotide for imaging somatostatin-receptor-positive tumors: preclinical evaluation and comparison with ^{111}In-octreotide. J. Nucl. Med. 41, 1114–1119.
Deshayes, S., Morris, M.C., Divita, G., Heitz, F., 2005. Interactions of primary amphipathic cell penetrating peptides with model membranes: consequences on the mechanisms of intracellular delivery of therapeutics. Curr. Pharm. Des. 11, 3629–3638.
de Visser, M., Verwijnen, S.M., de Jong, M., 2008. Improvement strategies for peptide receptor scintigraphy and radionuclide therapy. Cancer Biother. Radiopharm. 23, 137–157.
Dietz, G.P., Bähr, M., 2004. Delivery of bioactive molecules into the cell: the Trojan horse approach. Mol. Cell. Neurosci. 27, 85–131.
Drin, G., Cottin, S., Blanc, E., Rees, A., Temsamani, J., 2003. Studies on the internalization mechanism of cationic cell penetrating peptides. J. Biol. Chem. 278, 31192–31201.
Faintuch, B.L., Santos, R.L.S., Souza, A.L.F., Hoffman, J., Greeley, M., Smith, C.J., 2005. ^{99m}Tc-Hynic-bombesin (7–14)NH_2: radiochemical evaluation with coligands EDDA (EDDA = ethylenediamine-N,N′-diacetic acid), tricine and nicotinic acid. Synth. React. Inorg. Met.-Org. Nano-Met. Chem. 16, 438–442.
Ferro-Flores, G., de Ramírez, F.M., Meléndez-Alafort, L.G., Arteaga de Murphy, C., Pedraza-López, M., 2004. Molecular recognition and stability of ^{99m}Tc-UBI 29–41 based on experimental and semiempirical results. Appl. Radiat. Isot. 61, 1261–1268.
Ferro-Flores, G., Arteaga de Murphy, C., Melendez-Alafort, L., 2006a. Third generation radiopharmaceuticals for imaging and targeted therapy. Curr. Pharm. Anal. 2, 339–352.
Ferro-Flores, G., Arteaga de Murphy, C., Rodriguez-Cortes, J., Pedraza-Lopez, M., Ramirez-Iglesias, M.T., 2006b. Preparation and evaluation of ^{99m}Tc-EDDA/HYNIC-[Lys^3]-bombesin for imaging of GRP receptor-positive tumours. Nucl. Med. Commun. 27, 371–376.
Francesconi, L.C., Zheng, Y., Bartis, J., Blumenstein, M., Costello, C., De Rosch, M.A., 2004. Preparation and characterization of [^{99}TcO] apcitide: a technetium labeled peptide. Inorg. Chem. 43, 2867–2875.
Garcia-Garayoa, E., Ruegg, D., Blauenstein, P., Zwimpfer, M., Khan, I.U., Maes, V., Blanc, A., Beck-Sickinger, A.G., Tourwe, D.A., Schubiger, P.A., 2007. Chemical and biological characterization of new $Re(CO)_3$/[^{99m}Tc]$(CO)_3$ bombesin analogues. Nucl. Med. Biol. 34, 17–28.
Haimos, G., Wittliff, J.L., Schally, A.V., 1995. Characterization of bombesin/gastrin releasing peptide receptors in human breast cancer and their relationship to steroid receptor expression. Cancer Res. 55, 280–287.
Hu, M., Chen, P., Wang, J., Scollard, D.A., Vallis, K.A., Reilly, R.M., 2007. ^{123}I-labeled HIV-1 tat peptide radioimmuno conjugates are imported into the nucleus of human breast cancer cells and functionally interact in vitro and in vivo with the cyclin-dependent kinase inhibitor, p21(WAF-1/Cip-1). Eur. J. Nucl. Med. Mol. Imaging 34, 368–377.
Jain, M., Venkatraman, G., Batra, S.K., 2007. Cell-penetrating peptides and antibodies: a new direction for optimizing radioimmunotherapy. Eur. J. Nucl. Med. Mol. Imaging 34, 973–977.
Koch, A.M., Reynolds, F., Kircher, M.F., Merkle, H.P., Weissleder, R., Josephson, L., 2003. Uptake and metabolism of a dual fluorochrome Tat-nanoparticle in HeLa cells. Bioconjugate Chem. 14, 115–1121.
Kunstler, J.U., Veerendra, B., Figueroa, S.D., Sieckman, G.L., Rold, T.L., Hoffman, T.J., Smith, C.J., Pietzsch, H.J., 2007. Organometallic (99m)Tc(III) '4+1' Bombesin(7–14) conjugates: synthesis, radiolabeling, and in vitro/in vivo studies. Bioconjugate Chem. 18, 1651–1716.
La Bella, R., Garcia-Garayoa, E., Langer, M., Blauenstein, P., Beck-Sickinger, A.G., Schubiger, A., 2002. In vitro and in vivo evaluation of a ^{99m}Tc(1)-labeled bombesin analogue for imaging of gastrin releasing peptide receptor-positive tumors. Nucl. Med. Biol. 29, 553–560.
Lin, K.S., Liu, A., Baidoo, K.E., Hashemzadeh-Gargari, H., Chen, M.K., Brenneman, K., Pili, R., Pomper, M., Carducci, M.A., Wagner, H.N., 2005. A new high affinity technetium-99m-bombesin analogue with low abdominal accumulation. Bioconjugate Chem. 16, 43–50.
Liu, S., Edwards, D.S., 1999. ^{99m}Tc-labelled small peptides as diagnostic radiopharmaceuticals. Chem. Rev. 99, 2235–2251.
Lui, V.W., Thomas, S.M., Zhang, Q., Wentzel, A.L., Siegfried, J.M., Li, J.Y., Grandis, J.R., 2003. Mitogenic effects of gastrin-releasing peptide in head and neck squamous cancer cells are mediated by activation of the epidermal growth factor receptor. Oncogene 22, 6183–6193.
Melendez-Alafort, L., Ramirez, F., de, M., Ferro-Flores, G., Arteaga de Murphy, C., Pedraza-Lopez, M., Hnatowich, D.J., 2003. Lys and Arg in UBI: a specific site for a stable Tc-99m complex? Nucl. Med. Biol. 30, 605–615.
Nock, B.A., Nikolopoulou, A., Galanis, A., Cordopatis, P., Waser, B., Reubi, J.C., Maina, T., 2005. Potent bombesin-like peptides for GRP-receptor targeting of tumors with ^{99m}Tc: a preclinical study. J. Med. Chem. 48, 100–110.
Reubi, J.C., 2003. Peptide receptors as molecular targets for cancer diagnosis and therapy. Endocrine Rev. 24, 389–427.
Santos-Cuevas, C.L., Ferro-Flores, G., Arteaga de Murphy, C., Pichardo-Romero, P., 2008. Targeted imaging of GRP receptors with ^{99m}Tc-EDDA/HYNIC-[Lys^3]-bombesin: biokinetics and dosimetry in women. Nucl. Med. Commun. 29, 741–747.
Shriver, S.P., Bourdeau, H.A., Gubish, C.T., Tirpak, D.L., Davis, A.L., Luketich, J.D., Siegfried, J.M., 2000. Sex-specific expression of gastrin-releasing peptide receptor: relationship to smoking history and risk of lung cancer. J. Natl. Cancer Inst. 92, 24–33.
Smith, C.J., Sieckman, G.L., Owen, N.K., Hayes, D.L., Mazuru, D.G., Volkert, W.A., Hoffman, T.J., 2003. Radiochemical investigations of [^{188}Re$(H_2O)(CO)_3$-diaminopropionic acid-SSS-bombesin(7–14)NH_2]: synthesis, radiolabeling and in vitro/in vivo GRP receptor targeting studies. Anticancer Res. 23, 63–70.
Thakur, M., Lentle, B.C., 2005. Report of a summit on molecular imaging. Radiology 236, 753–755.
Varvarigou, A., Scopinaro, F., Leondiadis, L., Corleto, V., Schillaci, O., de Vincentis, G., 2002. Synthesis, chemical, radiochemical and radiobiological evaluation of a new ^{99m}Tc-labeled bombesin-like peptide. Cancer Biother. Radiopharm. 17, 317–326.
Youngblood, D.S., Hatlevig, S.A., Hassinger, J.N., Iversen, P.L., Moulton, H.M., 2007. Stability of cell-penetrating peptide-morpholino oligomer conjugates in human serum and in cells. Bioconjugate Chem. 18, 50–60.
Zhang, X., Cai, W., Cao, F., Schreibmann, E., Wu, Y., Wu, J.C., Xing, L., Chen, X., 2006a. ^{18}F-labeled bombesin analogs for targeting GRP receptor-expressing prostate cancer. J. Nucl. Med. 47, 492–501.
Zhang, Y.-M., Tung, C.H., He, J., Liu, N., Yanachkov, I., Liu, G., Rusckowski, M., Vanderheyden, J.L., 2006b. Construction of a novel chimera consisting of a chelator-containing Tat peptide conjugated to a morpholino antisense oligomer for technetium-99m labeling and accelerating cellular kinetics. Nucl. Med. Biol. 33, 263–269.

Multifunctional Targeted Radiotherapy System for Induced Tumours Expressing Gastrin-releasing Peptide Receptors

Nallely Jimenez-Mancilla[1,2], Guillermina Ferro-Flores[1]*, Blanca Ocampo-Garcia[1], Myrna Luna-Gutierrez[1,2], Flor De Maria Ramirez[1], Martha Pedraza-Lopez[3] And Eugenio Torres-Garcia[2]

[1]*Instituto Nacional de Investigaciones Nucleares, Estado de México, Mexico;* [2]*Universidad Autónoma del Estado de México, Mexico;* [3]*Instituto Nacional de Ciencias Médicas y Nutrición Salvador Zubirán, Mexico*

Abstract: The gastrin-releasingpeptide receptor (GRP-r)is overexpressed in breast and prostate cancer, and Lys^3-bombesin is a peptide that binds with high affinity to the GRP-r. HIV Tat(49-57) is a cell-penetrating peptide that reaches the DNA. In cancer cells,^{177}Lu shows efficient crossfire effect, while^{99m}Tc that is internalised to cancer cell nuclei acts as an effective system of targeted radiotherapy because of the Auger and IC electron emissions near the DNA. The aim of this research was to prepare a multifunctional system of ^{177}Lu- and ^{99m}Tc-labelled gold nanoparticles (AuNPs) that were conjugated to Tat(49-57)-Lys^3-bombesin (Tat-BN) and to evaluate the radiation absorbed dose to GRP receptor-positive PC3 tumours that were induced in mice. Cys-Gly-Cys-Tat-BN (CGC-Tat-BN), 1,4,7,10-tetraazacyclododecane-N',N",N"'-tetraacetic-Gly-Gly-Cys (DOTA-GGC)andhydrazinonicotinyl-Phe-Cys-Phe-Trp-Lys-Thr-Cys-Thr-ol (HYNIC-TOC) peptides were conjugated to AuNPs to prepare a multifunctional system by means of a spontaneous reaction of the thiol groups of cysteine. TEM, UV-Vis, XPS and Far-IR spectroscopy techniques demonstrated that AuNPs were functionalised with peptides through interactions with the-SHgroups. The^{99m}Tc labelling was performed via the HYNIC-TOC ligand, and the^{177}Lu labelling was performed through DOTA-GGC. The radiochemical puritywas 96 ± 2%. The ^{177}Lu-absorbed doseper injected activity that wasdelivered to the PC3 tumours was 7.9 Gy/MBq, and the ^{99m}Tc-absorbed dose that was delivered to the nuclei was 0.53 Gy/MBq. The ^{177}Lu/^{99m}Tc-AuNP-Tat-BN system showed properties suitable for a targeted radionuclide therapy of tumours expressing GRPreceptors due to the energy deposition from β-emissions and the Auger and IC electron emissions near the DNA.

Keywords: ^{177}Lu-gold nanoparticles; radiolabelled gold nanoparticles; radiolabelled Lys^3-bombesin-Tat(49-57); targeted radiotherapy; ^{99m}Tc-gold nanoparticles.

1. INTRODUCTION

The objective of targeted radiotherapies for cancer is to deliver a maximum radiation dose to tumours in a selective and localised manner, thereby generating a therapeutic effect through the energy deposition from charged particle emissions. The radionuclide^{177}Lu has a half-life of 6.71 d and a β_{max}emission of 0.497MeV (78%), andit has been successfully used for radiopeptide therapy with an efficient crossfire effect in cancer cells [1-4]. At the single-cell level, short-range charged particles, such as internal conversion (IC) electrons and Auger electrons, impart a dense ionising energy deposition pattern that is associated with an increased radiobiological effectiveness [5]. The^{99m}Tc that is internalised in cancer cell nuclei acts as an effective system of targeted radiotherapy because of the delivery of Auger energy (0.90 keV/decay) and IC electron energy (15.40 keV/decay) near the DNA [6].

The gastrin-releasingpeptide receptor (GRP-r) is overexpressed in breast and prostate cancer. Lys^3-bombesin is a peptide that binds with high affinity to theGRP-r [7-9]. Current challenges include conjugating biomolecules with cell-penetrating peptides and/or nuclear localisation peptide sequences (NLSs) to promote their internalisation and routing to the cell nucleus. Tat(49-57) is a peptide derived from thetransactivator of transcription protein of the HIV-1 virus that has a membrane translocation domain and an NLS [10,11]. Recently, Santos-Cuevas *et al.* [12,13] reported that the ^{99m}Tc-Tat(49-57)-Lys^3-Bombesin (^{99m}Tc-Tat-BN) was a new hybrid radiopharmaceutical that was internalised into the nuclei of prostate and breast cancer cells.

*Address correspondence to this author at the Departamento de Materiales Radiactivos, Instituto Nacional de Investigaciones Nucleares, Carretera México-Toluca S/N., La Marquesa, Ocoyoacac, Estado de México., C.P. 52750, México; Tel: + (52) (55)-53297200 ext. 3863; Fax: + (52) (55)-53297306; E-mail: ferro_flores@yahoo.com.mx; guillermina.ferro@inin.gob.mx

Several studies have demonstrated that conjugating peptides to gold nanoparticles (AuNPs) produces biocompatible and stable multimeric systems with target-specific molecular recognition [14-24]. Peptides can be conjugated to one AuNP by a spontaneous reaction of the AuNP surface with a thiol (cysteine) or an amine [16, 25].

The aim of this research was to prepare a multifunctional system of ^{177}Lu- and ^{99m}Tc-labelled gold nanoparticles (AuNPs) that were conjugated to Tat(49-57)-Lys^3-bombesin (^{177}Lu/^{99m}Tc-AuNP-Tat-BN) and to evaluate the radiation absorbed dose toGRP receptor-positive PC3 tumours that were induced in mice.

2. MATERIALS AND METHODS

Reagents. N,N-dimethylacetamide (DMA), tert-butyl bromoacetate, N,N-diisopropylethylamine (DIPEA), diisopropylcarbodiimide (DIC), dimethylformamide (DMF),dichloromethane (DCM), 2-(1H-benzotriazole-1-yl)-1,1,3,3-tetramethyluronium hexafluorophosphate (HBTU), hydroxybenzotriazole (HOBt),Fmoc-cys-Trt-OH, Fmoc-gly, 20-nm gold nanoparticles and other reagents were purchased from the Sigma-Aldrich Chemical Co. and used as received.Rink Amide MBHA was obtained from Novabiochem.

2.1. Synthesis of Peptides

2.1.1. Tat(49-57)-Lys^3-bombesin (Tat-BN)

The Tat(49-57) peptide (H-Arg-Lys-Lys-Arg-Arg-Gln-Arg-Arg-Arg-NH_2) was conjugated to Gly-Gly-Cys-Gly-Cys(Acm)-Gly-Cys(Acm)-NH_2 to produce the Tat(49-57)-spacer-GCGC peptide (H-Arg^1-Lys^2-Lys^3-Arg^4-Arg^5-Gln^6-Arg^7-Arg^8-Arg^9-Gly^{10}-Gly^{11}-Cys^{12}-Gly^{13}-Cys^{14}(Acm)-Gly^{15}-Cys^{16}(Acm)-NH_2). The sequence Gly^{13}-Cys^{14}-Gly^{15}-Cys^{16} was added for use as the specific chelating site by theAuNPs Fig. (1). The Lys^3-bombesin (Pyr-Gln-Lys-Leu-Gly-Asn-Gln-Trp-Ala-Vla-Gly-His-Leu-Met-NH2) was conjugated to a maleimidopropyl moiety through Lys^3, and the maleimidopropyl group was used as the branch position to form a thioether with the Cys^{12} side chain of the Tat(49-57)-spacer-GCGC

1573-4137/12 $58.00+.00

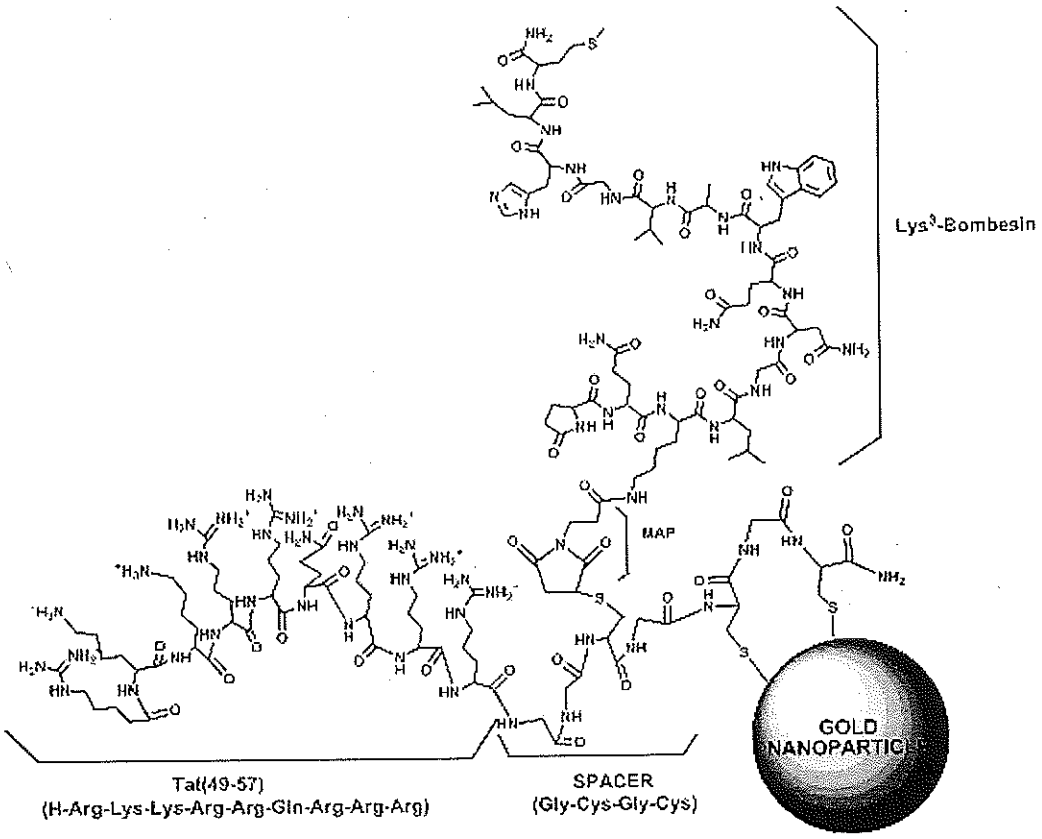

Fig. (1). General scheme of the Tat(49-57)-Lys³-Bombesin (Tat-BN) hybrid peptide conjugated to gold nanoparticles.

peptide Fig. (1). The synthesis, high-performance liquid chromatography (HPLC) analysis, matrix-assisted laser desorption/ionisation mass spectral analysis (MALDI), amino acid analysis and peptide content determination were carried out in the Bachem Laboratories (Bachem, California,USA) to ultimately obtain a certified white powder product with a chemical purity of more than 90% and a molecular weight of 3779.5 g/mol.

2.1.2. DOTA-GGC (1,4,7,10-tetraazacyclododecane-N',N'',N'''-tetraacetic-Gly-Gly-Cys)

*DO3A-tris-tertBu ester:*Tert-butyl bromoacetate (24.52 g, 0.12 mol) in DMA (50 mL) was added dropwise to a stirred DMA suspension (100 mL) containing cyclen (7.22 g, 0.04 mol) and sodium acetate (10.31 g, 0.12 mol) at 0°C. After the addition, the reaction mixture was stirred at room temperature for 2 days. Water (Milli-Q grade) was added until all solids were dissolved, yielding a light yellow solution. The pH of thesolution was adjusted to 9.0 by the addition of Na_2CO_3, and a precipitate was formed. Then,KBr (7.25 g) was added, and the resultant suspension was stirred for 2 d, which was followed by theaddition of ether (5 mL). The obtained white solid was filtered out,added to a 3 M NaOH solution (aqueous phase) and extracted with dichloromethane (2x, organic phase). The organic extract was then dried over anhydrous K_2CO_3 and filtered, and the solvent was evaporated on a rotary evaporator, yielding a light yellow oil 16.42 g (reaction yield=76%). The resulting product had the following properties: 1H NMR (200 MHz, $CDCl_3$): δ 1.45 (9H, s, ^{t}but), 1.46 (18H, s, ^{t}but), 2.92 (4H, sa, N-CH_2-CH_2-N)), 3.11(12H, sa, N-CH_2-CH_2-N), 3.29 (2H, s, N-CH_2-CO), 3.38 (4H, s, N-CH_2-CO) and ^{13}C NMR (50 MHz, $CDCl_3$): δ 28.2, 28.3, 47.6, 50.8, 52.33, 57.2, 80.8, 80.8, 171.2, 171.34. ES-MS [M+H]+=516 (Calc. 516).

DOTA-GGC: The peptide was synthesised on Rink Amide MBHA (with a 0.64 mmol/g resin load) at a 0.14 mmol scale. The resin was placed in a peptide reaction vessel and swelled in DMF. Aminoacids were attached by using single-step couplings with 5 equiv. of Fmoc-amino acid, 4.9 equiv. of HBTU and HOBt, and 6 equiv. of DIPEA in DMF in the order Fmoc-Cys-Trt-OH, Fmoc-Gly and Fmoc-Gly for 2 h each. Fmoc removal was performed by shaking the resin with 20 % piperidine in DMF for 30 min after aminoacid coupling. The resin was thoroughly washed with DMF after each step. The reaction progress was monitored by a ninhydrin test. After the last aminoacid couplingresin was treated with a DMF solution containing 2 M bromoacetic acid and 3.2 M DIC in DMF, the coupling was performed in a microwave oven set to deliver 10% power (2 × 15 s). After washing the resin with DMF, the reaction vessel was treated with DO3A-tris-tertBu ester (2.64 g, 5 mmol) and DIPEA (0.76 g, 6 mmol) in DMF, and the coupling was again performed in the microwave oven as described above. Once the peptide synthesis ended, the resin was washed with DMF and DCM and dried under a vacuum. Beads were then treated with a 95 % TFA, 2.5 % triisopropylsilane, and 2.5 % water mixture for 2 h to remove the side chain protection groups and the peptide from the resin. The resin was filtered out, and the acid from the filtrate was removed under a nitrogen flow. The residue was dissolved in 0.1 % TFA, and the product was purified by HPLC with a gradient of water/acetonitrile containing 0.1 % TFA from 95/5 to 80/20 over 35 min and lyophilised. Sixty milligrams of the peptide was obtained (reaction yield=69 %) with the following properties:t_R=4.4 min andm/z (MALDI+) m/z = 621.12 $[M+H]^+$(calc. 621.68).

2.1.3. HYNIC-TOC Lyophilised Formulations

The HYNIC-TOC peptide conjugate (hydrazinonicotinyl-D-Phe-Cys-Tyr-D-Trp-Lys-Thr-Cys-Thr(ol); MW 1170.29 g/mol) was synthesised by PiChem (Graz, Austria) with a purity > 98 %, as analysed by reversed phase HPLC (RP-HPLC) and mass spectrometry.

HYNIC-TOC lyophilised formulations were prepared as described by Ocampo-Garcíact *et al.* [26]. Briefly, 0.5 mg of HYNIC-TOC was dissolved in 1 mL of 10% ethanol,which was then added to a solution of EDDA-Tricine-Mannitol that had previously been prepared by mixing 1 g of EDDA (ethylenediamine-N,N'-diacetic acid), 2 g of tricine (N-tris-[hydroxymethyl]-methylglycine) and 2 g of mannitol in 97 mL of sterile apyrogenic water while stirring over low heat. Subsequently, 2 mL of a freshly prepared stannous chloride solution (1 mg/mL in 0.012 M HCl) was added under a nitrogen atmosphere. The mixture was sterilised by membrane filtration (Millipore; 0.22 μm), and 1.0 mL was dispensed into pre-sterilised serum vials and lyophilised for 24 h.

Additionally, 100 mL of a 0.2 M phosphate buffer solution, pH 7, was prepared under aseptic conditions and sterilised by membrane filtration (Millipore; 0.22 μm). A total of 5 mL of phosphate buffer was dispensed into pre-sterilised serum vials and stored at 4°C.

2.2. Conjugation of Peptides to the AuNPs

A 5-μM solution of Tat-BN, DOTA-GGC or HYNIC-TOC was prepared using injectable-grade water, and 0.05 mL of the solution was added to 1 mL of the AuNP solution (20 nm;6.99×10^{11} particles/mL)while stirring for 5 min. Under these conditions, an average of 215 molecules of Tat-BN, DOTA-GGC or HYNIC-TOC were attached per nanoparticle (20 nm; surface area = 1260 nm^2 and 37,000 surface Au atoms). The above peptides were also conjugated to the 5-nmdiameter AuNPs (Sigma-Aldrich; 3×10^{13} particles/mL with a surface area = 79 nm^2 and 951 surface Au atoms) under the same conditions, and it was estimated that 5 peptides were conjugated per AuNP.

2.3. Chemical Characterisation of the AuNP-peptide Conjugates

2.3.1. UV-Vis Spectroscopy

The absorption spectra from 400 to 700 nm were obtained with a Perkin-Elmer Lambda-Bio spectrometer using a 1-cm quartz cuvette. The nanoconjugates were measured by UV--Vis spectroscopy to monitor the shift in the AuNP surface plasmon band (~520 nm).

2.3.2. X-ray Photoelectron Spectroscopy (XPS)

The XPS spectra of AuNPs, DOTA-GGC-AuNP, HYNIC-TOC-AuNP and AuNP-Tat-BN were acquired on a K-Alpha Thermo Scientific spectrometer that was equipped with aMgK_{α} X-ray source (1253.6 eV). The source was operated at 10 kV/20 mA and calibrated using Au $4f_{7/2}$ (84.0 eV) and Ag $3d_{5/2}$ (368.2 eV) from foil samples. The samples were introduced into the ultra-high vacuum (UHV) chamber of the spectrometer (5×10^{-9} torr) and measured at 24°C (room temperature). The spot size of the beam was 100 μm. The pressure did not change during the analysis, and 20 scans for Au 4f were performed with an energy step size of 0.1 eV. The binding energies were referenced to the C1s peak at 284.3 eV. A Shirley background was subtracted from all of the spectra to perform peak fitting with a symmetric Gaussian-Lorentzian sum function (SpecSurf software).

2.3.3. Far-Infrared

The far-infrared spectra of the AuNP-conjugates were acquired on a Perkin Elmer spectrometer (Spectrum 400) with an ATR platform (Diamond GladiATR, Pike Technologies) using attenuated total reflection Fourier transform infrared (ATR-FTIR) spectroscopy from 200 to 300 cm^{-1}.

2.4. Preparation of ^{177}Lu-DOTA-GGC

A 5-μL aliquot of DOTA-GGC (1 mg/mL) was diluted with 50 μL of 1M acetate buffer at pH 5, which was followed by the addition of 7 μL of the $^{177}LuCl_3$ (~370 MBq, >3 TBq/mg, IRE, ELiT, Belgium) solution. The mixture was incubated at 90°C in a block heater for 30 min. All solutions were prepared using deionised water. A radiochemical purity >98 % was verified by TLC silica gel plates (aluminium backing, Merck).Ten-centimetre strips were used as the stationary phase and ammonium hydroxide:methanol:water (1:5:10) was used as the mobile phase to determine the amount of free ^{177}Lu (R_f=0) and ^{177}Lu-DOTA-GGC (R_f=0.4–0.5). The radiochemical purity was also determined by reverse phase HPLC on a C-18 column (μ-Bondapack C-18, Waters) using the Waters Millennium system with an in-line radioactivity detector and a gradient of water/acetonitrile containing 0.1 % TFA from 95/5 to 20/80 over 35 min at 1 mL/min ($^{177}LuCl_3$ t_R=3 min; ^{177}Lu-DOTA-GGC t_R=16 min).

2.5. Preparation of ^{99m}Tc-HYNIC-TOC

The ^{99m}Tc-pertechnetate was obtained from a GETEC ^{99}Mo/^{99m}Tc generator (ININ-Mexico). The ^{99m}Tc-EDDA/HYNIC-TOC was prepared by adding 1 mL of 0.2 M phosphate buffer, pH 7.0, that was followed immediately by 4 GBq (1 mL) of ^{99m}Tc-pertechnetate to the HYNIC-TOC freeze-dried kit formulation, which was then incubated at 92°C for 20 min in a dry block heater. A radiochemical purity >95 % of ^{99m}Tc-HYNIC-TOC was verified by ITLC-SG (Gelman Sciences, Pall Corporation, Port Washington, New York, USA) analyses using three mobile phases, 2-butanone to determine the amount of free $^{99m}TcO_4^-$ (R_f=1); 0.1 M sodium citrate, pH 5, to determine ^{99m}Tc-EDDA and $^{99m}TcO_4^-$ (R_f=1); and a 1:1 (v/v) methanol:1 M ammonium acetate solution for ^{99m}Tc-colloids (R_f=0), andthe R_f values of the radiolabelled peptide in these three systems were 0.0, 0.0 and 0.7–1.0, respectively.

2.6. Preparation of the ^{177}Lu/^{99m}Tc-AuNP-Tat-BN Multifunctional System

To 1 mL of AuNP (20 nm or 5 nm), 0.025 mL of Tat-BN (5 μM; 108 molecules per 20-nm nanoparticle and 2 molecules per 5-nmAuNP) was added that was followed by 25 μL (50 MBq) of ^{99m}Tc-HYNIC-TOC (0.063 μg of peptide; 3×10^{13} molecules; 43 molecules per 20-nmAuNP and 1 molecule per 5-nmAuNP) and 3 μL (18.5 MBq) of ^{177}Lu-DOTA-GGC (0.25 μg of peptide; 1.89×10^{14} molecules; 270 molecules per 20-nmAuNP and 6 molecule per 5-nmAuNP) with stirring for 5 min to form the ^{177}Lu/^{99m}Tc-AuNP-Tat-BN system Fig. (2). No further purification was performed.

Additionally, ^{177}Lu/^{99m}Tc-labelled AuNPs were prepared as described above but without the Tat-BN for comparative *in vivo* studies. The^{99m}Tc-Tat-BN was also prepared as previously reported [12].

The number of peptides per nanoparticle was corroborated by UV-Vis titration of peptides (8 μM) using increasing concentrations of gold nanoparticles (from 0 to 1 nM), as previously reported [21].

2.7. Radiochemical Purity

Size-exclusion chromatography and ultrafiltration were used as radiochemical control methods for the final radiopharmaceutical solution. A 0.1-mL sample of ^{177}Lu/^{99m}Tc-AuNP-Tat-BN was loaded into a PD-10 column, and injectable water was used as the eluent. The first radioactive and red eluted peak (3.0–4.0 mL) corresponded to the radiolabelled AuNP-Tat-BN. The free radiolabelled peptides appeared in the 5.0–7.0 mL eluted fraction, and $^{99m}TcO_4^-$and$^{177}LuCl_3$remained trapped in the column matrix. Using ultrafiltration (Centricon YM-30 regenerated cellulose 30,000 MW cut-off; Millipore, Bedford, MA, USA), the ^{177}Lu/^{99m}Tc-AuNP-Tat-BN remained in the filter, while free ^{99m}Tc-HYNIC-TOC, ^{177}Lu-

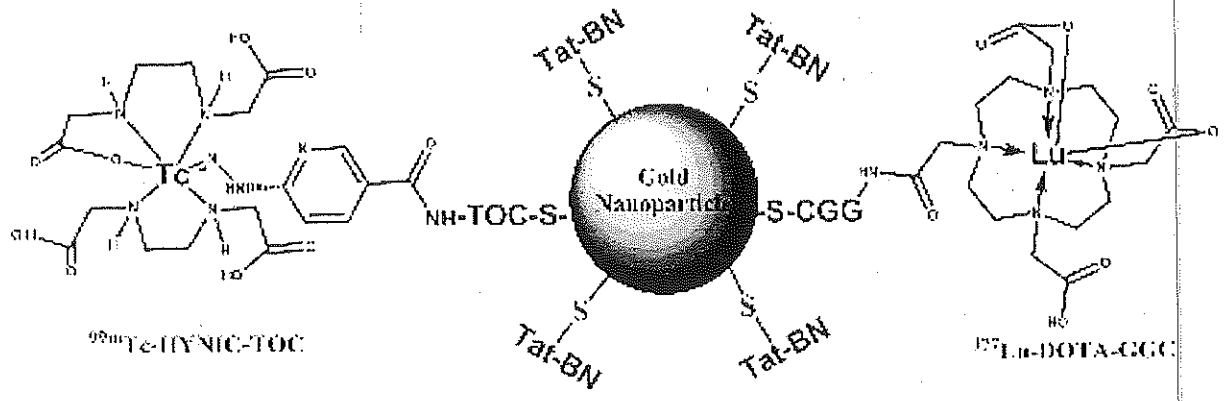

Fig. (2). Overall scheme of the multifunctional system of ^{177}Lu- and ^{99m}Tc-labelled gold nanoparticles (AuNPs) conjugated to Tat(49-57)-Lys^3-bombesin (^{177}Lu/^{99m}Tc-AuNP-Tat-BN).

DOTA-GGC, $^{177}LuCl_3$ and $^{99m}TcO_4^-$ passed through the filter. The activity was determined by using a well-type scintillation detector (Canberra), and the radiochemical purity (% R.P.) was estimated as follows:

$$\%\ R.P. = \frac{Activity\ in\ the\ filter}{Activity\ in\ the\ filter + Activity\ in\ the\ filtered\ solution} X100$$

In the radio-HPLC size exclusion system (ProteinPak 300SW, Waters; 1 mL/min with injectable water), the t_Rs for the ^{177}Lu/^{99m}Tc-AuNP-Tat-BN, ^{99m}Tc-HYNIC-TOC, ^{177}Lu-DOTA-GGC and $^{99m}TcO_4^-$ were 4.5–5, 8, 7.8 and 11 min, respectively.

2.8. Biological Evaluation

2.8.1. Cell lines

The human prostate cancer cell line PC3 was originally obtained from the American Type Culture Collection (USA). The cells were grown at 37°C with a 5 % CO_2 atmosphere and 100% humidity in RPMI medium supplemented with 10 % newborn calf serum and antibiotics (100 μg/mL streptomycin).

2.8.2. Animal Model

Tumour uptake and biodistribution studies in mice were carried out according to the rules and regulations of the Official Mexican Norm 062-ZOO-1999.

Athymic male BALB/c (nu/nu) mice (20-22 g) were kept in sterile cages with sterile wood-shavings for bedding at a constant temperature, humidity and noise level and a 12:12 light:dark period. Water and food (standard PMI 5001 feed) were given ad libitum.

2.8.3. Tumour Induction in Athymic Mice

Prostate tumours were induced by a subcutaneous injection of PC3 cells (1 X 10^6) resuspended in 0.2 mL of phosphate-buffered saline into the backsides of 6- to 7-week-old nude mice. The sites of injection were inspectedat regular intervals for tumour formation and progression. The type and size of the tumours play an important role in the radiopeptide uptake; therefore, after 9 days, only the mice with tumours between 0.5 and 0.6 g were usedtodecrease the biological variability.

2.8.4. Biodistribution

Athymic mice with induced tumours received the^{177}Lu/^{99m}Tc-AuNP-Tat-BN (0.05 mL; ~2.5 MBq of ^{99m}Tc and ~1 MBq of ^{177}Lu;AuNP=5 nm) by intratumoural injection. The mice were sacrificed at 0.5, 1, 3, 24, 48, 72 or96 h (n=3 at each time point) after the radiopharmaceutical administration. The whole heart, spleen, pancreas, liver, lung, kidneys and tumour and samples of the blood, intestines, bone and muscle were rinsedwith saline, blotted with paper and placed into pre-weighed plastic test tubes. The activity was determined in a well-type scintillation detector (Canberra) along with 3 x 0.5-mL aliquots of the diluted standard (^{177}Lu/^{99m}Tc-AuNP-Tat-BN, 0.05 mL; ~2.5 MBq of ^{99m}Tc and ~1 MBq of ^{177}Lu), which represented 100% of the injected dose, to obtain the activity corrected by decay. Mean activities were used to obtain the percentage of injected dose per gram of tissue (% ID/g) or % ID per organ.

A blocking study was performed in three mice with PC3-induced tumours. One hundred microlitres (0.1 mM) of unlabelled Lys^3-bombesin (Bachem) was intraperitoneally administered one hour before theintratumouralinjection (n=3) of ^{177}Lu/^{99m}Tc-AuNP-Tat-BN (0.05 mL; ~2.5 MBq of ^{99m}Tc and ~1 MBq of ^{177}Lu), and complete dissections were performed 1 h after the radiopharmaceutical administration, as described above.

The ^{177}Lu/^{99m}Tc-AuNP and^{99m}Tc-Tat-BN were also administered by an intratumoural injection in athymic mice with PC3-induced tumours, and complete dissections were performed at 1, 3 or24 h after the administration (n=3).

2.8.5. Biokinetic Model and Radiation Absorbed dose Estimation

The percentages of the injected dose at different times in the liver, kidney, spleen and tumour were used to derive the ^{177}Lu/^{99m}Tc-AuNP-Tat-BN time activity curves that were corrected for decay [$q_k(t) = A_k(t)e^{\lambda_R t}$] and that represent the biological behaviour in each organ. The $A_h(t)$ functions were thenobtained for ^{177}Lu [$A_k(t) = q_k(t)e^{-\lambda_{Lu-177}t}$] and ^{99m}Tc [$A_k(t) = q_k(t)e^{-\lambda_{Tc-99m}t}$] separatelyand then were integrated over time to give the total number of disintegrations (N)of each radionuclide in the source regionsnormalised to the unit of administered activity (MBq) (Table 2).

$$N_{source} = \int_{t=0}^{t=\infty} A_h(t)dt \quad (1)$$

The absorbed dose of the organs was evaluated according to equation 2:

$$\bar{D}_{target \leftarrow source} = \sum_{sources} N_{source} \times DF_{target \leftarrow source} \quad (2)$$

where $\bar{D}_{target \leftarrow source}$ is the mean absorbed dose to a target organ from a source organ and $DF_{target \leftarrow source}$ is a dose factor (equation 3).

$$DF_{target \leftarrow source} = \sum_i \Delta_i \Phi_{i\,(target \leftarrow source)} \quad (3)$$

The Δ_i term is the mean energy emitted per disintegration for the various i-type radiations (i-type emissions, $\sum n_i E_i$). The Φ_i term is the absorbed fraction that is dependent on the properties of the i-type emission and the size, shape, and separation of the source and target organs. DF values were calculated as reported by Miller *et al.* [27] using the beta-absorbed fractions in a mouse model as calculated by two Monte Carlo radiation transport codes, MCNP4C and PEREGRINE (voxel-based).

2.9. Statistical Analysis

Comparisons between groups in the blocking assay and for tumour uptake were made using Student's t-test (significance was defined as $P < 0.05$).

3. RESULTS

UV–Vis spectroscopy. The 20-nm AuNP spectrum showed a surface plasmon resonance (SPR) at 520 nm, and the 5-nm AuNPs exhibited an SPR at 523 nm. A red shift to 522 nm or 524 nm for the 20- or 5-nm AuNPs, respectively, was observed in the HYNIC-TOC-AuNP, DOTA-GGC-AuNP and AuNP-Tat-BN spectra due to changes in the refraction index and the surrounding dielectric medium as a consequence of the interactions between the peptides and the AuNP surfaces [28].

XP spectroscopy. The AuNP spectrum Fig. (3) showed two main peaks that corresponded to the binding energies (B.E.; eV) of electrons in the Au 4f orbitals at 87.5 eV ($Au4f_{5/2}$) and 83.8 eV ($Au4f_{7/2}$), with a characteristic difference of 3.6 eV and an intensity ratio of 3:4 between the two peaks. The AuNP-Tat-BN deconvoluted spectrum Fig. (3) displayed a peak at 84.7 eV, with a positive shift of 0.9 eV with respect to the Au $4f_{7/2}$ of the AuNPs. The peak that correlated with the Au $4f_{5/2}$ orbital appeared at 88.4 eV. The HYNIC-TOC deconvoluted spectrum reveals positive shifts at 87.9 eV ($Au4f_{5/2}$) and 84.3 eV ($Au4f_{7/2}$) with respect to the AuNPs. The orbital energies of the Au-Au or AuNP (Au^0) and Au-S (Au^{+1}) bonds are related to changes in the oxidative states (Au^0 to Au^{+1}); therefore, a shift of the electron-binding energies to higher values in the AuNP-Tat-BN and HYNIC-TOC-AuNP is an intrinsic property of the interaction between the gold core electrons and the peptides [28]. The XP spectrum confirms that the AuNP-Tat-BN bond has an important covalent character thatstabilises it because only a negligible amount of other species is found. In the XP-spectrum of the DOTA-GGC-AuNP, the shift of electron-binding energies to higher values but with a low intensity indicates that more than one type of interaction of the NH_2 (belonging to the amide group) with the Au–surface or the citrate-Au is possibly occurring, with the NH_2 groups also potentially forming hydrogen bonds. There was no difference between the 5-nm and 20-nm AuNP-conjugate spectra.

Far-IR spectroscopy. The AuNP-Tat-BN, DOTA-GGC-AuNP and AuNP-TOC showed a characteristic band at 279 ± 1 cm^{-1}, which was assigned to the Au-S bond [29] Fig. (4). However, the DOTA-GGC-AuNP band at 278 cm^{-1} is of low resolution with respect to that of the AuNP-Tat-BN at 280 cm^{-1}, which supports the idea that the Au-S bond in the DOTA-GGC-AuNP conjugate is not the only type of interaction with AuNP. In agreement with previous reports, at least three main peaks of the $\nu_{Au\text{-}S}$ were found in the range of 200-280 cm^{-1}, which was attributed to multiple adsorption sites [29, 30]. There was no difference between the 5-nm and 20-nm AuNP-conjugate spectra.

The radiochemical purity of the $^{177}Lu/^{99m}Tc$-AuNP-Tat-BN multifunctional radiopharmaceutical was determined by size exclu-

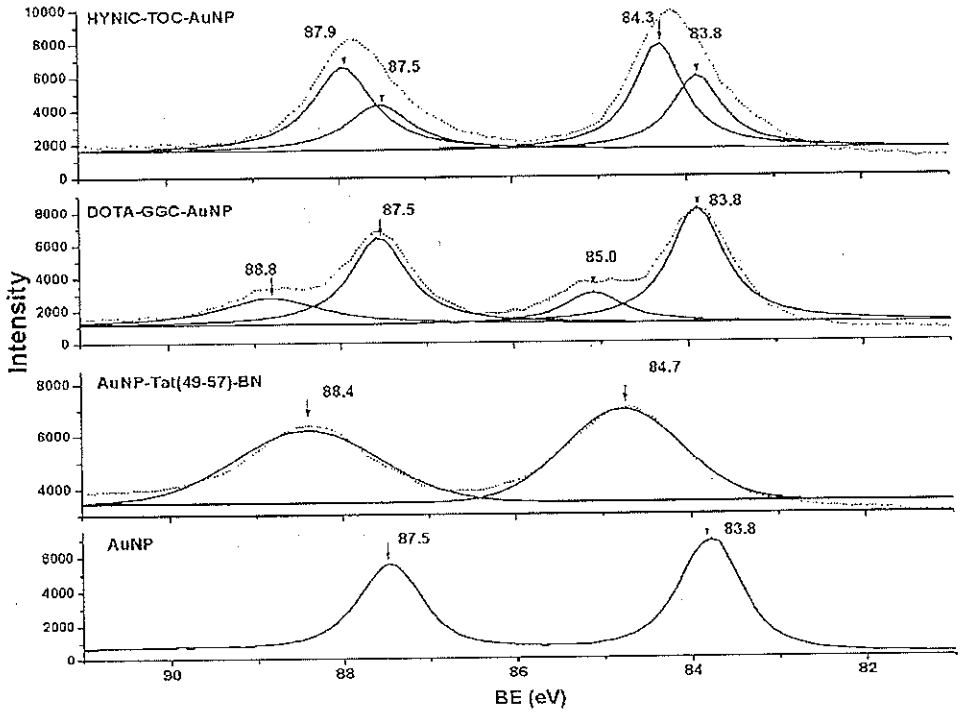

Fig. (3). The XPS spectra of AuNPs, AuNP-Tat-BN, DOTA-GGC-AuNP and HYNIC-TOC-AuNP. The experimental bands are represented by dotted lines, and the deconvoluted experimental bands are represented by solid lines.

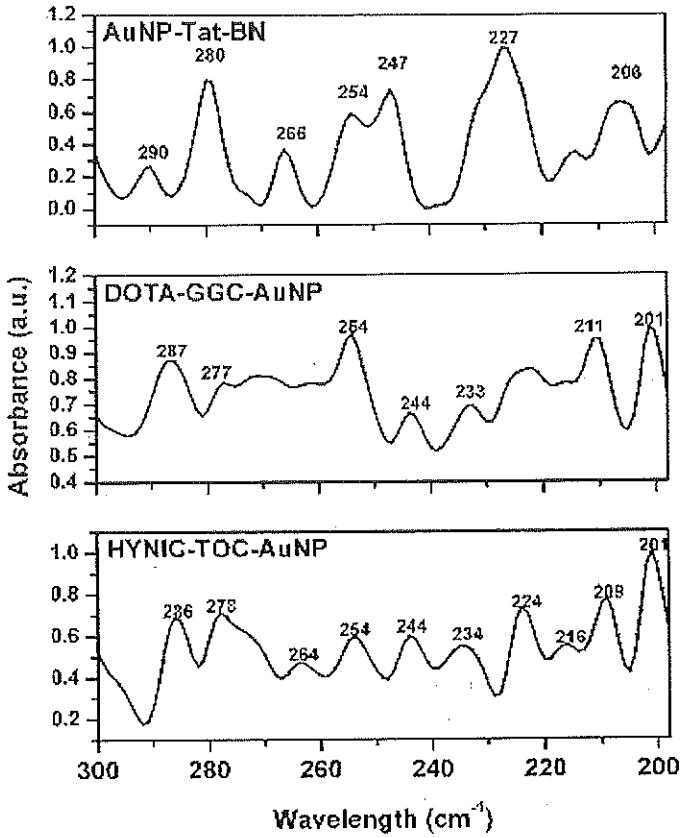

Fig. (4). The far-infrared spectra of AuNP-Tat-BN, DOTA-GGC-AuNP and HYNIC-TOC-AuNP.The characteristic band at 279 ± 1 cm^{-1}that is assigned to the Au-S bond can be observed.

sion chromatography and ultrafiltration to be 96 ± 2 %. No further purification was necessary, and after 8 d, the radiochemical purity decreased to 93 ± 3 % at room temperature (20°C). Previously, we had demonstrated that radiolabelled gold nanoparticles conjugated to peptides were stable in human serum [20,21].

Biodistribution studies showed that over 40 % of the $^{177}Lu/^{99m}Tc$-AuNP-Tat-BN remains in the tumour 24 h after the intratumoural administration (Table 1). The specificity was confirmed by a receptor blocking study, in which a previous injection of Lys^3-bombesin significantly diminished ($P<0.05$) the activity in the tumours, pancreas and intestine (Table 1) thereby demonstrating an ability to target *in vivo* GRP receptor-bearing cells. A recent studyfound that more than 300,000 bombesin receptor sites per cell are available in themouse pancreas and that prostate tumour PC3 cells have 44,000 receptor sites per cell [24]. The significant but minor uptake in the liver, intestine and bone could be related to the biological variability.

Tumour uptake of the $^{177}Lu/^{99m}Tc$-AuNP-Tat-BN multifunctional system was significantly higher than that of the $^{177}Lu/^{99m}Tc$-AuNP or ^{99m}Tc-Tat-BN Fig. (5). The $^{177}Lu/^{99m}Tc$-AuNP accumulation (27.32 ± 2.89 % at 1 h) in PC3 tumours was related to a passive uptake. Passive targeting depends on the accumulation of AuNPs in the tumours due to extravasations through leaky blood vessels (gaps - 100-800 nm), but with the conjugation of Tat-BN to the AuNPs, the tumour uptake was significantly increased (58.43 ± 6.19 % at 1h). The significant difference in tumour uptake results (27.32 % vs. 58.43 %) was due toactive targeting, suggesting that a specific GRP receptor was recognised.

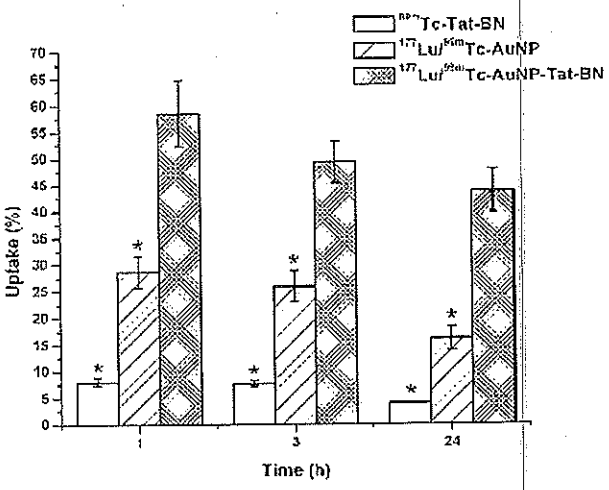

Fig. (5). Tumour uptake of ^{99m}Tc-Tat-BN, $^{177}Lu/^{99m}Tc$-AuNP and $^{177}Lu/^{99m}Tc$-AuNP-Tat-BN at 1, 3 and 24 h after intratumoural administration. *Statistically significant difference ($P<0.05$) vs. $^{177}Lu/^{99m}Tc$-AuNP-Tat-BN.

The$^{177}Lu/^{99m}Tc$-AuNP-Tat-BN showed a biological residence time of 80.6 h (Table 2). The radiation absorbed doses from ^{177}Lu and ^{99m}Tc to the tumour after normalisation to the unit of administered activity were 7.90 ± 0.95 Gy/MBq and 0.07 ± 0.01 Gy/MBq, respectively. The absorbed doses to the kidney, liver and spleen were0.80 ± 0.11, 0.18 ± 0.04 and 0.49± 0.09 Gy/MBq, respectively.

Table 1. The biodistribution in mice with PC3-induced tumours after an intratumoural administration of ^{99m}Tc- and ^{177}Lu-labelled gold nanoparticles conjugated to Tat(49-57)-Lys^3-Bombesin, which is expressed as a percentage of the injected dose per gram of tissue (% ID/g^{++}) or a percentage of the injected dose per organ (%ID^{+}) (mean ± SD, n=3).

TISSUE	Unblocked							Blocked[a]
	0.5 h	1 h	3 h	24 h	48 h	72 h	96 h	1 h
Blood^{++}	0.96 ± 0.17	0.37 ± 0.02*	0.46 ± 0.07	0.04 ± 0.03	0.03 ± 0.02	0.04± 0.02	0.02 ± 0.02	2.07 ± 0.98*
Heart^{+}	0.24 ± 0.09	0.18 ± 0.06	0.10 ± 0.08	0.00 ± 0.00	0.00 ± 0.00	0.00 ± 0.00	0.00 ± 0.00	0.93 ± 0.17
Lung^{+}	0.70 ± 0.13	0.51 ± 0.09	0.23 ± 0.04	0.05 ± 0.02	0.01 ± 0.01	0.00 ± 0.00	0.00 ± 0.00	1.24 ± 0.06
Liver^{+}	2.32 ± 0.16	2.37 ± 0.18	2.59 ± 0.04	1.23 ± 0.42	0.98 ± 0.23	0.93 ± 0.27	1.04 ± 0.18	3.96 ± 0.28
Pancreas^{+}	0.10 ± 0.05	1.46 ± 0.21	1.18 ± 0.14	0.88 ± 0.26	0.69 ± 0.12	0.18 ± 0.09	0.11 ± 0.04	0.83 ± 0.10
Spleen^{+}	0.21 ± 0.05	0.98 ± 0.17	1.79 ± 0.14	0.94 ± 0.64	0.71 ± 0.18	0.24 ± 0.08	0.21 ± 0.11	0.37 ± 0.22
Kidneys^{+}	5.01 ± 0.23	3.14 ± 0.12	4.90 ± 0.10	1.98 ± 0.22	1.23 ± 0.15	0.95 ± 0.10	0.87 ± 0.09	5.13 ± 1.03
Intestine^{++}	0.27 ± 0.14	0.78 ± 0.09	0.92 ± 0.14	0.38 ± 0.13	0.22 ± 0.11	0.09 ± 0.05	0.07 ± 0.01	0.39 ± 0.15
Muscle^{++}	0.34 ± 0.03	0.12 ± 0.01	0.07 ± 0.02	0.00 ± 0.00	0.00 ± 0.00	0.00 ± 0.00	0.00 ± 0.00	0.68 ± 0.12
Bone^{++}	0.19 ± 0.01	0.16 ± 0.06	0.05 ± 0.03	0.00 ± 0.00	0.00 ± 0.00	0.00 ± 0.00	0.00 ± 0.00	0.67 ± 0.21
PC3 Tumour^{+}(Average mass=0.5 g)	63.13±12.92	58.43±6.19*	49.22±3.92	43.73±4.07	35.85±3.83	31.58±4.12	27.69±3.19	39.19±5.04*

[a]Blocked with an additional intratumoural cold Lys^3-Bombesin blocking dose 1 h prior to the administration of ^{177}Lu/^{99m}Tc-AuNP-Tat(49-57)-Lys^3-Bombesin to determine the non-specific binding of the radioactivity.

*Significant difference (P< 0.05) between unblocked and blocked GRPreceptors.

In agreement with Santos-Cuevas *et al.* [13], 4,696,423 PC3cells were calculatedto form a 0.5-g tumour. After a 1MBq administration of ^{99m}Tc-AuNP-Tat-BN, the activity per cell would be 0.213 Bq/cell, and using the biokinetic subcellular model previously reported (Table 2; 2.49 Gy/Bq [13]), the radiation absorbed dose to the PC3 cell nuclei was estimated to be 0.53 Gy per MBq administered into the tumour. Nevertheless, immunofluorescent cell images and kinetic studies on the internalisation of the multifunctional system in PC3 tumour cells have to be accomplished.

4. DISCUSSION

Gold nanorods and silica-gold nanoshells were shown to be useful as photo-absorbing agents in photothermal therapy due to their strong and tunable linear absorption in the NIR region where tissues are optically transparent [31,32]. However, compared to the above nanostructures, spherical gold nanoparticles are particularlyappealing because of the easy methods for their synthesis and bioconjugation. Elbialy *et al.* [33] demonstrated irreversible thermal tumour damage for subcutaneous Ehrlich carcinomas in mice using spherical gold nanoparticles irradiated with a low-power argon laser. The use of gold nanospheres in photothermal cancer therapy can also be performed using short NIR laser pulses to generate a second harmonic or a two-photon absorption process [34]. Second harmonic generation converts the NIR photons into visible photons (400 nm) that are absorbed by the gold nanospheres through the surface plasmon absorption and the electron inter-band transition from the d band to the sp band with the consequential conversion of their energy into heat. NIR photons could also be directly absorbed and converted into heat through a nonlinear two-photon absorption process due to an aggregated alignment of nanoparticles bound to the cancer cells [34].

The goal of radiotherapy with internal emitters is to deliver therapeutic doses to a tumour without affecting healthy organs. The effectiveness of a radiopharmaceutical is a function of the absorbed dose (the mean energy imparted by ionising radiation to the matter or a unit of mass) and the total absorbed-dose rate that is delivered

Table 2. The Radiation Absorbeddose of ^{177}Lu- and ^{99m}Tc-labelled Gold Nanoparticles Conjugated to Tat(49-57)-Lys^3-bombesin (^{177}Lu/^{99m}Tc-AuNP-Tat-BN) in PC3tumoursthat Were Induced in Mice,Which was Normalised to the Unit of Administered Activity

Nuclide	Biokinetic model	$\int_0^{\infty} q_h(t)dt$ Biological residence time (h)	$\int_0^{\infty} A_h(t)dt$ (Total disintegrations)	Absorbed dose(Gy/MBq)
-	$^{*}q_h(t) = 22.5e^{-0.929t} + 49.3e^{-0.006t}$	80.6	-	
^{177}Lu (Tumour)	$A_h(t) = 22.5e^{-0.10t} + 49.3e^{-0.01t}$	-	1.714E11	7.90 ± 0.95
^{99m}Tc (Tumour)	$A_h(t) = 22.5e^{-1.04t} + 49.3e^{-0.12t}$	-	1.548E10	0.07 ± 0.01
^{99m}Tc (Cell nucleus[&])	$A_h(t) = -91.8^{-0.62Bt} + 54.4e^{-0.133t} + 63.9e^{-0.371t}$	-	17826	2.49 ± 0.01[&] (Gy/Bq bound to the cell)

$^{*}q_h(t)$ =activity corrected by decay, biological behaviour[$q_h(t) = A_h(t)e^{\lambda_{ef}t}$]

[&]Data reported by Santos-Cuevas *et al.*, 2011

to the tumour and to the normal tissues. The dose and its rate depend on the injected activity, the kinetics of uptake, the clearance of radioactivity within the tumour and the normal tissues/cells and the physical properties of the radionuclide (type of radiation, range of the emitted particles, etc.) [35]. In the ^{177}Lu/^{99m}Tc-AuNP-Tat-BN multifunctional system reported in this work, the beta particle (^{177}Lu) and the Auger electron (^{99m}Tc) emitters were readily conjugated onto gold nanoparticles with a molecular recognition for GRPreceptors. The linear energy transfer (LET) from beta particles is low, and they traverse several millimetres to deposit their energy over hundreds of cancer cells within the dimensions of the tumour. However, for microscopic tumours, micrometastases or single cancer cells, the low LET of beta particles is inefficient in causing lethal DNA damage or killing cells. In this case, the high LET of the Auger electrons near DNA is more efficient in producing lethal effects in the range of several nanometres. The *in vitro* and *in vivo* absorbed-dose assessments for the dual-labelled multifunctional system indicate a high potential for radiotherapy of tumours, micrometastases and individualcancer cells because the ^{177}Lu absorbed dose per injected activity delivered to the PC3 tumours was 7.9 Gy/MBq and the ^{99m}Tc absorbed dose delivered to nuclei was 0.53 Gy/MBq.

In addition, Berry *et al.* [36] demonstrated that 5-nm nanoparticles pass through the plasma membrane and achieve nuclear entry, while larger 30-nm particles are retained in the cytoplasm, which suggests that nuclear internalisation is blocked via the dimensions of the nuclear pore. Therefore, the ^{177}Lu/^{99m}Tc-AuNP-Tat-BN (5 nm) radiopharmaceutical could be a multifunctional system that is useful for the identification of malignant tumours and metastatic sites during treatment (SPECT imaging), for targeted radiotherapy (high β-particleenergy delivered per unit of targeted mass and Auger and internal conversion electron emissions near DNA) and for photothermal therapy (localised heating). However, for therapeutic purposes, NPs have to be administered by an intratumoural injection or via a selective artery to avoid a high uptake by organs of the reticuloendothelial system because of the colloidal nature of the nanoparticles. An injection of the multifunctional system into an artery of the affected organ would allow for a high uptake toa tumour, possible micrometastasesorindividual cancer cells. Studies on the toxicity, therapeutic efficacy and those to evaluate the potential of ^{177}Lu/^{99m}Tc-AuNP-Tat-BN for photothermal cancer therapy are in progress.

5. CONCLUSIONS

A multifunctional system of ^{177}Lu- and ^{99m}Tc-labelled gold nanoparticles conjugated to Lys^3-bombesin-Tat(49-57) was prepared with high radiochemical purity (>94 %) without post-labelling purification. The ^{177}Lu and ^{99m}Tc-AuNP-Tat-BN radiopharmaceuticals showed properties suitable for a targeted radionuclide therapy of tumours expressing GRPreceptors due to the energy deposition from β-emissions and the Auger and IC electron emissions near the DNA.

ACKNOWLEDGEMENTS

This study was supported by the Mexican National Council of Science and Technology (CONACYT-SEP-CB-2010-01-150942). There are no conflicts of interest.

REFERENCES

[1] Bakker, W.H.; Breeman, W.A.; Kwekkeboom, D.J.; De Jong, L.C.; Krenning, E.P. Practical aspects of peptide receptor radionuclide therapy with [^{177}Lu][DOTA^0,Tyr^3] octreotate. *Q. J. Nucl. Med. Mol. Imaging.*, 2006, *50*, 265-271.

[2] Panigone, S.; Nunn, A.D. Lutetium-177-labeled gastrin releasing peptide receptor binding analogs: a novel approach to radionuclide therapy. *Q. J. Nucl. Med. Mol. Imaging.*, 2006, *50*, 310-321.

[3] Pujatti, P.B.; Santos, J.S.; Couto, R.M.; Melero, L.T.; Suzuki, M.F.; Soares, C.R.; Grallert, S.R.; Mengatti, J.; De Araújo. E.B. Novel series of ^{177}Lu-labeled bombesin derivatives with amino acidic spacers for selective targeting of human PC-3 prostate tumor cells. *Q. J. Nucl. Med. Mol. Imaging.*, 2011, *55*, 310-323.

[4] Rodriguez-Cortes, J.; Arteaga De Murphy, C.; Ferro-Flores, G.; Pedraza-Lopez, M.; Murphy-Stack, E. Biokinetics and dosimetry with ^{177}Lu-DOTA-TATE in athymic mice with induced pancreatic malignant tumours: preclinical studies. *Radiat. Eff. Defects Solids.*, **2007**, *162*, 791-796.

[5] Buchegger, F.; Perillo-Adamer, F.; Dupertuis, Y.M.; Bischof, A. Auger radiation targeted into DNA: a therapy perspective. *Eur. J. Nucl. Med. Mol. Imaging*, **2006**, *33*, 1352-1363.

[6] Tavares, A.A.S.; Tavares, J.M.R.S. Evaluating ^{99m}Tc Auger electrons for targeted tumor radiotherapy by computational methods. *Med. Phys.*,**2010**, *37*, 3551-3559.

[7] Ferro-Flores, G.; Arteaga de Murphy, C.; Rodriguez-Cortes, J.; Pedraza-Lopez, M.; Ramirez-Iglesias, M.T. Preparation and evaluation of ^{99m}Tc-EDDA/HYNIC-[Lys^3]-bombesin for imaging gastrin-releasing peptide receptor-positive tumours. *Nucl. Med. Commun.*, **2006**, *27*, 371-376.

[8] Ferro-Flores, G.; Rivero, I.A.; Santos-Cuevas, C.L.; Sarmiento, J.I.; Arteaga de Murphy, C.; Ocampo-Garcia, B.E.; Garcia-Becerra, R.; Ordaz-Rosado, D. Clickchemistryfor [^{99m}Tc(CO)$_3$] labeling of Lys^3-bombesin. *Appl. Radiat. Isot.*, **2010**, *68*, 2274-2278.

[9] Santos-Cuevas, C.L.; Ferro-Flores, G.; Arteaga de Murphy, C.; Pichardo-Romero, P.A. Targeted imaging of gastrin-releasing peptide receptors with ^{99m}Tc-EDDA/HYNIC-[Lys^3]-bombesin: biokinetics and dosimetry in women. *Nucl. Med. Commun.*, **2008**, *29*, 741-747.

[10] Cornelissen, B.; McLarty, K.; Kersemans, V.; Scollard, D.; Reilly, R.; Properties of [^{111}In]-labelled HIV-1 tat peptide radioimmunoconjugates in tumor-bearing mice following intravenous or intratumoral injection. *Nucl. Med. Biol.*, **2008**, *35*, 101-110.

[11] Costantini, D.L.; Hu, M.; Reilly, R. Peptide motifs for insertion of radiolabeled biomolecules into cells and routing to the nucleus for cancer imaging or radiotherapeutic applications. *Cancer Biother. Radiopharm.*, **2008**, *23*, 3-24.

[12] Santos-Cuevas, C.L.; Ferro-Flores, G.; Arteaga de Murphy, C.; Ramirez, F. de M.; Luna-Gutierrez, M.A.; Pedraza-Lopez, M.; Garcia-Becerra, R.; Ordaz-Rosado, D. Design, preparation, *in vitro* and *in vivo* evaluation of ^{99m}Tc-N_2S_2-Tat(49-57)-bombesin: a target-specific hybrid radiopharmaceutical. *Int. J. Pharm.*, **2009**, *375*, 75-83.

[13] Santos-Cuevas, C.L.; Ferro-Flores, G.; Rojas-Calderon, E.L.; Garcia-Becerra, R.; Ordaz-Rosado, D.; Arteaga de Murphy, C.; Pedraza-Lopez, M. ^{99m}Tc-N_2S_2-Tat(49-57)-bombesin internalized in nuclei of prostate and breast cancer cells: kinetics, dosimetry and effect on cellular proliferation. *Nucl. Med. Commun.*, **2011**, *32*, 303-313.

[14] Levy, R.; Thanh, N.T.K.; Doty, R.C.; Hussain, I.; Nichols, R.J.; Schiffrin, D.J. Rational and combinatorial design of peptide capping ligands for gold nanoparticles. *J. Am. Chem. Soc.*, **2004**, *126*, 10076-10084.

[15] De la Fuente, J.M.; Berry, C.C. Tat peptide as an efficient molecule to translocate gold nanoparticles into the cell nucleus. *Bioconjug. Chem.*, **2005**, *16*, 1176-1180.

[16] Porta, F.; Speranza, G.; Krpetic, Z.; Santo, V.D.; Francescato, P.; Scari, G. Gold nanoparticles capped by peptides. *Mater. Sci. Eng. B.*, **2007**, *140*, 187-194.

[17] Olmedo, I.; Araya, E.; Sanz, F.; Medina, E.; Arbiol, J.; Toledo, P. How changes in the sequence of the peptide CLPFFD-NH_2 can modify the conjugation and stability of gold nanoparticles and their affinity for beta-amyloid fibrils. *Bioconjug. Chem.*,**2008**, *19*, 1154-1163.

[18] Surujpaul, P.P.; Gutierrez-Wing, C.; Ocampo-Garcia, B.; Ramirez, F. de M.; Arteaga de Murphy, C.; Pedraza-Lopez, M.; Camacho-Lopez, M.A.; Ferro-Flores, G. Gold nanoparticles conjugated to [Tyr^3]octreotide peptide. *Biophys. Chem.*, **2008**, *138*, 83-90.

[19] Mendoza-Sanchez, A.N.; Ferro-Flores, G.; Ocampo-Garcia, B.E.; Morales-Avila, E.; Ramirez, F. de M.; Leon-Rodriguez, L.M. Lys^3-bombesin conjugated to ^{99m}Tc-labeled gold nanoparticles for *in vivo* gastrin releasing peptide-receptor imaging. *J. Biomed. Nanotech.*, **2010**, *6*, 375-384.

[20] Ocampo-Garcia, B.E.; Ramirez, F. de M.; Ferro-Flores, G.; Leon-Rodriguez, L.M.; Santos-Cuevas, C.L.; Morales-Avila, E. ^{99m}Tc-labeled gold nanoparticles capped with HYNIC-peptide/mannose for sentinel lymph node detection. *Nucl. Med. Biol.*, **2011**, *38*, 1-11.

[21] Morales-Avila, E.; Ferro-Flores, G.; Ocampo-Garcia, B.E.; De Leon, L.M.; Santos-Cuevas C.L.; Medina, L.A. Multimeric System of ^{99m}Tc-labeled gold nanoparticles conjugated to c[RGDfK(C)] for molecular imaging of tumour $\alpha_v\beta_3$ expression. *Bioconjug. Chem.*, **2011**, *22*, 913-922.

[22] Wang, H.; Dimitrov, K. Conjugation of immunoglobulin M to gold nanoparticles. *Curr. Nanosci.*, **2011**, *7*, 874-878.

[23] Elfeky, S.A.; Al-Sherbini, A.A. Synthesis and spectral characteristics of gold nanoparticles labelled with fluorescein sodium. *Curr. Nanosci.*, **2011**, *7*, 1028-1033.

[24] Chanda, N.; Kattumuri, V.; Shukla, R.; Zambre, A.; Katti, K.; Upendran, A. Bombesin functionalized gold nanoparticles show *in vitro* and *in vivo* cancer receptor specificity. *Proc. Natl. Acad. Sci. USA*, **2010**, *107*, 8760-8765.

[25] Jadzinsky, P.D.; Calero, G.; Ackerson, C.J.; Bushnell, D.A.; Komberg, R.D. Structure of a thiol monolayer-protected gold nanoparticle at 1.1 A resolution. *Science*, **2007**, *318*, 430-433.

[26] Ocampo-Garcia, B.E.; Ferro-Flores, G.; Morales-Avila, E.; Ramirez, F. de M. Kit for preparation of multimeric receptor-specific ^{99m}Tc-radiopharmaceuticals based on gold nanoparticles. *Nucl. Med. Commun.*, **2011**, *32*, 1095-1104.

[27] Miller, W.H.; Hartmann-Siantar, C.; Fisher, D.; Descalle, M.A.; Daly, T.; Lehmann, J.; Lewis, M.R.; Hoffman, T.; Smith, J.; Situ, P.D.; Volkert, W.A.Evaluation of beta-absorbed fractions in a mouse model for ^{90}Y, ^{188}Re, ^{166}Ho, ^{149}Pm, ^{64}Cu, and ^{177}Lu radionuclides. *Cancer Biother. Radiopharm.*,**2005**, *20*, 436-449.

[28] Kogan, M.J.; Olmedo, I.; Hosta, L.; Guerrero, A.R.; Cruz, L.J.; Albericio, F. Peptides and metallic nanoparticles for biomedical applications. *Nanomedicine*,**2007**, *2*, 287-306.

[29] Petroski, J.; Chou, M.; Creutz, C. The coordination chemistry of gold surface: formation and far-infrared spectra of alkanethiolate-capped gold nanoparticles. *J. Organ. Chem.*, **2009**, *694*, 1138-1143.

[30] Kato, H.S.; Noh, J.; Hara, M.; Kawai, M.; An HREELS Study of Alkanethiol Self-Assembled Monolayers on Au(111). *J. Phys. Chem. B.*, **2002**, *106*, 9655-9658.

[31] Hirsch, L.R.; Stafford, R.J.; Bankson, J.A.; Sershen, S.R.; Rivera, B.; Price, R.E.; Hazle, J.D.; Hals, N.J. Nanoshell-mediated near-infrared thermal therapy of tumors under magnetic resonance guidance. *Proc. Natl. Acad. Sci. U SA.*, **2003**, *100*, 13549-13554.

[32] Huang, X.; Neretina, S.; El-Sayed, M.A. Gold nanorods: from synthesis and properties to biological and biomedical applications. *Adv. Mater.*, **2009**, *21*, 4880-4910.

[33] Elbialy, N.; Abdelhamid, M.; Youssef, T. Low power argon laser-induced thermal therapy for subcutaneous ehrlich carcinoma in mice using spherical gold nanoparticles. *J. Biomed. Nanotech.*, **2010**, *6*, 687-693.

[34] Huang, X.; Qian, W.; El-Sayed, I.H.; El-Sayed, M.A.The potential use of the enhanced nonlinear properties of gold nanospheres in photothermal cancer therapy. *Lasers Surg. Med.*, **2007**, *39*, 747-753.

[35] Ferro-Flores, G; Arteaga de Murphy, C. Pharmacokinetics and Dosimetry of ^{188}Re-pharmaceuticals. *Adv. Drug Deliv. Rev.*, **2008**, *60*, 1389-1401.

[36] Berry, C.C.; de la Fuente, J.M.; Mullin, M.; Chu, S.W.; Curtis A.S. Nuclear Localization of HIV-1 Tat Functionalized Gold Nanoparticles. *IEEE Trans. Nanobioscience*, **2007**, *6*, 262-269.

Received: September 28, 2011 Revised: November 22, 2011 Accepted: December 14, 2011

Nuclear Medicine and Biology 42 (2015) 109–114

Contents lists available at ScienceDirect

Nuclear Medicine and Biology

journal homepage: www.elsevier.com/locate/nucmedbio

Preparation and preclinical evaluation of ^{66}Ga-DOTA-E(c(RGDfK))$_2$ as a potential theranostic radiopharmaceutical

V. Lopez-Rodriguez [a], R.E. Gaspar-Carcamo [a], M. Pedraza-Lopez [b], E.L. Rojas-Calderon [c], C. Arteaga de Murphy [b], G. Ferro-Flores [c], M.A. Avila-Rodriguez [a,*]

[a] Unidad PET, Facultad de Medicina, Universidad Nacional Autónoma de México, México, D.F., Mexico
[b] Instituto Nacional de Ciencias Médicas y Nutrición Salvador Zubirán, México, D.F., Mexico
[c] Instituto Nacional de Investigaciones Nucleares, Estado de México, Mexico

ARTICLE INFO

Article history:
Received 28 August 2014
Received in revised form 26 September 2014
Accepted 30 September 2014

Keywords:
Gallium-66
RGD peptides
Integrin $\alpha_v\beta_3$
Angiogenesis
Theranostics
PET imaging

ABSTRACT

Introduction: Integrin $\alpha_v\beta_3$ plays an important role in angiogenesis and is over-expressed in tumoral endothelial cells and some other tumor cells. RGD (Arg-Gly-Asn) peptides labeled with ^{68}Ga ($t_{1/2}$ = 68 min) have showed good characteristics for imaging of $\alpha_v\beta_3$ expression using positron emission tomography (PET). Gallium-66 has been proposed as a PET imaging alternative to ^{68}Ga and given the unique high energy of its emitted positrons (E_{max} 4.15 MeV) it may also be useful for therapy. The aim of this research is to prepare [^{66}Ga]DOTA-E-[c(RGDfK)]$_2$ and evaluate in mice its potential as a new theranostic radiopharmaceutical.

Methods: High specific activity ^{66}Ga was produced via the ^{66}Zn(p,n) reaction, and the labelling method of DOTA-E-[c(RGDfK)]$_2$ with ^{66}Ga was optimized. Radiochemical purity was determined by TLC, and *in vitro* stability and protein binding were determined. Serial microPET imaging and biodistribution studies were carried out in nude mice bearing C6 xenografts. Radiation absorbed dose estimates were based on the biodistribution studies, where tumor and organs of interest were collected at 0.5, 1, 3, 5 and 24 h post-injection of [^{66}Ga]DOTA-E-[c(RGDfK)]$_2$.

Results: Our results have shown that [^{66}Ga]DOTA-E-[c(RGDfK)]$_2$ can be prepared with high radiochemical purity (>97%), specific activity (36–67 GBq/μmol), *in vitro* stability, and moderate protein binding. MicroPET imaging up to 24 post-injection showed contrasting tumors reflecting $\alpha_v\beta_3$-targeted tracer accumulation. Biodistribution studies and dosimetry estimations showed a stable tumor uptake, rapid blood clearance, and favorable tumor-to-tissue ratios.

Conclusions: The peptide conjugated DOTA-E-[c(RGDfK)]$_2$ labeled with ^{66}Ga may be attractive as a theranostic agent for tumors over-expressing $\alpha_v\beta_3$ integrins.

1. Introduction

During the past three decades, several radiopharmaceuticals have been developed for the early diagnosis of cancer through the use of novel molecular targets and predictive biomarkers, especially those aberrantly overexpressed in biological malignancy, invasiveness, metastasis and apoptosis [1–5].

It has been shown that peptides based on the Arg-Gly-Asp (RGD) amino acid sequence have a high affinity and selectivity for $\alpha_v\beta_3$ integrin receptors; specifically, it was found that cyclic analogues of RGD containing 5 amino acids (RGD sequence + a hydrophobic amino acid in position 4 + an additional amino acid in position 5) have the highest $\alpha_v\beta_3$ binding affinities [6,7]. Alpha(V)beta(3) integrin receptors are over expressed on endothelial cells during blood vessel formation affecting tumor growth, invasiveness and metastatic potential, and are therefore potential targets for receptor-mediated tumor imaging and therapy.

New approaches have been addressed in order to improve, with various ligands, the affinity of RGD. Due to the natural mode of interaction between $\alpha_v\beta_3$ and peptides containing the amino acid sequence RDG that may involve multivalent binding sites, the use of multivalent cyclic RGD peptides could improve the binding affinity and tumor uptake. Several research groups have compared the cyclic RGDfK monomer, dimer (E-[c(RGDfK)]$_2$) and tetramer (E-[c(RGDfK)]$_4$) as targeting biomolecule for diagnostic and therapeutic applications [8–11]. The short distances between the cyclic RGD peptides in dimmers (~20 bond distance), make it unlikely simultaneous binding to the adjacent $\alpha_v\beta_3$ receptors. It has been proposed that the binding of one RGD motif to the integrin $\alpha_v\beta_3$ will significantly increase "local concentration" of the multivalent RGD motif in the vicinity of the receptor-binding site leading to an enhanced integrin $\alpha_v\beta_3$ binding rate or the reduced dissociation rate of the cyclic RDG peptide from the integrin $\alpha_v\beta_3$[12]. This may explain the higher tumor uptake and longer tumor retention times of radiolabelled cyclic RGD tetramer and dimmer as compared

* Corresponding author at: Unidad PET, Facultad de Medicina, UNAM, Ciudad Universitaria, Delegación Coyoacán, México, D.F., C.P. 04510, Mexico. Tel.: +52 55 56232288; fax: +52 55 56232115.
E-mail address: avilarod@uwalumni.com (M.A. Avila-Rodriguez).

http://dx.doi.org/10.1016/j.nucmedbio.2014.09.010
0969-8051/

to their monomeric analogues [11–13]. The tetrameric RGD peptide labeled with ^{64}Cu ([^{64}Cu]DOTA-E{E-[c(RGDfK)]$_2$}$_2$), showed significantly higher receptor binding affinity than monomeric and dimeric RGD analogues, but demonstrated lower kidney clearance which may be related to the positively charge differences [14].

The positron emitting radionuclide ^{66}Ga ($t_{½}$ = 9.49 h, 56.5% β^+, 43.5% EC) has been proposed as a PET imaging alternative to ^{68}Ga. ^{66}Ga is of special interest because of its relative long half-life which makes it a suitable tracer for the study of long-term physiological processes and labeling of macromolecules with slow pharmacokinetics [15–17]. In addition, the most abundant positrons emitted by ^{66}Ga have a unique high energy (E_{max} 4.15 MeV, mean range 7.6 mm in tissue), which may also be useful for therapy [17].

At the intersection between treatment and diagnosis, interest has grown in combining both paradigms into clinically effective pharmaceuticals. This concept, recently named as theranostics, is highly relevant to agents that target molecular biomarkers of disease and is expected to contribute to personalized medicine [18].

The aim of this research was to prepare, characterize and perform the preclinical evaluation and dosimetry of [^{66}Ga]DOTA-Glu-[cyclo(Arg-Gly-Asp-D-Phe-Lys)]$_2$ ([^{66}Ga]DOTA-E-[c(RGDfK)]$_2$) in order to evaluate its potential as a theranostic radiopharmaceutical for molecular imaging diagnosis and targeted radiotherapy of $\alpha_v\beta_3$ over-expressing tumors.

2. Materials and methods

2.1. Reagents

All reagents used were TraceSelect grade, and water employed to prepare solutions was of Milli-Q grade (18 MΩ-cm) to ensure heavy metal-free aqueous solutions. Ultrapure HCl, HEPES and NH_4OAc (>99.999%) were purchased from Sigma-Aldrich (St. Louis, MO, USA). Cation exchange resin (AG50W-X4, 100–200 mesh) was purchased from BioRad (Hercules, CA, USA). Isotopically enriched ^{66}Zn (98.72 %) was obtained from Isoflex (San Francisco, CA, USA). DOTA-E-[c(RGDfK)]$_2$ was purchased from ABX advanced biomedical compounds GmbH (Radeberg, Germany), and centrifugal filters (cellulose, 30,000 MW cut off) and Millex-GV syringe filters (0.22 μm, PVDF, 33 mm) were obtained from Millipore (Bedford, MA, USA).

2.2. Cell lines and animal model

C6 rat glioma cell line was purchased from the American Type Culture Collection (ATCCW CCL-107, Rockville, USA). The cells were grown in RPMI 1640 medium (Invitrogen, USA) supplemented with 10% fetal bovine serum and antibiotics (100 mg/ml streptomycin) and incubated at 37 °C in an atmosphere with 5% CO_2.

Experimental animals were handled observing the technical specifications for the production, care and use of laboratory animals stated in the Official Mexican Norm NOM 0062-ZOO-1999. Studies with mice in this specific work were performed according to protocols approved by the Research and Ethics Committee of the Faculty of Medicine, at the National Autonomous University of Mexico (UNAM).

Female athymic Balb-C nu/nu mice (20–25 g) were supplied by the National Institute of Medical Sciences and Nutrition Salvador Zubiran (INCMNSZ), Mexico City, Mexico. All animals were kept in a pathogen free environment and fed *ad lib*.

C6 xenografts were induced by subcutaneous injection of 1×10^6 cells resuspended in 0.1 ml of phosphate buffered saline, in the dorsal surface of the scapula. The sites of injection were observed at regular intervals for the appearance of tumor formation and progression, and mice were used for *in vivo* experiments when the diameter of tumor reached about 0.5 cm.

2.3. Gallium-66 production

Gallium-66 was produced in a Siemens Eclipse HP cyclotron via the ^{66}Zn (p,n) ^{66}Ga reaction with 11 MeV protons as previously described by Engle et al. [19]. Briefly, ^{66}Zn was electrodeposited on Au backing and then irradiated for 10 to 20 min at a beam current of 10 to 20 μA. Radiochemical separation was performed by ion exchange chromatography using AG 50 W X-4 resin. The reactivity or effective specific activity of ^{66}Ga was determined by titration of [^{66}Ga]$GaCl_3$ with DOTA (1,4,7,10-Tetraazacyclododecane-1,4,7,10-tetraaceic acid).

2.4. Preparation of [^{66}Ga]DOTA-E-[c(RGDfK)]$_2$

For radiolabelling of DOTA-E-[c(RGDfK)]$_2$, 25 μl of the conjugated peptide solution (400 μg/ml, 1% EtOH), 25 μl 1.0 M HEPES (pH 7.0), and 25 μl 0.25 M NH_4OAc (pH 5.5), were mixed with 200–370 MBq of ^{66}Ga stock solution (50 μl 0.1 M HCl) and incubated for 20 min at 95 °C in a compact thermomixer (Eppendorf, USA) at 300 rpm [12]. When needed, purification of the final product was performed by SPE using Sep-Pak C18 Light cartridges. The final product was sterilized by passing through a 0.22 μm syringe filter (Millex-GV). The structural formula of [^{66}Ga]DOTA-E-[c(RGDfK)]$_2$ is shown in Fig. 1 [20].

2.5. Radiochemical purity

The radiochemical purity (RCP) was determined by thin layer chromatography (TLC) using silica gel (SG) strips as stationary phase and 1:1 MeOH:10% NH_4OAc (w/v) as mobile phase [21]. Evaluation of the TLC plates was performed by autoradiography in a Cyclone Plus Storage Phosphor System (Perkin Elmer).

2.6. In vitro stability

To determine the *in vitro* stability of [^{66}Ga]DOTA-E-[c(RGDfK)]$_2$ in physiological saline and serum, an aliquot (50 μl) of the labelled compound solution was incubated at 37 °C with 1 ml of 0.9% NaCl and fresh human serum. Radiochemical purity stability was evaluated up to 24 h by TLC-SG as described above.

2.7. Protein binding

To determine serum protein binding of [^{66}Ga]DOTA-E-[c(RGDfK)]$_2$, and aliquot of the labeled compound (100 μl) was incubated at 37 °C with 1 ml of fresh human serum up to 4 hours. After incubation the solution was analyzed by ultrafiltration (30,000 MW). Protein binding was determined by measuring the activity remaining in the filter, while the unbound [^{66}Ga]DOTA-E-[c(RGDfK)]$_2$ passed through the filter.

2.8. MicroPET imaging

Mice bearing glioma C6 tumors were scanned after a tail vein injection of 20 ± 0.5 MBq of [^{66}Ga]DOTA-E[c(RGDfK)]$_2$ under isoflourane anesthesia (1–3%). PET images were acquired in a MicroPET Focus 120 (Concorde Microsystems, Knoxville, TN, USA) at different post injection (p.i.) times (0.5, 1, 3, 5 and 24 h). Scan time was 20 min for images acquired at 0.5, 1, and 3 h p.i., 30 min for images acquired 5 h p.i., and 60 min for images acquired at 24 h. After PET acquisitions animals were sacrificed to perform the biodistribution studies. MicroPET images were reconstructed using a 3-D ordered subset expectation maximization (OSEM 3D) algorithm.

2.9. Biodistribution studies

After PET imaging acquisitions, animals were sacrificed by cervical dislocation at 0.5, 1, 3, 5, and 24 h p.i. (n = 3 per time point), and tissues

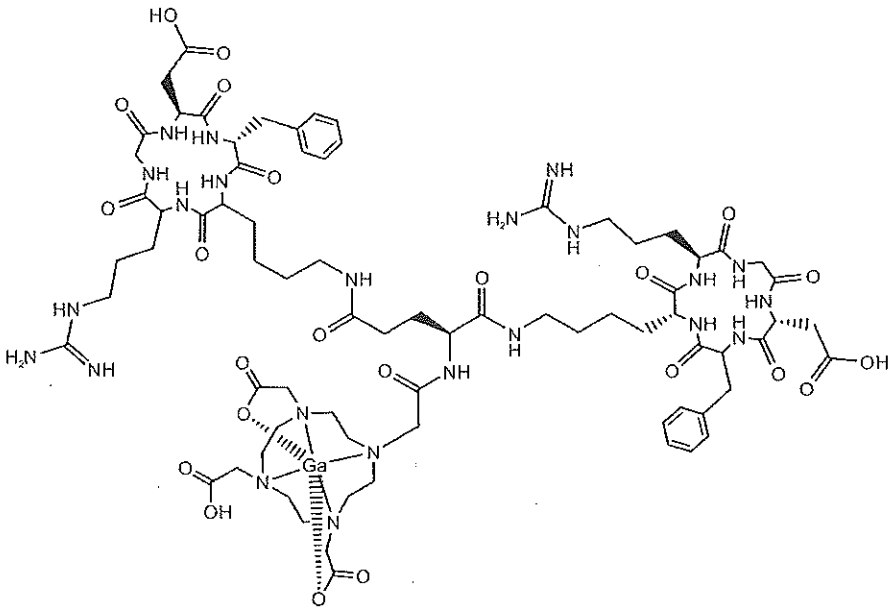

Fig. 1. Structural formula of the DOTA conjugated dimeric-RGD peptide labeled with Ga isotope [20].

of interest (blood, brain, heart, lungs, liver, spleen, blander, kidneys, bowel, muscle, femur and tumor) were removed immediately and weighed. Total blood volume, bone, and muscle mass were estimated as 5.4%, 10%, and 40% of the total body weight, respectively [22,23]. Activity in the different tissues was measured using a NaI(Tl) scintillation detector (ORTEC 905-1, AMETEK, USA). All the data were corrected for physical decay and to calculate uptake in each tissue sample as a fraction of the injected dose, aliquots of the injected dose were counted simultaneously. The results are expressed as a percentage of injected dose per gram of tissue (%ID/g) and percentage of injected dose per organ (%ID/organ).

2.10. Radiation dosimetry

Mice biodistribution data (%ID/organ) were used for estimation of the radiation absorbed dose for [^{66}Ga]DOTA-E[c(RGDfK)]$_2$. The mean activity in mice organs of interest (liver, spleen, kidneys and tumor) were used to calculate the biokinetic model, residence times and radiation absorbed doses according to the method described by Jimenez et al. [24] and Luna et al. [25]. The absorbed dose to organs was evaluated according to the equation:

$$D(r_k \leftarrow r_h) = \sum_h \tilde{A}_h \sum_i \Delta_i \Phi_i(r_k \leftarrow r_h)$$

where $\sum_i \Delta_i \Phi_i$ values were estimated in a mouse model by Monte Carlo methodology using the Penmain programme of Penelope 2008 [26] and $\sum_h \tilde{A}_h$ were estimated using OLINDA/EXM software [27].

2.11. Statistical methods

All of the data are presented as means ± SD.

3. Results

The experimental thin target yield (61 ± 14 mg/cm^2, 11 → 9.7 MeV) for ^{66}Zn targets was 3415 ± 681 MBq/μA with a radionuclide purity >97% at 2 h after the end of bombardment. Typical reactivity or effective specific activity of ^{66}Ga as determined by DOTA titration was in the range of 160–370 GBq/μmol.

The labeling yield of [^{66}Ga]DOTA-E-[c(RGDfK)]$_2$ was almost quantitative using 5.5 nmol of the conjugated peptide. It was observed that a mass as low as 2 nmol of DOTA-E-[c(RGDfK)]$_2$ was sufficient to reach nearly quantitative labeling. Fig. 2 shows that 7 min of incubation at 95 °C are enough to reach a complexation yield > 95%. Specific activity of the labeled conjugate was in the range of 36–67 GBq/μmol. The RCP as determined by TLC was >97% without the need of purification. With the chromatographic method used, the free [^{66}Ga]GaCl$_3$ stayed at the origin, while the R_f values of [^{66}Ga]DOTA-E-[c(RGDfK)]$_2$ and [^{66}Ga]DOTA were 0.6–0.7 and 0.7–0.8, respectively.

In vitro studies indicated high stability of the compound in physiological saline and fresh human serum after 1 h of incubation at 37 °C (RCP > 98%) and was degraded to ~95% at 24 h (Fig. 3) On the other hand, protein binding was negligible (<3%) after one hour of incubation in fresh human serum, but increased to almost 20% after 4 h of incubation at 37 °C.

MicroPET Images of C6 glioma tumor-bearing mice at different time points after injection of tracer showed a contrasting tumor reflecting $\alpha_V\beta_3$-targeted tracer accumulation. Typical decay-corrected images at 0.5, 1, 3, 5 and 24 h p.i. are shown in Fig. 4. Note that the C6 tumors were clearly visualized with good tumor-to-background contrast for all time points evaluated. Serial microPET imaging revealed a rapid

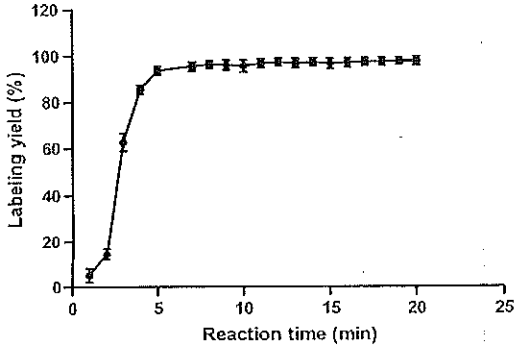

Fig. 2. Effect of incubation time on the complexation yield of [^{66}Ga]DOTA-E-[c(RGDfK)]$_2$ at 95 °C.

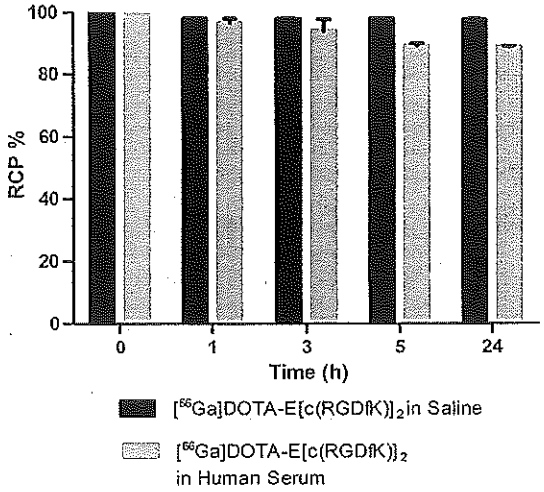

Fig. 3. Stability studies showed high stability of [^{66}Ga]DOTA-E-[c(RGDfK)]$_2$ up to 24 h in human serum and phisiological saline.

clearance from blood and kidneys and high uptake in the liver and spleen, which was consistent with biodistribution data.

Biodistribution data (%ID/g and %ID/organ) of [^{66}Ga]DOTA-E-[c(RGDfK)]$_2$ are shown in Fig. 5. High uptake was observed in organs such as liver, kidneys, lung, spleen, heart, bladder, and muscle at early times, but significantly decreased at 5 h p.i. Rapid blood clearance was also observed, reaching a blood uptake of only 2.81 ± 0.32 %ID/g at 1 h p.i. Uptake of [^{66}Ga]DOTA-E-[c(RGDfK)]$_2$ by the C6 tumor xenograft indicated stable retention of the tracer with minimal wash-out up to 24 h. Tumor-to-muscle ratios (% ID/g) were 1.40 ± 0.97 and 1.78 ± 0.57 at 0.5 h and 24 h p.i., respectively, while tumor-to-blood ratio was 0.20 ± 0.09 at 0.5 h, increasing to 1.97 ± 0.37 at 24 h p.i.

Fig. 6 shows the radiation absorbed doses normalized to unit injected activity (mGy/MBq) and the tumor-to-tissue absorbed dose ratios. As expected, the highest radiation absorbed dose was deposited in the tumor (65.53 ± 8.39 mGy/MBq), followed by the liver (48.06 ± 17.01), kidneys (32.72 ± 4.42), and spleen (27.2 ± 7.29). The biological residence time for the C6 glioma tumors was 5.57 h.

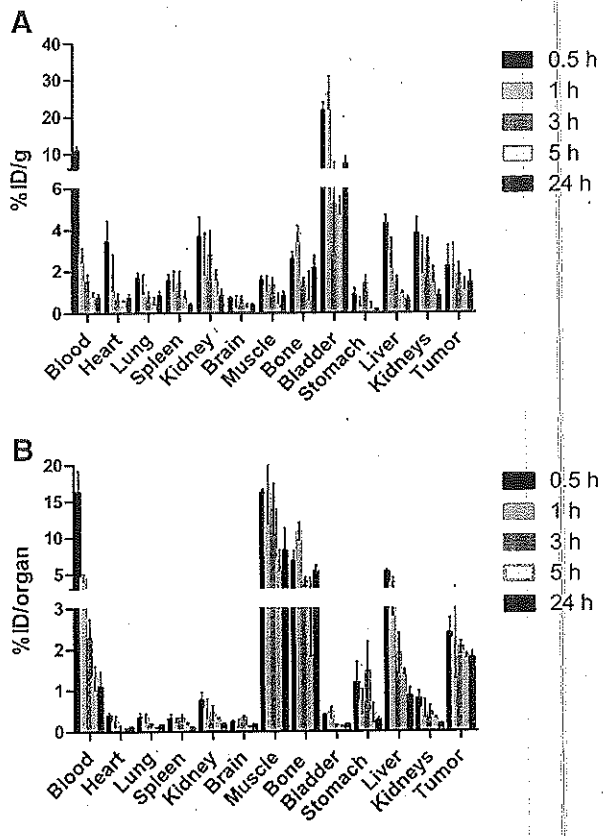

Fig. 5. Biodistribution data for [^{66}Ga]DOTA-E-[c(RGDfK)]$_2$ in mice 0.5, 1, 3, 5 and 24 h p.i. Results are shown as A) %ID/g (mean ± SD) and B) %ID/organ (mean ± SD).

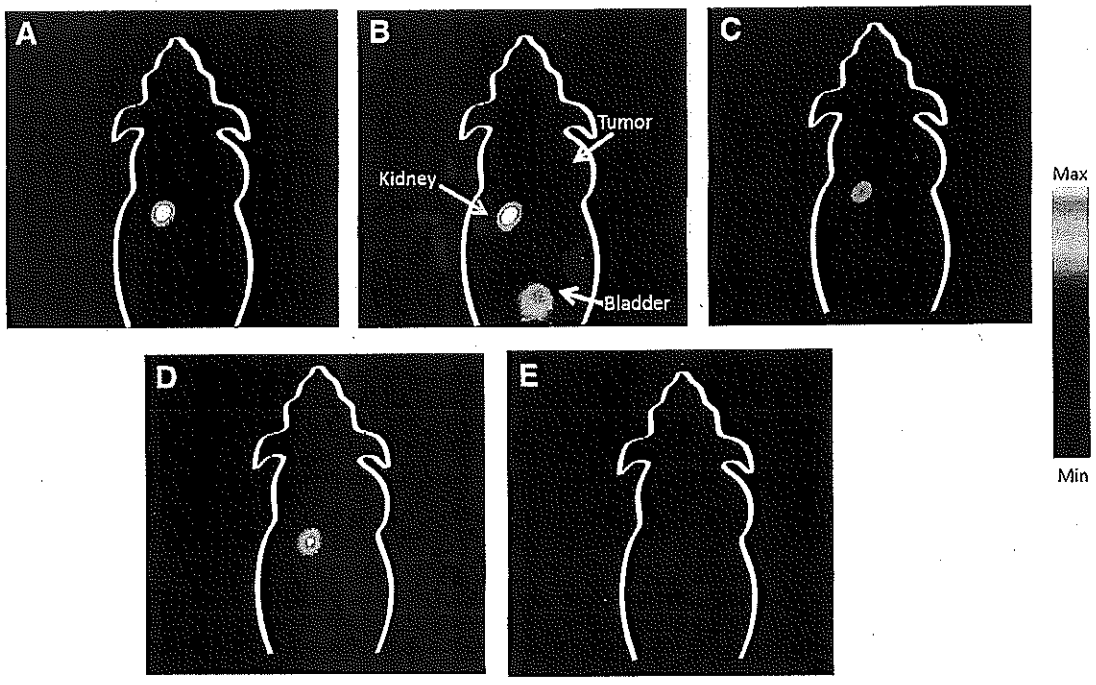

Fig. 4. Coronal microPET images of [^{66}Ga]DOTA -E-[c(RGDfK)]$_2$ in nude mice bearing C6 tumor xenograft at 0.5 h (A), 1 h (B), 3 h (C), 5 h (D) and 24 h (C) after injection of 20 ± 0.5 MBq of tracer under isoflourane anesthesia. Acquisition time was 20 min for A,B, and C); 30 min for D, and 60 min for E.

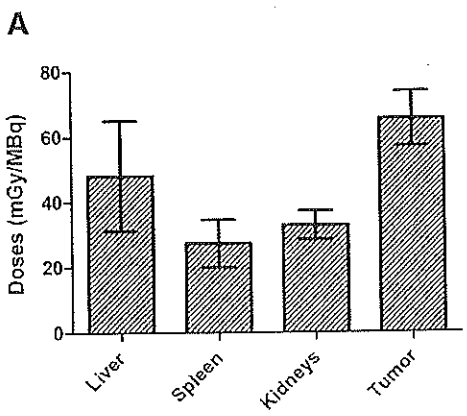

Tissue	Tumor to tissue absorbed dose ratio
Liver	1.36
Spleen	2.41
Kidneys	2.01
Tumor	1

Fig. 6. A)Estimated radiation absorbed doses normalized to unit injected activity and B) tumor-to-tissue absorbed dose ratios of [^{66}Ga]DOTA-E-[c(RGDfK)]$_2$ in nude mice bearing C6 tumor xenograft.

4. Discussion

During the past few years different multivalent cyclic RGD peptide conjugates have been used to target tumors over-expressing $\alpha_v\beta_3$ integrin receptors [25–39]; however, it has been demonstrated that the dimeric conjugate is more suitable for both, imaging and therapeutic applications. Li et al. [34] showed that despite the fact that the tetrameric peptide conjugate labeled with ^{68}Ga had the highest tumor uptake, its poor tumor-to-kidney ratio makes this compound less useful than the dimeric and monomeric counterparts. It was also found that the dimeric and monomeric peptide had similar tumor-to-kidney ratios but the dimer had higher tumor uptake and a prolonged retention time, making it more suitable than the monomer. On the other hand, Luna-Gutierrez et al. [25] investigated the potential of ^{177}Lu-labeled monomeric and dimeric cyclic RGD peptides ([c(RGDfK)]$_n$) for the treatment of tumors over-expressing $\alpha_v\beta_3$ integrins. *In vivo* evaluation in a mouse U87MG xenograft model showed that [^{177}Lu]DOTA-E-[c(RGDfK)]$_2$ had a higher uptake in tumor and a higher tumor-to-kidney ratio than [^{177}Lu]DOTA-E-c(RGDfK), making the dimer more suitable than the monomer for therapeutic applications.

In this light we evaluated the dimeric conjugated DOTA-E-[c(RGDfK)]$_2$ labeled with ^{66}Ga to target tumors over expressing $\alpha_v\beta_3$ integrin receptors. The glioma cell line used in this research was the C6 which is known to have a high tumor density of integrin $\alpha_v\beta_3$ receptors on the surface (1.51×10^{11} number of receptors/mg protein) [28], making this cell line a good candidate to evaluate theranostic applications with peptides containing the amino acid sequence RDG, labeled with the appropriate radionuclide. For imaging purposes, ^{68}Ga had shown to be a suitable radionuclide as it can be easily obtained from a ^{68}Ge/^{68}Ga generator [29–32], while for therapeutic applications the beta emitter ^{177}Lu is promising [34–37]. However, due to its decay scheme and the unique high energy of emitted positrons, ^{66}Ga has the potential to serve a dual role in the development of agents for PET-molecular imaging and radioimmunotherapy drugs for oncology. Additionally, high specific activity ^{66}Ga; in enough quantity and quality for clinical applications, can be efficiently produced in compact biomedical cyclotrons using enriched target material, which is relatively inexpensive (~2–3 USA dll/mg, ^{66}Zn > 99%) [19].

The most important feature of targeted radionuclide therapy is to deliver a tumoricidal dose for tumor ablation, without compromising other vital organs [38]. The [^{66}Ga]DOTA-E-[c(RGDfK)]$_2$ evaluated in this research showed good pharmacokinetic characteristics with a relatively stable tumor uptake and a rapid blood clearance. Dosimetry estimations from our biodistribution data showed that critical organs such as liver, kidneys, and spleen can receive a considerable radiation dose per unit injected activity, but in all cases the dose was lower than the one received by the tumor. Of particular interest in this research was to determine the tumor-to-tissue ratios that better define tumor targeting properties.

The 65 mGy/MBq radiation absorbed dose normalized to unit injected activity determined in this research for [^{66}Ga]DOTA-E-[c(RGDfK)]$_2$ in C6 tumors was significantly lower than the 230 mGy/MBq reported by Luna-Gutierrez et al. [25] for [^{177}Lu]DOTA-E-[c(RGDfK)]$_2$ in U87MG tumors; however, the tumor-to-tissue ratios reported in both cases are very similar. Note that for comparison purposes the higher density of integrin $\alpha_v\beta_3$ receptors on the surface of U87MG *vs.* C6 cells [28] is compensated in some way by the higher specific activity of ^{177}Lu *vs.* ^{66}Ga [25]. These results suggest that [^{66}Ga]DOTA-E-[c(RGDfK)]$_2$ possesses potential for targeted radionuclide therapy of tumors over expressing integrin $\alpha_v\beta_3$ receptors. Additionally, we had shown that, despite the high energy positrons emitted by ^{66}Ga, it is possible to get good quality microPET-images.

Since [^{66}Ga]DOTA-E-[c(RGDfK)]$_2$ combines imaging and radiotherapy in one preparation, it could be useful as a theranostic radiopharmaceutical for tumors over-expressing $\alpha_v\beta_3$ integrins. To plan a diagnosis/treatment scheme for an individual patient, the diagnosis and prospective radiation absorbed dose estimates could be made by administering a tracer activity of the radiopharmaceutical and subsequently the larger therapeutic activity. The quantitative patient-specific dosimetry work-up using a diagnostic dose before the therapeutic dose would be useful to identify cancer patients for whom the treatment is most likely to be effective, eliminating those patients for whom it would be unsuccessful ("personalized medicine"). In agreement with other radionuclide therapy protocols, positively charged amino acids could be coinfused to reduce the radiopeptide kidney retention considering that the maximum tolerated dose (MTD) for kidney is 25 Gy, while for spleen and liver the MTD value is almost twice [39].

5. Conclusions

To summarize, ^{66}Ga labeled DOTA-E-[c(RGDfK)]$_2$ was prepared with high yield, specific activity and radiochemical purity. The microPET imaging and biodistribution studies showed high affinity for the $\alpha_v\beta_3$ integrin receptors, with rapid blood clearance; and the radiation absorbed dose estimation suggested sub-toxic doses to critical organs. These results support the idea that [^{66}Ga]DOTA-E-[c(RGDfK)]$_2$ may be attractive as a theranostic agent for tumors over-expressing $\alpha_v\beta_3$ integrins.

Acknowledgements

We are grateful to A. Zarate-Morales and A. Flores-Moreno for cyclotron irradiations and to V.M. Lara-Camacho and M. Avila-Garcia for microPET imaging. This research was supported by CONACYT Grant

179218, UNAM-DGAPA-PAPIIT TA200512 and the International Atomic Energy Agency RC16467.

References

[1] Kai C, Conti PS. Target-specific delivery of peptide-based probes for PET imaging. Adv Drug Deliv Rev 2010;62:1005–22.

[2] Tolmachev V, Stone-Elander S. Radiolabelled proteins for positron emission tomography: pros and cons of labelling methods. Biochim Biophys Acta 1800;2010: 487–510.

[3] Lee S, Xie J, Chen X. Peptides and peptide hormones for molecular imaging and disease diagnosis. Chem Rev 2010;110:3087–111.

[4] Schottelius M, Wester HJ. Molecular imaging targeting peptide receptors. Methods 2009;48:161–77.

[5] Kaur S, Venktaraman G, Jain M, Senapati S, Garg PK, Batra SK. Recent trends in antibody-based oncologic imaging. Cancer Lett 2012;315:97–111.

[6] Plow EF, Haas TA, Zhang L, Loftusi J, Smith JW. Ligand binding to integrins. J Biol Chem 2000;275:21785–8.

[7] Gurrath M, Muller G, Kessler H, Aumailley M, Timpl R. Conformation/activity studies of rationally designed potent anti-adhesive RGD peptides. Eur J Biochem 1992;210: 911–21.

[8] Barrett JA, Croker AC, Onthank DC, Heminway S, Rajopadhye M, Liu S, et al. RP593 a ^{99m}Tc-labeled $\alpha_v\beta_3/\alpha_v\beta_5$ antagonist, rapidly detects spontaneous tumors in mice and dogs. Nucl Med Commun 2000;21:564.

[9] Janssen ML, Oyen WJ, Dijkgraaf I, Massuger LF, Frielink C, Edwards DS, et al. Tumor targeting with radiolabeled alpha(v)beta(3) integrin binding peptides in a nude mouse model. Cancer Res 2002;62:6146–51.

[10] Janssen ML, Oyen WJ, Massuger LF, Frielink C, Dijkgraaf I, Edwards DS, et al. Comparison of a monomeric and dimeric radiolabeled RGD-peptide for tumor targeting. Cancer Biother Radiopharm 2002;17:641–6.

[11] Janssen ML, Frielink C, Dijkgraaf I, Oyen WJ, Edwards DS, Liu S, et al. Improved tumor targeting of radiolabeled RGD peptides using rapid dose fractionation. Cancer Biother Radiopharm 2004;19:399–404.

[12] Dijkgraaf I, Yim C-B, Franssen MG, Schuit CR, Luurtsema G, et al. PET imaging of αvβ3 integrin expression in tumours with ^{68}Ga-labelled mono-, di- and tetrameric RGD peptides. Eur J Nucl Med Mol Imaging 2011;38:128–37.

[13] Chen X, Liu S, Hou Y, Tohme M, Park R, Bading JR, et al. MicroPET imaging of breast cancer alphav-integrin expression with ^{64}Cu-labeled dimeric RGD péptidos. Mol Imaging Biol 2004;6:350–9.

[14] Wu Y, Zhang X, Xiong Z, Cheng Z, Fisher DR, Liu S, et al. microPET imaging of glioma integrin αvβ3 expression using ^{64}Cu-labeled tetrameric RGD peptide. J Nucl Med 2005;46:1707–18.

[15] Lewis MR, Reichert DE, Laforest R, Margenau WH, Shefer RE, Klinkowstein RE, et al. Production and purification of gallium-66 for preparation of tumor-targeting radiopharmaceuticals. Nucl Med Biol 2002;29:701–6.

[16] Graham MC, Pentlow KS, Mawlawi O, Finn RD, Daghighian F, Larson SM. An investigation of the physical characteristics of ^{66}Ga as an isotope for PET imaging and quantification. Med Phys 1997;24:317–26.

[17] Ugur Ömer, Kothari Paresh J, Finn Ronald D, Zanzonico Pat, Ruan Shutian, Guenther Ilonka, et al. Ga-66 labeled somatostatin analogue DOTA-DPhe^1-Tyr^3-octreotide as a potential agent for positron emission tomography imaging and receptor mediated internal radiotherapy of somatostatin receptor positive tumors. Nucl Med Biol 2002;29:147–57.

[18] Janib SM, Moses AS, MacKay JA. Imaging and drug delivery using theranostic nanoparticles. Adv Drug Deliv Rev 2010;62:1052–63.

[19] Engle JW, Lopez Rodriguez V, Gaspar Carcamo RE, Valdovinos HF, Valle Gonzalez M, Trejo Ballado F, et al. Very high specific activity $^{66/68}$Ga from zinc targets for PET. Appl Radiat Isot 2012;70:1792–6.

[20] Kubíček Vojtěch, Havlíčkova Jana, Kotek Jan, Tircsó Gyula, Hermann Pert, Tóth Éva, et al. Gallium(III) complexes of DOTA and DOTA-monoamide: kinetic and thermodynamic studies. Inorg Chem 2010;49:10960–9.

[21] Karolin Pohle, Johannes Notni, Johanna Bussemer, Horst Kessler, Markus Schwaiger, Beer Ambros J. ^{68}Ga-NODAGA-RGD is a suitable substitute for ^{18}F-Galacto-RGD and can be produced with high specific activity in a cGMP/GRP compliant automated process. Nucl Med Biol 2012;39:777–84.

[22] Petty C. Research Techniques in the Rats. Springfield, IL: Charles C. Thomas; 1982.

[23] Frank DW. Physiological data of laboratory animals. Boca Raton, FL: CRC Press; 1976.

[24] Jimenez-Mancilla NP, Ferro-Flores G, Ocampo-García B, Luna-Gutiérrez M, Pedraza-Lopez M, Torres-Garcia E. Multifunctional targeted radiotherapy system for induced tumours expressing gastrin-releasing peptide receptor. Curr Nanosci 2012;8: 193–201.

[25] Luna-Gutiérrez M, Ferro-Flores G, Ocampo-García B, Jiménez-Mancilla NP, Morales-Avila E, De León Rodríguez LM, et al. ^{177}Lu-labeled monomeric, dimeric and multimeric RGD peptides for the therapy of tumors expressing α(v)β(3) integrins. J Labelled Comp Radiopharm 2012;50:140–8.

[26] Miller WH, Hartmann-Siantar C, Fisher D, Descalle MA, Daly T, Lehmann J, et al. Evaluation of beta-absorbed fraction in a mouse model for ^{90}Y, ^{188}Re, ^{166}Ho, ^{149}Pm, ^{64}Cu and ^{177}Lu radionuclides. Cancer Biother Radiopharm 2005;20:436–49.

[27] Stabin MG, Sparks RB, Crowe E. OLINDA/EXM: The second-generation personal computer software for internal dose assessment in nuclear medicine. J Nucl Med 2005; 46:1023–7.

[28] Zhang X, Xiong Z, Wu Y, Cai W, Tseng JR, Gambhir SS, et al. Quantitative PET imaging of tumor integrin αvβ3 expression with ^{18}F-FRGD$_2$. J Nucl Med 2006;47:113–21.

[29] Knetsch PA, Petrik M, Griessinger CM, Rangger C, Fani M, Kesenheimer C, et al. [^{68}Ga] NODAGA-RGD for imaging αvβ3 integrin expression. Eur J Nucl Med Mol Imaging 2011;38:1303–12.

[30] Knetsch PA, Petrik M, Rangger C, Seidel G, Pietzsch HJ, Virgolini I, et al. [68Ga]NS3-RGD and [68Ga] Oxo-DO3A-RGD for imaging $\alpha_v\beta_3$ integrin expression: synthesis, evaluation, and comparison. Nucl Med Biol 2013;40:65–72.

[31] Decristoforo C, Gonzalez Hernandez I, Carlsen J, Rupprich M, Huisman M, Virgolini I, et al. ^{68}Ga- and ^{111}In-labelled DOTA RGD peptides for imaging of $\alpha_v\beta_3$ integrin expression. Eur J Nucl Med Mol Imaging 2008;35:1507–15.

[32] Smith Daniel L, Breeman Wouter AP, Sims-Mourtada Jennifer. The untapped potential of Gallium68-PET:The next wave of ^{68}Ga-agents. Appl Radiat Isot 2013;76: 14–23.

[33] Oxboel Jytte, Brandt-Larsen Malene, Schjoeth-Eskesen Christina, Myschetzky Rebecca, El-Ali Henrik H, Madsen Jacob, et al. Comparison of two new angiogenesis PET tracers ^{68}Ga-NODAGA-E[c(RGDyK)]$_2$ and ^{64}Cu-NODAGA-E[c(RGDyK)]$_2$: in vivo imaging studies in human xenograft tumors. Nucl Med Biol 2014;41:259–67.

[34] Li ZB, Chen K, Chen X. ^{68}Ga-labeled multimeric RGD peptides for microPET imaging of integrin $\alpha_v\beta_3$ expression. Eur J Nucl Med Mol Imaging 2008;35:1100–8.

[35] Chakraborty S, Sarma HD, Vimalnath KV, Pillai MR. Tracer level radiochemistry to clinical dose preparation of ^{177}Lu-labeled cyclic RGD peptide dimer. Nucl Med Biol 2013;40:946–54.

[36] Jin-Hwan Kim, Jae-Cheong Lim, Ki-Cheol Yun, Sun-Ju Choi, Young-Don Hong. Preparation and preliminary biological evaluation of ^{177}Lu-labeled GluDTPA-cyclo (RGDfK) for integrin $\alpha_v\beta_3$ receptor-positive tumor targeting. J Labelled Comp Radiopharm 2012;55:10–7.

[37] Ju Chang Hwan, Jeong Jae Min, Lee Yun-Sang, Kim Young Joo, Lee Byung Chul, Lee Dong Soo, et al. Development of a ^{177}Lu-Labeled RGD derivative for targeting angiogenesis. Cancer Biother Radiopharm 2010;25:687–91.

[38] Fawwaz RA, Wang TS, Srivastava SC, Hardy MA. The use of radionuclides for tumor therapy. Int J Rad Appl Instrum B 1986;13:429–36.

[39] Zaknun J, Bodei L, Mueller-Brand J, Pavel ME, Baum RP, Hörsch D, et al. The joint IAEA, EANM, and SNMMI practical guidance on peptide receptor radionuclide therapy (PRRNT) in neuroendocrine tumours. Eur J Nucl Med Mol Imaging 2013;40: 800–16.

Journal of
Biomedical Nanotechnology
Vol. 10, 393–404, 2014
www.aspbs.com/jbn

Molecular Targeting Radiotherapy with Cyclo-RGDfK(C) Peptides Conjugated to ^{177}Lu-Labeled Gold Nanoparticles in Tumor-Bearing Mice

Andrea Vilchis-Juárez[1,2], Guillermina Ferro-Flores[1,*], Clara Santos-Cuevas[1], Enrique Morales-Avila[2], Blanca Ocampo-García[1], Lorenza Díaz-Nieto[3], Myrna Luna-Gutiérrez[1,2], Nallely Jiménez-Mancilla[1,2], Martha Pedraza-López[3], and Leobardo Gómez-Oliván[2]

[1]*Departamento de Materiales Radiactivos, Instituto Nacional de Investigaciones Nucleares, Carretera México-Toluca S/N, La Marquesa, Ocoyoacac, Estado de México, C.P. 52750, Mexico*
[2]*Universidad Autónoma del Estado de México, Estado de México 50180, Mexico*
[3]*Instituto Nacional de Ciencias Médicas y Nutrición Salvador Zubirán, México D.F., 14000, Mexico*

Peptides based on the cyclic Arg-Gly-Asp (RGD) sequence have been designed to antagonize the function of $\alpha(v)\beta(3)$ integrin, thereby inhibiting angiogenesis. The conjugation of RGD peptides to radiolabeled gold nanoparticles (AuNP) produces biocompatible and stable multimeric systems with target-specific molecular recognition. The aim of this research was to evaluate the therapeutic response of ^{177}Lu-AuNP-RGD in athymic mice bearing $\alpha(v)\beta(3)$-integrin-positive C6 gliomas and compare it with that of ^{177}Lu-AuNP or ^{177}Lu-RGD. The radiation absorbed dose, metabolic activity (SUV, [^{18}F]fluor-deoxy-glucose-microPET/CT), histological characteristics and VEGF gene expression (by real-time polymerase chain reaction) in tumor tissues following treatment with ^{177}Lu-AuNP-RGD, ^{177}Lu-AuNP or ^{177}Lu-RGD were assessed. Of the radiopharmaceuticals evaluated, ^{177}Lu-AuNP-RGD delivered the highest tumor radiation absorbed dose (63.8 ± 7.9 Gy). These results correlated with the observed therapeutic response, in which ^{177}Lu-AuNP-RGD significantly ($p < 0.05$) induced less tumor progression, less tumor metabolic activity, fewer intratumoral vessels and less VEGF gene expression than the other radiopharmaceuticals, a consequence of high tumor retention and a combination of molecular targeting therapy (multimeric RGD system) and radiotherapy (^{177}Lu). There was a low uptake in non-target organs and no induction of renal toxicity. ^{177}Lu-labeled gold nanoparticles conjugated to cyclo-RGDfK(C) demonstrate properties suitable for use as an agent for molecular targeting radiotherapy.

KEYWORDS: *Radiolabeled Gold Nanospheres, RGD Peptides, Lutetium-177, Targeted Radiotherapy.*

INTRODUCTION

Molecular targeting therapy has become a relevant therapeutic strategy for cancer.[1,2] The principle that peptide receptors can be used successfully for *in vivo* targeting of human cancers has been proven, and radiolabeled peptides have been demonstrated to be effective in patients with malignant tumors.[3–5] The effectiveness of targeted radiotherapy depends primarily on the absorbed-dose rate and the total absorbed dose delivered to the tumor and to normal tissues. The dose and its rate depend on the physical properties of the radionuclide, the injected activity and the kinetics of uptake and clearance of radioactivity within the tumor and normal tissue/cells.[6]

Angiogenesis is a physiological process involving the growth of new blood vessels. Angiogenesis is a requirement for tumor growth and metastasis and is stimulated by signal proteins such as the vascular endothelial growth factor (VEGF) and cell adhesion receptors, including integrins. The $\alpha(v)\beta(3)$ integrin, a transmembrane protein consisting of two noncovalently bound subunits (α and β), is over-expressed on activated endothelial cells in the tumor neovasculature and on the cell membrane of various tumor cell types such as ovarian cancer, neuroblastoma, glioblastoma, breast cancer and melanoma cells. Based on

*Author to whom correspondence should be addressed.
Emails: ferro_flores@yahoo.com.mx, guillermina.ferro@inin.gob.mx
Received: 20 March 2013
Accepted: 16 May 2013

the Arg-Gly-Asp (RGD) tripeptide sequence a series of small peptides have been designed to antagonize the function of the $\alpha(v)\beta(3)$ integrin and to inhibit angiogenesis.[7] Radiolabeled RGD peptides have been reported as radiopharmaceuticals with high affinity and selectivity for the $\alpha(v)\beta(3)$ integrin; therefore, these peptides have potential for use in the early detection of rapidly growing tumors and noninvasive visualization of tumor metastasis in cancer patients.[8–12]

Gold nanoparticles can be used to prepare multivalent pharmaceuticals.[13–15] Recently we demonstrated that covalent conjugation of 100 molecules of cyclo-RGDfK(C) to the surface of one radiolabeled gold nanosphere (20 nm, gold-thiol bond) produces a biocompatible and stable multimeric system with target-specific molecular recognition *in vitro* and *in vivo*.[16–19] Due to passive and active-targeting mechanisms, the radiolabeled multimeric and multivalent system exhibit higher tumor uptake than does a RGD-monomer or -dimer.[16, 17]

Lutetium-177 (^{177}Lu) is a radionuclide with a half-life of 6.71 d, a β_{max} emission of 0.497 MeV (78%) and γ radiation of 0.208 MeV (11%) and has been used successfully for radiotherapy with efficient cross-fire effect in cancer cells.[3–5, 20]

If cyclo-RGDfK(C) peptides conjugated to ^{177}Lu-gold nanoparticles (^{177}Lu-AuNP-RGD) are retained in tumors by both passive and active-targeting mechanisms, the total dose (RGD and ^{177}Lu molecules) delivered to the tumor would be significantly higher than that produced by ^{177}Lu-AuNP or ^{177}Lu-RGD, reducing the tumor angiogenic activity and increasing the effectiveness of molecular targeting radiotherapy.

The aim of this research was to evaluate the therapeutic response of ^{177}Lu-AuNP-RGD in athymic nude mice bearing $\alpha(v)\beta(3)$-integrin-positive C6 gliomas and compare the radiation absorbed dose, metabolic activity, histological characteristics and VEGF gene expression in tumor tissues following treatment with ^{177}Lu-AuNP-RGD, ^{177}Lu-AuNP or ^{177}Lu-RGD.

METHODS

Design and Synthesis of ^{177}Lu-DOTA-GGC-AuNP-c[RGDfK(C)](^{177}Lu-AuNP-RGD)

In the c[RGDfK(C)] molecule, the sequence-Arg-Gly-Asp-(-RGD-) acts as the active biological site, the D-Phe (*f*) and Lys (*K*) residues complete the cyclic and pentapeptide structure, and Cys (*C*) is the spacer and active thiol group that interacts with the gold nanoparticle surface (Fig. 1). The c[RGDfK(C)] was synthesized and characterized according to the method described by Morales-Avila et al.[16] In the DOTA-GGC (1,4,7,10-tetraazacyclododecane-*N′*,*N″*,*N‴*-tetraacetic-Gly-Gly-Cys) molecule, the GG sequence is the spacer, cysteine (active thiol group) is used to interact with the gold nanoparticle surface and DOTA is used as the lutetium-177 chelator (Fig. 1). The DOTA-GGC was synthesized and characterized according to the method described by Luna-Gutierrez et al.[17]

Gold nanoparticles (AuNP) in injectable-grade water (20 ± 2 nm, 7×10^{11} particles/mL) were synthesized as described by Ocampo-García et al.[19]

Preparation of ^{177}Lu-DOTA-GGC: A 5 μL aliquot of DOTA-GGC (1 mg/mL) was diluted with 40 μL of 1 M acetate buffer at pH 5, followed by the addition of 10 μL of a $^{177}LuCl_3$ (~740 MBq, > 3 TBq/mg, ITG Isotope Technologies Garching GmbH, Germany) solution. The mixture was incubated at 90 °C in a block heater for 30 min. All solutions were prepared using deionized water. A radiochemical purity of > 98% was verified by TLC silica gel plates (aluminum backing, Merck); 10-cm strips were used as the stationary phase, and ammonium hydroxide:methanol:water (1:5:10) was used as the mobile phase to determine the amount of free ^{177}Lu ($R_f = 0$) and ^{177}Lu-DOTA-GGC ($R_f = 0.4$–0.5). Radiochemical purity was also determined by reversed-phase HPLC on a C-18 column (μ-Bondapack C-18, Waters) using a Waters Empower system with an in-line radioactivity detector and a gradient of water/acetonitrile containing 0.1% TFA from 95/5 (v/v) to 20/80 (v/v) over 35 min at a flow rate of 1 mL/min ($^{177}LuCl_3$ $t_R = 3$–4 min; ^{177}Lu-DOTA-GGC $t_R = 12$–13 min).

Preparation of ^{177}Lu-DOTA-GGC-AuNP-c[RGDfK(C)]: To 1 mL of AuNP (20 nm), 0.025 mL of c[RGDfK(C)] (5 μM; 108 molecules per 20 nm nanoparticle) was added, followed by 3 μL (40 MBq) of ^{177}Lu-DOTA-GGC (0.25 μg of peptide; 1.89×10^{14} molecules; 270 molecules per 20 nm AuNP), and the mixture was stirred for 5 min to form the ^{177}Lu-DOTA-GGC-AuNP-c[RGDfK(C)] system (Fig. 1). No further purification was required because we have found that the maximum number of peptides that can be bound to one AuNP (20 nm) is between 520 and 1701 depending of the peptide structure.[16, 19] The number of peptides per nanoparticle was calculated by UV-Vis titration of peptides (8 μM) using increasing gold nanoparticle concentration (from 0 to 1 nM).[16, 19]

Radiochemical Purity of ^{177}Lu-AuNP-RGD: Size-exclusion chromatography and ultrafiltration were used as radiochemical control methods for the final radiopharmaceutical solution. A 0.1 mL sample of ^{177}Lu-DOTA-GGC-AuNP-c[RGDfK(C)] was loaded onto a PD-10 column and injectable water was used as the eluent. The first radioactive and red eluted peak (3.0–4.0 mL) corresponded to radiolabeled AuNP-c[RGDfK(C)]. The free radiolabeled peptide (^{177}Lu-DOTA-GGC) appeared in the fraction that eluted at 5.0–7.0 mL, and $^{177}LuCl_3$ remained trapped in the column matrix. Upon ultrafiltration (Centricron YM-30 regenerated cellulose 30,000 MW cut off, Millipore, Bedford, MA, USA), the ^{177}Lu-DOTA-GGC-AuNP-c[RGDfK(C)] remained in the filter, while free ^{177}Lu-DOTA-GGC and $^{177}LuCl_3$ passed through the filter. In the radio-HPLC size exclusion system (ProteinPak 300SW, Waters, 1 mL/min, injectable water),

P-269 ^{66}Ga labeled DOTA-E(c(RGDfK))$_2$ and NODAGA-E(c(RGDfK))$_2$ to target tumors over-expressing $\alpha_v\beta_3$ integrin receptors

Lopez-Rodriguez, V.[1]; Gaspar-Carcamo, R.E.[1]; Lara-Camacho, V.M.[1]; Avila-Garcia M.[1]; Ferro-Flores, G.[2]; Pedraza-Lopez, M.[3]; Arteaga de Murphy, C.[3]; Avila-Rodriguez, M.A.[1]

1 Unidad PET, Facultad de Medicina, Universidad Nacional Autónoma de México, Mexico City, Mexico; 2 Instituto Nacional de Investigaciones Nucleares, Estado de México, Mexic; 3 Instituto Nacional de Ciencias Médicas y Nutrición Salvador Zubirán, Mexico City, Mexico

Objectives: Angiogenesis plays an important role in neoplastic processes, one of the key players involved in this angiogenic process of $\alpha v\beta_3$ integrin. This integrin is overexpress on endothelial cells during blood vessel formation where it affects tumour growth, local invasiveness and metastatic potential. It has been shown that peptides based on the Arg-Gly-Asp (RGD) amino acid sequence have a high affinity and selectivity for $\alpha_v\beta_3$ integrin receptors [1]. The aim of this research was to prepare and evaluate ^{66}Ga-DOTA-Glu-[cyclo(Arg-Gly-Asp-D-Phe-Lys)]$_2$ and ^{66}Ga-NODAGA-Glu-[cyclo(Arg-Gly-Asp-D-Phe-Lys)]$_2$ as potential agents to target tumors over-expressing $\alpha_v\beta_3$ integrin receptors.

Methods: ^{66}Ga was produced in a cyclotron via the ^{66}Zn(p,n)^{66}Ga reaction with 11 MeV protons using ^{nat}Zn electrodeposited on Au backing as target material. Radiochemical separation was performed by ion exchange chromatography [2]. For radiolabelling, 40 µl of DOTA-E-[c(RGDfK)]$_2$ (0.4 mg/ml) or NODAGA-E-[c(RGDfK)]$_2$ (0.75 mg/ml), with 1M HEPES (pH 7) and0.25M NH_4OAc (pH 5.5), were mixed with 18.5-37 MBq of $^{66}GaCl_3$ stock solution (0.1M HCl) and incubated for 20 min at 95°C or room temperature, respectively. Radiochemical purity was determined by TLC using SG strips as stationary phase and 1:1 MeOH:10% NH_4OAc (v/v) as mobile phase. TLC-strips were analyzed by autoradiography. *In vitro* stability in human serum and 0.9% NaCl was evaluated up to 24 h at 37 °C and protein binding was determined in fresh human serum for 2 h at 37°C, samples were analyzed by ultrafiltration. Preclinical evaluation of the labelled peptide conjugates was performed in nude mice bearing C6 (glioma) xenografts using a microPET Focus 120.

Results: The radiochemical purity of ^{66}Ga-DOTA-E-[c(RGDfK)]$_2$ and ^{66}Ga-NODAGA-E-[c(RGDfK)]$_2$ were > 98 ± 2% (Figure 1A). *In vitro* studies indicated high stability of the compounds in 0.9% NaCl and human serum after 24 h incubation at 37°C. Protein binding was <5% after 2 h incubation as determined by ultrafiltration. MicroPET images showed contrasting tumors reflecting $\alpha_V\beta_3$-targeted tracer accumulation from 1 to 24 h after injection and receptor-specific-mediated uptake of the tracer was demonstrated by injecting unlabeled c(RGDfK)$_2$ prior to tracer injection.

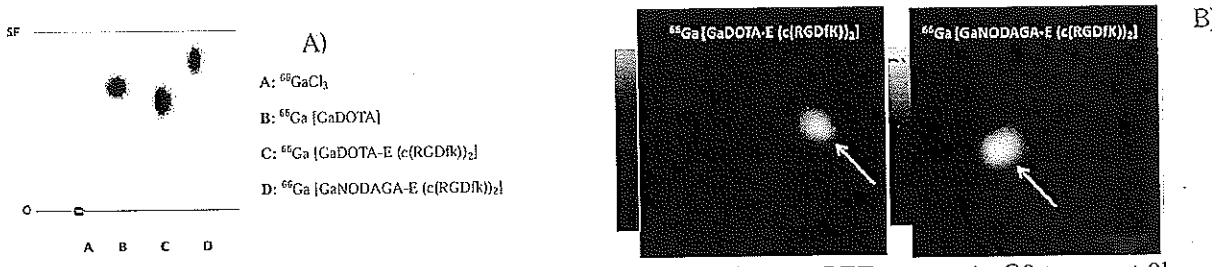

Figure 1. A) Autorradiography of radiochemical purity by TLC and B) MicroPET images in C6 tumor at 3h post-injection

Conclusions: ^{66}Ga-DOTA-E-[c(RGDfK)]$_2$ and ^{66}Ga-NODAGA-E-[c(RGDfK)]$_2$ were prepared with high radiochemical purity (>98) without post-labeling purification, high *in vitro* stability, low protein-bound activity and demonstrated high affinity for the $\alpha_v\beta_3$ integrin.

Research Support: This work was supported by CONACYT Grant 179218, UNAM-DGAPA-PAPIIT TA200512 and International Atomic Energy Agency RC16467.

References: [1] Dijkgraaf I,et al.(2011) Eur J Nucl Med Mol Imaging, 38, 128-37. [2] Engle JW,et al. (2012) Appl Radiat Isot, 70, 1792-96.

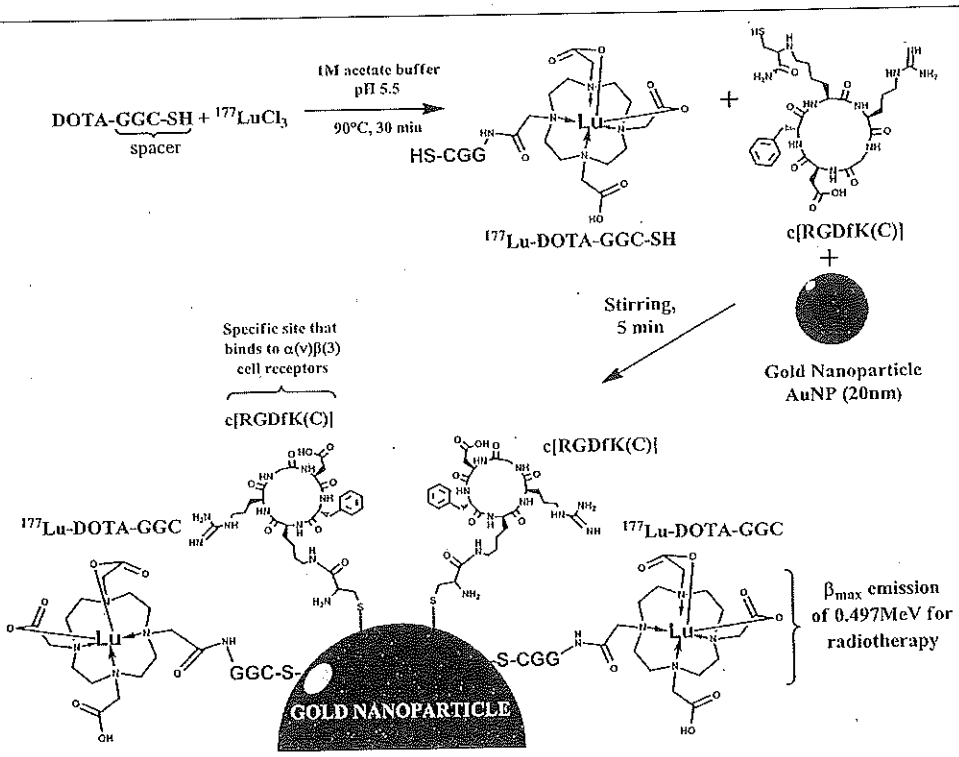

Figure 1. Overall scheme of ^{177}Lu-DOTA-GGC-AuNP-c[RGDfK(C)] (^{177}Lu-AuNP-RGD) preparation.

the t_Rs for the ^{177}Lu-DOTA-GGC-AuNP-c[RGDfK(C)] and ^{177}Lu-DOTA-GGC were 4–5 and 8 min, respectively (Fig. 2). Chromatographic profiles were obtained using two different detector systems, the UV-Vis detector and a radiometric detector. The sample first passed by the UV-Vis detector (photodiode array) and after 0.37 min (0.37 mL, 1 mL/min) it passed by the radioactive detector. Correspondence of retention times of the peaks of interest in the chromatogram is commonly accepted as a proof of the chemical identity of the radiopharmaceutical. The UV-Vis spectrum, assigned to the peak at 4–5 min using the photodiode array of the system, exhibited the AuNP surface plasmon band at 521 nm. Minor peaks corresponded to minor ^{177}Lu-AuNP-RGD-sizes. (Fig. 2).

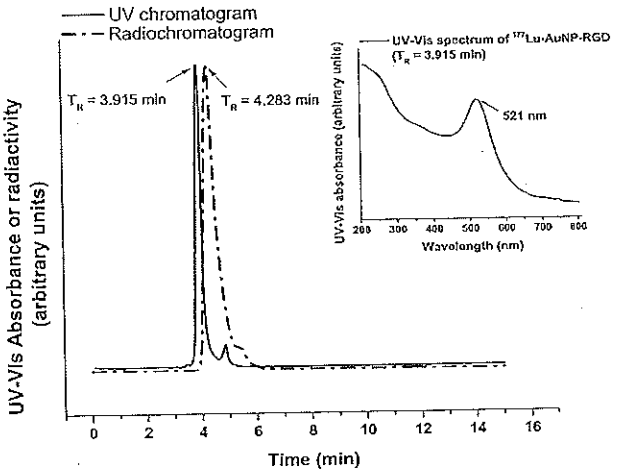

Figure 2. Size-exclusion HPLC chromatogram (520 nm; continuous line) and HPLC radiochromatogram (dotted line) of the ^{177}Lu-DOTA-GGC-AuNP-c[RGDfK(C)] (^{177}Lu-AuNP-RGD) conjugate. UV-Vis spectrum of the compound with retention time at 3.915 min (inset).

Preparation of ^{177}Lu-DOTA-GGC-AuNP (^{177}Lu-AuNP)

Three μL (40 MBq) of ^{177}Lu-DOTA-GGC (0.25 μg of peptide; 1.89×10^{14} molecules; 270 molecules per 20 nm AuNP) was added to 1 mL of AuNP (20 nm), and the mixture was stirred for 5 min to form the ^{177}Lu-DOTA-GGC-AuNP system. No further purification was performed. Radiochemical purity was evaluated as described above for ^{177}Lu-AuNP-RGD.

Chemical Characterization

The characterization of the DOTA-GGC and c[RGDfK(C)] conjugated to the gold nanoparticle surface by far infrared (FIR), UV-Vis, X-ray photoelectron spectroscopy (XPS) and Raman spectroscopy was previously reported in detail.[16–19]

Transmission Electron Microscopy (TEM): AuNP, ^{177}Lu-AuNP and ^{177}Lu-AuNP-RGD were characterized in size and shape by TEM using a JEOL JEM 2010 HT microscope operated at 200 kV. The samples were prepared for analysis by evaporating a drop of the aqueous product onto a carbon-coated TEM copper grid.

Particle size and zeta potential: AuNP, ^{177}Lu-AuNP or ^{177}Lu-AuNP-RGD were measured ($n = 5$) using

the particle size (dynamic light scattering = DLS) and Z potential Nanotrac-analyzer (Nanotrac Wave, Model MN401, Microtract, FL, USA).

Preparation of ^{177}Lu-DOTA-E-c(RGDfK)$_2$ (^{177}Lu-RGD)

DOTA-E-c(RGDfK)$_2$ was synthesized by Peptide International Inc. (Kentucky, USA) with a purity of > 98% as analyzed by reversed-phase HPLC (RP-HPLC) and mass spectroscopy. A 5 μL aliquot of DOTA-E-c(RGDfK)$_2$ (1 mg/mL) was diluted with 50 μL of 1 M acetate buffer at pH 5, followed by the addition of 10 μL of the ^{177}LuCl$_3$ (~370 MBq, > 3 TBq/mg, ITG Isotope Technologies Garching GmbH, Germany) solution. Each mixture was incubated at 90 °C in a block heater for 30 min and diluted to 18 mL with injectable-grade water. A radiochemical purity of > 98% was verified by TLC and HPLC as described above for ^{177}Lu-DOTA-GGC.

Cell Culture

The C6 rat cell line was originally obtained from ATCC (Atlanta, GA, USA). The cells were routinely cultured at 37 °C, with 5% CO_2 and 85% humidity in minimum essential medium eagle (MEM, Sigma-Aldrich Co., Saint Louis, Missouri, USA) supplemented with 10% fetal bovine serum and antibiotics (100 units/mL penicillin and 100 μg/mL streptomycin).

Solid-Phase $\alpha(v)\beta(3)$ Binding Assay

Microtiter 96-well vinyl assay plates (Corning, NY, USA) were coated with 100 μL/well of purified human integrin $\alpha(v)\beta(3)$ solution (150 ng/mL, Chemicon-Millipore Corporation, Billerica, MA, USA) in coating buffer (25 mM Tris-HCl, pH 7.4, 150 mM NaCl, 1 mM $CaCl_2$, 0.5 mM $MgCl_2$ and 1 mM $MnCl_2$) for 17 h at 4 °C. The plates were washed twice with binding buffer (0.1% bovine serum albumin (BSA) in coating buffer). The wells were blocked for 2 h with 200 μL of blocking buffer (1% BSA in coating buffer). The plates were washed twice with binding buffer. Then, 100 μL of binding buffer containing 10 kBq of ^{177}Lu-AuNP-RGD or ^{177}Lu-RGD and appropriate dilutions of c(RGDfK) (from 10.000 nM to 0.001 nM in binding buffer, Bachem-USA) were incubated in the wells at 37 °C for 1 h. After incubation, the plates were washed three times with binding buffer. The wells were cut out and counted in a gamma counter. The IC_{50} values of the RGD peptides were calculated by nonlinear regression analysis ($n = 5$).

In Vitro Cell Proliferation After ^{177}Lu-AuNP-RGD, ^{177}Lu-AuNP and ^{177}Lu-RGD Treatments

C6 cells suspended in fresh medium were incubated in a 96-well plate at a density of 1×10^3 cells/well. The cells were cultured for 24 h at 37 °C with 5% CO_2 and 85% humidity. The growth medium was removed, and the cells were exposed for 2 h (at 37 °C, with 5% CO_2 and 85% humidity) to one of the following treatments ($n = 6$):

(a) 100 μL of ^{177}Lu-AuNP-RGD (5 kBq) and 100 μL of PBS, pH 7,

(b) 100 μL of ^{177}Lu-AuNP (5 kBq) and 100 μL of PBS, pH 7,

(c) 100 μL of ^{177}Lu-RGD (5 kBq) and 100 μL of PBS, pH 7 or

(d) no treatment.

After 2 h, the solution in each well was removed and replaced with fresh culture medium. The cells were maintained for 3 days at 37 °C with 5% CO_2 and 85% humidity. After that, the percentage of cell proliferation in each well was evaluated by the spectrophotometric measurement of cell viability as a function of mitochondrial dehydrogenase activity, which involves the cleavage of the tetrazolium ring of XTT (sodium 3′-[1-[phenylaminocarbonyl]-3,4-tetrazolium]-bis[4-methoxy-6-nitro]benzene sulfonic acid hydrate) in viable cells to yield orange formazan crystals that are dissolved in acidified isopropanol (XTT kit, Roche Diagnostics GmbH, Mannheim, Germany). The resulting absorbance of the orange solution was measured at 480 nm in a microplate absorbance reader (EpochTM, BioTek, VT, USA). The absorbance of the untreated cells was considered as 100% of living C6 cells (or 100% proliferation).

Induction of C6 Tumors in Athymic Mice

Tumor uptake studies in mice were performed according to the rules and regulations of the Official Mexican Norm 062-ZOO-1999. The study was approved by the Institutional Committee for the Care and Use of Laboratory Animals ("*Instituto Nacional de Ciencias Médicas y Nutrición Salvador Zubirán*").

Athymic male mice (20–22 g) were kept in sterile cages with bedding of wood-shavings, constant temperature, humidity, noise and 12:12 light periods. Water and feed (standard PMI 5001 feed) were given *ad libitum*.

Glioma tumors were induced by subcutaneous injection of C6 cells (1.5×10^6) suspended in 0.2 mL of phosphate-buffered saline into the upper back of twenty 6–7-week-old nude mice. Injection sites were observed at regular intervals for tumor formation and progression.

Therapeutic Protocol

Four groups ($n = 5$, total mice = 20) of athymic nude mice bearing C6 gliomas (tumor size 0.05 ± 0.01 g) were used. Each group was treated with one of the following radiopharmaceuticals: (a) ^{177}Lu-AuNP-RGD or (b) ^{177}Lu-AuNP or (c) ^{177}Lu-RGD. There was an untreated control group. All radiopharmaceuticals (four administrations of 2 MBq/0.05 mL; in the case of ^{177}Lu-AuNP-RGD and ^{177}Lu-RGD ~ 3×10^{12} molecules of c-RGD) were injected intratumorally in mice under 2% isoflurane anesthesia. Doses were administered at day 1, 7, 14 and 21, for a total of four doses. Tumor growth was monitored weekly, the

length (L) and width (a) were measured with calipers and the volume was determined as $V = \pi/6 * (L) \times (a^2)$. Considering a tumor density of 1 g/cm^3, the tumor mass in grams was calculated. After 23 days, the mice were sacrificed and tumors and kidneys were dissected and prepared for histopathological or PCR studies as described below. Blood samples were also obtained for creatinine and urea quantification.

Biokinetic Studies

To evaluate biokinetics, the radiopharmaceuticals ^{177}Lu-AuNP-RGD, ^{177}Lu-AuNP or ^{177}Lu-RGD were administered intratumorally in mice with induced C6 tumors (0.05 mL, ~2 MBq). Mice were sacrificed at 3, 24, 48 and 96 h post-administration ($n = 3$ at each time, total mice = 12). Whole liver, heart, spleen, lung, kidneys and tumor as well as samples of blood, intestines, bone and muscle were placed into pre-weighed plastic test tubes. The activity was determined in a well-type scintillation detector (Auto In-V-tron 4010, Nuclear Medical laboratories Inc., CA, USA) along with 3×0.05 mL aliquots of the standard (~2 MBq) representing 100% of the injected dose to obtain the activity corrected by decay. Mean activities were used to obtain the percentage of the injected dose per organ (%ID). The time activity curves corrected by decay $[q_h(t) = A_h(t)e^{\lambda R^t}]$ (biological behavior) for ^{177}Lu-AuNP-RGD, ^{177}Lu-RGD or ^{177}Lu-AuNP were calculated using the %ID at different times.

Radiation Absorbed Dose Assessment

The $A_h(t)$ functions $[A_h(t) = q_h(t)e^{-\lambda_{Lu-177^t}}]$ obtained from the biokinetics studies were integrated to obtain the total number of disintegrations (N) in the main source regions (liver, spleen, kidneys and tumor) during the entire treatment:

$$N_{\text{source}} = \int_{t=0}^{t=23\ \text{d}} A_h(t)\,dt + \int_{t=7\ \text{d}}^{t=23\ \text{d}} A_h(t)\,dt + \int_{t=14\ \text{d}}^{t=23\ \text{d}} A_h(t)\,dt + \int_{t=21\ \text{d}}^{t=23\ \text{d}} A_h(t)\,dt$$

The absorbed dose to organs was evaluated according to the general equation:

$$\bar{D}_{\text{target}\leftarrow\text{source}} = \sum_{\text{sources}} N_{\text{source}} \times DF_{\text{target}\leftarrow\text{source}}$$

where $\bar{D}_{\text{target}\leftarrow\text{source}}$ is the mean absorbed dose to a target organ from a source organ and $DF_{\text{target}\leftarrow\text{source}}$ is a dose factor:

$$DF_{\text{target}\leftarrow\text{source}} = \sum_i \Delta_i \Phi_{i(\text{target}\leftarrow\text{source})}$$

The Δ_i terms are the mean energy emitted per disintegration for the various i-type radiations (i-type emissions, $\sum n_i E_i$). The Φ_i terms are the absorbed fractions that depend on the properties of the i-type emission and the size, shape and separation of the source and target organs. DF values were calculated according to Miller et al.[21] using the beta-absorbed fractions in a mouse model calculated by two Monte Carlo radiation transport codes, MCNP4C and PEREGRINE (voxel-based).

^{177}Lu-SPECT/CT Imaging

Single photon emission computed tomography (SPECT) and X-ray computed tomography (CT) images were acquired 24 h after the last injection (at 22 days of treatment) using a micro-SPECT/CT scanner (Albira, ONCOVISION, Spain) to verify the tumor uptake of ^{177}Lu-AuNP-RGD, ^{177}Lu-AuNP or ^{177}Lu-RGD. Mice under 2% isoflurane anesthesia were placed in the prone position and whole body imaging was performed. The micro-SPECT field of view was 60 mm, a symmetric 20% window was set at 208 keV and pinhole collimators were used to acquire a 3D SPECT image with a total of 64 projections of 30 s, over 360°. The image dataset was then reconstructed using the ordered subset expectation maximization (OSEM) algorithm with standard mode parameter as provided by manufacturer. CT parameters were 35 kV sure voltage, 700 μA current and 600 micro-CT projections.

Standardized Uptake Value (SUV) of [^{18}F]FDG in Tumors with PET/CT: Tumor Metabolic Activity

[^{18}F]FDG (2-deoxy-2-[^{18}F]fluoro-D-glucose)-positron emission tomography (PET) and X-ray CT imaging were performed using a micro-PET/CT scanner (Albira, ONCOVISION, Spain). The images were acquired at the end of the treatments (after 23 days). The micro-PET field of view was 60 mm. Mice were injected in the lateral tail vein with 9 MBq of [^{18}F]FDG in 100 μL PBS under 2% isoflurane anesthesia. After a resting period of 1 h the mice were transferred to the scanning room, placed in a prone position and the whole body imaging was performed. The PET acquisition time was 7.5 min. The CT parameters were those described above. From the [^{18}F]FDG dose and weight of each mouse, the mean standardized uptake value ($n = 5$) [mean SUV = (Bq/g)/(injected activity, Bq/body weight, g)] was calculated using PMOD Data Analysis Software (PMOD technologies).

Creatinine, Urea and BUN Quantification

Blood samples obtained at the end of the treatments were used to quantify creatinine, urea and urea nitrogen (BUN) in order to evaluate kidney function because renal toxicity is the primary obstacle to radiopeptide therapy.[22] Creatinine was measured titrimetrically using the conventional picrate method. Serum urea and BUN were quantified by an enzymatic *in vitro* assay using the coupled urease/glutamate dehydrogenase (GLDH) enzyme system.

Histopathological Evaluation

Tumors and kidneys samples were fixed in neutral 10% formaldehyde for 24 h, washed in 70% ethanol and

Table I. Primers and probes used in the VEGF gene expression assessment in tumor tissues by real time-PCR analysis.

Gen/Accession number	Upper primer	Lower primer	Amplicon (nt)	Probe number*
β-Actin/NM_031144.2	tgccctagacttcgagcaag	ggcagctcatagctcttctcc	72	69
VEGF/AY702972.1	cggagagcaacgtcactatg	tggtctgcattcacatctgc	104	4

Note: *From the universal probe library (Roche).

embedded in paraffin. Sections of 4 μm thickness were placed on slides and dried in an oven at 37 °C. Sections were dewaxed in xylene, rehydrated in a series of graded alcohols, and finally stained with Meyer's hematoxylin/eosin and coverslipped.

Evaluation of VEGF Expression in Tumors by Real-Time PCR

All the oligonucleotides for real-time polymerase chain reaction (qPCR) assays were obtained from Invitrogen (CA, USA). The TaqMan Master reaction, TaqMan probes, capillaries and the reverse transcription (RT) system were from Roche (Roche Applied Science, IN, USA).

Excised tumors were homogenized in 1 mL of Trizol reagent with a Polytron homogenizer (BioSpec Products, Inc.). Total RNA was then extracted following the manufacturer's instructions. Three μg of total RNA was reverse transcribed with the Transcriptor RT system. Real-time PCR was performed with the LightCycler® 2.0 from Roche (Roche Diagnostics, Mannheim, Germany), according to the following protocol: activation of Taq DNA polymerase and DNA denaturation at 95 °C for 10 min, followed by 45 amplification cycles consisting of 10 s at 95 °C, 30 s at 60 °C, and 1 s at 72 °C. Primers sequences, corresponding probe numbers and the sizes of the resulting amplicons are given in Table I. Gene expression of the housekeeping gene β-actin was used as an internal control and the results were expressed as a relative concentration (RC) of β-actin expression.

Statistical Analysis

Differences between the treatment groups were evaluated with Student's *t*-test. (Significance was defined as $p < 0.05$.)

RESULTS

Chemical Characterization and *In Vitro* Evaluation

^{177}Lu-AuNP-RGD, ^{177}Lu-RGD and ^{177}Lu-AuNP were obtained with radiochemical purities of > 92%. The TEM images of ^{177}Lu-AuNP-RGD and ^{177}Lu-AuNP showed monodisperse solutions (Fig. 3). The increase in the hydrodynamic diameter of the particle by the peptide conjugation-effect was observed by TEM as a low electronic density around the gold nanoparticle due to the poor interaction of the electron beam with the peptide molecules (low electron density), in contrast to the strong scattering of the electron beam when it interacted with the metallic nanoparticles (Fig. 3). The average particle hydrodynamic diameters determined by DLS were 26.6 ± 8.7 nm, 25.6 ± 9.4 nm and 23.8 ± 7.6 nm for ^{177}Lu-AuNP-RGD, ^{177}Lu-AuNP and AuNP, respectively (Fig. 3). The *Z* potential of ^{177}Lu-AuNP-RGD was −64.6 ± 2.8 mV and that of ^{177}Lu-AuNP was −56.9 ± 3.1 mV, versus −22.2 ± 1.7 mV for the AuNP, indicating that the peptide functionalization (both, DOTA-GGC and c[RGDfK(C)]) conferred a high colloidal stability to the nanosystem.[23]

The *in vitro* affinity, which was determined by a competitive binding assay, indicated that the concentration of c(RGDfK) required to displace 50% of the ^{177}Lu-AuNP-RGD ($IC_{50} = 10.2 \pm 1.1$ nM) or ^{177}Lu-RGD ($IC_{50} = 5.3 \pm 0.4$ nM) from the receptor was the same order of magnitude for both, demonstrating a high *in vitro* affinity for the $\alpha(v)\beta(3)$ integrin for both conjugates. However, the amount of c(RGDfK) required to displace ^{177}Lu-AuNP-RGD from the $\alpha(v)\beta(3)$ protein was twice of that necessary to displace ^{177}Lu-RGD, which may be attributed to the multivalent effect of the AuNP system.[8, 9, 24]

As shown in Figure 4, ^{177}Lu-AuNP-RGD significantly inhibited C6 cell proliferation (3.62 ± 1.07%) with respect to that of ^{177}Lu-AuNP (6.32 ± 1.16%) and ^{177}Lu-RGD (29.67 ± 2.82%), which was also attributed to the greater *in vitro* C6 cell internalization as a result of multivalency.

Biokinetics, Radiation Absorbed Dose and Therapeutic Response

After each of the four intratumoral administrations, the mean tumor uptakes 3 h post injection were 68.1 ± 7.1% ID (^{177}Lu-AuNP-RGD), 48.2 ± 5.5% ID (^{177}Lu-AuNP) and 26.8 ± 2.9% ID (^{177}Lu-RGD), with a high tumor retention for the radiolabeled nanoparticles. The tumor retention of ^{177}Lu-AuNP-RGD at 96 h (34.7 ± 4.3% ID) was significantly higher ($p < 0.05$) than that of ^{177}Lu-AuNP (15.5 ± 1.7% ID), whereas ^{177}Lu-RGD exhibited the highest tumor clearance (5.7 ± 0.8% ID). Uptake occurred mainly in the kidneys and liver, as well as in the spleen, with negligible uptake in other organs. The mean tumor residence times were 61.6 ± 5.8 h (^{177}Lu-AuNP-RGD), 38.7 ± 4.1 h (^{177}Lu-AuNP) and 17.3 ± 2.4 h (^{177}Lu-RGD), while the mean kidney residence times were 0.88 ± 0.11 h (^{177}Lu-AuNP-RGD), 0.72 ± 0.10 h (^{177}Lu-AuNP) and 1.20 ± 0.24 h (^{177}Lu-RGD). Figure 5 shows the total radiation absorbed doses to the kidney, liver and spleen that were received during the different treatment protocols. The kidneys are the major dose-limiting

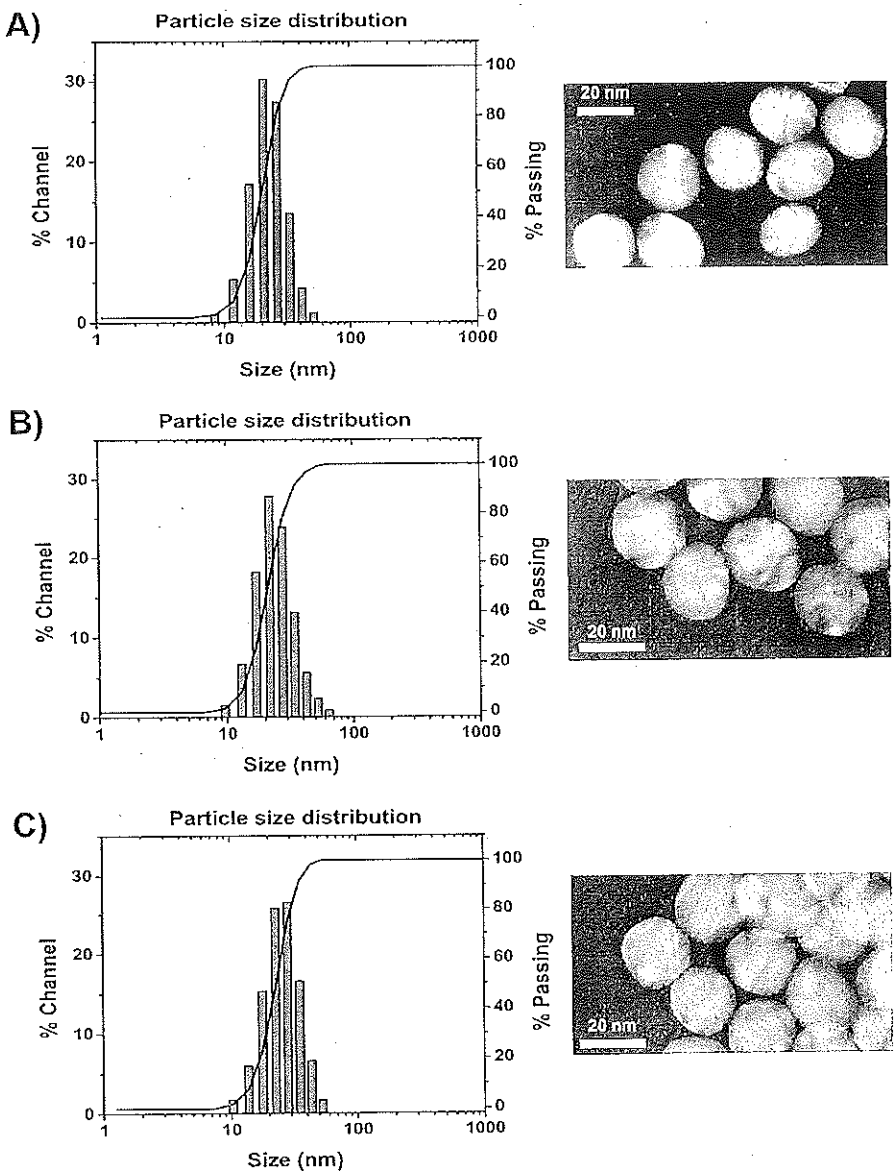

Figure 3. TEM image and size distribution of (A) AuNP, (B) ^{177}Lu-AuNP and (C) ^{177}Lu-AuNP-RGD.

organ because of the tubular re-absorption and retention of radioactivity, which may lead to radiation nephropathy.[22,25] The maximum tolerated dose to the kidneys is 25–30 Gy and the dose in our study was less than 1.5 Gy in the three ^{177}Lu treatments.[22]

The tumor size progression for all ^{177}Lu-conjugates was significantly lower ($p < 0.05$) after 23 days with respect to that of the control group (Fig. 6). At 23 days, tumor size in the ^{177}Lu-AuNP-RGD group was 27 times smaller than that of the controls and twelve-fold and three-fold smaller than in the ^{177}Lu-RGD and ^{177}Lu-AuNP groups, respectively (Fig. 6). These tumor size data correlate with the doses delivered to the tumor in the following order: ^{177}Lu-AuNP-RGD (63.8 ± 7.9 Gy), ^{177}Lu-AuNP (38.3 ± 4.2 Gy) and ^{177}Lu-RGD (16.6 ± 1.3 Gy) (Fig. 6). The experimental protocol was completed at 23 days because the control mice presented tumor sizes as large as 3 g, therefore, sacrifice was necessary.

Figure 7 shows the ^{177}Lu-micro-SPECT/CT images at 24 h after the last injection (at 22 days of treatment), in which the differences in tumor sizes and radiopharmaceutical accumulation in cancer tissues as well as the negligible uptake in non-target organs are visible. The tumor area in which no radioactivity is observed is necrotic tissue. It is important to mention that in advanced stages, the histopathological features of glioma are extensive necrotic foci surrounded by tumor cells, while in less-advanced neoplasms the necrosis occurs sparsely. Because ^{177}Lu-AuNP-RGD induced less tumor progression than the other radiopharmaceuticals, its tumor uptake in the micro-SPECT/CT image was more homogeneous indicating less necrosis.

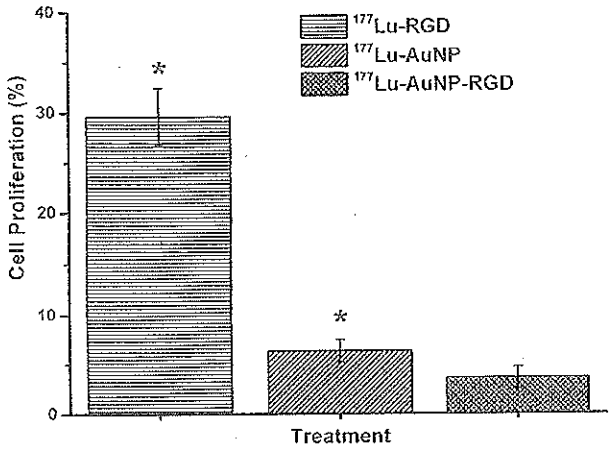

Figure 4. Effect of the ^{177}Lu-AuNP-RGD, ^{177}Lu-AuNP and ^{177}Lu-RGD on *in vitro* C6 cell proliferation. *Statistically significant difference ($p < 0.05$) versus ^{177}Lu-AuNP-RGD.

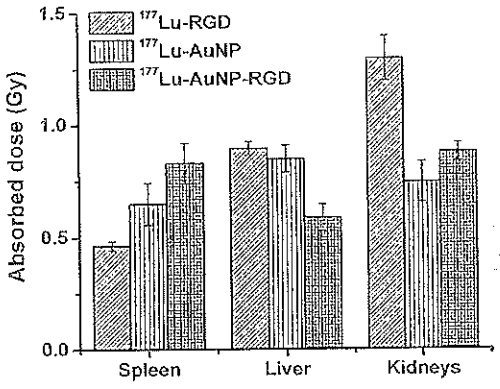

Figure 5. Radiation absorbed doses of ^{177}Lu-AuNP-RGD, ^{177}Lu-AuNP and ^{177}Lu-RGD to the spleen, liver and kidney induced in mice after 23 days of treatment.

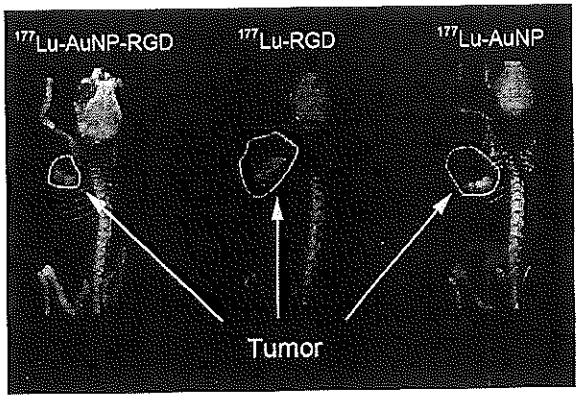

Figure 7. micro-SPECT/CT images of ^{177}Lu-AuNP-RGD, ^{177}Lu-AuNP and ^{177}Lu-RGD at 24 h after the last injection (at 22 days of treatment). The tumor areas in which no radioactivity is observed is necrotic tissue. Extensive necrotic foci are present in advanced stages of glioblastomas and in less-advanced neoplasms necrosis occurs sparsely. ^{177}Lu-AuNP-RGD tumor uptake is more homogeneous indicating less necrotic tissue.

Tumor Metabolic Activity

High accumulation of [^{18}F]FDG in the tumor and consequently high SUV values represent high metabolic activity in viable tumor cells. As shown in Table II, the SUV values of the groups treated with ^{177}Lu-radiopharmaceuticals were significantly lower than those of the control group ($p < 0.05$), while the SUV of the ^{177}Lu-AuNP-RGD group was significantly lower than that of ^{177}Lu-AuNP and ^{177}Lu-RGD groups ($p < 0.05$) (Fig. 8).

Histopathological Studies

Microscopic histological characteristics that define C6 gliomas were observed in tumors implanted in mice,

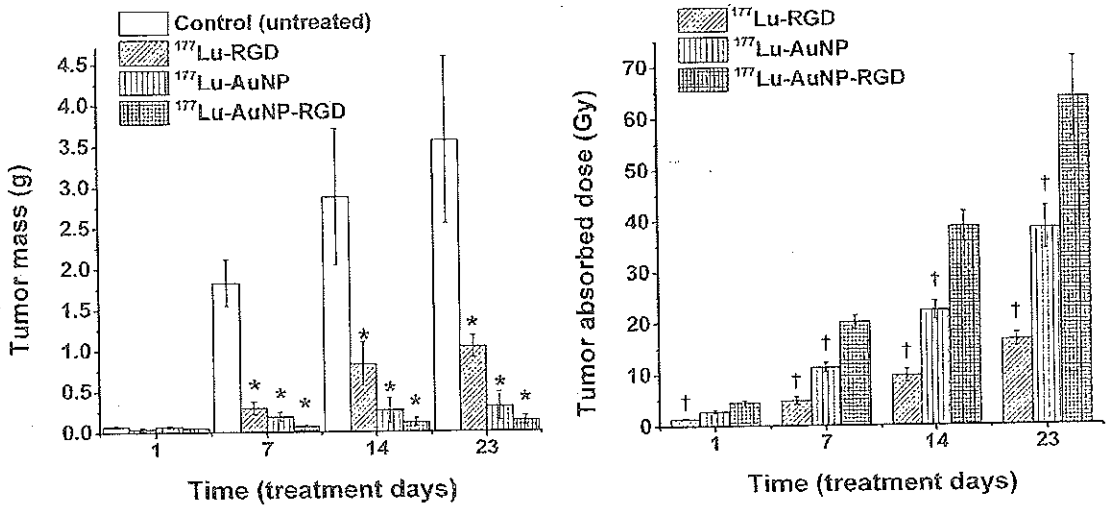

Figure 6. Tumor size progression for ^{177}Lu-AuNP-RGD, ^{177}Lu-AuNP and ^{177}Lu-RGD groups at different days of the treatment (left). The average radiation absorbed doses of ^{177}Lu-AuNP-RGD, ^{177}Lu-AuNP and ^{177}Lu-RGD delivered to C6 tumors (right). *Statistically significant difference ($p < 0.05$) versus control group. †Statistically significant difference ($p < 0.05$) versus ^{177}Lu-AuNP-RGD group.

Table II. Tumor metabolic activity (^{18}FDG standard uptake value, SUV), VEGF gene expression in tumor tissues (relative concentration versus β-actin) and urea, creatinine and urea nitrogen (BUN) serum concentrations in mice bearing C6 gliomas after 23 days of treatment with ^{177}Lu-AuNP-RGD, ^{177}Lu-RGD or ^{177}Lu-AuNP (mean ± standard deviation).

Treatment group	SUV	VEGF (RC)	Creatinine (mg/dL)	Urea (mg/dL)	BUN (mg/dL)
^{177}Lu-AuNP-RGD	0.335 ± 0.099*	0.012 ± 0.006*	0.230 ± 0.026	77.933 ± 7.497	30.417 ± 3.502
^{177}Lu-AuNP	0.584 ± 0.107*†	0.040 ± 0.012†	0.163 ± 0.050	67.025 ± 7.562	31.320 ± 3.534
^{177}Lu-RGD	2.740 ± 0.260*†	0.037 ± 0.006†	0.180 ± 0.036	59.267 ± 5.292	32.993 ± 2.433
Control	6.539 ± 0.052	0.070 ± 0.028	0.200 ± 0.057	63.550 ± 3.894	29.698 ± 1.821

Notes: *Statistically significant difference ($p < 0.05$) versus control (untreated group); †Statistically significant difference ($p < 0.05$) versus ^{177}Lu-AuNP-RGD group.

including giant cells and pleomorphic cell elements, mostly with vesicular nuclei and abundant eosinophil cytoplasm, mitotic forms and atypical nuclei. The following characteristics were observed in the different treatment groups.

^{177}Lu-AuNP-RGD: Tumors were delimited by a weak necrotic (N) area in the periphery (Fig. 9(A)); intratumoral vessels (V) observed in the necrotic zone were scarce and thinner than in other groups, with non-significant thick-wall (Figs. 9(B) and (C)); no inflammatory infiltrate was observed, and no detritus was formed in the tumor tissues.

^{177}Lu-RGD: Necrotic areas were surrounded and limited to the tumor periphery (Fig. 9(D)). Glomeruloid epithelial proliferations were occasionally present (Fig. 9(E)). Diffuse inflammatory infiltrate and cellular detritus were observed predominantly in necrotic sites, and intratumoral vessels were dispersed and occasional (Fig. 9(F)).

^{177}Lu-AuNP: Intratumoral thick-walled vessels were observed. Necrotic areas were dispersed in the periphery and within the tumor (Figs. 9(G) and (I)). In some cases, detritus accumulation and diffuse inflammatory infiltrate were present (Fig. 9(H)).

Control group: Extensive necrotic areas with pseudopalisading sections and thick-walled capillaries were observed (Figs. 9(J), (L)). The necrotic area exhibited more intratumoral vessels than in the ^{177}Lu-AuNP-RGD, ^{177}Lu-RGD or ^{177}Lu-AuNP groups. The vessel morphology was irregular in shape and size (Fig. 9(K)), and inflammatory infiltrate with an accumulation of cellular detritus was also observed (Fig. 9(L)).

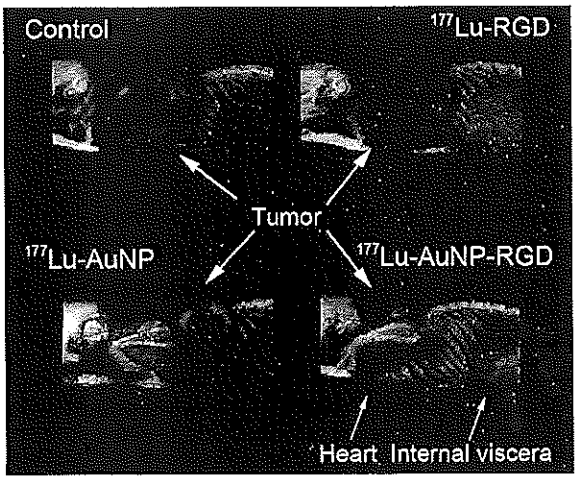

Figure 8. [^{18}F]FDG (2-deoxy-2-[^{18}F]fluoro-D-glucose)-micro PET/CT images of the control (untreated mouse), ^{177}Lu-AuNP-RGD, ^{177}Lu-RGD and ^{177}Lu-AuNP groups at 23 days of treatment. High accumulation of [^{18}F]FDG in the tumor represent high metabolic activity in the viable tumor cells.

No cytopathological damage was observed in kidneys. The glomerulus, proximal tube and distal tube exhibited no sign of necrosis or of damage any kind.

VEGF gene expression in tumor tissues. Real-time PCR analysis revealed that all treatments tended to reduce VEGF gene expression in tumor cells, although the effect in the ^{177}Lu-RGD group was not significant versus controls (Table II). However, treatment with ^{177}Lu-AuNP-RGD exerted the strongest and significant inhibition of VEGF gene expression when compared to the controls ($p < 0.05$). As ^{177}Lu-AuNP-RGD affinity for the $\alpha(v)\beta(3)$ integrin was demonstrated, the significant reduction in VEGF gene expression can be directly related to the $\alpha(v)\beta(3)$ blocking.[26]

Creatinine, urea and BUN quantification. Serum levels of creatinine, urea and BUN in the treatment groups were not statistically significant different with respect to control levels ($p > 0.05$) (Table II). This result correlates with the calculated low radiation absorbed dose to the kidneys, therefore, no renal toxicity was observed.

DISCUSSION

As expected, the radiopharmaceutical that yielded the greatest uptake and retention in tumors was ^{177}Lu-AuNP-RGD. The effects of this radiopharmaceutical can be attributed to passive and active-targeting mechanisms as well as multimeric and multivalent properties.[8] Consequently, the radiolabeled multimeric system delivered a greater radiation absorbed dose in tumors than did ^{177}Lu-AuNP or ^{177}Lu-RGD. The cRGD dose was also greater than that of ^{177}Lu-RGD, as ^{177}Lu-AuNP-RGD and ^{177}Lu-RGD were injected with the same cRGD concentration (~3×10^{12} molecules of cRGD/50 μL). These results correlated with the observed therapeutic response in which ^{177}Lu-AuNP-RGD was the radiopharmaceutical that induced significantly less tumor progression, less tumor metabolic activity, fewer intratumoral vessels and reduced VEGF gene expression.

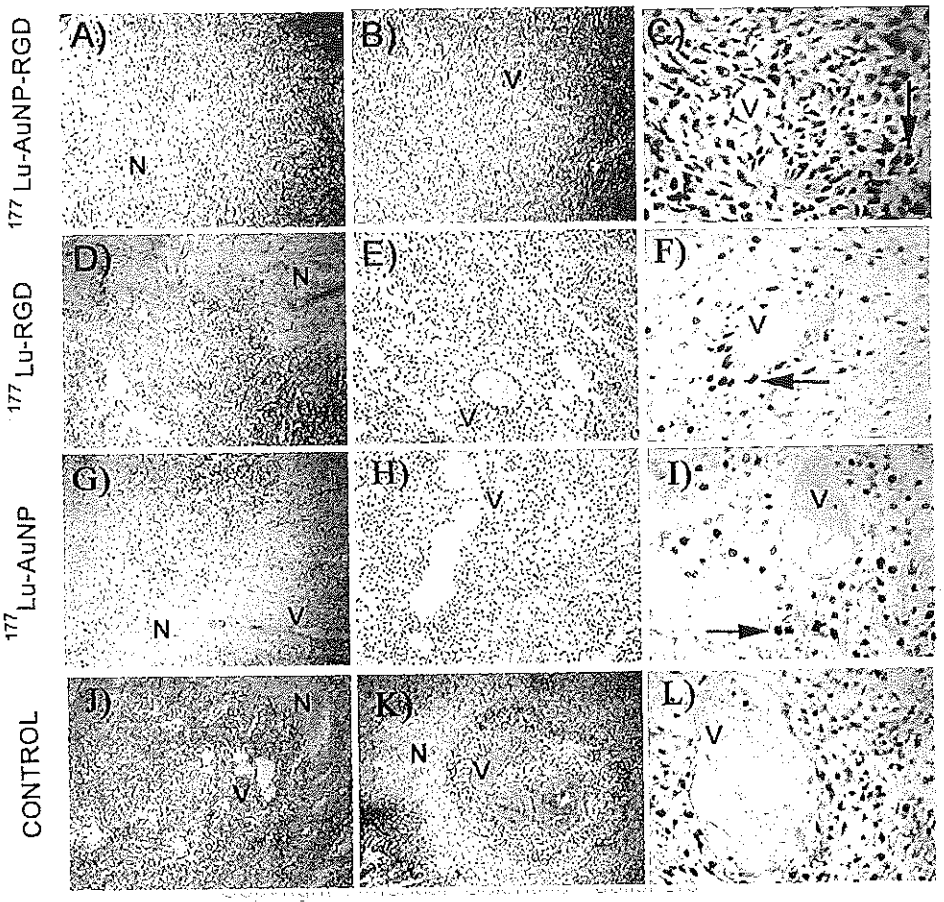

Figure 9. Three microscopic views ((A), (D); (G), (B), (E), (H), (J), (K): ×100; (C), (F), (I), (L): ×200) of tumor histopathology with ^{177}Lu-AuNP-RGD, ^{177}Lu-RGD or ^{177}Lu-AuNP after 23 days of treatment. The control is a tumor from an untreated mouse. Less necrosis (*N*) and less vascular proliferation (*V*) in the ^{177}Lu-treatments against the control are observed. Nuclear pleomorphism is indicated by arrows.

A peptide-nanoparticle conjugate bearing cRGD peptides provides a surface for simultaneous multiple interactions with the cell surface, giving rise to multivalent effects (defined as an affinity enhancement). Poethko et al.[24] reported that the minimum linker length is approximately 3.5 nm for the simultaneous binding of two c(RGD) motifs in the $\alpha(v)\beta(3)$ integrin. In the ^{177}Lu-AuNP-RGD system, the longest distance between two RGD motifs was calculated to be 11 nm, which is sufficiently long for the motifs to bind to adjacent $\alpha(v)\beta(3)$ integrins simultaneously.[8,12] The increase of peptide multiplicity in ^{177}Lu-AuNP-RGD may be at least partly responsible for the enhancement in tumor uptake (by an active-targeting mechanism) with respect to ^{177}Lu-RGD (^{177}Lu-DOTA-E-c(RGDfK)$_2$), in which the distance between the RGD molecules is 2.8 nm.[12]

Because the aim of this study was to evaluate and compare the therapeutic response, no tumor ablation was induced. However, in agreement with the radiation absorbed doses obtained in the non-target organs, the ^{177}Lu-AuNP-RGD dose could be increased ten-fold without exceeding the maximum tolerated radiation dose (MTD) to the kidneys (MTD = 25–30 Gy) or liver (MTD = 30–40 Gy), increasing the therapeutic efficacy and likely yielding complete tumor remission.[22,25]

The results indicated that ^{177}Lu-AuNP-RGD exerted the strongest and most significant inhibition of VEGF gene expression when compared to the controls ($p < 0.05$), potentially due to the multivalent RGD system, which may antagonize the function of the $\alpha(v)\beta(3)$ integrin, thereby inhibiting angiogenesis.[26] Cyclic RGD peptides have previously been reported to have limited activity as single agents in the treatment of glioblastoma, but when added to standard radiochemotherapy, appear to prolong progression-free and increase the overall survival in patients with newly diagnosed glioblastomas.[7] Therefore, the observed effect of ^{177}Lu-AuNP-RGD on VEGF gene expression could be due to the combined molecular targeting therapy (multimeric and multivalent RGD system) and radiotherapy (^{177}Lu) found in this one particular pharmaceutical.

Several trials have shown a significant improvement in clinical outcome when radiotherapy, chemotherapy or both were carried out under hyperthermic conditions in patients with advanced solid tumors such as cervical cancer.[27,28]

Hyperthermia increases the efficacy of radiotherapy by improving tumor oxygenation and interfering with DNA repair mechanisms.[27] In combination with chemotherapy, hyperthermia increases the drug concentration in the tumor area.[27] However, current techniques for hyperthermia induction display low spatial selectivity for the tissues that are heated. Lasers have been used for inducing hyperthermia, and spatial selectivity can be improved by adding gold nanoparticles to the tissue to be treated. By exposing nanoparticles to laser irradiation, it is possible to heat a localized area in tumors without any harmful heating of surrounding healthy tissues. The multifunctional ^{177}Lu-AuNP-RGD system prepared in this study, could also be used in photothermal cancer therapy using short NIR laser pulses to generate a second harmonic or a two-photon absorption process.[29] Second harmonic generation converts the NIR photons (800 nm) into visible photons (400 nm), which could be absorbed by the ^{177}Lu-AuNP-RGD nanospheres through surface plasmon and electron interband transition from the d band to the sp band with the consequent conversion of their energy into heat. NIR photons could also be directly absorbed and converted into heat through a nonlinear two-photon absorption process due to an aggregated alignment of the nanoparticles bound to cancer cells.[29,30]

If all the properties of the radiolabeled multifunctional system could be applied in nanomedicine, ^{177}Lu-AuNP-RGD could be potentially useful for the specific imaging of malignant tumors during treatment (SPECT imaging), for molecular targeting therapy/radiotherapy (multimeric RGD peptides plus high β-particle energy delivered per unit of targeted mass) and for photothermal therapy (localized heating). For therapeutic applications in humans, nanoparticles would have to be administered by an intratumoral injection or via a selective artery to avoid high uptake by organs of the reticuloendothelial system because of the colloidal nature of the nanoparticles.[31] Injection of the multimeric system into an artery of the affected organ would permit high uptake to a tumor and potentially to micrometastases or individual cancer cells.

CONCLUSIONS

^{177}Lu-labeled gold nanoparticles conjugated to cyclo-RGDfK(C) significantly decreased glioma tumor progression in mice through the effect of a combined molecular targeting therapy/radiotherapy. The inhibition of VEGF gene expression, involved in the angiogenesis process, indicated a molecular response. [^{18}F]fluor-deoxy-glucose-microPET/CT images showed a significant decrease in tumor metabolic activity. Therefore, ^{177}Lu-AuNP-RGD demonstrates properties suitable for use as an agent for molecular targeting radiotherapy.

Conflict of Interest

There are no conflicts of interest.

Author Disclosure Statement

No competing financial interests exist.

Acknowledgment: This study was supported by the Mexican National Council of Science and Technology (CONACYT-SEP-CB-2010-01-150942).

REFERENCES

1. D. L. Morse and R. J. Gillies, Molecular imaging and targeted therapies. *Biochem. Pharmacol.* 80, 731 (2010).
2. M. Patel, M. A. Vogelbaum, G. H. Barnett, R. Jalali, and M. S. Ahluwalia, Molecular targeted therapy in recurrent glioblastoma: current challenges and future directions. *Expert. Opin. Investig. Drugs* 21, 1247 (2012).
3. J. Kunikowska, L. Królicki, A. Hubalewska-Dydejczyk, R. Mikołajczak, A. Sowa-Staszczak, and D. Pawlak, Clinical results of radionuclide therapy of neuroendocrine tumours with ^{90}Y-DOTATATE and tandem ^{90}Y/^{177}Lu-DOTATATE: Which is a better therapy option?. *Eur. J. Nucl. Med. Mol. Imaging* 38, 1788 (2011).
4. R. Valkema, S. A. Pauwels, L. K. Kvols, D. J. Kwekkeboom, E. Jamar, M. de Jong, R. Barone, S. Walrand, P. P. Kooij, W. H. Bakker, J. Lasher, and E. P. Krenning, Long-term follow-up of renal function after peptide receptor radiation therapy with ^{90}Y-DOTA^0, Tyr^3-octreotide and ^{177}Lu-DOTA^0, Tyr^3-octreotate. *J. Nucl. Med.* 46, 83S (2005).
5. L. Bodei, M. Cremonesi, C. M. Grana, N. Fazio, S. Iodice, S. M. Baio, M. Bartolomei, D. Lombardo, M. E. Ferrari, M. Sansovini, M. Chinol, and G. Paganelli, Peptide receptor radionuclide therapy with ^{177}Lu-DOTATATE: The IEO phase I-II study. *Eur. J. Nucl. Med. Mol. Imaging* 38, 2125 (2011).
6. G. Ferro-Flores and C. A. Murphy, Pharmacokinetics and Dosimetry of ^{188}Re-pharmaceuticals. *Adv. Drug Deliv. Rev.* 60, 1389 (2008).
7. G. Tabatabai, J. C. Tonn, R. Stupp, and M. Weller, The role of integrins in glioma biology and anti-glioma therapies. *Curr. Pharm. Des.* 17, 2402 (2011).
8. S. Liu, Radiolabeled multimeric cyclic RGD peptides as integrin alphavbeta3 targeted radiotracers for tumor imaging. *Mol. Pharmaceutics* 3, 472 (2006).
9. S Liu, Radiolabeled cyclic RGD peptides as integrin $\alpha v\beta 3$-targeted radiotracers: Maximizing binding affinity via bivalency. *Bioconjugate Chem.* 20, 2199 (2009).
10. R. Haubner and C. Decristoforo, Radiolabeled RGD peptides and peptidomimetics for tumor targeting. *Front. Biosci.* 14, 872 (2009).
11. P. M. Mitrasinovic, Advances in $\alpha(v)\beta(3)$ integrin targeting cancer therapy and imaging with radiolabeled RGD peptides. *Curr. Radiopharm.* 2, 214 (2009).
12. X. Montet, M. Funovics, K. Montet-Abou, R. Weissleder, and J. Lee, Multivalent effects of RGD peptides obtained by nanoparticle display. *J. Med. Chem.* 49, 6087 (2006).
13. C. Huang, Q. Bao, D. Hunting, Y. Zheng, and L. Sanchez, Conformation-dependent DNA damage induced by gold nanoparticles. *J. Biomed. Nanotechnol.* 9, 856 (2013).
14. J. H. An, B. K. Oh, and J. W. Choi, Detection of tyrosine hydroxylase in dopaminergic neuron cell using gold nanoparticles-based barcode DNA. *J. Biomed. Nanotechnol.* 9, 639 (2013).
15. Y. Qu, Y. Huang, and X. Lü, Proteomic analysis of molecular biocompatibility of gold nanoparticles to human dermal fibroblasts-fetal. *J. Biomed. Nanotechnol.* 9, 40 (2013).
16. E. Morales-Avila, G. Ferro-Flores, B. E. Ocampo-García, L. M. De León-Rodríguez, C. L. Santos-Cuevas, R. García-Becerra, L. A. Medina, and L. Gómez-Oliván, Multimeric System of ^{99m}Tc-labeled Gold Nanoparticles Conjugated to c[RGDfK(C)] for Molecular Imaging of Tumor $\alpha(v)\beta(3)$ expression. *Bioconjugate Chem.* 22, 913 (2011).

17. M. Luna-Guitérrez, G. Ferro-Flores, B. E. Ocampo-García, N. Jiménez-Mancilla, E. Morales-Avila, L. de León Rodríguez, and K. Isaac-Olive, ^{177}Lu-labeled monomeric, dimeric and multimeric RGD peptides for the therapy of tumors expressing $\alpha(v)\beta(3)$ integrins. *J. Labelled Comp. Radiopharm.* 50, 140 (**2012**).
18. E. Morales-Avila, G. Ferro-Flores, B. E. Ocampo-García, and L. Gómez-Oliván, Engineered Multifunctional RGD-Gold Nanoparticles for the Detection of Tumour specific $\alpha(v)\beta(3)$ Expression: Chemical Characterisation and Ecotoxicological Risk Assessment. *J. Biomed. Nanotechnol.* 8, 991 (**2012**).
19. B. E. Ocampo-García, G. Ferro-Flores, E. Morales-Avila, and F. de M. Ramírez, Kit for Preparation of Multimeric Receptor-Specific ^{99m}Tc-Radiopharmaceuticals Based on Gold Nanoparticles. *Nucl. Med. Comm.* 32, 1095 (**2011**).
20. J. Rodriguez-Cortes, C. A. Murphy, G. Ferro-Flores, M. Pedraza-Lopez, and E. Murphy-Stack, Biokinetics and dosimetry with ^{177}Lu-DOTATATE in athymic mice with induced pancreatic malignant tumours: Preclinical studies. *Radiat. Eff. Defects Solids* 162, 791 (**2007**).
21. W. H. Miller, C. Hartmann-Siantar, D. Fisher, M. A. Descalle, T. Daly, J. Lehmann, M. R. Lewis, T. Hoffman, J. Smith, P. D. Situ, and W. A. Volkert, Evaluation of beta-absorbed fractions in a mouse model for ^{90}Y, ^{188}Re, ^{166}Ho,^{149}Pm, ^{64}Cu, and ^{177}Lu radionuclides. *Cancer Biother. Radiopharm.* 20, 436 (**2005**).
22. L. Bodei, M. Cremonesi, M. Ferrari, M. Pacifici, C. M. Grana, M. Bartolomei, S. M. Baio, M. Sansovini, and G. Paganelli, Long-term evaluation of renal toxicity after peptide receptor radionuclide therapy with ^{90}Y-DOTATOC and ^{177}Lu-DOTATATE: The role of associated risk factors. *Eur. J. Nucl. Med. Mol. Imaging* 35, 1847 (**2008**).
23. I. Olmedo, E. Araya, F. Sanz, E. Medina, J. Arbiol, and P. Toledo, How changes in the sequence of the peptide CLPFFD-NH_2 can modify the conjugation and stability of gold nanoparticles and their affinity for beta-amyloid fibrils. *Bioconjugate Chem.* 19, 1154 (**2008**).
24. T. Poethko, G. Thumshim, U. Hersel, F. Rau, R. Haubner, M. Schwaiger, H. Kessler, and H. J. Wester, Improved tumor uptake, tumor retention and tumor/background ratios of pegylated RGD multimers. *J. Nucl. Med.* 44, 46P (**2003**).
25. E. Vegt, M. Jong, J. Wetzels, R. Masereeuw, M. Melis, W. J. Oyen, M. Gotthardt, and O. C. Boerman, Renal toxicity of radiolabeled peptides and antibody fragments: Mechanisms, impact on radionuclide therapy, and strategies for prevention. *J. Nucl. Med.* 51, 1049 (**2010**).
26. C. F. Montenegro, C. L. Salla-Pontes, J. U. Ribeiro, A. Z. Machado, R. F. Ramos, C. C. Figueiredo, V. Morandi, and H. S. Selistre-de-Araujo, Blocking $\alpha v\beta 3$ integrin by a recombinant RGD disintegrin impairs VEGF signaling in endothelial cells. *Biochimie* 94, 1812 (**2012**).
27. M. Franckena, R. De Wit, A. C. Ansink, A. Notenboom, R. A. Canters, D. Fatehi, G. C. Van Rhoon, and J. Van Der Zee, Weekly systemic cisplatin plus locoregional hyperthermia: An effective treatment for patients with previously irradiated recurrent cervical carcinoma in a previously irradiated area. *Int. J. Hyperthermia* 23, 443 (**2007**).
28. M. Franckena, L. C. Lutgens, P. C. Koper, C. E. Kleynen, E. M. van der Steen-Banasik, J. J. Jobsen, J. W. Leer, C. L. Creutzberg, M. F. Dielwart, Y. van Norden, R. A. Canters, G. C. van Rhoon, and J. van der Zee, Radiotherapy and hyperthermia for treatment of primary locally advanced cervix cancer: Results in 378 patients. *Int. J. Radiat. Oncol. Biol. Phys.* 73, 242 (**2009**).
29. X. Huang, W. Qian, I. H. El-Sayed, and M. A. El-Sayed, The potential use of the enhanced nonlinear properties of gold nanospheres in photothermal cancer therapy. *Lasers Surg. Med.* 39, 747 (**2007**).
30. H. Mendoza-Nava, G. Ferro-Flores, B. Ocampo-García, J. Serment-Guerrero, C. Santos-Cuevas, N. Jiménez-Mancilla, M. Luna-Gutiérrez, and M. A. Camacho-López, Laser heating of gold nanospheres functionalized with octreotide: *In vitro* effect on HeLa cell viability. *Photomed. Laser Surg.* 31, 17 (**2013**).
31. N. Chanda, V. Kattumuri, R. Shukla, A. Zambre, K. Katti, A. Upendran, R. R. Kulkarni, P. Kan, G. M. Fent, S. W. Casteel, C. J. Smith, E. Boote, J. D. Robertson, C. Cutler, J. R. Lever, K. V. Katti, and R. Kannan, Bombesin functionalized gold nanoparticles show *in vitro* and *in vivo* cancer receptor specificity. *Proc. Natl. Acad. Sci. USA* 107, 8760 (**2010**).

Nuclear Medicine Communications

Original article

^{99m}Tc-N_2S_2-Tat (49-57)-bombesin internalized in nuclei of prostate and breast cancer cells: kinetics, dosimetry and effect on cellular proliferation

Clara L. Santos-Cuevas[a,b], Guillermina Ferro-Flores[a], Eva L. Rojas-Calderón[a], Rocío García-Becerra[c], David Ordaz-Rosado[c], Consuelo Arteaga de Murphy[c] and Martha Pedraza-López[c]

Background The gastrin-releasing peptide receptor (GRP-r) is overexpressed in prostate and breast cancers. tecnitium 99-bombesin (^{99m}Tc-BN) has been reported as a radiopharmaceutical with specific cell GRP-r binding. The HIV Tat (49-57)-derived peptide has been used to deliver a large variety of molecules to cell nuclei. A new hybrid radiopharmaceutical of type ^{99m}Tc-N_2S_2-Tat(49-57)-Lys^3-BN (^{99m}Tc-Tat-BN) internalized in cancer cell nuclei could act as an effective system of targeted radiotherapy using Auger and internal conversion electron emissions near DNA.

Aim The aim of this study was to assess the in-vitro nucleus internalization kinetics of ^{99m}Tc-Tat-BN in GRP r-positive cancer cells and to evaluate the subcellular-level radiation-absorbed dose associated with the observed effect on cancer cell DNA proliferation.

Methods ^{99m}Tc-Tat-BN in-vitro internalization kinetics were evaluated in human prostate cancer PC-3 cells and breast carcinoma cell lines MCF7 and MDA-MB231. Nuclei from cells were isolated using a nuclear extraction kit. Total disintegration in each subcellular compartment was calculated by the integration of experimental time–activity kinetic curves. Nucleus internalization was corroborated by confocal microscopy images using immunofluorescently labelled Tat–BN. The PENELOPE code was used to simulate and calculate the absorbed dose by the contribution of Auger and internal conversion electrons in the cytoplasm and nucleus using geometric models built from immunofluorescent cell images. A cell proliferation kit was used to evaluate DNA concentration after cancer cell incubation with ^{99m}Tc-Tat-BN.

Results The results showed that 59.7, 61.2 and 41.5% of total disintegration per unit of ^{99m}Tc-Tat-BN activity (1 Bq) bound to the cell occurred in the nucleus of PC-3, MCF7 and MDA-MB231, respectively. The ^{99m}Tc-Tat-BN absorbed doses delivered to nuclei were 0.142 mGy/decay (PC-3), 0.434 mGy/decay (MCF7) and 0.276 mGy/decay (MDA-MB231). ^{99m}Tc-Tat-BN produced a significant decrease in PC-3 (52.98%), MCF7 (45.71%) and MDA-MB231 (35.80%) cellular proliferation with respect to untreated cells.

Conclusion The hybrid radiopharmaceutical could be potentially useful as a therapeutic agent for prostate and breast cancers. *Nucl Med Commun* 32:303–311 © 2011 Wolters Kluwer Health | Lippincott Williams & Wilkins.

Nuclear Medicine Communications 2011,32 :303–311

Keywords: hybrid radiopharmaceutical, peptide-receptor therapy, radiolabelled bombesin, subcellular dosimetry, Tat-bombesin

[a]Instituto Nacional de Investigaciones Nucleares, [b]Universidad Autónoma del Estado de México, Estado de México and [c]Instituto Nacional de Ciencias Médicas y Nutrición Salvador Zubirán, México D.F., Mexico

Correspondence to Guillermina Ferro-Flores, PhD, Departamento de Materiales RadiactivosInstituto Nacional de Investigaciones NuclearesCarretera México-Toluca S/NLa Marquesa, Ocoyoacac, Estado de México, C.P. 52750, México
Tel: +52 55 53297200 x3863; fax: +52 55 53297306;
e-mail: ferro_flores@yahoo.com.mx; guillermina.ferro@inin.gob.mx

Received 8 September 2010 Revised 19 October 2010
Accepted 19 October 2010

Introduction

As interest in targeted therapies for cancer increases, radionuclides stand out not only for their ability to be detected by external scintigraphy, but also for their therapeutic capacity [1]. The objective is to deliver a maximum radiation dose to tumour areas in a selective and localized manner, generating a therapeutic effect because of energy deposition from charged particle emissions. At the single-cell level, short-range charged particles, such as α, internal conversion (IC) electrons and Auger electrons, impart a dense ionizing energy deposition pattern associated with increased radiobiological effectiveness. However, they must be able to penetrate the cytoplasm and reach the nucleus, which is considered to be the most radiosensitive component of the cell. Auger and IC electron emitters that can be targeted to the DNA of tumour cells represent an attractive system of radiation therapy because of their high linear energy transfer within nuclear dimensions (4–26 keV/μm) [2]. In contrast to α radiation, Auger and IC radiation are of low toxicity when decaying outside the cell nucleus, such as in the cytoplasm or outside the cells during blood transport. Technetium-99m (^{99m}Tc) is the most frequently used radionuclide for in-vivo diagnostic imaging studies because of its monoenergetic γ rays of 140 keV and easy complex formation with a large number of ligands. ^{99m}Tc produces

DOI: 10.1097/MNM.0b013e328341b27f

Multifunctional Targeted Radiotherapy System for Induced Tumours Expressing Gastrin-releasing Peptide Receptors

Nallely Jimenez-Mancilla[1,2], Guillermina Ferro-Flores[1]*, Blanca Ocampo-Garcia[1], Myrna Luna-Gutierrez[1,2], Flor De Maria Ramirez[1], Martha Pedraza-Lopez[3] And Eugenio Torres-Garcia[2]

[1]*Instituto Nacional de Investigaciones Nucleares, Estado de México, Mexico;* [2]*Universidad Autónoma del Estado de México, Mexico;* [3]*Instituto Nacional de Ciencias Médicas y Nutrición Salvador Zubirán, Mexico*

Abstract: The gastrin-releasingpeptide receptor (GRP-r)is overexpressed in breast and prostate cancer, and Lys^3-bombesin is a peptide that binds with high affinity to the GRP-r. HIV Tat(49-57) is a cell-penetrating peptide that reaches the DNA. In cancer cells,^{177}Lu shows efficient crossfire effect, while^{99m}Tc that is internalised to cancer cell nuclei acts as an effective system of targeted radiotherapy because of the Auger and IC electron emissions near the DNA. The aim of this research was to prepare a multifunctional system of ^{177}Lu- and ^{99m}Tc-labelled gold nanoparticles (AuNPs) that were conjugated to Tat(49-57)-Lys^3-bombesin (Tat-BN) and to evaluate the radiation absorbed dose to GRP receptor-positive PC3 tumours that were induced in mice. Cys-Gly-Cys-Tat-BN (CGC-Tat-BN), 1,4,7,10-tetraazacyclododecane-N',N",N'"-tetraacetic-Gly-Gly-Cys (DOTA-GGC)andhydrazinonicotinyl-Phe-Cys-Phe-Trp-Lys-Thr-Cys-Thr-ol (HYNIC-TOC) peptides were conjugated to AuNPs to prepare a multifunctional system by means of a spontaneous reaction of the thiol groups of cysteine. TEM, UV-Vis, XPS and Far-IR spectroscopy techniques demonstrated that AuNPs were functionalised with peptides through interactions with the-SHgroups. The^{99m}Tc labelling was performed via the HYNIC-TOC ligand, and the^{177}Lu labelling was performed through DOTA-GGC. The radiochemical purity was 96 ± 2%. The ^{177}Lu-absorbed dose per injected activity that wasdelivered to the PC3 tumours was 7.9 Gy/MBq, and the ^{99m}Tc-absorbed dose that was delivered to the nuclei was 0.53 Gy/MBq. The ^{177}Lu/^{99m}Tc-AuNP-Tat-BN system showed properties suitable for a targeted radionuclide therapy of tumours expressing GRPreceptors due to the energy deposition from β-emissions and the Auger and IC electron emissions near the DNA.

Keywords: ^{177}Lu-gold nanoparticles; radiolabelled gold nanoparticles; radiolabelled Lys^3-bombesin-Tat(49-57); targeted radiotherapy; ^{99m}Tc-gold nanoparticles.

1. INTRODUCTION

The objective of targeted radiotherapies for cancer is to deliver a maximum radiation dose to tumours in a selective and localised manner, thereby generating a therapeutic effect through the energy deposition from charged particle emissions. The radionuclide^{177}Lu has a half-life of 6.71 d and a β_{max}emission of 0.497MeV (78%), andit has been successfully used for radiopeptide therapy with an efficient crossfire effect in cancer cells [1-4]. At the single-cell level, short-range charged particles, such as internal conversion (IC) electrons and Auger electrons, impart a dense ionising energy deposition pattern that is associated with an increased radiobiological effectiveness [5]. The^{99m}Tc that is internalised in cancer cell nuclei acts as an effective system of targeted radiotherapy because of the delivery of Auger energy (0.90 keV/decay) and IC electron energy (15.40 keV/decay) near the DNA [6].

The gastrin-releasingpeptide receptor (GRP-r) is overexpressed in breast and prostate cancer. Lys^3-bombesin is a peptide that binds with high affinity to theGRP-r [7-9]. Current challenges include conjugating biomolecules with cell-penetrating peptides and/or nuclear localisation peptide sequences (NLSs) to promote their internalisation and routing to the cell nucleus. Tat(49-57) is a peptide derived from thetransactivator of transcription protein of the HIV-1 virus that has a membrane translocation domain and an NLS [10,11]. Recently, Santos-Cuevas *et al.* [12,13] reported that the ^{99m}Tc-Tat(49-57)-Lys^3-Bombesin (^{99m}Tc-Tat-BN) was a new hybrid radiopharmaceutical that was internalised into the nuclei of prostate and breast cancer cells.

*Address correspondence to this author at the Departamento de Materiales Radiactivos, Instituto Nacional de Investigaciones Nucleares, Carretera México-Toluca S/N., La Marquesa, Ocoyoacac, Estado de México., C.P. 52750, México; Tel: + (52) (55)-53297200 ext. 3863; Fax: + (52) (55)-53297306; E-mail: ferro_flores@yahoo.com.mx; guillermina.ferro@inin.gob.mx

Several studies have demonstrated that conjugating peptides to gold nanoparticles (AuNPs) produces biocompatible and stable multimeric systems with target-specific molecular recognition [14-24]. Peptides can be conjugated to one AuNP by a spontaneous reaction of the AuNP surface with a thiol (cysteine) or an amine [16, 25].

The aim of this research was to prepare a multifunctional system of ^{177}Lu- and ^{99m}Tc-labelled gold nanoparticles (AuNPs) that were conjugated to Tat(49-57)-Lys^3-bombesin (^{177}Lu/^{99m}Tc-AuNP-Tat-BN) and to evaluate the radiation absorbed dose toGRP receptor-positive PC3 tumours that were induced in mice.

2. MATERIALS AND METHODS

Reagents. N,N-dimethylacetamide (DMA), tert-butyl bromoacetate, N,N-diisopropylethylamine (DIPEA), diisopropylcarbodiimide (DIC), dimethylformamide (DMF),dichloromethane (DCM), 2-(1H-benzotriazole-1-yl)-1,1,3,3-tetramethyluronium hexafluorophosphate (HBTU), hydroxybenzotriazole (HOBt),Fmoc-cys-Trt-OH, Fmoc-gly, 20-nm gold nanoparticles and other reagents were purchased from the Sigma-Aldrich Chemical Co. and used as received.Rink Amide MBHA was obtained from Novabiochem.

2.1. Synthesis of Peptides

2.1.1. Tat(49-57)-Lys^3-bombesin (Tat-BN)

The Tat(49-57) peptide (H-Arg-Lys-Lys-Arg-Arg-Gln-Arg-Arg-Arg-NH_2) was conjugated to Gly-Gly-Cys-Gly-Cys(Acm)-Gly-Cys(Acm)-NH_2 to produce the Tat(49-57)-spacer-GCGC peptide (H-Arg^1-Lys^2-Lys^3-Arg^4-Arg^5-Gln^6-Arg^7-Arg^8-Arg^9-Gly^{10}-Gly^{11}-Cys^{12}-Gly^{13}-Cys^{14}(Acm)-Gly^{15}-Cys^{16}(Acm)-NH_2). The sequence Gly^{13}-Cys^{14}-Gly^{15}-Cys^{16} was added for use as the specific chelating site by theAuNPs Fig. (1). The Lys^3-bombesin (Pyr-Gln-Lys-Leu-Gly-Asn-Gln-Trp-Ala-Vla-Gly-His-Leu-Met-NH2) was conjugated to a maleimidopropyl moiety through Lys^3, and the maleimidopropyl group was used as the branch position to form a thioether with the Cys^{12} side chain of the Tat(49-57)-spacer-GCGC

1573-4137/12 $58.00+.00

INSTITUTO NACIONAL DE CIENCIAS MÉDICAS Y NUTRICIÓN SALVADOR ZUBIRÁN

11 de febrero de 2016

Dra. Norma Bobadilla Sandoval
Coordinadora de la Comisión en Animales
P r e s e n t e

Distinguida Dra. Bobadilla

Por este conducto me permito solicitar el cierre del protocolo: "EVALUACIÓN *IN VITRO* E *IN VIVO* DE PÉPTIDOS RADIOMACADOS PARA EL DIAGNÓSTICO ESPECÍFICO DE LESIONES TUMORALES POR IMÁGENES GAMMAGRÁFICAS EN MEDICINA NUCLEAR, No. de registro CINVA 243, debido a que el protocolo ha concluido.

Sin otro particular por el momento reciba un cordial saludo.

Atentamente

Dra. en C. Martha Pedraza López
Investigador en Ciencias Médicas "C"
Departamento de Medicina Nuclear

c.c.p. Dr. Gerardo Gamba Ayala. Director de Investigación
MVZ Mariela Contreras Escamilla. Jefa del DIEB

INSTITUTO NACIONAL DE CIENCIAS MEDICAS Y NUTRICION "SALVADOR ZUBIRAN"
11 FEB 2016
DEPARTAMENTO DE NEFROLOGÍA Y METABOLISMO MINERAL

Vasco de Quiroga No. 15
Colonia Sección XVI
Delegación Tlalpan
México, D. F. 14000
Tel. (52)54870900
www.incmnsz.mx

Acuse

INSTITUTO NACIONAL DE CIENCIAS MÉDICAS Y NUTRICIÓN SALVADOR ZUBIRÁN

México, D.F. a 10 de Febrero de 2016

INS. NACIONAL DE CIENCIAS MEDICAS Y NUTRICIÓN "SALVADOR ZUBIRÁN"
10 FEB 2016
DIRECCIÓN DE INVESTIGACIÓN

Dra. Martha Pedraza López
Depto. Medicina Nuclear
Presente

Estimada Dra. Pedraza:

Por este conducto me permito solicitar el cierre del Protocolo: "**EVALUACIÓN IN VITRO E IN VIVO DE PÉPTIDOS RADIOMARCADOS PARA EL DÍAGNÓSTICO DE LESIONES TUMORALES POR IMÁGENES GAMMAGRÁFICAS EN MEDICINA NUCLEAR..**", con registro **CINVA 243.**, debido a que el periodo de realización y la prórroga correspondiente autorizado por la CINVA ha concluido. Favor de llenar el formato de cierre del protocolo que se anexa a la presente. De no recibir el formato de su parte en el plazo de 30 días, el protocolo se dará por cerrado.

Sin otro particular por el momento, quedo de usted.

INST. NACIONAL DE CIENCIAS MEDICAS Y NUTRICIÓN "SALVADOR ZUBIRÁN"
11 FEB 2016 9:12
MEDICINA NUCLEAR

Atentamente,

Dra. Norma A. Bobadilla Sandoval
Coordinadora de la Comisión de Investigación en Animales

Avenida Vasco de Quiroga No. 15
Colonia Belisario Domínguez Sección XVI
Delegación Tlalpan
Código Postal 14080
México, Distrito Federal
Tel. (52)54870900
www.incmnsz.mx

c.c.p. Dr. Gerardo Gamba Ayala, Director de Investigación
MVZ Mariela Contreras Escamilla, Jefa del DIEB

NAB/nom

INSTITUTO NACIONAL DE CIENCIAS MEDICAS Y NUTRICIÓN
10 FEB 2016
INVESTIGACION EXPERIMENTAL

F12

INNSZ

INSTITUTO NACIONAL DE CIENCIAS MÉDICAS Y NUTRICIÓN
SALVADOR ZUBIRÁN

Abril 23, 2012

Dra. Martha Pedraza López
Departamento de Medicina Nuclear
P r e s e n t e .

Por este medio me permito informar a usted que se aprueba su solicitud de ampliación de fecha de término a diciembre de 2015, del proyecto "Evaluación *in vitro* de péptidos radiomarcados para el diagnóstico específico de lesiones tumorales por imágenes gammagráficas en Medicina Nuclear".

A t e n t a m e n t e

MVZ. MSc. Cert.L.A.M. Rafael Hernández González
Coordinador de la Comisión de Investigación en Animales
Jefe del Departamento de Investigación Experimental y Bioterio

Recibí Hayde 3-05-2012.

Investigación
Tradición Servicio
Asistencia Docencia

• Vasco de Quiroga 15,
• Delegación Tlalpan
• C. P. 14000 México, D. F.
• Tel. 54-87-09-00

Lili,
Por favor hacer respuesta positiva
Mtka

INNSZ

INSTITUTO NACIONAL DE CIENCIAS MÉDICAS Y NUTRICIÓN
SALVADOR ZUBIRÁN

30 de marzo del 2012

Dr. Rafael Hernández González
Coordinador de la CINVA
Presente

Estimado Dr. Hernández:

Por este conducto le solicito de la manera más atenta la prorroga hasta diciembre del año 2015 para la continuación del proyecto: Evaluación *in vitro* de péptidos radiomarcados para el diagnóstico específico de lesiones tumorales por imágenes gammagráficas en Medicina Nuclear, No. CINVA 243. La continuidad en este trabajo ha permitido la aplicación exitosa de péptidos radiomarcados para la localización de lesiones tumorales en pacientes. Así mismo se han publicado artículos a este respecto en revistas internacionales de alto impacto.

Sin otro particular por el momento.

Atentamente.

Dra. Martha Pedraza López
Departamento de Medicina Nuclear

• Vasco de Quiroga 15,
• Delegación Tlalpan
• C. P. 14000 México, D. F.
• Tel. 54-87-09-00

INNSZ

INSTITUTO NACIONAL DE CIENCIAS MÉDICAS Y NUTRICIÓN
SALVADOR ZUBIRÁN

INSTITUTO NACIONAL DE CIENCIAS MEDICAS Y NUTRICION SALVADOR ZUBIRAN
23 OCT 2007
DIRECCION DE INVESTIGACION

22 de octubre de 2007

Dra. en C. Martha Pedraza López
Departamento de Medicina Nuclear
P r e s e n t e .

En referencia con el proyecto de investigación: **"Evaluación in *vitro* e in *vivo* de Péptidos Radiomarcados para el Diagnóstico Específico de Lesiones Tumorales por Imágenes Gammagráficas en Medicina Nuclear"**

Registro CINVA: 243

El Comité de Investigación en Animales ha revisado su respuesta de fecha 04 de octubre y el (CINVA) decidió **APROBAR** el proyecto con las siguientes observaciones:

1. La metodología está mejor presentada y queda más claro pero deben justificar el uso de las líneas celulares de páncreas y próstata (en los Antecedentes no incluyen ninguna referencia relacionada con estas líneas que justifique su uso, no proveen de antecedentes donde se demuestre que esas líneas celulares presentan receptores a oxcitocina e integrinas (células AR42J de páncreas y PC3 de próstata).

2. Dentro de sus objetivos, el marcado como 3 no puede realizarse con el protocolo que proponen y debe eliminarse.

Sin otro particular, le deseo éxito en su proyecto.

Atentamente

MVZ., M. Sc. Rafael Hernández González
Coordinador del Comité de Investigación en Animales

ccp. Dr. Rubén Lisker Y. Director de Investigación
Dr. Patricio Santillán Doherty. Comité de Investigación en Animales.
Dr. Gerardo Gamba Ayala. Comité de Investigación en Animales.
MVZ., M. en C. Ma. de la Luz Streber J. Comité de Investigación en Animales.

Investigación

Tradición Servicio

Asistencia Docencia

20007700

• Vasco de Quiroga 15,
• Delegación Tlalpan
• C. P. 14000 México, D. F.
• Tel. 54-87-09-00

INCMNSZ

Dirección de Investigación

FORMA ÚNICA PARA REGISTRO DE PROYECTOS

No invada las zonas sombreadas

CLAVE: MNT - 032 - 07/08 - 1

FECHA DE RECEPCIÓN : 27-JUNIO-2007

TÍTULO: EVALUACION IN VITRO E IN VIVO DE PEPTIDOS RADIOMARCADOS PARA EL DIAGNOSTICO ESPECIFICO DE LESIONES TUMORALES POR IMAGENES GAMMAGRAFICAS EN MED. NUCLEAR

INVESTIGADOR RESPONSABLE: DRA. EN C. MARTHA PEDRAZA LOPEZ

DEPARTAMENTO O SERVICIO: MEDICINA NUCLEAR

TIPO DE INVESTIGACIÓN:

	1. Investigación Clínica	(incluye seres humanos o sus productos biológicos)
X	*2. Investigación Experimental*	(incluye animales de investigación o sus productos biológicos)
	3. Investigación Documental	(revisión de expedientes, revisión bibliográfica, informe de casos, etc.)
	4. Desarrollo Tecnológico	(instrumental, equipo, metodos diagnósticos, drogas nuevas, etc)
	5. Investigación Epidemiológica	(estudios en poblaciones, en comunidad o en hospital)
	6. Otros	(organización de eventos, asistencia a reuniones, donativos, etc)

PATROCINADORES:

	Cantidad:	
CONACyT	$100,000.00	$100,000.00 *TOTAL*

Fondo de Apoyo

PERÍODO DE UTILIZACIÓN DE LOS RECURSOS: *de mes:* JULIO *año:* 2007 *a mes:* JULIO *año:* 2008

FORMA EN LA QUE SE RECIBIRÁN LOS FONDOS:

	primer trimestre	segundo trimestre	tercer trimestre	cuarto trimestre
Primer año:	$100,000.00			
Segundo año:				
Tercer año:				
Cuarto año:				
Quinto año:				

COSTOS TOTALES DE LA INVESTIGACIÓN (ver instrucciones al reverso)	
1. Personal: (sueldos y sobresueldos al personal)	
2. Equipos: (de laboratorio, cómputo, transporte, etc.)	$40,000.00
3. Materiales: (reactivos, consumibles, desechables, etc.)	$30,000.00
4. Animales: (adquisición, cuidado, procedimientos, etc.)	
5. Estudios: (de laboratorio, gabinete, especiales, etc.)	
6. Viáticos: (reuniones científicas y trabajo de campo)	$10,000.00
7. Publicaciones: (costos directos de publicación, sobretiros)	
8. Suscripción: (libros, revistas, software, periódico, etc.)	$20,000.00
9. Varios: (teléfono, fax, fotocopias, mensajería, etc.)	
10. Fondo de Apoyo:	

INSTITUCIONES PARTICIPANTES

INCMNSZ, ININ.

FIRMAS

Investigador Responsable

Jefe del Departamento

Comité de Investigación en Humanos

Comité de Investigación en Animales

Director de Investigación

Director General

22-10-2007

INCMNSZ

INSTITUTO NACIONAL DE CIENCIAS MEDICAS Y NUTRICION
SALVADOR ZUBIRAN

04 de octubre de 2007
Ref. CINVA 243

MVZ. M. Sc. Rafael Hernández González
Coordinador del Comité de Investigación en Animales.
INCMNSZ

Estimado Dr. Hernández:

Recibimos su comunicación del 17 de septiembre con observaciones al proyecto "Evaluación *in vitro* e *in vivo* de péptidos radiomarcados para el diagnóstico específico de lesiones tumorales por imágenes gammagráficas en medicina nuclear"

En respuesta a sus observaciones se anexa un documento con el protocolo modificado incluyendo todas las correcciones sugeridas amablemente por usted.

Agradezco todas sus observaciones esperando haber respondido a todas ellas y quedo a su disposición para cualquier aclaración.

Atentamente,

Dra. en C. Martha Pedraza López
Investigador en Ciencias Médicas
Departamento de Medicina Nuclear.
Ext. 2402

• Vasco de Quiroga 15,
• Delegación Tlalpan
• C.P. 14000 México, D.F.
• Tel. 54-87-09-00

EVALUACIÓN *IN VITRO* E *IN VIVO* DE PÉPTIDOS RADIOMARCADOS PARA EL DIAGNÓSTICO ESPECÍFICO DE LESIONES TUMORALES POR IMÁGENES GAMMAGRÁFICAS EN MEDICINA NUCLEAR

Investigador Responsable Dra. Martha Pedraza López
Departamento de Medicina Nuclear

ANTECEDENTES

En Medicina Nuclear el, ^{99m}Tc es el radionúclido más utilizado para estudios de diagnóstico debido a sus características físicas y químicas, emite radiaciones gamma de 140 keV (90%), (monoenergético), fácilmente detectada que proporciona imágenes gammagráficas de alta calidad, su tiempo de vida media física es de seis horas, desintegrándose por transición isomérica sin radiaciones beta, por lo que se pueden administrar dosis relativamente altas para efectuar estudios clínicos en menos tiempo y con menor tiempo de exposición. Además, el ^{99m}Tc tiene una gran disponibilidad debido a su bajo costo, ya que se obtiene fácilmente de un generador de ^{99}Mo/^{99m}Tc.

Se utiliza en forma de pertecneciato y, en estado reducido se une a un gran número de ligantes o moléculas acarreadoras, formando complejos (radiofármacos) en un tiempo de reacción relativamente corto (5 a 30 min) con altas eficiencias de marcado (>90%) [Verduyckt y cols 2003; FEUM, 2004]. Una alta selectividad por el sitio del tumor y un periodo de permanencia largo del radiofármaco en el sitio de interés son las bases para un diagnóstico clínico exitoso.

Las hormonas peptídicas (ácidos α-aminocarboxílicos) han sido diseñadas por la naturaleza para estimular, regular, inhibir numerosas funciones de la vida y actúan por medio de sus receptores principalmente, como transmisores de información y coordinadores de actividades de varios tejidos en el organismo. Comparados con los anticuerpos, los péptidos pequeños ofrecen varias ventajas: son fáciles de sintetizar y modificar, tienen menos probabilidad de ser inmunogénicos y rápida depuración sanguínea. En muchos casos la afinidad de los péptidos pequeños por sus receptores es significativamente mayor que la de los anticuerpos o sus fragmentos [Lui y cols., 1997; Reubi, 2003, De Jong y cols., 2003].

Los receptores se unen específicamente a los correspondientes péptidos marcados con radionucleidos. Los receptores de péptidos están sobre expresados en las células de numerosos cánceres. Estos receptores han sido usados como blancos moleculares para peptidos radiomarcados y así localizar el tumor, uno de esos complejos es el octreótido (^{99m}Tc-HYNIC-TOC) que ha demostrado ser una buena opción para la detección de tumores que presentan receptores de somatostatina, ya que es captado rápidamente y retenido por el tumor. Las aplicaciones exitosas del octreótido radiomarcado en centelleografía para la localización de linfomas, granulomatosis, meningiomas y tumores de origen neuroendócrino y cáncer pulmonar, sobre todo en Europa son indicativas de la importancia que tiene investigar otro tipo de péptidos radiomarcados, tanto nativos como sus derivados (análogos), para diagnóstico por imagen en medicina nuclear [Breeman y cols., 2001; Krenning y cols., 2004, Kaltsas y cols., 2004; Kwekkeboom y cols., 2005a, 2005b].

Otros péptidos de mucho interés en medicina debido a que sus receptores estimulan el crecimiento en las células neoplásicas son la oxitocina en el cáncer de mama y cérvico uterino, y las integrinas en la estimulación de la angiogénesis.

a) **Oxitociona** Químicamente la oxitocina (OT) es un nanopéptido cíclico, con la secuencia cisteína-tirosina-isoleucina-glutamina-asparagina-cisteína-prolina-leucina-glicina. Es una hormona neuropeptidica sintetizada en los núcleos paraventricular y supraóptico del hipotálamo. La acción hormonal periférica de la OT está mediada por receptores. Los receptores (OTRs) se unen específicamente y con gran afinidad a la OT y a algunos de sus análogos. Los OTRs se expresan principalmente en las células mioepiteliales de la glándula mamaria, en el miometrio y el endometrio del útero, al término del embarazo y en el parto y post parto. Además por estudios in vivo e in vitro se demostró que también se encuentran en carcinomas de mama y de endometrio, en neuroblastomas, glioblastomas, osteoblastos y osteosarcomas [Cassoni y col. 2000, 2004].

b) **Integrinas** Las integrinas son glucoproteínas heterodiméricas de adhesión transmembranal, constituidas por cadenas alfa y beta que cruzan de parte a parte la membrana celular. Hay 14 clases de subunidades α y 8 clases de subunidades β, que producen al menos 20 heterodímeros de integrinas. Hay muchas integrinas que están expresadas ampliamente, y la mayoría de las células tienen más de una integrina en su superficie celular, por ejemplo, las células de melanoma expresan $\alpha_v\beta_3$, $\alpha_1\beta_1$, $\alpha_3\beta_1$ y $\alpha_5\beta_1$; en las células de carcinoma pulmonar se expresan $\alpha_v\beta_5$ y en muchas otras células tumorales se encuentran $\alpha_v\beta_6$ [Knight y cols 2003; Mitra y cols. 2006]. Se han encontrado una gran variedad de integrinas sobre la superficie de células tumorales, las integrinas $\alpha_v\beta_3$ se encuentran elevadas en la angiogénesis de tumores y sus metástasis [Friedlander y cols. 1995];

La unión específica de los receptores $\alpha_v\beta_3$ de las integrinas a los péptidos que contienen el residuo de amino ácidos Arg-Gly-Asp (RGD) ha sido útil para obtener la imagen de tumores específicos, mediante el radiomarcado del péptido RGD [Janssen y cols. 2002].

OBJETIVOS E HIPÓTESIS

EL OBJETIVO PRINCIPAL:
Evaluar la especificidad *in vivo* de las formulaciones de péptidos marcados con ^{99m}Tc para el diagnóstico específico de lesiones tumorales que sobre expresan receptores de oxitocina y de integrinas por imágenes gammagráficas en medicina nuclear. Los estudios in vitro han sido previamente realizados y la hipótesis anterior sobre la captación in vitro ya se corroboró con estudios anteriores.

LOS OBJETIVOS GENERALES SON:

1. Determinar la biodistribución de los radiofármacos en un modelo animal (ratones sanos y en ratones con tumores inducidos).
2. Obtener imágenes gammagráficas de la biodistribución de cada uno de los radiofármacos en animales con tumores inducidos.

3. Elaborar un protocolo clínico que permita la obtención de imágenes diagnósticas en pacientes con los radiofármacos obtenidos y que pudieran ser utilizados para el diagnóstico de cáncer de páncreas, próstata y mama.

HIPÓTESIS:

Si los péptidos marcados son receptor-específicos serán captados *in vivo* en lesiones tumorales y podrían ser un buen agente para el diagnóstico por imágenes gammagráficas en medicina nuclear.

MATERIAL Y MÉTODOS

Todo lo referente marcado de la oxitocina (^{99m}Tc-oxitocina) y del ciclo-Lys-D-Phe-RGD (^{99m}Tc-RGD), estudios de estabilidad de los radiofármaco y captación *in vitro* en las líneas de células tumorales son objetivos ya realizados. En este protocolo solo se realizarán los estudios *in vivo* en ratones sano y ratones con tumor inducido

Material biológico

Ratones atímicos, de 6 semanas de edad mantenidos en jaulas de plástico con aserrín, a temperatura constante (23 -25 °C) y períodos regulados de luz y oscuridad (12 h cada uno). Alimentación *ad libitum.*

Tamaño de la muestra

90 ratones atímicos, divididos en 6 grupos de 15 ratones cada uno para los estudios radiofarmacocinéticos.

Los datos de biodistribución (como se detallará más adelante) se obtendrán sacrificando a los ratones a las 0.5, 1, 2, 3, 24 h, postinyección, (tiempos necesarios para conocer la cinética de eliminación) y serán 3 animales por cada tiempo, dando un total de 15 ratones por grupo.

Con el radiofármaco ^{99m}Tc-oxitocina se utilizaran 2 grupos de 15 ratones cada uno y se evaluará la biodistribución del radiofármaco en ratones atímicos sanos y en ratones atímicos con tumor inducido que presentan receptores de oxitocina (cáncer de mama).

Con el radiofármaco ^{99m}Tc-RGD se utilizaran 4 grupos de 15 ratones, se evaluará la biodistribución del radiofármaco en ratones atímicos sanos y en ratones atímicos con tumores inducidos de páncreas (15 ratones), próstata (15 ratones) y mama (15 ratones), que presentan receptores de integrinas

Solo se utilizarán 3 ratones por tiempo porque es el número necesario para tener un nivel de confianza del 95 % es decir que la probabilidad de que el intervalo de confianza calculado contenga al verdadero valor del parámetro.

Además si el número de ratones es excesivo, el estudio se encarece desde el punto de vista económico y humano y es poco ético el someter a más animales al experimento cuando se puede tener un panorama general del efecto con el menor número de animales de experimentación.

Inducir tumores en ratones atímicos (Inoculación de agentes biológicos)

Se utilizarán diferentes líneas celulares de cáncer:
Células AR42J de tejido canceroso de páncreas, (origen murino)

Células PC3 de tejido canceroso de próstata, (origen humano)
Células MCF-7 de tejido canceroso de mama, (origen humano)

Los ratones atímicos se utilizarán de acuerdo a las especificaciones del reglamento sobre el manejo ético de los animales de laboratorio del bioterio del INCMNSZ (Norma Oficial Mexicana, NOM-062-ZOO-1999).
Para inducir los tumores en los ratones atímicos se inoculará de manera subcutánea 100 μL de una solución de células cancerosas en flancos (en un solo sitio), con los cuidados de manejo y sujeción del animal para minimizar riesgos durante el procedimiento de inyección tanto para el animal como para la persona que realiza el procedimiento. Una vez que el tumor tenga un tamaño de 0.5 a 1 cm de diámetro como máximo, se procederá a realizar el estudio de biodistribución

Estudios de Biodistribución

Se evaluará la biodistribución de los radiofármacos en ratones atímicos sanos y en ratones atímicos con tumores inducidos que presenten receptores de oxitocina y de integrinas para determinar la actividad acumulada en cada uno de los tejidos a diferentes tiempos.

Antes de la inyección del radiofármaco los ratones atímicos se pesan y la inyección en la cola del animal produce trauma mínimo.
Los datos de biodistribución se obtendrán despues de inyectar en la vena de la cola del ratón 20 μL a 40 μL del radiofármaco en estudio con una concentración radiactiva de aproximadamente de 40 microcuries (37 MBq/mL). Sacrificar a los ratones atímicos en la cámara de acrílico con una dosis letal de bióxido de carbono a las 0.5, 1, 2, 3, 24 h, postinyección con objeto de extraer y pesar los órganos, sangre, corazón, pulmón, músculo, riñones, estómago, vesícula biliar, intestino, hígado, fémur y el tumor en el caso de los ratones con inoculados previamente con células cancerosas. Se obtendrá las cpm de cada órgano, utilizando para el conteo un detector precalibrado de NaI(Tl). La captación en cada órgano se calculará y expresará como el % de actividad inyectada por g de órgano (%AI/g órgano). Todas las cuentas se corregirán por fondo, geometría (volúmenes iguales) y decaimiento físico.

Las curvas de actividad contra tiempo obtenidas en cada órgano, se ajustarán a un modelo biexponencial o triexponencial según el caso, con la finalidad de obtener las constantes de captación y eliminación efectivas.

La actividad determinada en las muestras de sangre a los diferentes intervalos de tiempo, se ajustarán a un modelo biexponencial de dos compartimentos; el compartimento central Cc y el compartimento perifério Cp , esto es, que el radiofármaco llega directamente a la circulación sistémica y se distribuye entre el torrente sanguíneo y los órganos más irrigados, como son el corazón, hígado y riñones, que constituyen el Cc; desde este compartimento la actividad pasa más lenta, a órganos o tejidos que reciben un menor flujo de sangre y éste nuevo espacio se denomina Cp.

Los resultados se analizarán con el programa biexp, para calcular las constantes de distribución rápida y constante de eliminación lenta, el volumen aparente de distribución en el compartimento central (Vdcc), el volumen aparente de distribución en el estado de equilibrio

(Vdss), la depuración total, el tiempo promedio de residencia y la constante de eliminación (kss) se calcularán.

Obtención de imágenes gammagráficas

Se obtendra una imagen gammagráfica del ratón inyectado con el radiofármaco utilizando el gammágrafo E-cam del departamento de medicina nuclear, 2 h postinyección del radiofármaco.

Disposición de cadáveres

Todo lo referente al uso de material radiactivo se trabajará dentro de un área que tiene licencia de uso de material radiactivo (laboratorio de medicina nuclear), el personal involucrado en este proyecto es POE y solo se usarán 40 microcuries que es una actividad muy baja, comparada con los 10 milicuries (10000 microcuries) que se usan en los estudios de rutina en pacientes. Además el Tc-99m tiene un tiempo de vida media física de seis horas, desintegrándose sin radiaciones beta, por lo que no existe ningún riesgo para el usuario y está clasificado dentro de los radionúclidos de toxicidad baja de acuerdo a la NOM-003-NUCL-1994 "Clasificación de instalaciones o laboratorios que utilizan fuentes abiertas"

En cuanto al manejo de desechos, se realizará de acuerdo al manual oficial de procedimiento del departamento de medicina nuclear. Los órganos del ratón y el cadáver se colocarán en una bolsa de plástico de color amarillo que tiene la leyenda "residuos biológico-infecciosos" y se almacenará dentro del cuarto frío del departamento de Medicina Nuclear. Después de 3 días de decaimiento, la bolsa amarilla de plástico que contienen los restos de cada tejido ya sin radiactividad, se desechará en el contenedor correspondiente de este tipo de desechos biológicos.

Análisis estadístico propuesto

Se usará la prueba de t pareada para evaluar el efecto del porcentaje de captación comparando la biodistribución del radiofármaco ^{99m}Tc-RGD en ratones con tumor inducido de mama y la biodistribución de la ^{99m} Tc-oxitocina también en ratones con tumor inducido de mama y determinar si hay diferencia significativa entre los dos radiofármacos. Se considerará diferencia significativa una $p<0.05$.

Para el análisis estadístico de la biodistribución de la ^{99m}Tc-RGD con las diferentes líneas celulares (3) se utilizara un ANOVA con un nivel de significancia de 0.05.

Otros aspectos

La metodología no incluye: maniobras conductuales, modificaciones ambientales, restricción física y ejercicio, inmunización, administración de medicamentos, substancias peligrosas ni cirugía

BIBLIOGRAFÍA

1. Breeman W.A., de Jong M., Kwekkeboom D. J., Valkema R., Bakker W.H. Kooij P.P., et al. Somatostatin receptor-mediated imaging and therapy: basic science, current knowledge, limitations and future perspectives. *Eur J Nucl Med.* **2001**, *28:1421-1429*
2. Bussolati G., Chinol M., Chini B., Nacca A., Cassoni P., Paganelli G. ^{111}In-labeled 1,4,7,10-Tetraazacyclododecane-N,N',N'',N'''-tetraacetic Acid-Lys^{8}-Vasoticin: A new Powerful Radioligand for Oxytocin Receptor-expressin Tumors *Cancer Research.* **2001**, *6:4393-43-97.*
3. Cassoni P., Fulcheri E., Carcangiu M. L., Stella A., Deaglio S., Bussolati G. Oxytocin receptors in human adenocarcinomas of the endometrium: presence and biological significance. *J. Pathol.* **2000**, *190:470-477.*
4. Cassoni P., Sapino A., Marrocco T., Bussolati G. Oxytocin and Oxytocin Receptors in Cancer Cells an Proliferation. *J. Neuroendocrinology.* **2004**, *16:362-364.*
5. Costopoulos, B.; Benaki, D.; Pelecanou, M.; Mikros, E.; Stassinopoulou, C.I.; Varvarigou, A.D.; Archimandritis, S.C. *Inorg. Chem.,* **2004**, *43*, 5598.
6. De Jong M., Kwekkeboom D., Valkema R., Krenning E. P. Tumor Therapy with radiolabelled peptides: current satatus and future directions. *Eur. J. Nucl. Med. Mol. Imaging.* **2003**, *30:463-469.*
7. FEUM. Farmacopea de los Estados Unidos Mexicanos. Capítulo de radiofármacos Octava edición, Vol.I, Secretaria de Salud. **2004**, México.
8. Friedlander M, Brooks PC, Shaffer RW, Kincaid CM, Varner JA, Cheresh DA. Definition of two angiogenic pathways by distinct alpha v integrins. Sc*ience.* **1995** *Dec 1;270(5241):1500-2*
9. Haubner, R.; Bruchertseifer, F.; Bock, M.; Kessler, H.; Schwaiger, M.; Wester, H.J. *Nuklearmedizin*, **2004**, *43*, 26
10. Janssen M, Frielink C, Dijkgraaf I, Oyen W, Edwards DS, Liu S, Rajopadhye M, Massuger L, Corstens F, Boerman O. Improved tumor targeting of radiolabeled RGD peptides using rapid dose fractionation. *Cancer Biother Radiopharm.* **2004***;19(4):399-404.*
11. Janssen M, Oyen WJ, Massuger LF, Frielink C, Dijkgraaf I, Edwards DS, Radjopadhye M, Corstens FH, Boerman OC.Comparison of a monomeric and dimeric radiolabeled RGD-peptide for tumor targeting. *Cancer Biother Radiopharm.* **2002***;17(6):641-6.*
12. Janssen ML, Oyen WJ, Dijkgraaf I, Massuger LF, Frielink C, Edwards DS, Rajopadhye M, Boonstra H, Corstens FH, Boerman OC. Tumor targeting with radiolabeled alpha(v)beta(3) integrin binding peptides in a nude mouse model. *Cancer Res.* **2002** *;62(21):6146-51.*
13. Kaltsas G., Rockall A., Papadogias D., Reznek R., Grossman A. B. Recent advances in radiological and radionuclide imaging and therapy of neuroendocrine tumours. *Eur. J. Endocrinol.* **2004**; *151:15-27*
14. Knight LC. In Handbook of Radiopharmaceuticals; Welch MJ and Redvanly CS eds. John Wiley & Sons: England, **2003**; pp. 643-684.
15. Krenning E.P., Kwekkeboom D.J.,Valkema R., Pauwels S., Kvols L.K., Marion de Jong. Peptide Receptor Radionuclide Therapy. *Ann. N.Y. Acad. Sci.* **2004**, *1014:234–245.*

16. Kwekkeboom D.J., Teunissen J.J., Bakker W.H., Kooij P.P., de Herder W.W., Feelders R.A., et al. Radiolabeled somatostatin analog [177Lu-DOTA0,Tyr3]octreotate in patients with endocrine gastroenteropancreatic tumors. *J. Clin. Oncol.* **2005a**; *23:2754-2762.*

17. Kwekkeboom D.J., Muller-Brand J., Paganelli G., Lowell B. A., Pauwels S., Kvols K. L., O'Dorisio T. M., et al. Overview of Results of Peptide Receptor Radionuclide Therapy with 3 Radiolabeled Somatostatin Analog. *J. Nucl. Med.* **2005b**; *46:62S-66S*

18. Liu, S.; Hsieh, W.Y.; Kim, Y.S.; Mohammed, S.I.; Effect of coligands on biodistribution characteristics of ternary ligand 99mTc complexes of a HYNIC-conjugated cyclic RGDfK dimer. *Bioconjug Chem. **2005** Nov-Dec;16(6):1580-8*

19. Lui S, Edwards S, Barnet AS. Reviews 99mTc. Labeling of highly potent small peptides. *Bioconjugate Chem.* **1997**; *5:621-636.*

20. Mitra A, Nan A, Papadimitriou JC, Ghandehari H, Line BR. Polymer-peptide conjugates for angiogenesis targeted tumor radiotherapy. *Nucl Med Biol.* **2006**; *33(1):43-52.*

21. Reubi J.C. Peptide Receptors as Molecular Targets for Cancer Diagnosis and Therapy. *Endocrine Reviews.* **2003**; *24(4): 389-427.*

22. Su ZF, Liu G, Gupta S, Zhu Z, Rusckowski M, Hnatowich DJ. In vitro and in vivo evaluation of a Technetium-99m-labeled cyclic RGD peptide as a specific marker of alpha(V)beta(3) integrin for tumor imaging. *Bioconjug Chem.* **2002**;*13(3):561-70*

23. Varner JA; Brooks PC; Cheresh DA. REVIEW: the integrin alpha V beta 3: angiogenesis and apoptosis. *Cell adhesion & communications*, **1995**;*3(4):367-74*

24. Varner JA, Cheresh DA. Integrins and cancer. *Curr. Opin. Cell. Biol.* **1996**; 8(5):724-30.

25. Verduyckt, T.; Kieffer, D.; Huyghe, D.; Cleynhens, B.; Verbeke, K.; Verbruggen, A.; Bormans, G. *J. Pharm. Biomed. Anal.*, **2003**, *32*, 669.

26. Facilities for Experimental Animals, Information for new users 1987, University of Cambridge, Central Biomedical Services

27. Norma Oficial Mexicana NOM-062-ZOO-1999. Diario Oficial del 22 de agosto del 2001

28. Manual de seguridad radiológica del departamento de medicina nuclear, INCMNSZ.

INNSZ

INSTITUTO NACIONAL DE CIENCIAS MÉDICAS Y NUTRICIÓN
SALVADOR ZUBIRÁN

México, D.F., a 17 de septiembre 2007

Dra. en C. Martha Pedraza López
Investigadora
Depto. Medicina Nuclear

Estimada Dra. Pedraza,

En referencia con el proyecto de investigación: CINVA 243
"Evaluación in *vitro* de péptidos radiomarcados para el diagnóstico de lesiones tumorales por imágenes gammagráficas en medicina nuclear"

El Comité recibió su comunicación que da respuesta a las observaciones emitidas por el mismo en su primera revisión, sin embargo, la información que presenta en su carta no ha sido suficiente para aclarar las dudas del CINVA, pro lo que a continuación se expone:

1. No se presentó el protocolo con las modificaciones a que se hacen referencia en su carta.
2. En lo referente a la justificación para mantener el título del trabajo. No es un argumento convincente.
3. La nueva hipótesis que se presenta no cumple con la definición metodológica acerca de la relación de una variable dependiente y una variable independiente.
4. Se establecen el protocolo al menos 8 objetivos generales. Sin embargo en la sección de Material y Método únicamente se presenta la metodología para cumplir con la primera parte del objetivo 5.
5. Se sugiere presentar el protocolo de manera continua, particularmente en su sección de Material y Métodos incluyendo detalladamente la metodología para cada uno de los experimentos que se realizarán.
6. En lo referente al la determinación para el tamaño de muestra, no se presenta ningún calculo estadístico que apoye la selección del tamaño.
7. Se menciona que se tienen control de bioseguridad de los materiales y desechos biológicos, pero no se cuenta con el protocolo en donde se incluyen estos procedimientos.
8. Explicar como determinaran con base en los datos estadísticos la utilidad de los productos biológicos marcados.

Sin otro particular,

Recibí Original
17/Sept/2007

Atentamente

M.V.Z., M.Sc. Rafael Hernández González
Coordinador del Comité de Investigación en Animales

• Vasco de Quiroga 15,
• Delegación Tlalpan
• C. P. 14000 México, D. F.
• Tel. 54-87-09-00

INCMNSZ

INSTITUTO NACIONAL DE CIENCIAS MEDICAS Y NUTRICION
SALVADOR ZUBIRAN

viernes, 13 de julio de 2007
Ref. CINVA 243

MVZ. M. Sc. Rafael Hernández González
Coordinador del Comité de Investigación en Animales.
INCMNSZ

Distinguido Dr. Hernández:

Recibimos su comunicación del 9 de julio con observaciones al proyecto "Evaluación *in vitro* e *in vivo* de péptidos radiomarcados para el diagnóstico específico de lesiones tumorales por imágenes gammagráficas en medicina nuclear"

Las respuestas a sus observaciones son:

1. El titulo no se puede cambiar porque así se registró en CONACYT.
   Se realizarán estudios preclínicos en animales y la finalidad es demostrar que los péptidos que serán marcados y evaluados serían útiles en un futuro para el diagnóstico específico de lesiones tumorales por imágenes gammagráficas en medicina nuclear.
   Los estudios preclínicos de obtención de imágenes se mencionaron en el protocolo enviado, en los objetivos generales, No. 7 "Obtener imágenes gammagráficas de la biodistribución de cada uno de los radiofármacos en animales con tumores inducidos"

2. La hipótesis se replanteó y queda como sigue:
   Si los péptidos marcados son específicos serán útiles para ser captados in vitro e in vivo en lesiones tumorales y podrían ser un buen agente para el diagnóstico por imágenes gammagráficas en medicina nuclear"

3. La inoculación de células tumorales se mencionó en el protocolo enviado, en los objetivos generales, No. 5 "Determinar la biodistribución de los 3 radiofármacos en un modelo animal (animales sanos y en animales con tumores inducidos)" y No. 6 "Comparar la especificidad *in vivo* de los 3 radiofármacos en tumores inducidos en un modelo animal", y se describió en el punto 6.10 del protocolo enviado.

4. Con respecto al tamaño de la muestra:
   El número de animales se modifica a 60 ratone atímicos, 30 hembras y 30 machos. No se puede utilizar un número menor de animales ya que para poder realizar un estudio estadístico es necesario al menos 3 datos por cada uno de los tiempos.

• Vasco de Quiroga 15,
• Delegación Tlalpan
• C.P. 14000 México, D.F.
• Tel. 54-87-09-00

Los datos de biodistribución como se menciona en el del protocolo se obtendrán sacrificando a los ratones a las 0.5, 1, 2, 3, 24 h, postinyección, (se elimina el tiempo de 0.25 h) y serán 3 animales por cada tiempo, dando un total de 15 y si se pretende comparar las líneas celulares y dos radiofármacos son necesarios 60 animales.

5. No es necesaria la aprobación por el Comité Institucional de Bioseguridad porque todo lo referente al uso de material radiactivo se trabajará dentro de un área que tiene licencia de uso de material radiactivo (laboratorio de medicina nuclear), el personal involucrado en este proyecto es POE y solo se usarán 40 microcuries que es una actividad muy baja, comparada con los 10 milicuries (10000 microcuries) que se usan en los estudios de rutina en pacientes. Además el Tc-99m tiene un tiempo de vida media física de seis horas, desintegrándose sin radiaciones beta, por lo que no existe ningún riesgo para el usuario y está clasificado dentro de los radionúclidos de toxicidad baja de acuerdo a la NOM-003-NUCL-1994 "Clasificación de instalaciones o laboratorios que utilizan fuentes abiertas"

   En cuanto al manejo de desechos, los órganos del ratón y el cadáver se colocarán en una bolsa de plástico de color amarillo que tiene la leyenda "residuos biológico-infecciosos" y se almacenará dentro del cuarto frío del departamento de Medicina Nuclear. Después de 3 días de decaimiento, la bolsa amarilla de plástico que contienen los restos de cada tejido ya sin radiactividad, se desechará en el contenedor correspondiente de este tipo de desechos biológicos.

6. El análisis estadístico se modificó y queda como sigue:
   Se usará la prueba de t pareada para evaluar el efecto del porcentaje de captación de los radiofármacos y determinar si hay diferencia significativa entre las diferentes líneas celulares y los diferentes péptidos. Se considerará efecto significativo una $p<0.05$

Agradezco todas sus observaciones esperando haber respondido a todas ellas y quedo a su disposición para cualquier aclaración.

Atentamente,

Dra. en C. Martha Pedraza López
Investigador en Ciencias Médicas
Departamento de Medicina Nuclear.
Ext. 2402

• Vasco de Quiroga 15,
• Delegación Tlalpan
• C.P. 14000 México, D.F.
• Tel. 54-87-09-00

INCMNSZ

INSTITUTO NACIONAL DE CIENCIAS MEDICAS Y NUTRICION
SALVADOR ZUBIRAN

viernes, 13 de julio de 2007
Ref. CINVA 243

MVZ. M. Sc. Rafael Hernández González
Coordinador del Comité de Investigación en Animales.
INCMNSZ

Distinguido Dr. Hernández:

Recibimos su comunicación del 9 de julio con observaciones al proyecto "Evaluación *in vitro* e *in vivo* de péptidos radiomarcados para el diagnóstico específico de lesiones tumorales por imágenes gammagráficas en medicina nuclear"

Las respuestas a sus observaciones son:

1. El titulo no se puede cambiar porque así se registró en CONACYT.
   Se realizarán estudios preclínicos en animales y la finalidad es demostrar que los péptidos que serán marcados y evaluados serían útiles en un futuro para el diagnóstico específico de lesiones tumorales por imágenes gammagráficas en medicina nuclear.
   Los estudios preclínicos de obtención de imágenes se mencionaron en el protocolo enviado, en los objetivos generales, No. 7 "Obtener imágenes gammagráficas de la biodistribución de cada uno de los radiofármacos en animales con tumores inducidos"

2. La hipótesis se replanteó y queda como sigue:
   Si los péptidos marcados son específicos serán útiles para ser captados in vitro e in vivo en lesiones tumorales y podrían ser un buen agente para el diagnóstico por imágenes gammagráficas en medicina nuclear"

3. La inoculación de células tumorales se mencionó en el protocolo enviado, en los objetivos generales, No. 5 "Determinar la biodistribución de los 3 radiofármacos en un modelo animal (animales sanos y en animales con tumores inducidos)" y No. 6 "Comparar la especificidad *in vivo* de los 3 radiofármacos en tumores inducidos en un modelo animal", y se describió en el punto 6.10 del protocolo enviado.

4. Con respecto al tamaño de la muestra:
   El número de animales se modifica a 60 ratone atímicos, 30 hembras y 30 machos. No se puede utilizar un número menor de animales ya que para poder realizar un estudio estadístico es necesario al menos 3 datos por cada uno de los tiempos.

Investigación
Tradición Servicio
Asistencia Docencia
20007700

. Vasco de Quiroga 15,
. Delegación Tlalpan
. C.P. 14000 México, D.F.
. Tel. 54-87-09-00

Recibí original
13-07-07

Los datos de biodistribución como se menciona en el del protocolo se obtendrán sacrificando a los ratones a las 0.5, 1, 2, 3, 24 h, postinyección, (se elimina el tiempo de 0.25 h) y serán 3 animales por cada tiempo, dando un total de 15 y si se pretende comparar las líneas celulares y dos radiofármacos son necesarios 60 animales.

5. No es necesaria la aprobación por el Comité Institucional de Bioseguridad porque todo lo referente al uso de material radiactivo se trabajará dentro de un área que tiene licencia de uso de material radiactivo (laboratorio de medicina nuclear), el personal involucrado en este proyecto es POE y solo se usarán 40 microcuries que es una actividad muy baja, comparada con los 10 milicuries (10000 microcuries) que se usan en los estudios de rutina en pacientes. Además el Tc-99m tiene un tiempo de vida media física de seis horas, desintegrándose sin radiaciones beta, por lo que no existe ningún riesgo para el usuario y está clasificado dentro de los radionúclidos de toxicidad baja de acuerdo a la NOM-003-NUCL-1994 "Clasificación de instalaciones o laboratorios que utilizan fuentes abiertas"

   En cuanto al manejo de desechos, los órganos del ratón y el cadáver se colocarán en una bolsa de plástico de color amarillo que tiene la leyenda "residuos biológico-infecciosos" y se almacenará dentro del cuarto frío del departamento de Medicina Nuclear. Después de 3 días de decaimiento, la bolsa amarilla de plástico que contienen los restos de cada tejido ya sin radiactividad, se desechará en el contenedor correspondiente de este tipo de desechos biológicos.

6. El análisis estadístico se modificó y queda como sigue:
   Se usará la prueba de t pareada para evaluar el efecto del porcentaje de captación de los radiofármacos y determinar si hay diferencia significativa entre las diferentes líneas celulares y los diferentes péptidos. Se considerará efecto significativo una $p<0.05$

Agradezco todas sus observaciones esperando haber respondido a todas ellas y quedo a su disposición para cualquier aclaración.

Atentamente,

Dra. en C. Martha Pedraza López
Investigador en Ciencias Médicas
Departamento de Medicina Nuclear.
Ext. 2402

INNSZ

INSTITUTO NACIONAL DE CIENCIAS MÉDICAS Y NUTRICIÓN SALVADOR ZUBIRÁN

09de julio de 2007

Dra. en C. Martha Pedraza López
Departamento de Medicina Nuclear
P r e s e n t e.

En referencia con el proyecto de investigación: CINVA 243.

"Evaluación *in Vitro e in Vivo* de Péptidos Radiomarcados para el Diagnóstico de Lesiones Tumorales por Imágenes Gammagráficas en Medicina Nuclear".

El Comité de Investigación en Animales, ha revisado el proyecto y requiere se de respuesta a las siguientes observaciones:

1. El título no refleja lo que realmente van a realizar y debería modificarse. En ningún momento hablan de imágenes sino de medición de actividad radioactiva por cpm y cálculos de su distribución en los distintos órganos (página 3).
2. La Hipótesis debe replantearse ya que la propuesta no se relaciona con lo que mencionan posteriormente en Material y Métodos. Nunca mencionan cómo es que van a determinar la producción del "...complejo estable 99mTc-HYNIV-ciclo-Lys-D-Phe_RGD con una pureza radioquímica mayor al 95%...",ni tampoco como van a demostrar que este es "captado *in vivo* en sitios específicos de angiogénesis".
3. En Material y Métodos (página 3), nunca mencionan la inoculación de células tumorales en los animales (ni siquiera en la justificación, los objetivos ni la hipótesis); posteriormente en la página 6 de repente mencionan la inoculación de tres líneas celulares sin jamás haber mencionado esto anteriormente y sin especificar una serie de cuestiones relevantes para el análisis del proyecto. Debemos conocer la justificación del inóculo de células tumorales (cuando ni siquiera conocen la distribución normal de los radiopéptidos), el momento en que van a realizar el inóculo, el tiempo que mantendrán a los animales inoculados antes de hacer el estudio de radiofarmacología, criterios de eliminación de los animales (si presentan deterioro importante en su salud o manifestaciones potenciales de sufrimiento innecesario), etc.
4. En caso de replantear el proyecto deben realizar un cálculo de tamaño de muestra que justifique los 120 animales solicitados (ratones nu/un, 60 machos, 60 hembras).
5. El estudio requiere aprobación por el Comité institucional de Bioseguridad (¿?). No estoy seguro de que el manejo propuesto de los desechos de ratones radioactivos y sus tejidos sea el adecuado.
6. El punto 4.5 Análisis Estadístico Propuesto (página 3) es inaceptable.

Recibí Original
10/Julio/2007

Investigación

Tradición Servicio

Asistencia Docencia

A t e n t a m e n t e

MVZ. M. Sc. Rafael Hernández González
Coordinador del Comité de Investigación en Animales

• Vasco de Quiroga 15,
• Delegación Tlalpan
• C. P. 14000 México, D. F.
• Tel. 54-87-09-00

20007700

INSTITUTO NACIONAL DE CIENCIAS MEDICAS Y NUTRICION
"SALVADOR ZUBIRAN"
Dirección de Investigación
Comité de Investigación en Animales (CINVA)

SOLICITUD DE EVALUACION DE PROYECTOS

No invada las zonas sombreadas

No. CINVA: 243
CLAVE:

Fecha de Recepción: Fecha de revisión:

TITULO DEL PROYECTO: EVALUACION IN VITRO E IN VIVO DE PEPTIDOS RADIOMARCADOS PARA EL DIAGNOSTICO DE LESIONES TUMORALES POR IMAGENES GAMMAGRAFICAS EN MEDICINA NUCLEAR

INVESTIGADOR PRINCIPAL (IP): DRA. EN C. MARTHA PEDRAZA LOPEZ
DEPARTAMENTO DE ADSCRIPCION: MEDICINA NUCLEAR EXT. 2402-2400
TELEFONOS PARA EMERGENCIAS: 54-87-09-00
CORREO ELECTRONICO: mpedraza@quetzal.innsz.mx OBSERVACIONES:

Personal que trabajará directamente con los animales (investigadores asociados, alumnos, tesistas, etc)

Nombre	Puesto en el INCMNSZ	EXT.	Tel. en caso de emergencia
1. DRA. MARTHA PEDRAZA LOPEZ	INV.CIENC.MEDICAS	2402	54870900
2. DRA. CONSUELO ARTEAGA DE MURPHY	INV.CIENC.MEDICAS	2402	54870900
3. M en C. OCTAVIO VILLANUEVA SANCHEZ	J.LAB. CLIN.	2253	54870900
4. Q. FRED ALONSO LOPEZ DURAN	TESISTA	2402	56222288

Los animales utilizados en el proyecto de investigación serán adquiridos, mantenidos, manejados y utilizados de acuerdo al reglamento, a los manuales y guías de procedimientos del Departamento de Investigación Experimental y Bioterio, mismos que contienen la Norma Oficial Mexicana NOM-062-ZOO-1999, Especificaciones técnicas para la producción, cuidado y uso de los animales de laboratorio. Publicada por la SAGARPA en el Diario Oficial el miércoles 22 de agosto del 2001, y los lineamientos nacionales e internacionales para el buen uso de los animales de experimentación.

Sólo el suscrito, los investigadores y personal registrado y autorizado por el CINVA trabajarán con los animales, siendo el investigador principal el responsable de que cada uno de ellos cuente con los conocimientos, habilidades y experiencia en el manejo de los animales para realizar las maniobras experimentales descritas en el proyecto.

Los animales serán sometidos exclusivamente a los procedimientos especificados en este protocolo, siendo indispensable solicitar **por escrito** al CINVA cualquier modificación, incluyendo las fechas de inicio y terminación del estudio.

DRA. EN C. MARTHA PEDRAZA LOPEZ
Nombre y firma del Investigador Principal

El presente formulario pretende facilitar la evaluación de suproyecto e identifcar las necesidades de animales de laboratorio, equipo y manejo para su proyecto de investigación. Para el llenado de los cuadros consulte la información que describe cada sección de los mismos:

Fecha de inicio del estudio: JULIO 2007

Fecha de terminación del estudio: JULIO 2008

Indique con el inciso correspondiente las características de los animales, condiciones de alojamiento y maniobras experimentales que requiere el proyecto:

1. Especie	2. Raza, cepa	3. Condición microbiol.	4.No. H	Total M	5. Distribución	6. Alojamiento	7. Densidad	8. Nivel biosegur.	9. Nivel de afectación	10. Destino	11. Eutanasia
RATON	NU/NU	A	60	60	30/MES	A	10/CAJA	I	B	D	CO2

1. **Nombre genérico o especie:** Escriba el nombre común o científico de los animales que empleará en su estudio.

2. **Raza, cepa o tipo genético:** Escriba la nomenclatura que mejor describe las características genéticas del animal que necesita (ej: ratón: BALB/c, C57BL6, Cd1, nu/nu, Rata: wistar, fischer 344, sprague-dawley, NIH, Conejo: nueva zelanda albino, Hámster: dorado)

3. **Tipo o condición microbiológica:** A) Convencional: animal con flora microbiológica desconocida, sin signos aparentes de enfermedad, B) SPF: (specific pathogen free) libre de patógenos especificos (indicar el tipo de patógenos indeseables ej: virus, bacterias, hongos, parásitos), C) Otro: especifique

4. **Número total:** Indique el número de animales que utilizará en el estudio, H: hembras, M: machos, incluyendo grupos piloto. En caso de utilizar animales de un sólo sexo favor de invalidar la columna correspondiente.

5. **Distribución:** Indique la cantidad y la frecuencia en que requiere se le entreguen los animales ej: todos en una entrega, 10 cada semana, al mes, bimestre, trimestre, semestre, etc.

6. **Alojamiento:** Indique con la letra el tipo que corresponda:
A) caja de policarbonato de piso sólido
B) jaula con piso de malla o rejilla
C) jaula metabólica
D) microaislador
E) caja de policarbonato de piso sólido con filtro
F) perrera
G) corral
H) corraleta metabólica
I) pecera

7. **Densidad poblacional:** Indique como alojará a los animales ej: un animal por caja, parejas, 3, 5, etc. Consultar la Norma Oficial Mexicana NOM-062-ZOO-1999, Especificaciones técnicas para la producción, cuidado y uso de los animales de laboratorio. Publicada por la SAGARPA en el Diario Oficial el miércoles 22 de agosto del 2001.

8. **Nivel de bioseguridad:** Deberá indicar el nivel de riesgo biológico que existe para el personal que maneja a los animales o sus desechos, tanto para investigadores, alumnos y técnicos de bioterio.
Nivel I) Trabajo con agentes químicos, físicos o biológicos que no producen enfermedad y no son un riesgo para la salud de personas sanas y el medio ambiente.
Nivel II) Trabajo con agentes químicos, físicos o biológicos que tienen un peligro potencial bajo o moderado para la salud del personal y el medio ambiente (Ej: Salmonelosis, Toxoplasmosis, Hepatitis B)
Nivel III) Trabajo con agentes químicos, físicos o biológicos que tienen un peligro potencial alto para la salud humana y animal o pueden producir la muerte cuando se inhalan (Ej: Tuberculosis, *Coxiella burnetti*)
Nivel IV) Trabajo con agentes químicos, físicos o biológicos exóticos transmisibles por aerosoles y mortales para seres humanos y animales (Ej: virus ébola, virus hanta)

9. **Nivel de afectación de los animales:** Indique el nivel de invasividad y el grado de dolor que sentirá el animal durante los procedimientos experimentales o manipulación:
Categoría A) Experimentos con invertebrados, huevos, protozoarios, organismos unicelulares. Uso de metazoarios, cultivo de tejidos u órganos obtenidos después de la muerte del animal.
Categoría B) Experimentos que causen molestia o estrés mínimo (inyección no dolorosa, restricción de movimiento, marcado o aretado de orejas)
Categoría C) Experimentos que causan estrés menor o dolor de corta duración, realizados con analgesia o anestesia (colocación de cánula, biopsia, cirugía menor)
Categoría D) Experimentos que causan estrés o dolor de moderado a severo controlado con anestesia (procedimientos quirúrgicos mayores)

10. **Destino final:** indicar el destino final de los animales al término de los experimentos:
A) vivo sin cirugía
B) vivo post-cirugía
C) cirugía terminal (no despierta de la anestesia)
D) eutanasia

11. **Eutanasia:** Indique el método empleado para dar muerte al animal. Consultar la Norma Oficial Mexicana NOM-062-ZOO-1999, Especificaciones técnicas para la producción, cuidado y uso de los animales de laboratorio. Publicada por la SAGARPA en el Diario Oficial el miércoles 22 de agosto del 2001, capítulo 9, eutanasia.

En el siguiente cuadro marque con la clave que se indica el nivel de habilidad y experiencia de usted y su personal para realizar las maniobras experimentales mencionadas en la columna de la izquierda.

Clave:

A) Entrenado, hábil y con experiencia.
B) Será entrenado y supervisado por el I.P.
C) Requiere instrucción, entrenamiento y supervisión por el personal del D.I.E.B.

En caso de que las maniobras experimentales sean realizadas por el personal del bioterio se marcará con una x el espacio correspondiente en la columna D.I.E.B.

Investigador ó personal que trabajará directamente con los animales (investigadores asociados, alumnos, tesistas), etc

MANIOBRA	I.P.	1	2	3	4	D.I.E.B.
Inmovilización	X	X	X	X	X	
Anestesia						
Medicación Enteral						
Medicación parenteral						
Toma de sangre	X	X	X	X	X	
Otras muestras *	X	X	X	X	X	
Cirugía						
Eutanasia	X	X	X	X	X	
Otras **						

* Especificar de qué, cantidad y frecuencia de muestreo:
SE DESCRIBE EN MATERIAL Y METODO

** Especificar : _____

DRA. EN C. MARTHA PEDRAZA LOPEZ
Nombre y firma del Investigador Principal

RHG/mlsj, agosto del 2001

EVALUACIÓN *IN VITRO* E *IN VIVO* DE PÉPTIDOS RADIOMARCADOS PARA EL DIAGNÓSTICO ESPECÍFICO DE LESIONES TUMORALES POR IMÁGENES GAMMAGRÁFICAS EN MEDICINA NUCLEAR

Investigador Responsable Dra. Martha Pedraza López
Departamento de Medicina Nuclear

ANTECEDENTES

En Medicina Nuclear el, ^{99m}Tc es el radionúclido más utilizado para estudios de diagnóstico debido a sus características físicas y químicas, emite radiaciones gamma de 140 keV (90%), (monoenergético), fácilmente detectada que proporciona imágenes gammagráficas de alta calidad, su tiempo de vida media física es de seis horas, desintegrándose por transición isomérica sin radiaciones beta, por lo que se pueden administrar dosis relativamente altas para efectuar estudios clínicos en menos tiempo y con menor tiempo de exposición. Además, el ^{99m}Tc tiene una gran disponibilidad debido a su bajo costo, ya que se obtiene fácilmente de un generador de ^{99}Mo/^{99m}Tc.

Se utiliza en forma de pertecneciato y, en estado reducido se une a un gran número de ligantes o moléculas acarreadoras, formando complejos (radiofármacos) en un tiempo de reacción relativamente corto (5 a 30 min) con altas eficiencias de marcado (>90%) [Verduyckt y cols 2003; FEUM, 2004]. Una alta selectividad por el sitio del tumor y un periodo de permanencia largo del radiofármaco en el sitio de interés son las bases para un diagnóstico clínico exitoso.

Las hormonas peptídicas (ácidos α-aminocarboxílicos) han sido diseñadas por la naturaleza para estimular, regular, inhibir numerosas funciones de la vida y actúan por medio de sus receptores principalmente, como transmisores de información y coordinadores de actividades de varios tejidos en el organismo. Comparados con los anticuerpos, los péptidos pequeños ofrecen varias ventajas: son fáciles de sintetizar y modificar, tienen menos probabilidad de ser inmunogénicos y rápida depuración sanguínea. En muchos casos la afinidad de los péptidos pequeños por sus receptores es significativamente mayor que la de los anticuerpos o sus fragmentos [Lui y cols., 1997; Reubi, 2003, De Jong y cols., 2003].

Los receptores se unen específicamente a los correspondientes péptidos marcados con radionucleidos. Los receptores de péptidos están sobre expresados en las células de numerosos cánceres. Estos receptores han sido usados como blancos moleculares para peptidos radiomarcados y así localizar el tumor, uno de esos complejos es el octreótido (^{99m}Tc-HYNIC-TOC) que ha demostrado ser una buena opción para la detección de tumores que presentan receptores de somatostatina, ya que es captado rápidamente y retenido por el tumor. Las aplicaciones exitosas del octreótido radiomarcado en centelleografía para la localización de linfomas, granulomatosis, meningiomas y tumores de origen neuroendócrino y cáncer pulmonar, sobre todo en Europa son indicativas de la importancia que tiene investigar otro tipo de péptidos radiomarcados, tanto nativos como sus derivados (análogos), para diagnóstico por imagen en medicina nuclear [Breeman y cols., 2001; Krenning y cols., 2004, Kaltsas y cols., 2004; Kwekkeboom y cols., 2005a, 2005b].

Otros péptidos de mucho interés en medicina debido a que sus receptores estimulan el crecimiento en las células neoplásicas son la oxitocina en el cáncer de mama y cérvico uterino, y las integrinas en la estimulación de la angiogénesis.

a) **Oxitociona** Químicamente la oxitocina (OT) es un nanopéptido cíclico, con la secuencia cisteína-tirosina-isoleucina-glutamina-asparagina-cisteína-prolina-leucina-glicina. Es una hormona neuropeptidica sintetizada en los núcleos paraventricular y supraóptico del hipotálamo. La acción hormonal periférica de la OT está mediada por receptores. Los receptores (OTRs) se unen específicamente y con gran afinidad a la OT y a algunos de sus análogos. Los OTRs se expresan principalmente en las células mioepiteliales de la glándula mamaria, en el miometrio y el endometrio del útero, al término del embarazo y en el parto y post parto. Además por estudios in vivo e in vitro se demostró que también se encuentran en carcinomas de mama y de endometrio, en neuroblastomas, glioblastomas, osteoblastos y osteosarcomas [Cassoni y col. 2000, 2004].

b) **Integrinas** Las integrinas son glucoproteínas heterodiméricas de adhesión transmembranal, constituidas por cadenas alfa y beta que cruzan de parte a parte la membrana celular. Hay 14 clases de subunidades α y 8 clases de subunidades β, que producen al menos 20 heterodímeros de integrinas. Hay muchas integrinas que están expresadas ampliamente, y la mayoría de las células tienen más de una integrina en su superficie celular, por ejemplo, las células de melanoma expresan $\alpha_v\beta_3$, $\alpha_1\beta_1$, $\alpha_3\beta_1$ y $\alpha_5\beta_1$; en las células de carcinoma pulmonar se expresan $\alpha_v\beta_5$ y en muchas otras células tumorales se encuentran $\alpha_v\beta_6$ [Knight y cols 2003; Mitra y cols. 2006]. Se han encontrado una gran variedad de integrinas sobre la superficie de células tumorales, las integrinas $\alpha_v\beta_3$ se encuentran elevadas en la angiogénesis de tumores y sus metástasis [Friedlander y cols. 1995];

La unión específica de los receptores $\alpha_v\beta_3$ de las integrinas a los péptidos que contienen el residuo de amino ácidos Arg-Gly-Asp (RGD) ha sido útil para obtener la imagen de tumores específicos, mediante el radiomarcado del péptido RGD [Janssen y cols. 2002].

OBJETIVOS E HIPÓTESIS

EL OBJETIVO PRINCIPAL:
Evaluar la especificidad *in vivo* de las formulaciones de péptidos marcados con ^{99m}Tc para el diagnóstico específico de lesiones tumorales que sobre expresan receptores de oxitocina y de integrinas por imágenes gammagráficas en medicina nuclear. Los estudios in vitro han sido previamente realizados y la hipótesis anterior sobre la captación in vitro ya se corroboró con estudios anteriores.

Cambio Ref.

LOS OBJETIVOS GENERALES SON:

1. Determinar la biodistribución de los radiofármacos en un modelo animal (ratones sanos y en ratones con tumores inducidos).
2. Obtener imágenes gammagráficas de la biodistribución de cada uno de los radiofármacos en animales con tumores inducidos.

3. Elaborar un protocolo clínico que permita la obtención de imágenes diagnósticas en pacientes con los radiofármacos obtenidos y que pudieran ser utilizados para el diagnóstico de cáncer de páncreas, próstata y mama.

HIPÓTESIS:

Si los péptidos marcados son receptor-específicos serán captados *in vivo* en lesiones tumorales y podrían ser un buen agente para el diagnóstico por imágenes gammagráficas en medicina nuclear.

MATERIAL Y MÉTODOS

Todo lo referente marcado de la oxitocina (^{99m}Tc-oxitocina) y del ciclo-Lys-D-Phe-RGD (^{99m}Tc-RGD), estudios de estabilidad de los radiofármaco y captación *in vitro* en las líneas de células tumorales son objetivos ya realizados. En este protocolo solo se realizarán los estudios *in vivo* en ratones sano y ratones con tumor inducido

Material biológico

Ratones atímicos, de 6 semanas de edad mantenidos en jaulas de plástico con aserrín, a temperatura constante (23 -25 °C) y períodos regulados de luz y oscuridad (12 h cada uno). Alimentación *ad libitum.*

Tamaño de la muestra

90 ratones atímicos, divididos en 6 grupos de 15 ratones cada uno para los estudios radiofarmacocinéticos.

Los datos de biodistribución (como se detallará más adelante) se obtendrán sacrificando a los ratones a las 0.5, 1, 2, 3, 24 h, postinyección, (tiempos necesarios para conocer la cinética de eliminación) y serán 3 animales por cada tiempo, dando un total de 15 ratones por grupo.

Con el radiofármaco ^{99m}Tc-oxitocina se utilizaran 2 grupos de 15 ratones cada uno y se evaluará la biodistribución del radiofármaco en ratones atímicos sanos y en ratones atímicos con tumor inducido que presentan receptores de oxitocina (cáncer de mama).

Con el radiofármaco ^{99m}Tc-RGD se utilizaran 4 grupos de 15 ratones, se evaluará la biodistribución del radiofármaco en ratones atímicos sanos y en ratones atímicos con tumores inducidos de páncreas (15 ratones), próstata (15 ratones) y mama (15 ratones), que presentan receptores de integrinas

Solo se utilizarán 3 ratones por tiempo porque es el número necesario para tener un nivel de confianza del 95 % es decir que la probabilidad de que el intervalo de confianza calculado contenga al verdadero valor del parámetro.

Además si el número de ratones es excesivo, el estudio se encarece desde el punto de vista económico y humano y es poco ético el someter a más animales al experimento cuando se puede tener un panorama general del efecto con el menor número de animales de experimentación.

Inducir tumores en ratones atímicos (Inoculación de agentes biológicos)

Se utilizarán diferentes líneas celulares de cáncer:
Células AR42J de tejido canceroso de páncreas, (origen murino)

Células PC3 de tejido canceroso de próstata, (origen humano)
Células MCF-7 de tejido canceroso de mama, (origen humano)

Los ratones atímicos se utilizarán de acuerdo a las especificaciones del reglamento sobre el manejo ético de los animales de laboratorio del bioterio del INCMNSZ (Norma Oficial Mexicana, NOM-062-ZOO-1999).
Para inducir los tumores en los ratones atímicos se inoculará de manera subcutánea 100 µL de una solución de células cancerosas en flancos (en un solo sitio), con los cuidados de manejo y sujeción del animal para minimizar riesgos durante el procedimiento de inyección tanto para el animal como para la persona que realiza el procedimiento. Una vez que el tumor tenga un tamaño de 0.5 a 1 cm de diámetro como máximo, se procederá a realizar el estudio de biodistribución

Estudios de Biodistribución

Se evaluará la biodistribución de los radiofármacos en ratones atímicos sanos y en ratones atímicos con tumores inducidos que presenten receptores de oxitocina y de integrinas para determinar la actividad acumulada en cada uno de los tejidos a diferentes tiempos.

Antes de la inyección del radiofármaco los ratones atímicos se pesan y la inyección en la cola del animal produce trauma mínimo.
Los datos de biodistribución se obtendrán despues de inyectar en la vena de la cola del ratón 20 µL a 40 µL del radiofármaco en estudio con una concentración radiactiva de aproximadamente de 40 microcuries (37 MBq/mL). Sacrificar a los ratones atímicos en la cámara de acrílico con una dosis letal de bióxido de carbono a las 0.5, 1, 2, 3, 24 h, postinyección con objeto de extraer y pesar los órganos, sangre, corazón, pulmón, músculo, riñones, estómago, vesícula biliar, intestino, hígado, fémur y el tumor en el caso de los ratones con inoculados previamente con células cancerosas. Se obtendrá las cpm de cada órgano, utilizando para el conteo un detector precalibrado de NaI(Tl). La captación en cada órgano se calculará y expresará como el % de actividad inyectada por g de órgano (%AI/g órgano). Todas las cuentas se corregirán por fondo, geometría (volúmenes iguales) y decaimiento físico.

Las curvas de actividad contra tiempo obtenidas en cada órgano, se ajustarán a un modelo biexponencial o triexponencial según el caso, con la finalidad de obtener las constantes de captación y eliminación efectivas.

La actividad determinada en las muestras de sangre a los diferentes intervalos de tiempo, se ajustarán a un modelo biexponencial de dos compartimentos; el compartimento central Cc y el compartimento perifério Cp , esto es, que el radiofármaco llega directamente a la circulación sistémica y se distribuye entre el torrente sanguíneo y los órganos más irrigados, como son el corazón, hígado y riñones, que constituyen el Cc; desde este compartimento la actividad pasa más lenta, a órganos o tejidos que reciben un menor flujo de sangre y éste nuevo espacio se denomina Cp.

Los resultados se analizarán con el programa biexp, para calcular las constantes de distribución rápida y constante de eliminación lenta, el volumen aparente de distribución en el compartimento central (Vdcc), el volumen aparente de distribución en el estado de equilibrio

(Vdss), la depuración total, el tiempo promedio de residencia y la constante de eliminación (kss) se calcularán.

Obtención de imágenes gammagráficas

Se obtendra una imagen gammagráfica del ratón inyectado con el radiofármaco utilizando el gammágrafo E-cam del departamento de medicina nuclear, 2 h postinyección del radiofármaco.

Disposición de cadáveres

Todo lo referente al uso de material radiactivo se trabajará dentro de un área que tiene licencia de uso de material radiactivo (laboratorio de medicina nuclear), el personal involucrado en este proyecto es POE y solo se usarán 40 microcuries que es una actividad muy baja, comparada con los 10 milicuries (10000 microcuries) que se usan en los estudios de rutina en pacientes. Además el Tc-99m tiene un tiempo de vida media física de seis horas, desintegrándose sin radiaciones beta, por lo que no existe ningún riesgo para el usuario y está clasificado dentro de los radionúclidos de toxicidad baja de acuerdo a la NOM-003-NUCL-1994 "Clasificación de instalaciones o laboratorios que utilizan fuentes abiertas"

En cuanto al manejo de desechos, se realizará de acuerdo al manual oficial de procedimiento del departamento de medicina nuclear. Los órganos del ratón y el cadáver se colocarán en una bolsa de plástico de color amarillo que tiene la leyenda "residuos biológico-infecciosos" y se almacenará dentro del cuarto frío del departamento de Medicina Nuclear. Después de 3 días de decaimiento, la bolsa amarilla de plástico que contienen los restos de cada tejido ya sin radiactividad, se desechará en el contenedor correspondiente de este tipo de desechos biológicos.

Análisis estadístico propuesto

Se usará la prueba de t pareada para evaluar el efecto del porcentaje de captación comparando la biodistribución del radiofármaco ^{99m}Tc-RGD en ratones con tumor inducido de mama y la biodistribución de la ^{99m} Tc-oxitocina también en ratones con tumor inducido de mama y determinar si hay diferencia significativa entre los dos radiofármacos. Se considerará diferencia significativa una $p<0.05$.

Para el análisis estadístico de la biodistribución de la ^{99m}Tc-RGD con las diferentes líneas celulares (3) se utilizara un ANOVA con un nivel de significancia de 0.05.

Otros aspectos

La metodología no incluye: maniobras conductuales, modificaciones ambientales, restricción física y ejercicio, inmunización, administración de medicamentos, substancias peligrosas ni cirugía

BIBLIOGRAFÍA

1. Breeman W.A., de Jong M., Kwekkeboom D. J., Valkema R., Bakker W.H. Kooij P.P., et al. Somatostatin receptor-mediated imaging and therapy: basic science, current knowledge, limitations and future perspectives. *Eur J Nucl Med.* **2001**, *28:1421-1429*

2. Bussolati G., Chinol M., Chini B., Nacca A., Cassoni P., Paganelli G. ^{111}In-labeled 1,4,7,10-Tetraazacyclododecane-N,N',N'',N'''-tetraacetic Acid-Lys^{8}-Vasoticin: A new Powerful Radioligand for Oxytocin Receptor-expressin Tumors *Cancer Research.* **2001**, *6:4393-43-97.*

3. Cassoni P., Fulcheri E., Carcangiu M. L., Stella A., Deaglio S., Bussolati G. Oxytocin receptors in human adenocarcinomas of the endometrium: presence and biological significance. *J. Pathol.* **2000**, *190:470-477.*

4. Cassoni P., Sapino A., Marrocco T., Bussolati G. Oxytocin and Oxytocin Receptors in Cancer Cells an Proliferation. *J. Neuroendocrinology.* **2004**, *16:362-364.*

5. Costopoulos, B.; Benaki, D.; Pelecanou, M.; Mikros, E.; Stassinopoulou, C.I.; Varvarigou, A.D.; Archimandritis, S.C. *Inorg. Chem.*, **2004**, *43*, 5598.

6. De Jong M., Kwekkeboom D., Valkema R., Krenning E. P. Tumor Therapy with radiolabelled peptides: current satatus and future directions. *Eur. J. Nucl. Med. Mol. Imaging.* **2003**, *30:463-469.*

7. FEUM. Farmacopea de los Estados Unidos Mexicanos. Capítulo de radiofármacos Octava edición, Vol.I, Secretaria de Salud. **2004**, México.

8. Friedlander M, Brooks PC, Shaffer RW, Kincaid CM, Varner JA, Cheresh DA. Definition of two angiogenic pathways by distinct alpha v integrins. Sc*ience.* **1995** *Dec 1;270(5241):1500-2*

9. Haubner, R.; Bruchertseifer, F.; Bock, M.; Kessler, H.; Schwaiger, M.; Wester, H.J. *Nuklearmedizin*, **2004**, *43*, 26

10. Janssen M, Frielink C, Dijkgraaf I, Oyen W, Edwards DS, Liu S, Rajopadhye M, Massuger L, Corstens F, Boerman O. Improved tumor targeting of radiolabeled RGD peptides using rapid dose fractionation. *Cancer Biother Radiopharm.* **2004***;19(4):399-404.*

11. Janssen M, Oyen WJ, Massuger LF, Frielink C, Dijkgraaf I, Edwards DS, Radjopadhye M, Corstens FH, Boerman OC.Comparison of a monomeric and dimeric radiolabeled RGD-peptide for tumor targeting. *Cancer Biother Radiopharm.* **2002***;17(6):641-6.*

12. Janssen ML, Oyen WJ, Dijkgraaf I, Massuger LF, Frielink C, Edwards DS, Rajopadhye M, Boonstra H, Corstens FH, Boerman OC. Tumor targeting with radiolabeled alpha(v)beta(3) integrin binding peptides in a nude mouse model. *Cancer Res.* **2002** *;62(21):6146-51.*

13. Kaltsas G., Rockall A., Papadogias D., Reznek R., Grossman A. B. Recent advances in radiological and radionuclide imaging and therapy of neuroendocrine tumours. *Eur. J. Endocrinol.* **2004**; *151:15-27*

14. Knight LC. In Handbook of Radiopharmaceuticals; Welch MJ and Redvanly CS eds. John Wiley & Sons: England, **2003**; pp. 643-684.

15. Krenning E.P., Kwekkeboom D.J.,Valkema R., Pauwels S., Kvols L.K., Marion de Jong. Peptide Receptor Radionuclide Therapy. *Ann. N.Y. Acad. Sci.* **2004**, *1014:234–245.*

16. Kwekkeboom D.J., Teunissen J.J., Bakker W.H., Kooij P.P., de Herder W.W., Feelders R.A., et al. Radiolabeled somatostatin analog [177Lu-DOTA0,Tyr3]octreotate in patients with endocrine gastroenteropancreatic tumors. *J. Clin. Oncol.* **2005a**; *23:2754-2762.*

17. Kwekkeboom D.J., Muller-Brand J., Paganelli G., Lowell B. A., Pauwels S., Kvols K. L., O'Dorisio T. M., et al. Overview of Results of Peptide Receptor Radionuclide Therapy with 3 Radiolabeled Somatostatin Analog. *J. Nucl. Med.* **2005b**; *46:62S-66S*

18. Liu, S.; Hsieh, W.Y.; Kim, Y.S.; Mohammed, S.I.; Effect of coligands on biodistribution characteristics of ternary ligand 99mTc complexes of a HYNIC-conjugated cyclic RGDfK dimer. *Bioconjug Chem. **2005** Nov-Dec;16(6):1580-8*

19. Lui S, Edwards S, Barnet AS. Reviews 99mTc. Labeling of highly potent small peptides. *Bioconjugate Chem.* **1997**; *5:621-636.*

20. Mitra A, Nan A, Papadimitriou JC, Ghandehari H, Line BR. Polymer-peptide conjugates for angiogenesis targeted tumor radiotherapy. *Nucl Med Biol.* **2006**; *33(1):43-52.*

21. Reubi J.C. Peptide Receptors as Molecular Targets for Cancer Diagnosis and Therapy. *Endocrine Reviews.* **2003**; *24(4): 389-427.*

22. Su ZF, Liu G, Gupta S, Zhu Z, Rusckowski M, Hnatowich DJ. In vitro and in vivo evaluation of a Technetium-99m-labeled cyclic RGD peptide as a specific marker of alpha(V)beta(3) integrin for tumor imaging. *Bioconjug Chem.* **2002**;*13(3):561-70*

23. Varner JA; Brooks PC; Cheresh DA. REVIEW: the integrin alpha V beta 3: angiogenesis and apoptosis. *Cell adhesion & communications*, **1995**;*3(4):367-74*

24. Varner JA, Cheresh DA. Integrins and cancer. *Curr. Opin. Cell. Biol.* **1996**; 8(5):724-30.

25. Verduyckt, T.; Kieffer, D.; Huyghe, D.; Cleynhens, B.; Verbeke, K.; Verbruggen, A.; Bormans, G. *J. Pharm. Biomed. Anal.*, **2003**, *32*, 669.

26. Facilities for Experimental Animals, Information for new users 1987, University of Cambridge, Central Biomedical Services

27. Norma Oficial Mexicana NOM-062-ZOO-1999. Diario Oficial del 22 de agosto del 2001

28. Manual de seguridad radiológica del departamento de medicina nuclear, INCMNSZ.

4.2 ANTECEDENTES

En Medicina Nuclear el, ^{99m}Tc es el radionúclido más utilizado para estudios de diagnóstico debido a sus características físicas y químicas, emite radiaciones gamma de 140 keV (90%), (monoenergético), fácilmente detectada que proporciona imágenes gammagráficas de alta calidad, su tiempo de vida media física es de seis horas, desintegrándose por transición isomérica sin radiaciones beta, por lo que se pueden administrar dosis relativamente altas para efectuar estudios clínicos en menos tiempo y con menor tiempo de exposición. Además, el ^{99m}Tc tiene una gran disponibilidad debido a su bajo costo, ya que se obtiene fácilmente de un generador de ^{99}Mo/^{99m}Tc.

Se utiliza en forma de pertecneciato y, en estado reducido se une a un gran número de ligantes o moléculas acarreadoras, formando complejos (radiofármacos) en un tiempo de reacción relativamente corto (5 a 30 min) con altas eficiencias de marcado (>90%) [Verduyckt y cols 2003; FEUM, 2004]. Una alta selectividad por el sitio del tumor y un periodo de permanencia largo del radiofármaco en el sitio de interés son las bases para un diagnóstico clínico exitoso.

Las hormonas peptídicas (ácidos α-aminocarboxílicos) han sido diseñadas por la naturaleza para estimular, regular, inhibir numerosas funciones de la vida y actúan por medio de sus receptores principalmente, como transmisores de información y coordinadores de actividades de varios tejidos en el organismo. Comparados con los anticuerpos, los péptidos pequeños ofrecen varias ventajas: son fáciles de sintetizar y modificar, tienen menos probabilidad de ser inmunogénicos y rápida depuración sanguínea. En muchos casos la afinidad de los péptidos pequeños por sus receptores es significativamente mayor que la de los anticuerpos o sus fragmentos [Lui y cols., 1997; Reubi, 2003, De Jong y cols., 2003].

Los receptores se unen específicamente a los correspondientes péptidos marcados con radionucleidos. Los receptores de péptidos están sobre expresados en las células de numerosos cánceres. Estos receptores han sido usados como blancos moleculares para peptidos radiomarcados y así localizar el tumor. El agente biquelante ácido hidrazinonicotínico (HYNIC) y el coligante ácido etilendiaminodiacético (EDDA) se han utilizado para formar complejos de ^{99m}Tc con péptidos análogos de la somatostatina, uno de esos complejos es el octreótido (^{99m}Tc-HYNIC-TOC) que ha demostrado ser una buena opción para la detección de tumores que presentan receptores de somatostatina, ya que es captado rápidamente y retenido por el tumor. Las aplicaciones exitosas del octreótido radiomarcado en centelleografía para la localización de linfomas, granulomatosis, meningiomas y tumores de origen neuroendócrino y cáncer pulmonar, sobre todo en Europa son indicativas de la importancia que tiene investigar otro tipo de péptidos radiomarcados, tanto nativos como sus derivados (análogos), para diagnóstico por imagen en medicina nuclear [Breeman y cols., 2001; Krenning y cols., 2004, Kaltsas y cols., 2004; Kwekkeboom y cols., 2005a, 2005b].

Otros péptidos de mucho interés en medicina debido a que sus receptores estimulan el crecimiento en las células neoplásicas son la oxitocina en el cáncer de mama y cérvico uterino, y las integrinas en la estimulación de la angiogénesis.

a) **Oxitociona** Químicamente la oxitocina (OT) es un nanopéptido cíclico, con la secuencia cisteína-tirosina-isoleucina-glutamina-asparagina-cisteína-prolina-leucina-glicina. Es una hormona neuropeptidica sintetizada en los núcleos paraventricular y supraóptico del hipotálamo. La acción

hormonal periférica de la OT está mediada por receptores. Los receptores (OTRs) se unen específicamente y con gran afinidad a la OT y a algunos de sus análogos. Los OTRs se expresan principalmente en las células mioepiteliales de la glándula mamaria, en el miometrio y el endometrio del útero, al término del embarazo y en el parto y post parto. Además por estudios in vivo e in vitro se demostró que también se encuentran en carcinomas de mama y de endometrio, en neuroblastomas, glioblastomas, osteoblastos y osteosarcomas [Cassoni y col. 2000, 2004].

b) **Integrinas** Las integrinas son glucoproteínas heterodiméricas de adhesión transmembranal, constituidas por cadenas alfa y beta que cruzan de parte a parte la membrana celular. Hay 14 clases de subunidades α y 8 clases de subunidades β, que producen al menos 20 heterodímeros de integrinas. Hay muchas integrinas que están expresadas ampliamente, y la mayoría de las células tienen más de una integrina en su superficie celular, por ejemplo, las células de melanoma expresan $\alpha_v\beta_3$, $\alpha_1\beta_1$, $\alpha_3\beta_1$ y $\alpha_5\beta_1$; en las células de carcinoma pulmonar se expresan $\alpha_v\beta_5$ y en muchas otras células tumorales se encuentran $\alpha_v\beta_6$ [Knight y cols 2003; Mitra y cols. 2006]. Se han encontrado una gran variedad de integrinas sobre la superficie de células tumorales, las integrinas $\alpha_v\beta_3$ se encuentran elevadas en la angiogénesis de tumores y sus metástasis [Friedlander y cols. 1995];

La unión específica de los receptores $\alpha_v\beta_3$ de las integrinas a los péptidos que contienen el residuo de amino ácidos Arg-Gly-Asp (RGD) ha sido útil para obtener la imagen de tumores específicos, mediante el radiomarcado del péptido RGD [Janssen y cols. 2002].

4.3 OBJETIVOS E HIPÓTESIS

EL OBJETIVO PRINCIPAL:
Evaluar la especificidad *in vitro* e *in vivo* de las formulaciones de péptidos marcados con ^{99m}Tc para el diagnóstico de cánceres que sobre expresan receptores de oxitocina y de integrinas.

LOS OBJETIVOS GENERALES SON:

1. Marcar con ^{99m}Tc las formulaciones de los conjugados de oxitocina: EDDA/HYNIC-[Cys^1]-oxitocina-NH_2 y EDDA/HYNIC-[Lys^8]-oxitocina-NH_2, y del conjugado: EDDA/HYNIC-ciclo-Lys-D-Phe-RGD.
2. Evaluar la integridad de los radiofármacos y la estabilidad a la dilución en solución isotónica y plasma humano y la unión a proteínas séricas de cada uno de los 3 radiofármacos.
3. Evaluar la inmunoreactividad *in vitro* de cada uno de los radiofármacos midiendo la afinidad por los receptores de oxitocina y de integrinas presentes en líneas de células tumorales.
4. Realizar estudios de biocinética de internalización y externalización en líneas de células tumorales.
5. Determinar la biodistribución de los 3 radiofármacos en un modelo animal (animales sanos y en animales con tumores inducidos).
6. Comparar la especificidad *in vivo* de los 3 radiofármacos en tumores inducidos en un modelo animal.
7. Obtener imágenes gammagráficas de la biodistribución de cada uno de los radiofármacos en animales con tumores inducidos.
8. Cálculos dosimétricos.

9. Elaborar un protocolo clínico que permita la obtención de imágenes diagnósticas en pacientes con todos o con alguno de los radiofármacos obtenidos y que pudieran ser utilizados para el diagnóstico de cáncer.

HIPÓTESIS:
Si los coligantes EDDA y Tricina completan la esfera de coordinación en los complejos de ^{99m}Tc, entonces su uso en la formulación para el marcaje del conjugado HYNIC-ciclo-Lys-D-Phe-RGD, producirá el complejo estable ^{99m}Tc-HYNIC-ciclo-Lys-D-Phe-RGD con una pureza radioquímica mayor al 95% y tendrá las propiedades biológicas adecuadas para ser captado *in vivo* en sitios específicos de angiogénesis.

4.4 MATERIAL Y MÉTODOS

Los ratones atímicos se utilizarán de acuerdo a las especificaciones del reglamento sobre el manejo ético de los animales de laboratorio del bioterio del INCMNSZ y se realizará bajo las normas de seguridad radiológica el siguiente procedimiento: Los datos de biodistribución se obtendrán despues de inyectar en la vena de la cola del ratón 20 µL a 40 µL del péptido marcado ^{99m}Tc-EDDA/HYNIC-[Cys^1]-oxitocina-NH_2, y ^{99m}Tc-EDDA/HYNIC-ciclo-Lys-D-Phe-RGD con una concentración radiactiva de aproximadamente de 40 microcuries (37 MBq/mL). Sacrificar a los ratones atímicos a las 0.25, 0.5, 1, 2, 3, y 24 h postinyección. La finalidad es extraer y pesar los órganos, sangre, corazón, pulmón, músculo, riñones, estómago, vesícula biliar, intestino, hígado y fémur. Se obtendrá las cpm de cada órgano, utilizando para el conteo un detector precalibrado de NaI(Tl). La captación en cada órgano se calculará y expresará como el % de actividad inyectada por g de órgano (%AI/g órgano). Todas las cuentas se corregirán por fondo, geometría (volúmenes iguales) y decaimiento físico. Las curvas de actividad contra tiempo obtenidas en cada órgano, se ajustarán a un modelo biexponencial o triexponencial según el caso, con la finalidad de obtener las constantes de captación y eliminación efectivas.

La actividad determinada en las muestras de sangre a los diferentes intervalos de tiempo, se ajustarán a un modelo biexponencial de dos compartimentos; el compartimento central Cc y el compartimento perifério Cp , esto es, que el radiofármaco llega directamente a la circulación sistémica y se distribuye entre el torrente sanguíneo y los órganos más irrigados, como son el corazón, hígado y riñones, que constituyen el Cc; desde este compartimento la actividad pasa más lenta, a órganos o tejidos que reciben un menor flujo de sangre y éste nuevo espacio se denomina Cp.

Los resultados se analizarán con el programa biexp, para calcular las constantes de distribución rápida y constante de eliminación lenta, el volumen aparente de distribución en el compartimento central (Vdcc), el volumen aparente de distribución en el estado de equilibrio (Vdss), la depuración total, el tiempo promedio de residencia y la constante de eliminación (kss) se calcularán.

4.5 ANÁLISIS ESTADÍSTICO PROPUESTO

Coeficiente de variación.

4.6 BIBLIOGRAFÍA

1. Breeman W.A., de Jong M., Kwekkeboom D. J., Valkema R., Bakker W.H. Kooij P.P., et al. Somatostatin receptor-mediated imaging and therapy: basic science, current knowledge, limitations and future perspectives. *Eur J Nucl Med.* **2001**, *28:1421-1429*

2. Bussolati G., Chinol M., Chini B., Nacca A., Cassoni P., Paganelli G. ^{111}In-labeled 1,4,7,10-Tetraazacyclododecane-N,N',N'',N'''-tetraacetic Acid-Lys^{8}-Vasoticin: A new Powerful Radioligand for Oxytocin Receptor-expressin Tumors *Cancer Research.* **2001**, *6:4393-43-97.*

3. Cassoni P., Fulcheri E., Carcangiu M. L., Stella A., Deaglio S., Bussolati G. Oxytocin receptors in human adenocarcinomas of the endometrium: presence and biological significance. *J. Pathol.* **2000**, *190:470-477.*

4. Cassoni P., Sapino A., Marrocco T., Bussolati G. Oxytocin and Oxytocin Receptors in Cancer Cells an Proliferation. *J. Neuroendocrinology.* **2004**, *16:362-364.*

5. Costopoulos, B.; Benaki, D.; Pelecanou, M.; Mikros, E.; Stassinopoulou, C.I.; Varvarigou, A.D.; Archimandritis, S.C. *Inorg. Chem.,* **2004**, *43*, 5598.

6. De Jong M., Kwekkeboom D., Valkema R., Krenning E. P. Tumor Therapy with radiolabelled peptides: current satatus and future directions. *Eur. J. Nucl. Med. Mol. Imaging.* **2003**, *30:463-469.*

7. FEUM. Farmacopea de los Estados Unidos Mexicanos. Capítulo de radiofármacos Octava edición, Vol.I, Secretaria de Salud. **2004**, México.

8. Friedlander M, Brooks PC, Shaffer RW, Kincaid CM, Varner JA, Cheresh DA. Definition of two angiogenic pathways by distinct alpha v integrins. Sc*ience.* **1995** *Dec 1;270(5241):1500-2*

9. Haubner, R.; Bruchertseifer, F.; Bock, M.; Kessler, H.; Schwaiger, M.; Wester, H.J. *Nuklearmedizin*, **2004**, *43*, 26

10. Janssen M, Frielink C, Dijkgraaf I, Oyen W, Edwards DS, Liu S, Rajopadhye M, Massuger L, Corstens F, Boerman O. Improved tumor targeting of radiolabeled RGD peptides using rapid dose fractionation. *Cancer Biother Radiopharm.* **2004***;19(4):399-404.*

11. Janssen M, Oyen WJ, Massuger LF, Frielink C, Dijkgraaf I, Edwards DS, Radjopadhye M, Corstens FH, Boerman OC.Comparison of a monomeric and dimeric radiolabeled RGD-peptide for tumor targeting. *Cancer Biother Radiopharm.* **2002***;17(6):641-6.*

12. Janssen ML, Oyen WJ, Dijkgraaf I, Massuger LF, Frielink C, Edwards DS, Rajopadhye M, Boonstra H, Corstens FH, Boerman OC. Tumor targeting with radiolabeled alpha(v)beta(3) integrin binding peptides in a nude mouse model. *Cancer Res.* **2002** *;62(21):6146-51.*

13. Kaltsas G., Rockall A., Papadogias D., Reznek R., Grossman A. B. Recent advances in radiological and radionuclide imaging and therapy of neuroendocrine tumours. *Eur. J. Endocrinol.* **2004**; *151:15-27*

14. Knight LC. In Handbook of Radiopharmaceuticals; Welch MJ and Redvanly CS eds. John Wiley & Sons: England, **2003**; pp. 643-684.

15. Krenning E.P., Kwekkeboom D.J.,Valkema R., Pauwels S., Kvols L.K., Marion de Jong. Peptide Receptor Radionuclide Therapy. *Ann. N.Y. Acad. Sci.* **2004**, *1014:234–245.*

16. Kwekkeboom D.J., Teunissen J.J., Bakker W.H., Kooij P.P., de Herder W.W., Feelders R.A., et al. Radiolabeled somatostatin analog [177Lu-DOTA0,Tyr3]octreotate in patients with endocrine gastroenteropancreatic tumors. *J. Clin. Oncol.* **2005a**; *23:2754-2762.*

17. Kwekkeboom D.J., Muller-Brand J., Paganelli G., Lowell B. A., Pauwels S., Kvols K. L., O'Dorisio T. M., et al. Overview of Results of Peptide Receptor Radionuclide Therapy with 3 Radiolabeled Somatostatin Analog. *J. Nucl. Med.* **2005b**; *46:62S-66S*

18. Liu, S.; Hsieh, W.Y.; Kim, Y.S.; Mohammed, S.I.; Effect of coligands on biodistribution characteristics of ternary ligand 99mTc complexes of a HYNIC-conjugated cyclic RGDfK dimer. *Bioconjug Chem. **2005** Nov-Dec;16(6):1580-8*

19. Lui S, Edwards S, Barnet AS. Reviews 99mTc. Labeling of highly potent small peptides. *Bioconjugate Chem.* **1997**; *5:621-636.*

20. Mitra A, Nan A, Papadimitriou JC, Ghandehari H, Line BR. Polymer-peptide conjugates for angiogenesis targeted tumor radiotherapy. *Nucl Med Biol.* **2006**; *33(1):43-52.*

21. Reubi J.C. Peptide Receptors as Molecular Targets for Cancer Diagnosis and Therapy. *Endocrine Reviews.* **2003**; *24(4): 389-427.*

22. Su ZF, Liu G, Gupta S, Zhu Z, Rusckowski M, Hnatowich DJ. In vitro and in vivo evaluation of a Technetium-99m-labeled cyclic RGD peptide as a specific marker of alpha(V)beta(3) integrin for tumor imaging. *Bioconjug Chem.* **2002**;*13(3):561-70*

23. Varner JA; Brooks PC; Cheresh DA. REVIEW: the integrin alpha V beta 3: angiogenesis and apoptosis. *Cell adhesion & communications*, **1995**;*3(4):367-74*

24. Varner JA, Cheresh DA. Integrins and cancer. *Curr. Opin. Cell. Biol.* **1996**; 8(5):724-30.

25. Verduyckt, T.; Kieffer, D.; Huyghe, D.; Cleynhens, B.; Verbeke, K.; Verbruggen, A.; Bormans, G. *J. Pharm. Biomed. Anal.*, **2003**, *32*, 669.

26. Facilities for Experimental Animals, Information for new users 1987, University of Cambridge, Central Biomedical Services

27. Norma Oficial Mexicana NOM-062-ZOO-1999. Diario Oficial del 22 de agosto del 2001

4.5 ANÁLISIS ESTADÍSTICO PROPUESTO
Coeficiente de variación.

6. 1 TAMAÑO DE LA MUESTRA
90 ratones atímicos, divididos en 3 grupos de 30 ratones para los estudios radiofarmacocinéticos, terapéuticos y dosimétricos.

6.2 MEDICIONES FISIOLÓGICAS
Antes de la inyección del radiofármaco los ratones atímicos se pesan.

6.3 ALIMENTACIÓN
SIN ESPECIFICACIONES, *ad libitum*

6.4 AGUA
POTABLE, *ad libitum*

6.5 MANIOBRAS CONDUCTUALES
NINGUNA

6.6 MODIFICACIONES AMBIENTALES
NINGUNA

6.7 RESTRICCIÓN FÍSICA Y EJERCICIO
NINGUNO

6.8 INMUNIZACIÓN
NO PROCEDE

6.9 ADMINISTRACIÓN DE MEDICAMENTOS
NINGUNO

6.10 INOCULACIÓN DE AGENTES BIOLÓGICOS
Se utilizarán diferentes líneas celulares de cáncer:
Células AR42J de tejido canceroso de páncreas, (origen humano)
Células MCF-7 de tejido canceroso de mama, (origen humano)
Células PC3 de tejido canceroso de próstata, (origen murino)

Se inoculará de manera subcutánea 100 µL de una solución de células cancerosas en flancos (en un solo sitio), con los cuidados de manejo y sujeción del animal para minimizar riesgos durante el procedimiento de inyección tanto para el animal como para la persona que realiza el procedimiento. Una vez que el tumor tenga un tamaño de 0.5 a 1 cm de diámetro como máximo, se procederá a realizar el estudio de biodistribución.

6.11 SUBSTANCIAS PELIGROSAS
NINGUNA

6.12 RADIACIONES
Se inyectarán en la vena de la cola del ratón 40 microcuries del péptido marcado con Tc-99m. El radiofármaco inyectado no representa ningún peligro para el ratón ni para el operador.

6.13 TRAUMA
La inyección en la cola del animal produce trauma mínimo.

6.14 CIRUGÍA
NO PROCEDE

6.15 OBTENCIÓN DE MUESTRAS
Se obtiene una cantidad de sangre de aproximadamente 0.5 mL por punción cardiaca inmediatamente después de la muerte del ratón.

6.16 OBTENCIÓN DE TEJIDOS

Tomar una muestra de tejidos de diferentes órganos (corazón, pulmón, hígado, bazo, vesícula biliar, estómago, intestino, heces, riñón, músculo, hueso y tejido canceroso).

6.17 EUTANASIA

Se usará una dosis letal de bióxido de carbono en la cámara de acrílico.

6.18 DISPOSICIÓN DE CADÁVERES

Después de extirpar los órganos del ratón, el cadáver se coloca en una bolsa de plástico de color amarillo y se almacena dentro del cuarto frío del departamento. Después de 3 días de decaimiento los tubos de ensaye de plástico que contienen los restos de cada tejido se desechan en el contenedor correspondiente.